Phytochemical Mediated Modulation Of Breast Cancer Resistance Protein At The Blood Brain Barrier And Blood Cerebrospinal Fluid Barrier

MANJIT KAUR

Thesis submitted for the degree of

Doctor of Philosophy

ASTON UNIVERSITY

January 2016

Aston University

Phytochemical Mediated Modulation Of Breast Cancer Resistance Protein At The Blood Brain Barrier And Blood Cerebrospinal Fluid Barrier

Manjit Kaur

Doctor of philosophy
2016

Thesis Summary

Drug delivery to the central nervous system (CNS) is significantly hindered by the presence of the blood brain barrier (BBB) and blood cerebrospinal fluid barrier (BCSFB) and associated drug efflux transporter proteins. The aim of this work was to modulate the expression of breast cancer resistance protein (BCRP) at each barrier site using phytochemical modulators. *In-vitro* cellular models of both the BBB (porcine brain microvascular endothelial cells (PBMEC/C1-2)) and BCSFB (rat choroid plexus cells (Z310)) were utilised and 18 phytochemical modulators screened for their cellular toxicity with IC_{50} values for the majority of phytochemicals being in excess of 100 µM. Intracellular accumulation of Hoechst 33342 (H33342) was assessed in each barrier cell line to determine short-term modulation of BCRP efflux or long-term modulation of protein expression. Incubations with modulators demonstrated significant inhibition of BCRP efflux activity for a range of modulators in both cell lines with TMF (1-100 µM) demonstrating a > 6 fold increase in intracellular accumulation. Similarly, many modulators demonstrated proposed protein-level modulation of BCRP resulting in increases or decreases in H33342 accumulation following a 24 hour exposure. Western blotting subsequently confirmed that quercetin and naringin for PBMEC/C1-2 and baiclain and flavone for Z310 induced BCRP expression (to 2-3 fold of control) whereas curcumin and 17-β-estradiol for PBMEC/C1-2 and silymarin, quercetin and 17-β-estradiol for Z310 down-regulated BCRP expression (to 0.24-0.4 fold of control). This was further confirmed in substrate transport studies using 12- well permeable insert models, which demonstrated functional changes in the permeability of BCRP substrates across both barrier models.

Subsequently the regulation of BCRP by AhR was confirmed through siRNA knockdown of AhR, which resulted in a significant decrease in BCRP gene expression in both cell lines. Furthermore the induction/down-regulation effects on BCRP were, in general, diminished following AhR knockdown, suggesting AhR plays an important role in mediating the genomic/proteomic alterations in BCRP expression when exposed to phytochemicals.

Acknowledgements

Firstly, I would like to express my sincere gratitude to my supervisor Dr. Raj K Singh Badhan for his great amount of patience, help, guidance and encouragement throughout this journey for the past few years. You are the best teacher I have ever had.

I would like to thank all the others in the drug delivery group at Aston University for their support, the lab technicians: Jiteen Ahmed, Tom and Chris for the enormous help they have given with regard to all the equipment and materials I needed throughout this project.

I would like to thanks my colleagues and friends Mandeep, Eman, Sheetal, Swapnil and Affiong to support and encouragement during tough times. We all had fun together and you all will be my friends forever.

I would like to thanks Aston University for providing funding for this research.

I would like to thank my family and friends who have all been so supportive throughout the years, thank you so much. Finally, I reserve my greatest expression of gratitude to my husband Charnjit Singh, who has always believed in me and has always been there for me. I am truly and earnestly grateful for your support, encouragement, love and praise. You are my pillar of strength and without you, this would never have been possible.

List of Publications

Peer Reviewed Articles

1. **Kaur M** and Badhan RK., (2015). Phytoestrogens modulate breast cancer resistance protein expression and function at the blood-cerebrospinal fluid barrier. *Journal of pharmacy and pharmaceutical sciences*. 18(2): 132-154.

2. Badhan RK, **Kaur M,** Lungare S and Obuobi S., (2014). Improving brain drug targeting through exploitation of the nose-to-brain route: a physiological and pharmacokinetic perspective. *Current Drug Delivery.*11 (4):458-71.

Article in Preparation

Kaur M and R.K.Singh Badhan., (2015). Phytoestrogens modulate breast cancer resistance protein expression and function at the blood-brain barrier. In preparation.

Abstracts

1. **Manjit Kaur** and Raj K Singh Badhan.,2014. Flavonoids down regulate breast cancer resistance protein function and expression at the blood cerebrospinal fluid barrier. Blood brain barrier symposium, University College London, London, UK.

2. **Manjit Kaur and** Raj K Singh Badhan, 2014. Flavonoids are modulators of BCRP at the Blood brain barrier and Blood cerebrospinal fluid barrier. LHS PG Research day, Aston University, Birmingham, UK.

3. **Manjit Kaur** and Raj K Singh Badhan., 2014. Determination of genomic and protein expression of Breast Cancer Resistance Protein and its modulation at the blood cerebrospinal fluid barrier (Z310 cells). M5 Biomedical imaging conference, University of Nottingham, Nottingham, UK.

4. **Manjit Kaur** and Raj Singh Badhan., 2013., Silencing the central nervous system: A gene silencing approach to enhance the neuropharmacokinetics of the CNS drug delivery. UKICRS. The University of Reading, Reading. UK.

5. Raj K Singh Badhan and **Manjit Kaur,** 2012., The art of miniaturisation: A microfluidic approach to the design and delivery of nanoparticle drug formulations. UKICRS. Aston University, Birmingham.UK

6. **Manjit Kaur**, Raj K Singh Badhan and Yvonne Perrie. 2012. Overcoming drug delivery to the central nervous system: A novel CNS drug delivery platform. Aston University PG. Birmingham, UK.

List of Contents

List of Abbreviations

ABC	Adenosine 5’-triphosphate binding cassette
AD	Alzheimer’s disease
ANOVA	Analysis of variance
ATP	Adenosine 5"- triphosphate
BBB	Blood-brain barrier
BCRP	Breast cancer resistance protein
BCSFB	Blood-cerebral spinal fluid barrier
BSA	Bovine serum albumin
BCA	Bicinchoninic acid assay
C	Celsius
CEC	Cerebral endothelial cell
cm	Centimetre
CNS	Central nervous system
CO2	Carbon dioxide
CP	Choroid plexus
CSF	Cerebral spinal fluid
D	Dilution factor
Da	Daltons
DMEM	Dulbecco’s modified eagle medium
DMSO	Dimethylsulfoxide
DNA	Deoxyribonucleic acid
DPBS	Dulbecco’s phosphate buffered saline
°	Degree
EC	Endothelial cells
EDTA	Potassium ethylene diamine tetra acetic acid

EGF	Epidermal growth factor
FBS	Foetal bovine serum
g	Gram
h	Hour
HBSS	Hank's buffered salt solution
HEPES	4-(2-hydroxyethyl)-1-piperazineethanesulfonic acid
H2O	Water
ICF	Intracellular fluid
ISF	Interstitial fluid
L	Litre
MDCK	Madin-Darby Canine Kidney
MEM	Minimal Essential Medium
mg	Milligram
min	Minute
µL	Microlitre
mL	Millilitre
µM	Micromolar
mM	Millimolar
MRP	Multidrug resistance associated protein
MTT	Methylthiazolyldiphenyl-tetrazolium bromide **(**3-(4, 5-dimethylthiazol-2-yl)-2, 5-diphenyltetrazolium bromide,
MW	Molecular weight
nM	Nanomolar
NVU	Neurovascular Unit
Ω	Ohm
PBEC	Porcine brain endothelial cell
PBS	Phosphate-buffered saline

PET	Positron emission tomography
PXR	Pregnane X receptor
qPCR	Quantitative polymerase chain reaction
RNA	Ribonucleic acid
RT	Room temperature
RT-PCR	Reverse transcriptase polymerase chain reaction
s	Second
SFM	Serum free media
t	Time
TAE	Tris-Acetate EDTA buffer
TBST	Tris-Buffered Saline with Tween 20
T-25	25 cm^2 tissue culture flask
T-75	75 cm^2 tissue culture flask
TEER	Transendothelial or epithelial resistance
TJ	Tight junctions
U	Units
UV	Ultraviolet
V	Volts
v	Volume
w	Weigh

List of Figures

Chapter 1: Introduction

Chapter 2: Assessment of the interactions of phytochemicals on BCRP expression and function at the porcine blood brain barrier

Chapter 3: Assessment of the interactions of phytochemicals on BCRP expression and function at the rat blood cerebrospinal fluid barrier

Chapter 4: Transcriptional regulation of BCRP by the aryl hydrocarbon receptor at the BBB and BCSFB

List of Tables

Chapter 1: Introduction

Chapter 2: Assessment of the interactions of phytochemicals on BCRP expression and function at the porcine blood brain barrier

Chapter 3: Assessment of the interactions of phytochemicals on BCRP expression and function at the rat blood cerebrospinal fluid barrier

Chapter 4: Transcriptional regulation of BCRP by the aryl hydrocarbon receptor at the BBB and BCSFB

Chapter 1

Introduction

1.1. Background

The development of neurodegenerative diseases is one of the most devastating illnesses which can affect people across all age groups (Manji and DeSouza, 2008). The World Health Organization (WHO) reported that neurological disorders contributed to 92 million disability adjusted life years (DALYs) in 2005 and which is thought to increase to 103 million (approximately 12% rise) in 2030 (Eigenmann et al., 2013). In Europe the WHO described that CNS disorders contributes 37% of the total disease burden (Stins et al., 2001, Prudhomme et al., 1996), with an estimated cost of treatment thought to be at $798 billion (Prudhomme et al., 1996). Age related neurodegenerative diseases, such as Alzheimer's disease (AD) and Parkinson's disease (PD), are major health problems in developed countries. AD is the sixth leading cause of deaths in the USA and an estimated 5 million Americans are living with AD (Hurd et al., 2013). The treatment costs for AD and other 'dementias' (in United States) was estimated to be $226 billion in 2015 and is expected to rise to $1.2 trillion by 2050 (Kameremail et al., 2015). This figure is made even more striking when considering that in 2010 it was estimated that there were 35.6 million people with dementia with the figure nearly doubling every 20 years, increasing to 65.7 million in 2030, and 115.4 million in 2050 (Wimo and Prince, 2010).

Similarly, PD is the second most neurodegenerative illness after AD in United States. 10 million people are living with PD worldwide. The economic burden of PD exceeds $14.4 billion in 2010 and expected to be double by 2040 (Kowal et al., 2013).The total annual cost of care in the UK has been estimated at approximately £599 million per year for 100,000 individuals with PD only (2015b). Costs to the National Health Service (NHS) were approximately 38% of the total care costs (Findley et al., 2003).

A major cause of this increase in the incidence of untreated CNS disorders is not due to a lack of therapeutics, but rather a lack of understanding of CNS disease pathology and how this may impact upon the delivery of drugs to the CNS. In recent years, the pharmaceutical industry have struggled to provide novel drug therapies for CNS disorders, primarily as a result of higher cost to market, longer development times (an average 13 years) compared to non-CNS diseases (an average 8 -10 years) (Alavijeh et al., 2005), higher risk of clinical failure and changing regulatory hurdles (Manji and DeSouza, 2008). A report by the Tufts Centre for the Study of Drug Development (Tufts CSDD) suggests that only 8.2 % of CNS drug candidates ever become available for

clinical use, compared with 15% for non-CNS indicated drugs (Riordan and Cutler, 2012).

1.2. The physiology of the brain and central nervous system

The brain is a highly vascularised organ with a combined microvascular surface area of 150-200 cm^2/g , which results in a large area for molecular/fluid transfer (12-18 m^2) in the adult human brain (Abbott et al., 2010, Tang et al., 2014, Zhao et al., 2009a). The delivery of drugs to the CNS is often hindered by its complex anatomy and physiology (Abbott, 2005). The CNS is a complicated and delicate organ and has its own self-protective mechanism to exchange nutrients, neurotoxins, pathogens and xenobiotics. This self-protective mechanism has become a significant hurdle to deliver drugs to the brain (Begley, 2003). A key obstacle to the delivery of drugs to the CNS is the presence of physiological barriers located between the blood and brain (termed the blood brain barrier [BBB]) and the blood and cerebrospinal fluid (termed the blood cerebrospinal fluid barrier [BCSFB]). A prerequisite for therapeutic molecules to gain access to the CNS biophase is the permeation of these barriers (Begley, 2003).

1.2.1. The blood brain barrier

1.2.1.1. Discovery

In 1878, the German scientist Paul Ehrlich injected several mice with trypan blue dye and discovered that the dye stained all other tissue and organs except for the brain and the spinal cord. Thereafter Edwin Goldman (one of Ehrlich's student), injected the same dye into the cerebrospinal fluid (CSF) and found that it stained the brain but no other body organs (Goldmann, 1909, Goldmann, 1913). Ehrlich's experimental findings were later confirmed by a number of other researches (Goldmann, 1909, Goldmann, 1913) (Friedemann, 1942) and led to the idea of a compartmentalisation between the brain and cerebral capillaries, that is to say that BBB.

1.2.1.2. Physiology of the blood brain barrier

The BBB is essentially formed by microvascular endothelial cells, which surround blood capillaries within the brain (Figure 1.1). The BBB is further formed into a complex mesh of astrocytes, basement membranes, pericytes and neurons (Stamatovic et al., 2008), and which is often termed the 'neurovascular unit'. Endothelial cells primarily form the

'barrier' function by hindering xenobiotic transport, with endothelial cells held tightly packed together with adjacent endothelial cells through a tight network of tight junctions (TJs). Furthermore endothelial cells have no fenestrations (Fenstermacher and Kaye, 1988), an increased number of mitochondria (Oldendorf et al., 1977) and low pinocytotic activity (Sedlakova et al., 1999) which restricts the diffusion of hydrophilic solutes (Abbott, 2002).

Endothelial cells and the neurovascular unit (NVU) function to regulate transport and metabolism of substances from blood to brain and brain to the peripheral blood. As part of the NVU, astrocytes form networks which surround the endothelial cells and basement membrane (Bernoud et al., 1998). The NVU also includes a basement membrane which is comprised of a range extracellular matrix proteins such as collagen, elastin, fibronectin, laminin and proteoglycans and cell adhesion molecules (CAMs), as well as signalling proteins (Carvey et al., 2009, Wolburg et al., 2009). Disruption of basement membrane can lead to alteration of brain micro vessel cytoskeleton which can affect the barrier integrity (Cardoso et al., 2010).

Pericytes communicate with the other elements of the NVU through signalling pathways and regulate the normal function of the BBB (Ryota et al., 2007). From a BBB perspective, neurons are known to induce enzymes, which regulate the function of blood vessels (Persidsky et al., 2006).

Figure 1.1: Schematic representation of the blood brain barrier.

Blood capillaries are surrounded by endothelial cells which also have astrocytes and pericytes overlying that together form the blood brain barrier (Chen and Liu, 2012).

Tight Junctions (TJs) are formed by contact zones between cells or between parts of the same cell, in which the intercellular cleft is occluded. TJs are regulated by a set of interacting proteins including occludin, claudins and junctional adhesion molecules (JAMs) that seals the space between adjacent endothelial cells (Figure 1.2) and further hinder the passage of xenobiotic across the BBB.

Occludin (molecular weight ~65kDa) was the first reported TJ transmembrane protein. Occludin contains two equal extracellular loops, four transmembrane domains and three cytoplasmic domains. The C-terminal domain forms an α-helix coiled loop structure (Li et al., 2005) and mediates communication with other cytoplasmic proteins such as ZO-1, ZO-2 and ZO-3 and interactions with other regulatory proteins (Peng et al., 2003).

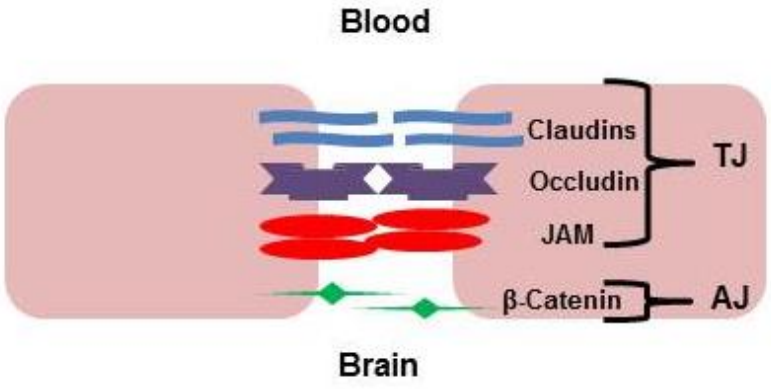

Figure 1.2: Structure of tight junctions.

Adjacent endothelial cells are linked by tight junction, which expresses TJs proteins such as claudins, occludin that interact with each other and seals the space between the cells. AJs are the junctions formed between the cells or surrounding matrix.

Claudin (molecular weight ~20-27 kDa) is a major constituent of TJs. Claudin binds to claudins present on the adjacent endothelial cells and to cytoplasmic proteins (ZO-1, ZO-2 and ZO-3) and contributes to the tightly linked endothelial cell structure (Furuse et al., 1999). Adheren junctions (AJs) are cellular junctions formed between two adjacent endothelial cells. The main functions of AJs are to mediate cell adhesion, cell polarity and also contribute to the BBB function (Hawkins and Davis, 2005). The main constituents of AJs are cadherin and catenins. Cadherin mediates cell adhesion, limits cell proliferation and decreases cellular permeability (Cook et al., 2008). Catenins act as linking proteins which link cadherin adhesion to the cortical actin cytoskeleton.

1.2.2. The blood cerebrospinal fluid barrier

1.2.2.1. Discovery

The cerebrospinal fluid (CSF) was first described in a document by ancient Egyptians as 'water surrounding the brain' over 2700 years ago (Hajdu, 2003). This was followed by a description by Hippocrates (129-219 AD) who described the water in the skull as 'hydrocephalus'. Galen (130-200 AD.) identified a 'fluid' found to be leaking from the nasal cavity of sick patients was a originating from the pituitary gland (Nutton, 1973). In 1664 Thomas Willis first correctly evaluated the choroid plexus as a source of CSF production in a body of work called the "*Cerebri Anatome*" (Stephen Porter et al., 1977). In the mid-1700s Albrecht von Haller (Frixione, 2006) describes the circulation of CSF and thereafter the ventricle structures and presence of CSF within brain and spinal cord was identified.

1.2.2.2. Physiology of the blood cerebrospinal fluid barrier

The choroid plexuses (CP) are highly vascular tissues found in all four cerebral ventricles (Figure 1.3). The CP is comprised of a rich capillary bed of pia matter and choroidal epithelial cells (Siegel GJ et al., 1999) and consists of three layers of cells: apical epithelial cells, connective tissues and inner layer of endothelial cells.

The primary function of the CP is to secrete cerebrospinal fluid (CSF) (Pollay and Curl, 1967). CSF is formed by the filtration of plasma by choroidal capillaries (Xie and Hammarlund-Udenaes, 1998). The osmotically active ions such as Na^+, Cl^-, K^+ ,HCO_3^- and water from the plasma are filtered to the CSF. The total volume of CSF is estimated to be 150-200 mL in humans, 1.4-2.3 mL in rabbits (Siegel GJ et al., 1999, Brown et al., 2004) and 0.28-0.3 mL in rats (Han et al., 2009). The rate of CSF production in humans is 0.3-0.4 mL/min and 0.003 mL/min in rodents (Hammarlund-Udenaes, 2000).

Villi and microvilli present on the choroidal epithelial cells enhances the macroscopic folding of the choroid plexus and increases the surface area of choroidal epithelial (Nolte, 1993). The surface area of the CP is reported to range from 0.02-5 m^2 (Cornford et al., 1997, Dohrmann, 1970b, Pardridge, 2011), and if assumed to be in the range of > 1 m^2, places the surface area within an order of magnitude of brain microvascular endothelial cell surface area.

Figure 1.3: Location of the choroid plexus within the human brain.

Lateral, central, third and fourth ventricles are the primary location of the choroid epithelial tissue and the sites of cerebrospinal fluid secretion into ventricles (1991b).

The epithelial cells of the choroid plexus form a barrier which restricts the free movement of molecules from blood into the CSF and brain biophase-to-CSF-to-blood (Siegel GJ et al., 1999) and is termed the blood-cerebrospinal fluid barrier (BCSFB) (Figure 1.4).

1.2.2.3. Functional role of the choroid plexuses

In addition to the secretion of CSF, the CP epithelium also synthesises large numbers of bioactive peptides (Redzic et al., 2005) such as adrenomodulin, endothelin-1 and vasopressin (Chodobski et al., 1997). The level of these peptides and proteins change during CNS disorders, supporting the evidence that the CP plays important role in the brain injury and repair process (http://alzheimers.org.uk/site/scripts/download_info.php?downloadID=1491, 2014, Happich et al., 2016).

Figure 1.4: The CP epithelial structure.

Microvilli structure on the CSF-facing region of the CP act to increase the surface area of the apical membrane of the choroid plexus epithelial cells. These cells also express a variety of drug efflux transporters (Siegel GJ et al., 1999).

The adult human brain weights approximately 1400 g whereas the CP tissue weighs only 2-3 g, however perfusion to the CP capillaries is 5 to 10 times greater than the mean blood flow (mL/min/g) to brain (Nolte, 1988, Thomsen et al., 2015, Wimo and Prince, 2010, 2015b). When considering that the total surface area of the CP may also be within the same order of magnitude as the BBB (Johanson et al., 2008a, Christy and Fishman, 1961, Pardridge, 1991, Blasberg et al., 1975, Tang et al., 2014), the importance of the CP infiltration of plasma across the choroidal capillaries (Johanson et al., 2008a) clearly is vitally important in helping to maintain and stabilise the fluid environment within the brain and CNS.

1.2.2.4. Barrier function of the BCSFB

The BCSFB is situated between the systemic circulation and the CSF and hence, acts to restrict the entry of xenobiotics into the CSF in addition to aiding in the removal of compounds from the CSF back into the systemic circulation (Redzic et al., 2005). This barrier function is imparted as a result of the network of tight junctions between the epithelial cells which regulate exchange of compounds between the blood and CSF (Ebada et al., 2011).

Furthermore, the surface area of the choroidal epithelial is significantly enhanced because of villi and microvilli structures projecting from the apical surface of the cells into the ventricle (Figure 1.4). This increases the surface area available for drug transfer and fluid secretion (Redzic and Segal, 2004).

1.3. Drug transport across the BBB and BCSFB

1.3.1. Transport pathways

Although a number of cellular factors govern the permeability of drugs across the BBB and BCSFB and include the expression of membrane transporters, transcytotic vesicles and the inherent barrier function formed by the endothelial/epithelial (Persidsky et al., 2006), the physicochemical properties of any compounds attempting to permeate across the BBB and BCSFB is also a driving factor in its ability to distribute into the CNS. The primary physicochemical factors governing molecular transport include lipophilicity and ionisation states, molecular size and the extent of plasma protein binding. In order for a drug molecule to diffuse across the BBB and BCSFB, passive transport is a common pathway and highly dependent upon the lipophilicity and molecular weight of the drug (Figure 1.5). Other drug molecules can often exploit energy-dependant carrier mediated transport pathways to enable drug transfer across concentrations gradients (Figure 1.5). On the other hand larger peptides/proteins can often exploit cell-surface receptors to enable transport across cell membranes in a process termed receptor-mediated transcytosis (Figure 1.5) (Norinder and Haeberlein, 2002).

The 'Rule of 5' of Lipinski states that poor drug absorption is more common if the molecular weight is > 500 Da, log P > 5 and more than 5 hydrogen bond donors and 10 hydrogen bond acceptors are present in a drug molecule (Lipinski, 2000). However in the case of drug delivery across the BBB and BCSFB, CNS –indicated drugs possess the above properties but Lipinski's role often do not apply as the majority of these drugs display limited measurable CNS uptake (Evans and Skalak, 1980).

Figure 1.5: A schematic representation of drug transport pathways across the BBB.

The primary pathways for drug transport across cellular barriers include passive transport, carrier-mediated transport, absorptive-mediated and receptor-mediated transcytosis(Norinder and Haeberlein, 2002).

The rate and extent of drug transport across the barriers are the two key factors, which govern their eventual delivery into the CNS. The permeability rate of a molecule at the BBB or BCSFB is reflected in the rate of drug entry to the CNS and processes which hinder the permeation of drugs across the barriers. Furthermore permeability rate may also inherently be hindered by poor physicochemical properties of the drug molecules. The extent of drug transport into the CNS is primarily a factor of the ability of the drug to partition into the CNS and is often related to fraction of drug which is not bound onto either plasma protein (free fraction in plasma) or within CNS tissues (e.g. free fraction in brain) (Figure 1.6) (Summerfield et al., 2007).

Figure 1.6: Schematic illustration of the equilibrium processes at the BBB and BCSFB. (Billiau et al., 1981)

Compartmentalisation of CNS barriers and factors governing the equilibrium of drug distribution within the CNS. Arrows indicate direction of transport.

1.3.2. Transporter proteins

Adenosine 5'- triphosphate binding cassette (ABC) transporter proteins form a major family of drug transporter proteins which play a significant role in hindering the tissue distribution of many drugs, particularly at CNS barrier (2015a, Kameremail et al., 2015, Nicolazzo and Katneni, 2009). The term 'ABC transporters' was introduced in 1992 (Higgins, 1992) and it is now known that 49 human ABC transporters exist (The Nutrition, Metabolism and Genomics Group, Wageningen University, Netherlands: http://nutrigene.4t.com/humanabc.htm) and are divided into several subclasses on the similarities between their nucleotide binding domains (NBD) (Table 1.1).

Table 1.1: List of important human ABC genes

Family	Alternative name	Transporters hindering drug transport
ABCA	ABC1	ABCA2
ABCB	MDR	ABCB1 (P-gp)
		ABCB4 (MDR2)
ABCC	MRP	ABCC1 (MRP1)
		ABCC2-6
		ABCC10
		ABCC11
ABCD	ALD	
ABCE	OABP	
ABCF	GCH20	
ABCG		ABCG2 (BCRP)

The ABC transporter family are one of the largest known transporter protein families and are widely distributed in all major tissues and in many different species (Schinkel and Jonker, 2012). ABC transporter proteins generally consist of a membrane-spanning region termed the trans-membrane domain (TMD) and a cytoplasmically located nucleotide-binding domain (NBD) (Figure 1.7). To function they require energy released from the hydrolysis of adenosine 5'-triphosphate (ATP), process which takes place within the NBD (Gupta et al., 2004) and which leads to the 'transport' process of molecules across cell membranes (Abbott, 2005, Nies et al., 2004).Typically, drug transporters are located apically or basolaterally at cell membranes and exhibit an influx (into the cell) or efflux (out of the cell) property.

Figure 1.7: A typical structure of ABC transporter

The structure of an ABC transport typically includes TMDs, which often contain 6 trans-membrane (TM) segments followed by a NBD, and the functional transporter is formed from a second repeating unit of TMD-NBD. 'Half transporters' are formed of one TMD and one NBD that, upon translation, combine to form a functional unit (Reginald A Kavishe et al., 2009).

Functionally active transporters are often formed from two linked monomer units (NBD-TMD-NBD-TMD) but can formed from multiple-monomer units combined in an intricate three and four-dimensional structure. Well-known example of ABC-transporters, which hinder the distribution drugs into tissues, includes breast cancer resistance protein (BCRP), P-glycoprotein (P-gp) and multidrug resistance protein (MRP).

1.3.3. Breast cancer resistance protein

BCRP is a member of the G-family of ATP-binding cassette. BCRP was first identified from human MCF-7 breast cancer cells and termed it as a breast cancer resistant protein (Doyle et al., 1998). At the same time another group described the role of this transporter in mitoxantrone resistance and termed it mitoxantrone resistance factor (MXR) (Miyake et al., 1999), with a third group (Allikmets et al., 1998) reporting its discovery in placental tissue and terming it called ABCP (Staud and Pavek, 2005). BCRP is composed of one single N-terminal intracellular NBD followed by six trans-membrane domain (Mao, 2005) and four N-glycosylation (Figure 1.8).

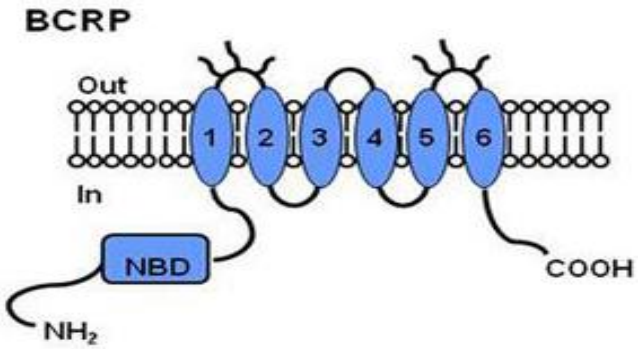

Figure 1.8: Breast cancer resistance protein structure

BCRP is known as a half transporters consisting of one nucleotide binding domain (NBD) and one trans-membrane binding domain (TMD), comprised of 6 trans-membrane spanning regions.

BCRP is often termed a half transporter and is thought to homodimerise through the formation of disulfide bridges in order to function (You and Morris, 2007). A study (Kage et al., 2002) confirmed that BCRP migrated as a 70 kDa band on a SDS-PAGE gel in the presence of reducing agent, but 140 kDa band in the absence of reducing agent suggesting BCRP could exist in the monomeric (70 kDa) and dimer (140 kDa) structure. However recent studies have suggested that BCRP may exist as higher order oligomers (Saito et al., 2006, Xu et al., 2004).The role of oligomerisation in BCRP is not clear yet but it has been suggested that the function of BCRP could be regulated by the dynamic association and dissociation of BCRP monomers by protein-protein interactions (Mo and Zhang, 2009).Therefore, prevention of oligomerisation or prevention of formation of higher active oligomers may be a future strategy to inhibit BCRP.

Chemotherapeutic agents were the first identified substrates for BCRP and it is now known that BCRP possess a diverse substrate specificity (Table 1.2) (Mao, 2005). BCRP confers resistant to a wide range of drugs and particularly anti-neoplastic agents such as topotecan, doxorubicin, mitoxanthrone, irinotecan, etoposide, methotrexate (MTX) and imatinib (Breedveld et al., 2004).

Table1.2: Substrates and inhibitors of BCRP

Substrates	Inhibitors
Drugs	**Drugs**
Mitoxantrone,Topotecan Doxorubicin,Epirubicin, Metoxantrate,Imatinib, Getfitinib,Ciprofloxacin, Erythromycin Folic Acid	Fumitremorgin C (FTC) KO143, GF120918, Digoxin,Dexamethasone, Cyclosporin A, Flavopiridol Novobiocin, Gefitnib
Dyes Pheophorbide a, Rhodamine 123, BODIPY Prazosin, Hoechst 33342, Lysotracker Green	
Natural compounds	**Natural compounds**
Genistein, Quercetin 17β-Estradiol Sulphate	Estrone, Chrysin, Biochanin A,Naringin Acastein,Genistein, Quercetin, 17β-Estradiol Sulphate

1.3.4. Expression and localisation of BCRP

BCRP has been reported to be expressed at the BBB in many species including mice, bovine and porcine origins) (Warren et al., 2009), where its function is thought to be a protective one in preventing the entry of drugs and xenobiotics into the brain biophase through its' inherent efflux transporter properties. Elsewhere, it has been reported to be expressed in the gut, blood-testis barrier (Bart et al., 2004), placenta (Doyle and Ross, 2003b) intestine and mammary glands (Jonker et al., 2005) of humans.

At the BBB, BCRP is located abluminally (Bendayan et al., 2006) and functions to transport xenobiotics in a brain-to-blood direction. However, at the BCSFB, BCRP is located luminally and results in transfer of drugs into the CSF from the brain biophase or blood (Figure 1.9). The high expression of BCRP in key sanctuary sites such as the small intestine, breast, liver, kidney, blood brain barrier and placenta confirms its important role in controlling the distribution of drugs into the most tissues.

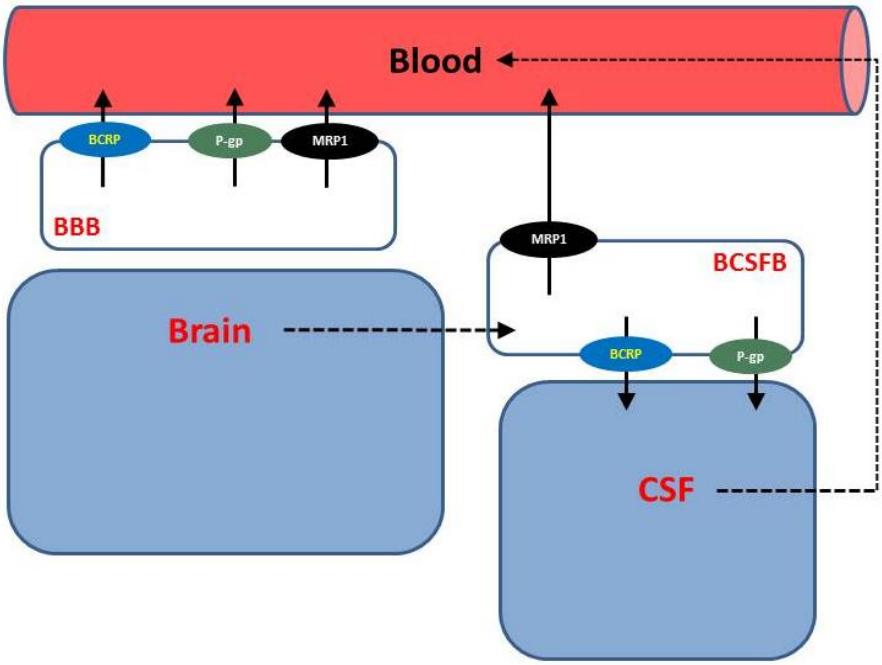

Figure 1.9: Localisation of drug transporters at the BBB and BCSFB.

At the BBB, the ABC transporters such as BCRP located abluminally (blood side), whereas at the BCSFB BCRP is expressed at the luminal side (brain side). The dashed lines represent bulk fluid flow (brain to BCSFB is the bulk flow of ISF and CSF to blood is CSF drainage) (solid arrows represent direction of transport).

The absolute protein expression of transporter proteins has recently been reported using quantitative proteomics approaches at the BBB and BCSFB (Lee et al., 2003) from human brain capillaries using liquid chromatography-tandem mass spectrometric quantification method (Esser, 2009). BCRP protein expression was reported to be 8.14 fmol/µg protein, and is higher than another well characterised drug efflux transporter protein, P-gp (6.06 fmol/µg protein), reinforcing the importance of BCRP. Furthermore, in monkeys the protein expression of BCRP has been reported to be 12.5-16.2 (fmol/µg protein) compared to P-gp: (6.49-2.65 fmol/µg protein) (Caldwell and Yan, 2013). In mice, BCRP was found to be expressed 1.85-fold greater than P-gp in mice (Lee et al., 2003) and in a further human study from freshly isolated human brain capillary

endothelial cells, BCRP expression was 1.6-fold higher than that of P-gp (Dauchy et al., 2008b).

Similarly, the absolute protein quantification of transporters at the choroid plexus was investigated in the isolated rat and human choroid plexus plasma membrane fractions. It was reported that the levels of BCRP in humans were 6.56- and 2.12-fold greater than those of mdr1a (P-gp) and Bcrp in rat, respectively (Uchida et al., 2015).

1.4. The role of BCRP in health and disease

BCRP is widely expressed in tissues and cells and plays important role in tissue and cellular protection. BCRP protects normal tissues such as the placenta, hepatocytes, intestinal mucosal and brain by eliminating xenobiotics and toxic compounds (Doyle and Ross, 2003a). Its role at the BBB has recently been elucidated using positron emission tomography (PET) and single photon emission computed tomography (SPECT), powerful nuclear imagining techniques. A PET method has been developed to investigate the BCRP function at the BBB in a BCRP wild-type and knockout mouse model (Takashima et al., 2013). In their study [^{11}C] tariquidar, a BCRP (Pohl et al., 2006) substrate, was used to assess the BCRP function by PET and it was demonstrated that knockdown of BCRP resulted in significantly increased signal intensity in the brain compared to wild-type mice.

BCRP also imparts a protective role from relatively toxic molecules. Heterocyclic amines and polycyclic aromatic hydrocarbons (a group of chemical components formed while cooking or barbecue food (meat) at high temperatures) (Ebert et al., 2005) in addition to protoporphyrin IX (a metabolic product of δ-aminolevulinic acid) and hematoporphyrin (a sonosensitizers) (Krishnamurthy et al., 2004) are common substrates for BCRP. Furthermore, BCRP also play important role in the control of and transport of folic acid (water soluble vitamins which plays important role in growth, differentiation and homeostasis) and it's conjugates (Volk and Schneider, 2003).

Other endogenous substrates include steroids such as estrone and estradiol (Imai et al., 2003). Estrone is hormone associated with the female reproductive functions and estradiol is a female sex hormone produced by the ovaries. Moreover, BCRP function in the elimination of uric acid was discovered in proximal tubular cells (Woodward et al., 2009). BCRP has also been implicated in limiting the progression of Alzheimer's disease (AD) because of the neurotoxic β-amyloid peptides being substrates for BCRP (Zhang et al., 2004b) (Zhao et al., 2010). Furthermore, BCRP genomic and protein

expression was found to be increased in AD brain (Zhao et al., 2010) (Xiong et al., 2009) highlighting the important role BCRP plays in brain protection for age associated CNS disorders.

BCRP has also been implicated in disease states, particularly in relation to tumour cells and the associated multi-drug resistance phenomena, whereby BCRP is overexpressed because of exposure to antineoplastic agents. In cell culture systems, the multi drug resistance cell lines MCF-7 (myeloma 8226 and colon carcinoma cell line) shows resistance to BCRP substrates such as mitoxantrone, topotecan, flavopiridol and doxorubicin with an associated overexpression of BCRP mRNA (Zhao et al., 2013, Novotna et al., 2014).

1.5. Other CNS drug transporter proteins

1.5.1. P-glycoprotein (P-gp)

P-glycoprotein (P-gp) was one of the first efflux transporter proteins discovered in 1976 (Juliano and Ling, 1976). P-gp was found to be highly expressed in Chinese hamster ovarian cells when discovered, and was resistance to a wide variety of amphiphilic drugs (Juliano and Ling, 1976). P-gp has an apparent molecular weight of 170 kDa (Löscher and Potschka, 2005) and a member of the P-gp family are found in humans (ABCB1) with and three members identified in mice (mdr1a, mdr1b and mdr2) (Gottesman and Pastan, 1993). P-gp exhibits a high nucleotide sequence homology to other members of the B-subfamily (Cornford et al., 1997). The primary role of P-gp is similar to that of BCRP, to protect tissue from toxic compounds through efflux transport processes. It is highly expressed at the luminal membrane of endothelial cells forming the blood–brain and blood–testis barriers (Schinkel, 1999, Cordon-Cardo et al., 1989, Dohrmann, 1970a, Melaine et al., 2002), blood-mammary barrier (Edwards et al., 2005) and the maternal–fetal barrier of the placenta (Gil et al., 2005).

1.5.2. Multidrug resistance protein (MRP)

Multidrug resistance protein (MRP) was first discovered in 1992 in human small cell lung carcinoma cell line H69AR (Cole et al., 1992). The MRP family of transporter proteins (ABCC1-6, 10-11), together with the ATP-gated chloride channel, CFTR (ABCC7), and the ATP-dependent sulfonylurea receptors, SURs (ABCC8, 9), comprise the ‘C’ branch of the ABC superfamily (Table 1.1). There is also an overlap with the substrate specificity of MRP1 and P-gp. MRP1 transports a large number of drugs

including antineoplastic or therapeutic agents, including folate-based antimetabolites, anthracyclines, vinca-alkaloids, antiandrogens, and numerous glutathione (GSH)- and glucuronide conjugates of these compounds as well as organic anions and heavy metals (Deeley and Cole, 2006). Transport of several compounds by MRP1 depends on the presence of reduced glutathione (GSH). This has been confirmed by using MRP1 overexpressing cell lines, where in the presence of transport inhibitor (probenecid), decreased GSH release and increased drug accumulation (Versantvoort et al., 1995). MRP transports organic molecules and confer resistance to a wide variety of drugs.

1.6. Current approaches to assess drug delivery across the BBB/BCSFB

Currently there are no *ex-vivo* models, which can mimic the function of the BBB or BCSFB to study the transport of drugs. However, a number of surrogate *in-vitro*, *in-vivo* and *in-silico* models exists to support the development of approaches to mechanistically understand and predict how drug molecules are able to cross the BBB and BCSFB. Core to the development of such models is the requirement that they should include aspects of the expression of tight junctional proteins (Roberts et al., 2008) along with the distribution and functional expression of efflux transporters such as P-gp, BCRP and MRPs (Miller, 2010, Kusuhara and Sugiyama, 2005, Naik and Cucullo, 2012), which are vitally important in controlling the rate and extent drug distribution into the CNS.

1.6.1. *In-vitro* models

1.6.1.1. Non-cerebral cell lines

A large number of studies reporting the use of different types of epithelial cells or endothelial cells of non-cerebral origin for the study of different aspects of BBB and BCSFB function have been reported and include Madin-Darby canine kidney (MDCK) cells (Wang et al., 2005) (Nazer et al., 2008) and human umbilical endothelial cells (HUVECs) (Langford et al., 2005). The use of these cell lines as a BBB models is limited because of their non-cerebral origin, although they are useful for screening for drug transporter substrates.

1.6.1.2. Rodent origin cell lines

Rat brain endothelial (RBE) cell lines have been established and characterised by Roux et al (Roux et al., 1994) to develop an *in-vitro* BBB model. RBE cells express most of the enzymes and transporters that are considered as specific for the blood-brain endothelium. Other rat origin cell lines include GP8, GPNT. The bEND.3-5 cells are murine origin and have been widely used for the signalling (Stins et al., 2001), permeability and drug uptake studies (Prudhomme et al., 1996, Eigenmann et al., 2013). Other mouse origin brain cell lines include cEND and bEND3, and have been widely used to study brain drug transport (Franke et al., 2000, 1991b, 1991a).

Z310 (Zheng and Zhao, 2002) and TR-CSFB (Kitazawa et al., 2001) cell lines are immortalised in nature and obtained from rat CP tissues. They have been established and characterised for drug transporter expression, TJs proteins and drug transport (Juliane Kläs et al., 2010, Szmydynger-Chodobska et al., 2007), in an attempt to mimic the BCSFB. The choroid plexus cell lines such as TR-CSFB shows low TEER values, requires growth at lower temperatures, and have been less widely characterised (Juliane Kläs et al., 2010, Kitazawa et al., 2001). The CP epithelial cells form leaky barriers (TEER value of 150-200Ω.cm^2) compared to BBB cell systems (Hakvoort et al., 1998, Baehr et al., 2006) and monolayer formation and resistances are greater for Z310 cells (~140 Ω.cm^2) (Kitazawa et al., 2001) compared with TR-CSF cells (90 Ω.cm^2) (Hosoya et al., 2004). Furhermore, the Z310 cell lline has previoulsy been demonstrated to expression BCRP (Halwachs et al., 2011, Kaur and Badhan, 2015).

1.6.1.3. Bovine origin cell lines

Bovine brain endothelial cells have been widely used to develop an *in-vitro* BBB model, and cell monolayers typically give resistance values in the range of 160-200 Ω.cm^2 (Zhang et al., 2004b, Zhao et al., 2010). Bovine immortalised cell lines include t-BBEC-117(Allen et al., 2002a), SV-BEC (Stephen Porter et al., 1977) and BBEC-SV (Frixione, 2006). Additionally, primary bovine blood brain barrier cell models have been used to study BBB properties and drug transport (Spector et al., 2015, Lindsey and Papoutsakis, 2012, Tan et al., 2010), but as a novel BBB model, are often restricted in use due to the historical risk of Creutzfeldt-Jakob disease infections in brain tissues.

1.6.1.4. Porcine origin cell lines

The most widely used immortalised porcine BBB model is the PBMEC/C1-2 cell line (Teifel and Friedl, 1996). The presence of tight junctions gives a relatively high monolayer resistance of 250–300 Ωcm^2, and it has been well characterised for drug permeation and drug transporter protein studies (Lauer et al., 2004, Neuhaus et al., 2010, Neuhaus et al., 2012). Primary cultured porcine brain microvascular endothelial cells (PBMECs) have recently increased in use, having been first developed (Ulrike Tontsch and Bauer, 1989) and subsequently modified by Patabendige et al (Patabendige et al., 2013). Such cellular models give robust monolayer with high TEER values in excess of 800 $\Omega.cm^2$. Furthermore, the expression of endothelial brain cell markers and drug transporter proteins has been extensively studied using these cells (Skinner et al., 2009, Cohen-Kashi-Malina et al., 2012, Patabendige et al., 2013).

1.6.1.5. Human original cell lines

Due to the restricted availability of human brain tissues for the isolation of primary human brain endothelial cells, the development of a reliable immortalised human brain cerebral endothelial cell line was fulfilled in the hCMEC/D3 (Weksler et al., 2005) which has been shown to retain important BBB characteristics and which has been extensively studied for the expression of junctional proteins (Cohen-Kashi-Malina et al., 2012), drug transporters such as BCRP (Dauchy et al., 2009, Skinner et al., 2009), neurosignalling (Hammarlund-Udenaes, 2000, Xie and Hammarlund-Udenaes, 1998, Thomsen et al., 2015) and drug transport studies (Wimo and Prince, 2010). Other conditionally immortalised human brain microvascular endothelial cell lines include TY08 (2015b), hBMEC (Stins et al., 2001) and BB-19 (Prudhomme et al., 1996) and have been characterised for the markers of brain endothelial cells and expression of drug transporters. A comparative study between the four cell lines confirmed that hBMEC is the most suitable human cell line to develop an *in-vitro* BBB model (Eigenmann et al., 2013).

Only one human chorodial epithelial immortalised cell culture model has been developed, and is derived from choroid plexus papilloma cells (HIBCPP) (Ishiwata et al., 2005). The use of HIBCPP is limited due the lack of morphological characteristics of epithelial cells (cells differ in size and do not display cobblestone like appearance) and difference in protein expression and metabolism (due to isolation from anaplastic choroid plexus rather than a normal human) (Schwerk et al., 2012). Furthermore, HIBCPP cells have not been recommended to be used after more than 30 passages

and hence may limit studies. HIBCPP cells have tendency to grow in multiple layers, a careful consideration of seeding density and trypsinisation is required to obtain a monolayer (Ishiwata et al., 2005).

1.6.2. *In-silico* models

As a result of the variability in available *in-vitro* cellular models and the limited use of *in-vivo* models to assess CNS drug delivery, *in-silico* approaches such as pharmacokinetic modelling and simulations, have often been used to collate a range of different *in-vitro* data (e.g. physicochemical, metabolic and permeability) generated to describe the pharmacokinetics of a drug to be able to predict both brain and CSF temporal drug concentrations (Ball et al., 2012, Badhan et al., 2014).

1.6.3. *In-vivo* models

To been able to predict and assess distribution of drugs *in-vivo*, the brain slice method is precise and robust technique to measure the uptake of drugs into the brain tissues by determining unbound drug concentration in *ex-vivo* brain sections. Further the temporal concentration of drugs can also be measured directly by micro dialysis techniques (Hammarlund-Udenaes, 2000). This involves the insertion of a probe into the tissue or fluid and multiple regional brain sampling from the same animal can be achieved. This technique has been used in the pre-clinical studies (Xie and Hammarlund-Udenaes, 1998, Zhang et al., 2015, Wei et al., 2015, Kitamura et al., 2015, Chiang et al., 2015). However, poor recovery of lipophilic compounds, low throughput and local tissue damage at the site of probe insertion limit its use in drug discovery (Hammarlund-Udenaes, 2000).

Another widely used technique is that of *in-situ* brain perfusion, which allows the quantitative measurement of brain uptake of solutes by perfusion of saline or blood to the right external carotid artery and been commonly applied to a wide variety of drugs (Zhao et al., 2009b, Youdim et al., 2004, Tournier et al., 2015, Suzuki et al., 2015, Cisternino et al., 2001, Alata et al., 2014).

In-vivo molecular imaging approaches such PET has also been widely used to investigate BCRP function at the BBB in a BCRP wild-type and knockout mouse model (Takashima et al., 2013) for a range of radiolabelled compounds including [^{11}C] tariquidar, [^{125}I]-or [^{3}H]-Aβ peptides (Zhang et al., 2013), [^{11}C] sorafenib (Asakawa et

al., 2011) , [^{11}C] XR9576(Kawamura et al., 2010) and [^{11}C] elacridar (Bankstahl et al., 2013).

1.7. The regulation of BCRP at the BBB and BCSFB

The transcriptional regulation of BCRP at both the BBB and BCSFB, as with many ABC transporters, is thought to be governed by a range of nuclear hormone receptors (Wang and Negishi, 2003, Xu et al., 2005) and the interference of these signalling pathways under physiological and pathophysiological conditions provides a new approach to modulate BCRP function at the CNS barrier (Mahringer and Fricker, 2010, Hartz and Bauer, 2011, Bauer et al., 2006). Many members of the nuclear receptor superfamily are known to regulate drug transporters includes the pregnane-X-receptor (PXR), the constitutive androstane receptor (CAR) and the aryl hydrocarbon receptor (AhR) (Jacob et al., 2011, Xu et al., 2005, Dauchy et al., 2008a, Granberg et al., 2003) (Table 1.3). The regulation of many of the transporter proteins is controlled by endogenous and exogenous compounds which act to activate the receptors and subsequently leads to changes in transporter gene expression.

Table 1.3: Regulation of drug transporters by nuclear hormone receptors

Nuclear receptor	Drug transporters
PXR	P-gp (Bauer et al., 2004, Narang et al., 2008a, Ott et al., 2009, Chan et al., 2011), **BCRP** and Mrp2 (Narang et al., 2008a)
GR	P-gp and **BCRP**(Narang et al., 2008a)
CAR	P-gp, Mrp2 (Narang et al., 2008a, Wang et al., 2010),**BCRP**(Lemmen et al., 2013)
PPARα	**BCRP** (Hoque et al., 2012)
ER	**BCRP**(Hartz et al., 2010, Mahringer and Fricker, 2010, Imai et al., 2005b, Wang et al., 2006, Wang et al., 2008b)
AhR	P-gp, **BCRP** and Mrp2 (Wang et al., 2011, Fernandez-Salguero et al., 1996, Guo et al., 2000, Tompkins et al., 2010).

PXR is a xenobiotic-activated nuclear transcription factor which translocates from the cytoplasm to the nucleus following ligand binding, leading to transcriptional activation of a range of drug metabolising enzymes and transporter proteins (Geick et al., 2001a, Kast et al., 2002, Xu et al., 2005). A large number of endogenous and exogenous compounds can activate PXR and include St.John's wort, bile acids, steroids and antibiotics (di Masi et al., 2009, Mahringer et al., 2011, Chang, 2009). PXR has been found to be expressed in rat brain capillaries (Bauer et al., 2004) and regulates phase-I metabolising enzymes such as CYP3A4, CYP2B6, CYP2Cs, and CYP7A and phase-II metabolising enzymes such as sulfotransferases (SULTs), glutathione *S*-transferases (GSTs) and UDP-glucuronosyltransferases (UGTs) (Wang and LeCluyse, 2003, Geick et al., 2001b). PXR also regulates the expression of ABC drug transporters such as P-gp (Bauer et al., 2004, Geick et al., 2001b), Mrp2 (Bauer et al., 2008a, Johnson et al., 2002) and Mrp3 (Teng et al., 2003). Pregnenolone 16α-carbonitrile (PCN) and dexamethasone, both ligands for rodent PXR increased the expression of P-gp, Mrp1 and BCRP in the rodent brain capillaries (Bauer et al., 2006, Narang et al., 2008b, Bauer et al., 2004).

CAR functions in the similar way as PXR and demonstrating an overlapping ligand profile as PXR (Moore et al., 2003). Typical ligands for CAR includes bile acids, environmental pollutants and therapeutic drugs (Stanley et al., 2006). Wang et al (Wang et al., 2010) identified the expression of CAR in rat and mouse brain capillaries and demonstrating that it plays a role in regulation of ABC transporters.

Cyclooxygenase-2 (COX-2) is an enzyme involved in the production of prostanoids and a key enzyme involved in the development of inflammatory responses. The role of COX-2 in the regulation of drug transporters proteins have been demonstrated in a number of studies. Bauer et al (Bauer et al., 2008b) reported that the expression of P-gp was increased in isolated rat brain capillaries when exposed to glutamate and that P-gp expression was attenuated by using an NMDA receptor antagonist and COX-2 inhibitors. The study suggested that the inhibition of COX-2 can enhance the uptake of antiepileptic drugs (Bauer et al., 2008b). This study was further supported by Schlichtiger et al (Schlichtiger et al., 2010), where exposure to celecoxib, a COX-2 inhibitor, significantly reduced the occurrence of seizures in a phenobarbital-resistant epilepsy rat model. In a further study by Yousif et al (Yousif et al., 2012), the expression of BCRP and P-gp was increased after exposure to morphine in rat brain vessels. This up-regulation was reversed in the presence of MK-801 (NMDA antagonist) and

meloxicam (COX-2 inhibitor), suggesting the role of NMDA and COX-2 in regulation of BCRP and P-gp in the rat brain.

The regulation of drug transporter proteins at CNS barriers (primarily the BBB) has been limited, and regulation has largely been demonstrated for a limited range of transporters by nuclear receptors such as PXR, CAR, Estrogen receptor (ER) and AhR (Bauer et al., 2004, Bauer et al., 2006, Hartz et al., 2010).

The regulation of BCRP has largely been under-researched and is currently not well characterised. In the 5'-flanking section of the gene promoter region of BCRP a novel estrogen responsive element (ERE) is present and it is thought that transcriptional regulation of BCRP may involve the activation and binding of 17-β-estradiol (E2) within an estrogen receptor (ER) complex (Ee et al., 2004a). Hormonal regulation of BCRP by progesterone and testosterone was further identified and studied in human placental BeWo cells. These studies confirmed that progesterone and testosterone increased, whereas E2 decreased, the mRNA and protein expression of BCRP in human placental BeWo cells (Wang et al., 2008b, Wang et al., 2006). Other studies have also demonstrated that E2 plays a significant role in down regulating BCRP expression in brain capillaries (Hartz et al., 2010) (Mahringer and Fricker, 2010).

Cytokines such as tumour necrosis factor-α (TNF-α) and interleukin-1β (IL-1β) have also been shown to down-regulate BCRP mRNA expression in primary porcine brain endothelial cells (von Wedel-Parlow et al., 2009) human hCMEC/D3 cells (Poller et al., 2010).

1.8. Regulation of BCRP by the Aryl Hydrocarbon Receptor

The aryl hydrocarbon receptor (AhR) has been reported to be highly expressed in the kidney, liver, whole brain, brain microvessels and the choroid plexus (Dauchy et al., 2008a, Jacob et al., 2011) (Dauchy et al., 2008a, Dauchy et al., 2009, Kainu et al., 1995). The prototypical ligand for the induction of AhR activity are dioxins such as the 2,3,7,8-tetrachlorodibenzo-p-dioxin (TCDD) and induction of AhR activity by TCDD was first studied in hepatic cells (Poland et al., 1976). The majority of the genes known to be regulated by AhR are involved in xenobiotic metabolism and include CYP1A1, CYP1A2 and CYP1B1 (Nebert et al., 1993) (Nebert et al., 2000).

1.8.1. Structure and function of AhR

AhR is a member of the bHLH-PAS family of DNA-binding proteins. The bHLH domain is a specific DNA binding domain and the HLH region interacts with cellular proteins such as the AhR nuclear translocator (ARNT) and chaperone proteins such as the heat shock protein 90 (HSP90) (Figure 1.10).

The PER-ARNT-SIM (PAS) signalling domain plays an important role in controlling a conformational change in the structure of the AhR complex upon ligand binding (Fukunaga et al., 1995, Hoffman et al., 1991).

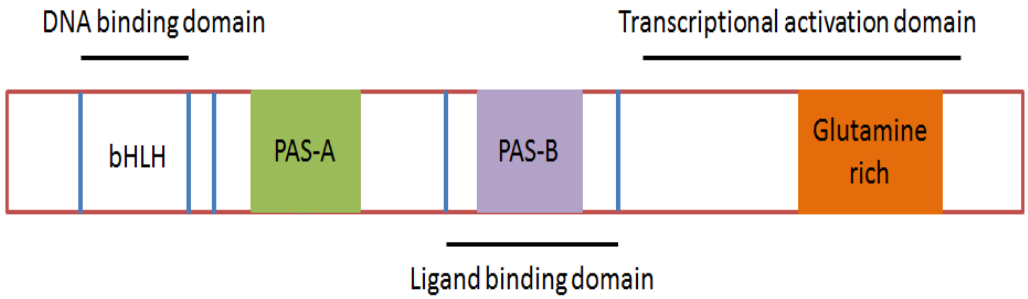

Figure 1.10: Schematic representation of the AhR domain.

The bHLH motif is present at the N-terminal and facilitates the binding of transcription factor to DNA. PAS acts as a ligand binding domain and the C-terminal region consists of transcriptional activation domain.

AhR is located in the cytoplasm and agonist binding at the PAS domain leads to a conformational change in the receptor (Wilhelmsson et al., 1990). This conformational change alters its binding with chaperones and as a result of this, the receptor complex migrates into the nucleus (Ikuta et al., 1998, Ikuta et al., 2000). Within the nucleus of the cell, AhR then undergoes heterodimerisation with another bHLH-PAS protein ARNT (T et al., 1998, Reyes et al., 1992). The AHR/ARNT heterodimer complex then interacts with the responsive elements of the target genes and leads to activation of target genes expression. When in the nucleus of the cell, AhR dissociate from its chaperones and the resulting AhR translocate to the cytoplasm where it can be degraded by proteasomes, a process that can be inhibited when using proteasome inhibitors such MG-132 (Davarinos and Pollenz, 1999).

At the BBB, AhR regulates the expression of drug metabolising enzymes such as CYP1A1 and CYP1B1 and ABC transporters (Granberg et al., 2003, Dauchy et al., 2008a). Guo et al (Guo et al., 2000) treated MCF10A-Neo cells (transfected human breast cancer epithelium cell) with the AhR ligand TCDD and found the transcriptional activation of CYP1A1. Jacob et al (Jacob et al., 2011) examined rat brain microvessels after exposure to a range of AhR ligands such as TCDD, Δ^9-tetrahydrocannabinol (Δ^9-THC) and diesel exhaust particles. It was reported that AhR activation mediated the up-regulation of CYP1A1 gene and protein after exposure, which was capable of being reversed using the AhR antagonist CH-223191.

Whilst most studies have focused on the role of AhR in regulating the expression of xenobiotic metabolism pathways (e.g. CYP isozymes), a few studies have demonstrated the role AhR plays in regulating BCRP expression. 3-methylcholanthrene (3MC) is a known AhR agonists and has shown to activate estrogen receptor-α (Abdelrahim et al., 2006). Tompkins et al (Tompkins et al., 2010) demonstrated AhR mediated an 80-fold induction of BCRP in LS174T cells when exposed to 3MC, which was reduced by 65% in AhR knockdown cells (Tompkins et al., 2010). Wang et al (Wang et al., 2011) demonstrated that TCDD up-regulated the expression and transporter activity of BCRP in rat brain capillaries. In a further study by Campos et al (Campos et al., 2012), exposure of TCDD to rat spinal cord capillaries increased protein expression of BCRP.

AhR is therefore an important regulatory element in controlling the homeostatic balance of xenobiotic transporter/clearance pathways, but is also a potentially important target for modulating the expression of drug transporter proteins such as BCRP at the BBB and BCSFB, with a view to enhancing the delivery of therapeutic agents into the CNS. This is particularly important when considering the poor progress made in the clinical translation of BCRP inhibitors, which have demonstrated *in-vitro* inhibition of BCRP. First generation inhibitors of BCRP such as cyclosporine A and verapamil showed limited clinical efficacy in trials due to significant toxicity and interaction with drug metabolising enzymes cytochrome P450 3A (CYP3A) (Suzuki and Sugiyama, 2000). Second generation inhibitors such as topotecan, irinotecan and SN-38 are analogous of first generation inhibitors and also possess both cellular toxicity and an ability to mediate drug–drug interactions at the level of phase-I metabolic enzymes. Third generation inhibitors represent molecules that have been recently developed and

include fungal toxins such as fumitremorgin-C and Ko143, but their use is limited due to severe neurotoxicity (Nutton, 1973, Allen et al., 2002a) (Allen et al., 2002b).

Whilst the activity of many inhibitors of BCRP is positive, their toxicity often precludes clinical progression. Therefore there is a need to identity and develop newer inhibitors or modulators of both drug transporters and their regulatory elements to enable a broad approach to the modulation of the transport function at CNS barriers. One potential novel group of candidate compound which are often perceived as being 'safe' are natural product derived phytochemicals, typically flavonoids, which have demonstrated an ability to modulate the expression and function of xenobiotic clearance pathways (Frixione, 2006, Spector et al., 2015, Lindsey and Papoutsakis, 2012, Tan et al., 2010). Flavonoids are a class of polyphenolic compounds that are found in fruits, vegetables and wine. Previous reports demonstrated that flavonoids belonging to the subclasses of flavones, flavonols, flavanones and catechins are able to act directly as AhR antagonists (Ashida et al., 2000, Ciolino et al., 1998a, Nishiumi et al., 2007b) and hence may present as a viable group of candidate molecules with which to exploit the modulation of target gene activity, i.e. BCRP in the CNS, as a novel mechanisms to reverse the barrier function BCRP provides to drug entry into the brain and wider CNS.

1.8.2. Structure of flavonoids

Over 6500 compounds has been identified as belonging to the general category of 'flavonoids' (Morris and Zhang, 2006). Flavonoids consists a backbone of two aromatic rings (A and C ring) and a heterocyclic benzene ring (B ring) (Figure 1.11). Flavonoids are divided into several sub-groups based on the position of the substitution group (R_x) attached and level of oxidation (Middleton Jr, 1998). The main subclasses includes: flavones (e.g. flavone), flavonols (e.g. quercetin, fistein), flavonones (e.g. flavanone, hesperetin and naringin), flavanonol (e.g. taxifolin), isoflavones (e.g. genistein, daidzein), flavan-3-ols (e.g. catechin , epicatechin) (Narayana et al., 2001).

Figure 1.11: The structure of flavonoid.

Flavonids consist of two aromatic rings (A and B) linked through three carbons that usually form a heterocyclic ring (C). Based on the pattern of hydroxylation and substitution (R_x), there are 7 subclasses of flavonoids.

1.8.3. Systemic absorption and permeation of the BBB and BCSFB

The dietary ingestion of flavonoids results in the exposure of the gastrointestinal system to the glycoside conjugate form of the flavonoids, which often possess limited absorption into the systemic circulation (Donovan et al., 2006). Within the stomach and small-intestine, these glyosidic forms come into contact with lactase phloridzin hydrolase (LPH), which results in an aglycone form of the flavonoids which is then absorbed by passive diffusion (Day et al., 2000). When passing through the small-intestine and liver, the aglycone form of most flavonoids are then exposed to metabolic pathways resulting in the final form found in the circulation being the sulfate, glucuronide and/or methylated metabolites as a result of the action of sulfotransferases (SULT), uridine-5′-diphosphate glucuronosyltransferases (UGTs) and catechol-*O*-methyltransferases (COMT) (Donovan et al., 2006). It is therefore unlikely that the conjugated form of the flavonoids would naturally be capable of crossing the BCSFB or BBB.

The ability of flavonoids to cross both the BBB and BCSFB and reach the brain/CNS biophase has been investigated. In cell culture systems the permeability of naringenin and hesperetin (30 μM) have been demonstrated in two brain endothelial cell lines (mouse b.END5 and rat RBE4) and an *in-vitro* model of the BBB (ECV304 cells co-cultured with C6 glioma cells) (Youdim et al., 2003). Furthermore the aglycone form of flavonoids demonstrated a significantly greater penetration across the BBB compared to the conjugated form [aglycone: naringenin (P_{app}=350 nm/s) and hesperetin (P_{app} =

290 nm/s); conjugated (P_{app} = 113-182 nm/s)] (Youdim et al., 2003). In an *in-situ* rat brain perfusion model the aglycone form of [^{3}H]-naringenin was detected in most brains regions (Youdim et al., 2004). *In-vivo* studies in rats have demonstrated that kaempferol and isorhamnetin were detected in brain tissues (293 ng/g brain) and high concentrations of quercetin detected in the hippocampus, stratum and cerebellum, with levels exceed 1000 ng/g protein, following the administration of a standard extract of *Ginkgo biloba* (extract EGb761) given to rats at a single dose of 600mg/kg (Rangel-Ordonez et al., 2010). Furthermore Peng et al (Peng et al., 1998) demonstrated that the aglycone form of naringenin was detected in the cerebral cortex of rats following an IV bolus dose.

1.8.4. Flavonoids as modulators of BCRP efflux function

As a result of their ability to penetrate the BBB and BCSFB, flavonoids have also been shown to act directly upon BCRP. Quercetin, genistein and 17-β-estradiol were able to prevent the efflux of the BCRP substrate mitoxantrone in MCF-7 cells with limited accumulation in BCRP knockdown cells (Zhang and Morris, 2003). In another study, the effects of flavonoids on mitoxantrone accumulation in both MCF-7 MX100 and NCI-H460 MX20 cells were investigated for apigenin, biochanin A, chrysin, genistein and kaempferol and which all demonstrated high BCRP inhibition activity and significantly increased mitoxantrone accumulation (Zhang and Morris, 2003). In a robust screening study 20 out of 33 flavonoids screened in K562/BCRP possessed BCRP inhibition properties, with 3',4',7-trimethoxyflavone showing the strongest inhibition (Katayama et al., 2007). In a recently study a number of grape-fruit juice constituents (bergamottin, 6′,7′-dihydroxybergamottin (DHB), quercetin, and kaempferol), orange juice constituents (tangeretin and nobiletin) and apple juice constituents (hesperetin) greatly inhibited BCRP-mediated dasatinib efflux at the concentration of 50 μM ($p < 0.001$) (Fleisher et al., 2015). In another study, the role of phytochemicals such as quercetin, epicatechin, chrysin, genistein, curcumin, resveratrol and flavone on their ability to modulate BCRP gene expression was investigated (Ebert et al., 2007).

1.8.5. Flavonoids as modulators of AhR function

Only a few studies have previously been reported demonstrating the agonist/antagonism of AhR regulatory functions by flavonoids (Mukai et al., 2010, Ashida et al., 2000, Nishiumi et al., 2007a, Ciolino et al., 1998b) with the ability to

modulate AhR function being concentration dependent (Nishiumi et al., 2007a, Ciolino et al., 1998b). At concentrations of 10 μM apigenin and kaempferol have been shown to suppress the transformation of AhR by hindering the dissociation of HSP90 and and hepatitis-B virus X-associated protein 2 (XAP2), which are important complexes formed during the functional role of AhR. Apigenin and kaempferol suppress the dissociation of these proteins in Hepa-1c1c7 and hence antagonise the function of AhR (Mukai et al., 2010). In HepG2 cells, quercetin (25 μg/mL) and kaempferol (20 μg/mL) demonstrated activation of AhR (Li et al., 2009). Resveratrol (0.5-20 μM) has shown to inhibit CYP1A1 expression by preventing the binding of AhR to the promoter sequences which induces CYP1A1 transcription (Ciolino et al., 1998b).

1.9. Novel approaches to modulating BCRP function at the CNS barriers

BCRP expression and function at the BBB and BCSFB has been studied in a number of cellular and *in-vivo* systems, with a large body of research supporting the view that BCRP is a vital transporter and gatekeeper directly affecting the pharmacokinetics of drug delivery to the CNS. Existing approaches to modulate its activity, to overcome its efflux properties and thereby enhancing delivery of therapeutic agents into the CNS shows promise *in-vitro*, but there is paucity in the clinical translation of such inhibitors.

It is also clear that the regulation of BCRP is highly controlled by nuclear hormone receptors, and a clear relationship between the expression of BCRP and AhR has recently been identified and reported by Tan et al (Tan et al., 2010). In an attempt to identify new and novel candidates that can modulate the activity and function of BCRP, phytochemicals are of increasing interest due to their relatively large dietary intake and apparent lack of associated cytotoxicity. Furthermore, clear evidence is now available demonstrating the ability of phytoestrogens such as flavonoids to both directly inhibits the function of BCRP and to modulate the activity of AhR.

When considering the fact that many of these flavonoids are capable of crossing the BBB (and potential therefor the BCSFB), phytoestrogens/flavonoids are potentially viable novel leads for modulating BCRP expression and function at the BBB and BCSFB to enhance CNS drug delivery.

1.10. Aims and Objectives

The overall aim of the thesis was examining the approaches that can modulate the expression of BCRP at the BBB and BCSFB with the phytochemicals using *in-vitro* porcine and rat cell culture models respectively. Furthermore, the work also investigated the AhR mediated transcriptional regulation of BCRP at the BBB and BCSFB.

To achieve the aims the overall objectives were:

- To demonstrate the expression of BCRP in PBMEC/C1-2 and Z310 cells
- Evaluate the cytotoxicity profile of phytochemicals for BBB and BCSFB *in-vitro* cell culture models
- Investigate the modulation of genomic, protein and transport expression of BCRP in the cell culture models
- Evaluate the modulation of BCRP and AhR following phytochemical exposure
- Silencing AhR gene to investigate the AhR mediated modulation of BCRP gene

Chapter 2

Assessment of the interactions of phytochemicals on BCRP expression and function at the porcine blood brain barrier

2.1. Introduction

Microvascular brain endothelial cells act as a primary physical and cellular barrier to the delivery of drugs and therapeutic agents into the brain and wider CNS. These cells are formed into an intricate network of cerebral capillaries and, at a cellular level, are held tightly together by tight junctional proteins to form the blood-brain barrier. A range of *in-vitro* models are commonly used to assess the extent to which new therapeutic entities are able to permeate the BBB, and a primary goal of many of these models is to assess the potential impact of membrane localised drug transporter proteins, such as BCRP, on controlling the permeation of drugs across the BBB. Inhibition of BCRP at the BBB has been demonstrated to lead to significantly enhanced penetration of BCRP substrates into the brain (Shi et al., 2007). However, many known inhibitors of BCRP demonstrate neurotoxicity and have shown limited success clinically (Allen et al., 2002b). Approaches are therefore required to identify alternative compounds that can diminish the function of BCRP at the BBB to enhance CNS drug delivery.

Natural compound phytochemicals, such as flavonoids, represent a group of natural substances found in fruit, vegetables, grains, tea and wine. Furthermore many flavonoids have been shown to directly impact upon the function of BCRP at the BBB (Zhang et al., 2000) (Hartz et al., 2010) (Zhang and Morris, 2003) and hence have gained increasing interest as modulators of BCRP function.

2.2. Aims and objectives

The aim of the chapter is to characterise the expression of BCRP at the BBB and to examine approaches that enable modulation of BCRP at the BBB with phytochemical (primarily flavonoids) compounds using a porcine brain microvascular endothelial cell culture model (PBMEC/C1-2) and primary porcine brain microvascular endothelial cell culture model.

To achieve the aims the overall objectives were:

- To demonstrate gene and protein expression of BCRP in PBMEC/C1-2 cells
- To investigate the cytotoxicity of phytochemical modulators towards PBMEC/C1-2 cells
- Evaluate the modulation of genomic and protein expression and transport function of BCRP when exposed to phytochemical modulators in PBMEC/C1-2 cells

- Isolation and growth of primary porcine endothelial cells in specific cell culture conditions and determine the expression of BCRP and evaluate the modulation of BCRP transport function in PBMEC/C1-2 cells
- Evaluate the modulation of transport function of BCRP when exposed to phytochemical modulators in a primary BBB cell culture model

2.3. Materials

Hams F12, IMDM and Dulbecco's modified essential media with glucose (DMEM), new born calf serum (NCS), fetal bovine serum (FBS), penicillin/streptomycin and L-glutamine were obtained from Biosera (Sussex, UK); GenElute Total RNA extraction kits were purchased from Sigma (Dorset, UK); Rat tail I collagen solution from First Link (Birmingham, UK) and unless otherwise indicated all other chemicals were obtained from Sigma (Dorset, UK). My Taq™ One-step RT-PCR kit and Easy Ladder I obtained from Bioline (London, UK). All reverse transcriptase PCR primers were synthesised by IDTDna (Leuven, Belgium); Resveratrol and Ko143 from Santa Cruz Biotechnology (Texas, USA); Curcumin from Cayman Chemical (Cambridge, UK); Real time PCR housekeeping gene primers were obtained from Invitrogen and BCRP primers were obtained from PrimerDesign (Sheffield ,UK); total RNA extraction kits were purchased from Qiagen (Manchester, UK) and qPCR master-mixes were obtained from PrimerDesign (Sheffield ,UK). Optiblot SDS-page gel and western blot reagents obtained from Abcam (Cambridge, UK); ABCG2 antibody, beta-actin (C4), broad range markers, goat anti-rabbit IgG-FITC and protease inhibitor cocktail were obtained from Santa Cruz Biotechnology (Texas, USA). Stock solutions of all test compounds were prepared in dimethylsulfoxide (DMSO) and stored at -20°C until use.

A total of 18 phytochemical derived modulators were selected for studies and their structures are detailed in Appendix A.

2.4. Methods

2.4.1. Culture of C6 rat astrocytes

C6 cells were obtained from Cell Line Services (Germany). The cells were resuspended in a T25 flask containing C6 media (Hams F12 50%, IMDM 50%, 7.5% NCS, 7mM L-glutamine, 5µg/mL transferrin, 0.5U/mL heparin and 100 U/mL penicillin G sodium, 100 µg/mL streptomycin sulphate). Cells were grown at 37°C in a humidified atmosphere of 5% CO_2 for 24 h and media changed after 24 h. Thereafter the cells were passaged 3-4 days post seeding (at 70-80% confluency) by washing with pre-warmed PBS followed by the addition of 1 mL of trypsin-EDTA to the flask. The flask was then placed in an incubator for 5 min and cell suspension was resuspended in 5 mL of growth media. Cell suspensions were then transferred to a 15 mL centrifuge tube and centrifuged at 1500 rpm for 5 min and the pellet was resuspended in 2 mL of the media and transferred to a T75. The media was aspirated every other day, sterile filtered (0.22 µm) and stored at 4°C for further use.
This media was labelled as astrocyte conditioning media (ACM).

2.4.2. Culture of PBMEC/C1-2 cells

2.4.2.1. Preparation and coating of an gelatine extracellular matrix

PBMEC/C-12 cells do not demonstrate optimum growth on the plastic surfaces. In order to allow growth on cell culture surfaces, an extracellular matrix support was required to enhance attachment and proliferation. To support the growth of PBMEC/C1-2 cells on plasticware, a 2 % w/v gelatine stock solution was prepared in the water by the addition of 4 g of gelatine powder to a sterilised bottle containing 200 mL of water. The suspension was autoclaved and stored at 4°C for further use.

Each flask was coated with 1:5 dilution of the gelatine stock with cell culture water to obtain a final surface coating of 0.4 % w/v gelatine. The flasks were left to dry in a laminar airflow hood for 2 h to ensure thorough surface coating, and any excess gelatine was aspirated before the flasks were washed with cell culture water.

2.4.2.2. PBMEC/C1-2 cell growth on tissue culture surfaces

PBMEC/C1-2 cells were a kind gift from Dr M.Teifel (Institut für Biochemie, Technische Hochschule Darmstadt, Germany). Cells were resuspended in a 50:50 mixture of C6 media and ACM, referred to as PBMEC media, and seeded onto gelatine coated T25 flasks. PBMEC media was replaced every other day until the cells reached confluency. Subsequently, PBMEC media was aspirated and cells were washed twice with the pre-warmed PBS and incubated with 1 mL of a 0.25 % w/v trypsin-EDTA solution, sufficient to cover the entire cell layer. Flask were then incubated at 37°C in a humidified atmosphere of 5% CO_2 in air with the slight agitation for 5 minutes. Once cells had detached, fresh PBMEC media was added to inactivate trypsin and the cell suspension was transferred to a 15 mL centrifuge tube and centrifuged at 1500 rpm for 10 min. The supernatant was removed and cell pellet resuspended in 2 mL of PBMEC media and reseeded into appropriately coated plasticware for further use. The coating process was performed on all surfaces used to grow PBMEC/C1-2 cells including flasks, 6-well and 96-well plates. Approximately 3-4 days post seeding, the cell monolayers were examined under an inverted DMI400B microscope (Leica microscope systems (UK) Ltd, Milton Keynes, UK).

2.4.2.3. Cryopreservation of the cells

Cells were cryopreserved for further use by centrifugation a cell suspension at 1500 rpm for 10 min to obtain a cell pellet, followed by resuspension of the pellet in cryopreservation media (10% DMSO and 90% PBMEC media). A 1 mL volume of the cell suspension was aliquoted to the cryovials and stored overnight at -80˚C in cell cooling box (Mr. Frosty, Nalgene®, Thermo Fisher Scientific, UK). After 24 h, cryovials were transferred to liquid nitrogen for long-term storage.

2.4.2.4. Development of a permeable insert based BBB model

To develop an *in-vitro* BBB model, 12-well permeable inserts (ThinCert® with 0.4µm pore size) were used as a support for cell growth, with the addition of a matrix coating of 5 µg/cm^2 of rat-tail collagen. Inserts were left to dry for 3-4 h in a laminar airflow hood before excess collagen was aspirated and inserts washed twice with PBS. Cell suspensions were introduced into the apical chamber of coated inserts at a density of

1 x10^5 cells/cm^2 with the basolateral chamber receiving PBMEC media only. Cells were grown for 3-4 days in PBMEC media supplemented with 1 µg/mL fibronectin to enhance attachment. Monolayer formation was monitored by measuring the transendothelial electrical resistance (TEER) using a voltohmmeter (EVOM) (World Precision Instrument) directly before and after all transport studies. TEER values were calculated as follows:

$$\text{TEER Values } (\Omega.\text{cm}^2) = (\text{R}_{\text{Cell monolayer}} - \text{R}_{\text{Blank filter}})\text{xA} \qquad (1)$$

where A = Surface area of the permeable insert (cm^2), $R_{Cell\ monolayer}$ = Resistance across permeable insert with cell monolayer and $R_{Blank\ filter}$ = Resistance across permeable insert without cells.

Control measurements were made using filters without cells (blank filter). The cut-off TEER values for an acceptable *in-vitro* model was set at 300 Ω.cm^2 (Lauer et al., 2004).

2.4.3. Cytotoxicity of modulators towards PBMEC/C1-2 cells: methylthiazolyldiphenyl-tetrazolium bromide assay

Stock solutions of methylthiazolyldiphenyl-tetrazolium bromide (MTT) were prepared in DMSO. Sterile dilutions of each modulator across a 7-fold log concentration range of 0.001 µM- 1000 µM were freshly prepared on the day. Culture media was used as the diluent and the final solvent concentrations did not exceed 1 % (v/v).

PBMEC/C1-2 cells were seeded with a density of 15,000 cells per well onto clear flat bottom 96-well plates and incubated for 24 h to attach. The media was subsequently removed and fresh media containing the test compounds was added and incubated for 24 h for subsequent experiments. The medium was then removed and cells were washed with the pre-warmed PBS and incubated with fresh media for 30 min. MTT powder was dissolved in PBS (5 mg/mL) and filtered through a 0.2 µm pore size. 20 µL of the pre-warmed MTT solution was added to each well. The plates were protected from light and incubated at 37°C in a humidified atmosphere of 5% CO_2 for 4 h. Thereafter the media was removed and 100µL of DMSO added to the each well to solubilise the purple formazan crystals. The plates were incubated for a further 10-15 min at room temperature (RT). The UV-absorbance of the formazan product was measured on a multi-plate reader (Bio-Rad laboratories, Hercules, CA) using 570 nm as a test wavelength and 600 nm as a reference wavelength.

The mean of the blank UV-absorbance was subtracted from the UV-absorbance of each controls and samples and percentage viability was calculated. The percentage of cellular viability was calculated (Equation 2).

$$\%\ \text{cell viability} = \frac{\text{absorbance of sample}}{\text{absorbance of control}} * 100 \qquad (2)$$

The IC_{50} was subsequently calculated using a sigmoidal dose response function within the Graphpad Prism version 5.0 (GraphPad Software, Inc. USA).

2.4.4. Immunostaining detection of BCRP in PBMEC/C1-2 cells

PBMEC/C1-2 cells were grown on coverslips coated with 0.4 % w/v gelatine for 48 hours. Media was then aspirated and coverslips were washed three times with pre-warmed PBS. Cells were fixed with methanol at -20°C for 20 min and washed three times with pre-warmed PBS before being rehydrated in PBS for 20 min at room temperature. Blocking solution (1 % goat serum in PBS) was added to the coverslips and incubated for 30 min at room temperature. The coverslips were then incubated with primary anti-ABCG2 antibody (Sigma-Aldrich company ltd, Dorset, UK) (1:200) for 2 h at 37 °C. Subsequently, the coverslips were washed twice with PBS and incubated with the secondary antibody fluorescein iso-thiocyanate (FITC)-labelled mouse anti-rabbit IgG (1:500) in blocking solution, for 45 min at room temperature in the dark. The secondary antibody was then aspirated and cells were washed three times with pre-warmed PBS. The coverslips were then rinsed with sterile water and mounted onto the glass slide with mounting media containing 4',6-diamidino-2-phenylindole (DAPI). The staining of cells with anti-ABCG2 was analysed using an upright confocal microscope (Leica SP5 TCS II MP) and visualised with a 40x oil immersion objective. All images were acquired using an argon laser at 494 nm to visualise FITC and a helium laser to visualise DAPI at 461 nm.

2.4.5. Measurement of BCRP cellular functional activity in PBMEC/C1-2 cells

2.4.5.1. Determination of PBMEC/C1-2 optimum seeding density and modulator incubation time

To develop a high-throughput *in-vitro* screening system to detect modulators of BCRP the optimum seeding density of PBMEC/C1-2 cells was assessed to enable the intracellular detection of the BCRP substrate H33342. Cells were seeded at densities of 1000, 20,000, 50,000 and 100,000 cells per well of a 96-well plate and left to adhere for 24 h. Wells were subsequently washed twice with pre-warmed PBS at 37 °C. 100 µL of PBMEC media containing 10 µM Hoechst 33342 was added to each well and incubated for 30 min, 60 min and 90 min at 37°C. Cells were washed twice with warm PBS and lysed by storing plates at -80°C for 20 minutes before resuspending in pre-warmed PBS. The fluorescence of H33342 was determined on a fluorescent plate reader with an excitation wavelength of 355 nm and emission wavelength of 460 nm.

2.4.5.2. Functional activity of BCRP in PBMEC/C1-2 using a 96-well plate assay

The functional activity of BCRP in PBMEC/C1-2 cells was assessed using Ko143, a known potent inhibitor of BCRP. 20,000 cells per well were seeded into a 96-well plate and allowed to attach for 24 h. Thereafter cells were washed with pre-warmed PBS at 37°C and fresh media added containing 3.9 nM-5 µM Ko143 and left to pre-incubate for 1 h. 100 µL of media containing 10 µM of H33342 and 3.9 nM-5 µM Ko143 was then added to the appropriate wells and incubated for a further 30 min at 37°C. Wells were then washed twice with ice cold PBS and cells lysed by storage of plates at -80°C for 20 min before being read on a fluorescent plate reader at an excitation wavelength of 355 nm and emission wavelength of 460 nm.

2.4.5.3. Assessment of the intracellular accumulation of H33342 in the presence of modulators.

Prior to assessment the impact of modulators on intracellular H33342 accumulation, the auto-fluorescence of all modulators was determined. Non-toxic concentrations of modulators were prepared in cell culture media and 100 µL added to wells of a 96-well plate with H33342 (10 µM) acting as a positive control and a fluorescent substrate for BCRP and prepared in the cell culture media with 100 µL added to wells of a 96-well plate. The fluorescence of flavonoids was measured using a fluorescent plate reader

at an excitation wavelength of 355 nm and emission wavelength of 460nm and compared to the fluorescence obtained from H33342.

The potential for modulators to alter the functional activity of BCRP was then assessed by measuring changes in the intracellular accumulation of H33342 in the absence and presence of modulators. PBMEC/C1-2 cells were seeded onto clear-bottomed 96-well plates for 24 h, where optimal seeding densities and incubation times were determined from previous experiments (section 2.4.5.1). To assess the potential for direct inhibition of BCRP function, cells were washed with pre-warmed PBS at 37 °C and pre-treated with 25 µM of modulators (unless or otherwise stated) and incubated at 37 °C for 1 h. Cells were also incubated with 1 µM Ko143 for 1 h (used as a positive control comparator). Following pre-incubation with modulators, media was removed and cells were washed twice with pre-warmed PBS at 37 °C before the addition of 10 µM H33342 containing 25 µM of modulators (unless otherwise indicated) and incubated for a further 30 min. Thereafter cells were washed twice with ice cold PBS and lysed at -80°C for 20 min before being resuspended in 100 µL of water and fluorescence measured with dual-scanning microplate spectroflurometer (Spectra Max Gemini XS, molecular devices, Sunnyvale, California) at an excitation wavelength of 355 nm and emission wavelength of 460 nm.

To assess the potential for modulation of BCRP protein expression, cells were washed with pre-warmed PBS at 37°C cells and incubated with 25 µM of modulators (unless otherwise stated) for 24 h in PBMEC media at 37°C. Following pre-incubation with modulators, media was removed and cells were incubated fresh PBMEC media (without modulators) for 1 hour (wash-out period). Thereafter the media was removed and cells washed twice with pre-warmed PBS at 37°C before the addition of 10 µM H33342 for 30 min. At the end of the incubation period cells were washed twice with ice cold PBS and lysed at -80°C for 20 min before being resuspended in 100 µL of water and fluorescence measured with dual-scanning microplate spectroflurometer (Spectra Max Gemini XS, molecular devices, Sunnyvale, California) at an excitation of wavelength of 355 nm and emission wavelength of 460 nm.

2.4.6. Determination of BCRP gene expression by reverse-transcriptase PCR (RT-PCR) in PBMEC/C1-2 cells

2.4.6.1. Extraction of total RNA

RNA was extracted according to the manufacturer's instructions (RNeasy® Mini kit, Qiagen). In brief, 50,000 cells per well were seeded in a 6-well plate. Cells were washed twice with PBS and 350 µL of the RLT buffer was added to each well. 350 µL of the 70 % ethanol was added and mixed by pipetting up and down. The lysate was transferred to the RNeasy mini spin column placed in 2 mL collection tube and centrifuged for 15 s at 8000 g. The flow through liquid was discarded and 700 µL of the RW1 buffer was added to the column and centrifuge for 15 s at 8000 g and flow through liquid was then discarded. 500 µL of the RPE buffer was added to the column and spun for a further 2 min at 8000 g and the flow through liquid was discarded and column was placed into a 2 mL collection tube. 30-40 µL of RNA free water was added to the column and spun for 1 min at 8000 g. The final resultant RNA was collected in the collection tube and aliquoted before being stored at -80°C for further use.

2.4.6.2. One-step reverse-transcriptase PCR

A one-step PCR reaction was setup using 80 ng of the template RNA, spectrophotometrically determined using a NanoDrop 1000 spectrophotometer (ThermoScientific, UK). The ratio of UV-absorbance at 260 nm and 280 nm was used to determine the purity of the sample. PCR tube reactions were setup as detailed in Table 2.1.

Table 2.1: Preparation of PCR samples

Reagents	Volume
My Taq One-Step Mix	25 µL
Primer Forward	1.5 µL
Primer Reverse	1.5 µL
Reverse Transcriptase Enzyme	0.5 µL
Ribosafe Inhibitor	1 µL
DEPC Water	15.5 µL
Template (80 ng)	5 µL
Total Volume	50 µL

Forward and reverse primers (HKG: β-actin; GOI: BCRP) were designed using the PrimerQuest tool (http://www.idtdna.com/primerquest/home/index) and custom synthesised (IDTDna, Germany) (Table 2.2). The thermal cycling was conducted using a Hybaid OmniGene Thermal Cycler using a three-step protocol (Table 2.3)

Table 2.2: Primers used for RT-PCR

Gene	Size	Forward Primers	Reverse Primers
β-actin	806	AAGCCAACCGTGAGAAGATG	CAACTAACAGTCCGCCTAGAAG
BCRP	652	TCCGACCACCATGACAAATC	GTACACCGAGCTCTTCTTCTTC

Table 2.3: Thermal cycle reactions for PCR

Cycles	Temperature	Time	Procedure
1	45°C	20 min	Reverse Transcription
1	95°C	1 min	Polymerase Activation
40	95°C	10 s	Denaturation
	55°C	10 s	Annealing
	72°C	30 s	Extension

2.4.6.3. Gel electrophoresis

Confirmation of a successful PCR product was assessed by gel electrophoresis. A 2 % w/v agarose gel was prepared in TAE buffer with 5 µL of ethidium bromide to allow visualisation under UV light. 6 µL of the PCR-product was mixed with 8 µL loading buffer and loaded into wells. Gel electrophoresis was carried out at 50 Volts for 1.5 h and visualised under a UV-transilluminator (Geneflash, Syngene Bioimaging, Cambridge, UK) with a 1kbp DNA ladder (Easyladder I) used as a marker ladder for size analysis.

2.4.7. Determination of BCRP protein expression by SDS-PAGE and Western blotting in PBMEC/C1-2 cells

2.4.7.1. Preparation of cell lysate

PBMEC/C1-2 cells were grown on gelatine coated 6-well plates with a seeding density of 50,000 cells per well for 24 h and allowed to attach. Cells were trypsinised and centrifuged at 1500 g for 10 min and pellet was dissolved in 40 µL of RIPA buffer containing TBS, 1% nonidet P-40, 0.5% sodium deoxycholate, 0.1% SDS, 0.004%

sodium azide, PMSF, protease inhibitor and sodium orthovanadate (Santa Cruz Biotechnology, Canada) and transferred to an ice cold Eppendorf's tube before being sonicated for 10 s and centrifuged at 4°C at 16000 rcf for 30min. The supernatant was then aliquoted and frozen at -80°C until further use.

To assess the impact of modulators on BCRP protein expression, PBMEC/C1-2 cells were grown on 6-well plates and incubated with modulators at 25 µM (unless otherwise stated) for a further 24 h. The media was aspirated and whole cell lysate was extracted as described above.

2.4.7.2. Determination of protein concentration: bicinchoninic acid assay

Total protein was quantified using a bicinchoninic acid (BCA) assay (Novagen, BCA assay protein kit). In brief, the assay is based upon the reduction of Cu^{2+} to Cu^{1+} by protein in an alkaline solution. Bicinchoninic acid is a chromogenic reagent that chelates with the reduced copper, producing a purple reaction complex with strong UV-absorbance at 562nm. A standard curve with bovine serum albumin (BSA) was prepared in RIPA buffer. BCA working stock was prepared by adding 1 mL of BCA solution and 20 µL of the 4 % cupric sulphate just before use. 25 µL of the sample or BSA standards were added to the clear 96-well plate and 200 µL of BCA working stock was added and plate was incubated for 30 min at 37 °C and the UV-absorbance was measured using a multi-plate reader at 570 nm as a test wavelength and 600 nm as a reference wavelength (Bio-Rad laboratories, Hercules, CA).

2.4.7.3. Sodium dodecyl sulphate polyacrylamide gel electrophoresis

Optiblot SDS-PAGE precast gels (8%) (Abcam, UK) were used to conduct SDS-PAGE electrophoresis. Optiblot SDS reducing running buffer (Abcam, UK) was prepared by the addition of 40 mL of Optiblot 20 X run buffer (Abcam, UK) and 760 mL of ultrapure water and stored at 4°C for further use. Samples for SDS-PAGE were prepared as outlined in Table 2.4.

Table 2.4: Reagents composition for SDS-PAGE

Reagents	Volume
Sample	X µL
Water	13-X µL
LDS Loading Buffer 4X	5 µL
DTT Reducer 10X	2 µL
Total Volume	20 µL

A total reaction volume of 20 µL (containing 50 µg of protein) was used for SDS-PAGE. Samples were heated at 37°C for 30 min. The gel cassette was placed in the tank and wells were washed twice with ultrapure water. 20 µL of the SDS-PAGE protein sample mix was loaded onto the gel in addition to 7 µL of a broad range marker (6-200 kDa). Approximately 400 mL of the running buffer was added to the outer chamber and tank was assembled. The gel was run at 180 V for at least 30 min or until the blue dye front neared the bottom of the cassette.

2.4.7.4. Electrophoretic transfer and blotting of proteins

A Bio-Rad mini trans-blot system was used to transfer the proteins from the gel to a polyvinylidene fluoride (PVDF) membrane. The blotting buffer was prepared while the SDS-PAGE was running, the trans-blot system and sponges were washed with distilled water and sponges were soaked in the blot buffer (Optiblot blot buffer supplemented with 20% methanol). The PVDF membrane was activated by subsequently transfer into methanol for 15 s, 2 min in ultrapure water and finally 5 min in blotting buffer. The gel was placed on the PVDF membrane and sandwiched between blotting paper and sponge pads. The electrophoresis tank was placed on ice and two ice packs were placed in the tank to avoid overheating. Electrophoretic transfer of protein was conducted with ice-cold buffer at 50 V for at least 2 h and 30 min. Following transfer membrane was washed in ultrapure water for 2 min, deactivated in methanol for 10 s and finally exposed to Ponceau stain (0.1 % w/v Ponceau S in 5% v/v acetic acid) for 1 min to allow visual observation of the protein transfer.

2.4.7.5. Immunological detection of BCRP

Protein-transferred membranes were washed with TBST buffer for 30 min and blocked with blocking buffer (5 % w/v milk and TBST) for 1 h at room temperature. The membrane was then incubated with the polyclonal anti-ABCG2 antibody (Sigma-Aldrich,UK) (1:4000) in blocking buffer and incubated for 24 h at 4 °C. Thereafter, the

membrane was placed onto an orbital shaker for 2 h before the antibody solution was removed and membrane washed with TBST for 30 min and blocked with blocking buffer for 30 min at room temperature. The membrane was then incubated for 2 h at room temperature with goat anti-rabbit IgG-horse radish peroxidise-conjugated (Santa Cruz biotechnology, Sc-2004) (1:7500) in blocking buffer.

2.4.7.6. Chemiluminescent detection of BCRP

Detection of BCRP was conducted using laboratory prepared enhanced chemiluminescent detection solution (Table 2.5), with 3 µL of solution B combined with per 1 mL of solution A prior to detection.

Table 2.5: Chemiluminescent reagents

Solution A	Volume	Solution B	Volume
Coumaric acid (90 mM)	110 µL	30 % Hydrogen peroxide	100 µL
Luminol (250 mM)	250 µL	Ultra-pure water	900 µL
Tris (1 M)	5 mL		

The chemiluminescent solution was poured onto the PVDF membrane and incubated on an orbital shaker for 2 min, before the membrane was then placed on a transparent plastic film and transferred to a developing cassette. Subsequent steps were performed in a dark room. An X-ray film (CL-X Posure™ film, Thermo Scientific, Belgium) was placed on top of the membrane and the developing cassette was closed for 1 min. The membrane was carefully transferred to a fixer solution (Kodak GBX fixer, Sigma-Aldrich, UK) for 10-20 s and then placed into the developer solution (Kodak GBX developer, Sigma-Aldrich, UK) for 30 s before being thoroughly washed with water and dried in the air for 2-4h.

2.4.7.7. Membrane stripping

Following BCRP detection, antibody was removed by membrane stripped using a mild stripping method adapted from Legocki and Verma (Bendayan et al., 2006) (Table 2.6).

Table 2.6: Composition of buffer used for stripping

Reagents	Quantity
Glycine	15 g
SDS	1 g
Tween 20	10 mL
Water	To 1000 mL

The membrane was washed with TBST and sufficient stripping buffer added to cover the membrane, before being gently shaken on an orbital shaker for 10 min. The membrane was subsequently washed for 10 min, twice in PBS followed by twice with TBST in 2 min intervals before being blocked with TBST and milk for 1 h.

2.4.7.8. Immunological detection of β-actin

To reprobe the membrane for the loading control (β-actin) the membrane was incubated with blocking buffer, followed by mouse β-actin horseradish peroxidase conjugated monoclonal antibody (1:7500) in blocking buffer for 24 h at 4°C. The membrane was then washed with TBST for 45 min before β-actin was detected by a chemiluminescent detection approach (section 2.4.7.6).

2.4.8. Modulation of BCRP gene expression by phytochemicals compound in PBMEC/C1-2 cells

2.4.8.1. Extraction of RNA

PBMEC/C1-2 cells were grown on gelatine coated 6-well plates for 24 h and modulators demonstrating BCRP protein induction or down-regulation were incubated with cells for 24 h at, unless otherwise stated, 25 μM. RNA was extracted as stated in section 2.4.6.1.

2.4.8.2. Reverse transcription

A two-step reverse transcription protocol was utilised involving both annealing and extension steps. RNA samples were prepared as recommended by the manufacturer (Precision Nanoscript RT kit, PrimerDesign, UK).

For the annealing step, the samples were prepared by the addition of 1 μL of gene specific RT primers, 600 ng of RNA template and a final volume of 10 μL was achieved

by the addition of RNase-free water. Samples were then transferred to a heat block for 5 min at 65 °C. For the extension step, the reagent were prepared as described in Table 2.7.

Table 2.7: Preparation of extension reagents

Reagents	Volume
Nano Script 10x Buffer	2 µL
dNTP Mix 10mM	1 µL
DTT 100mM	2 µL
RNase-free Water	4 µL
Nano Script Enzyme	1 µL
Annealing mix end-product	10µL

10 µL of the extension reagent mix was added to the 10 µL of each pre-heated sample and tubes were vortexed. Samples were then incubated at 55 °C for 20 min on a heat block before the temperature was raised to 75°C for 15 min. The subsequent cDNA was quantified spectrophotometrically and samples were stored at -20°C for future use.

2.4.8.3. qPCR cycle parameters

The qPCR reaction mixture was prepared as outlined in Table 2.8.

Table 2.8: Preparation of qPCR samples

Reagents	Volume
10x Master Mix	10 µL
Primer Forward (6 pmol)	1 µL
Primer Reverse (6 pmol)	1 µL
RNase-free Water	3 µL
Template (25 ng)	5 µL
Total Volume	20 µL

qPCR primers were custom synthesised as follows: *HPRT1* (NCBI Accession: NM_001032376.2) forward primer GGTCAAGCAGCATAATCCAAAG, reverse primer CAAGGGCATAGCCTACCACAA and a custom synthesised porcine *BCRP* (NCBI Accession: NM_214010) gene primers (PrimerDesign, UK). qPCR was conducted using a Stratagene MX3000p thermal cycler (Agilent technologies, United States) with a SYBR-green detection probe and a two-step cycling protocol (Table 2.9).

Table 2.9: qPCR cycles

Cycles	Step	Time	Temperature
	Enzyme activation	2 min	95°C
40 Cycles	Denaturation	15 s	95°C
40 Cycles	Data Collection	60 s	60°C

2.4.8.4. qPCR quantification method

Relative quantification determines the mRNA changes in gene of interest (*BCRP*) relative to the levels of a housekeeping gene (*HPRT1*) RNA. Threshold cycle (Ct) values were determined and changes in the expression of target gene normalised with HPRT1 calculated for each reaction condition (ddCT method) (Livak and Schmittgen, 2001) (see equation 3)

$$\text{Fold change} = 2^{-\Delta(\Delta Ct)} \qquad (3)$$

where $\Delta Ct = C_{T,BCRP} - C_{T,HPRT1}$

The efficiency of all genes were pre-validated for specificity by the manufacturer.

2.4.9. Assessing the functional activity of BCRP in an *in-vitro* permeable insert BBB monolayer model

2.4.9.1. Pheophorbide A (PhA) calibration curve

To assess the function of BCRP *in-vitro*, the specific BCRP fluorescent substrate pheophorbide A (PhA) was used. Stock solutions of PhA were prepared in DMSO and a standard curve generated over a concentration range of 0.001 µM to 50 µM, prepared in serum free PBMEC media. PhA fluorescence was quantified by transferring 100 µL of each standard solution into wells of a black 96-well plate before quantifying on a fluorescent plate reader at an excitation wavelength of 395 nm and emission wavelength of 670 nm using a dual-scanning microplate spectroflurometer (Spectra Max Gemini XS, Molecular Devices, Sunnyvale, California).

2.4.9.2. Optimisation of the *in-vitro* transport media

Permeable PBMEC/C1-2 inserts were prepared according to section 2.4.2.4. TEER values were used as a measure of monolayer formation and suitability of transport media. Preliminary experiments were performed to assess the integrity of monolayers when incubated with either HBSS supplemented with glucose (10 mM) and HEPES (10 mM) or PBMEC serum free media (SFM). TEER values were determined after 30 min, 60 min, 90 min, 120 min, 150 min and 180 min exposure to media.

2.4.9.3. Lucifer yellow permeability assay

To further assess the formation of a suitable monolayer, Lucifer yellow (LY) was used as a passive diffusion marker. Solutions of LY were prepared in SFM and added to the apical chamber of the inserts to achieve a final concentration of 100 µM, and LY-free SFM added to the basolateral chamber (1.5 mL). The inserts were then placed on an orbital shaker at 100 rpm at 37 °C for 1 h. Thereafter, a sample of the basolateral media was then collected and quantified for LY permeation on a fluorescent plate reader at an excitation wavelength of 428 nm and emission wavelength of 536 nm using dual-scanning microplate spectroflurometer (Spectra Max Gemini XS, Molecular Devices, Sunnyvale, California). The percentage transport of LY across the permeable inserts were calculated (Equation 4).

$$\%\ \text{Lucifer yellow transported} = 100 \cdot \left(1 - \frac{RFU_{basolateral}}{RFU_{apical}}\right) \quad (4)$$

where $RFU_{basolateral}$ is the relative fluorescence units in the sample taken from basolateral compartment and RFU_{apical} is the relative fluorescence unit in the sample taken from the apical compartment. Inserts were rejected for permeability assays if the percentage LY transport was greater than 1 %.

2.4.9.4. Modulation of BCRP transport function

To assess the potential for phytochemical modulators to modulate the *in-vitro* transporter function of BCRP in the permeable insert BBB model, modulators identified as resulting in induction or down-regulation of BCRP protein from western blotting studies (section 2.4.7) were selected to then assess their potential to modulate the efflux of PhA. PBMEC/C1-2 seeded permeable inserts were washed with pre-warmed

PBS and freshly prepared working stocks of modulators (optimal non-toxic concentrations were used and determined from cytotoxicity and western blotting studies) and Ko143 in SFM were added to the permeable inserts and incubated for either 1 h (Ko143: to pre-load cells with inhibitor) or 24h (modulators: to modulate the protein expression of BCRP) at 37°C.

Cells were subsequently washed with pre-warmed PBS followed by the addition of SFM containing Ko143 (1 µM) or modulators and 10 µM PhA into the apical compartment. The basolateral compartment received media with modulators only. 50 µL aliquots were taken at 0, 30, 60, 90, 120, 150, 180 and 210 min, replaced by fresh SFM, and the fluorescence of PhA determined at an excitation wavelength of 395 nm and emission wavelength of 670 nm using a dual-scanning microplate spectrofluorometer (Spectra Max Gemini XS, molecular devices, Sunnyvale, California). For modulators demonstrating induction of BCRP, all compounds were added into the basolateral compartment and sampling of the apical compartment was conducted.

2.4.9.5. Measurement of the apparent membrane permeability coefficient

The apparent membrane permeability (P_{app}: $x10^{-6}$ cm/s) of PhA was calculated according to equation 5.

$$\mathrm{Papp} = {}^{dQ}/_{dt} \cdot \frac{1}{AC_0} \qquad (5)$$

where dQ/dt is the rate of appearance of PhA on the receiver side (calculated from the slope of the cumulative transport graph), C_0 is the initial concentration of PhA in the donor compartment and A (cm^2) is the surface area of the insert.

2.4.10. Development of an *in-vitro* primary porcine brain microvascular endothelial cell culture model

BBB cellular models derived from immortalised cells are widely used to study the phenotype and genotype of the BBB. However, immortalised systems are often fraught with loss of key BBB markers, reduced expression of regulators and transporter proteins and often demonstrate lower TEER values compared to the microvasculature *in-vivo*.

Cells isolated directly from freshly obtained brain tissues can be used to develop a more representative *in-vitro* BBB model, and a recently described primary porcine BBB model system has been demonstrated to yield a high number of cells from brain

hemispheres, retention of BBB phonotypic characteristics, close reflection of human and porcine genome, anatomy and disease progression (Krishnamurthy et al., 2004, Doyle and Ross, 2003a, Patabendige et al., 2013).

2.4.10.1. Isolation of the primary porcine brain endothelial cells

Porcine brain endothelial cells were isolated according to the methods described by Patabendige et al (Patabendige et al., 2013). Porcine brains were acquired from a local abattoir (Long Compton Abbatoir, Oxford, UK) within 1-hour of sacrifice. The brains were transferred to the laboratory in sterile box containing L-15 media supplemented with 1 % penicillin/streptomycin on ice. Each brain was separated into respective hemispheres and thoroughly washed with ice-cold PBS media supplemented with 1 % v/v penicillin/streptomycin. The meninges and blood vessels were removed along with the choroid plexus and capillaries located within brain sulci. The hemispheres were then placed in a clean beaker containing PBS supplemented with HEPES (10 mM) and penicillin/streptomycin sulphate. White matter was then carefully removed and grey matter dissected and transferred to a beaker containing MEM supplemented with HEPES (10 mM) and 1% v/v penicillin/streptomycin. The grey matter tissue was then chopped into small 1 cm^3 sections using a sterile scalpel before being transferred into a 50 mL syringe and passed into a T75 containing 50 mL of MEM supplemented with HEPES (10 mM) and 1 % v/v penicillin /streptomycin.

15 mL of this brain extract was transferred into a homogeniser (Dounce Homogeniser, Jencons, UK) and 25 mL of MEM supplemented with HEPES (10 mM) and penicillin/streptomycin sulphate was added to the homogeniser. The brain extract was then homogenised gently for 15 strokes with a loose pestle (Type B) followed by 15 strokes with tight pestle (Type A). The resulting homogenate was then transferred to a sterile T175 and process repeated for the remaining tissue.

200 mL of homogenate was then filtered through a 150 µm pore nylon mesh and the filtrate collected and subsequently filtered again through a 60 µm pore nylon mesh (Plastok Associates Ltd, Wirral, UK). The filters were removed and placed into separate 15 cm Petri dishes containing 80 mL of digest mix (M199 containing collagenase (223 U/mg), trypsin (211 U/mg), DNase I (2108 U/mg), 10 % v/v FCS and 1 % v/v penicillin/streptomycin). Filters were then incubated at 37°C for 1 h in an orbital shaker and labelled as 150 and 60s.

There after the filters were thoroughly washed and the digest mix transferred to 50 mL centrifuge tubes labelled '150s' and '60s' and centrifuged at 4°C for 5 min at 240 g. The pellet was resuspended in 10 mL of MEM supplemented with HEPES (10 mM) and 1% v/v penicillin /streptomycin sulphate and centrifuged again at 4 °C for 5 min at 240 g. This was repeated 3 times. The final pellets were resuspended in cryopreservation media (90 % FBS and 10% DMSO) and cryovials maintained at -80°c for 24 h before being transferred to liquid nitrogen (-196°C) for long term storage until use.

2.4.11. Characterisation of the *in-vitro* primary porcine BBB model

2.4.11.1. Morphology of the cells

T75 cell culture flasks were coated with rat-tail type-1 collagen (300 µg/mL in cell culture water) for 2-3 h in a laminar air hood. The collagen was aspirated and flasks were washed twice with the pre-warmed HBSS. The larger microvessels (150s) were resuspended in 16 mL of basic growth media (DMEM supplemented with 10% v/v FCS, 1% v/v penicillin/streptomycin, 1% v/v L-glutamine, 125 µg/mL heparin) and 8 mL of this cell suspension was transferred into two T75s and cells allowed to attached at 37 °C in a humidified atmosphere of 5 % CO_2 in air for 24 h.

In order to remove contaminating cells, such as pericytes, 3 µg/mL of puromycin was added to the flasks 24 h post seeding, and the media maintained for 3 days of exposure. Thereafter the media was removed and fresh basic growth media (without puromycin) was added to the flasks maintained at 37 °C in a humidified atmosphere of 5 % CO_2 in air until confluent. At 70-80 % confluency, the cell culture medium was removed and cells were washed with pre-warmed PBS and 2 mL of trypsin-EDTA solution was added. The flasks were returned to the incubator at 37°C for 10 min. An equal volume of the media was then added and the resulting cell suspension was centrifuged at 1500 rpm for 10 min and pellet was resuspended with the basic growth media and cells were seeded for subsequent experiments.

2.4.11.2. Assessment of barrier integrity

To develop the *in-vitro* BBB model, the smaller microvessel fractions (60s) were seeded into permeable inserts (ThinCert™, pore size 1 µm) that had been pre-coated with 300 µg/mL collagen for 3-4 h in a laminar air hood. 1 x10^5 cells/cm^2 were seeded into the permeable inserts and the inserts maintained in basic growth media and

allowed to attach for 24 h. To enhance the formation of the monolayer, the cell culture media was switched on day 4 to serum free media supplemented with 250 µM CPT-cAMP, 17.5 µM RO20-1724 and 500 nM of hydrocortisone (Woodward et al., 2009, Ishiwata et al., 2005, Schwerk et al., 2012) and TEER values used to assess the development of a tight monolayer with an acceptable cut-off of 400-500 $\Omega.cm^2$ in a 6-well transwell system (Patabendige et al., 2013).

2.4.11.3. Immunostaining detection of BCRP grown on permeable inserts

Primary porcine brain endothelial cells (60s) were grown on pre-coated permeable inserts for the detection of BCRP as described in section 2.4.2.4. Cell culture media was aspirated and inserts washed three times with pre-warmed PBS before being fixed with methanol at -20°C for 20 min and thereafter washed three times with pre-warmed PBS. Cells were subsequently rehydrated in PBS for 20 min at room temperature followed by incubation with blocking solution (1% goat serum in PBS) for 30 min at room temperature. The cell monolayers were then incubated with primary anti-ABCG2 antibody (Sigma-Aldrich, Dorset, UK) (1:200 dilution) for 2 h at 37 °C. Cell monolayers were washed twice with PBS and incubated with secondary antibody fluorescein iso-thiocyanate (FITC)-labelled mouse anti-rabbit IgG (1:500 dilution) prepared in blocking solution, for 45 min at room temperature in the dark. Secondary antibody was then aspirated and cells were washed three times with pre-warmed PBS. The insert membranes were then carefully cut and rinsed with MilliQ water and mounted onto glass slides with mounting media containing 4',6-diamidino-2-phenylindole(DAPI). The localisation of BCRP was determined using an upright confocal microscope (Leica SP5 TCS II MP) and visualised with a 40x oil immersion objective. All images were acquired using an argon laser at 494 nm to visualise FITC and a helium laser to visualise DAPI at 461 nm.

2.4.11.4. Determination of BCRP protein in primary porcine brain microvascular endothelial cells.

Primary porcine brain endothelial cells (150s) were grown on collagen coated 6-well plates for 10 days. Whole cell lysate was extracted as described in section 2.4.7.1. Protein was quantified using the BCA assay as described in section 2.4.7.2. SDS-PAGE was performed by loading 50 µg of protein onto gels as described in section 2.4.7.3 and proteins immunological detection of BCRP was performed as detailed in section 2.4.7.4 and 2.4.7.6.

2.4.11.5. Cytotoxicity of modulators towards primary porcine brain microvascular endothelial cells: methylthiazolyldiphenyl-tetrazolium bromide

Primary porcine brain microvascular endothelial cells (150s) were seeded with a seeding density of 25,000 cells per well onto a clear flat bottom 96-well plates. 8-10 days post seeding the media was carefully removed and fresh media containing the modulator compounds at concentrations optimised from PBMEC/C1-2 studies (MTT section 2.4.3, Hoechst 33342 section 2.4.5.3 and WB section 2.4.7) were added and incubated for 24 h. The medium was then removed and cells were washed with the pre-warmed PBS and incubated with fresh media for 30 min. MTT powder was dissolved in PBS (5 mg/mL) and filtered through a 0.2 µm pore. 20 µL of the pre-warmed MTT solution was added to each well. The plates were protected from light and incubated at 37°C in a humidified atmosphere of 5% CO_2 for 4 h. Thereafter the media was removed and 100 µL DMSO added to each well of a 96-well plate to solubilise the purple formazan crystals. The plates were incubated for a further 10-15 min at room temperature (RT).The UV-absorbance of the formazan product was measured on a multi-plate reader (Bio-Rad laboratories, Hercules, CA) using 570 nm as a test wavelength and 600 nm as a reference wavelength. The mean of the blank UV-absorbance was subtracted from the UV-absorbance of each control and samples and percentage viability (see equation 2). The IC_{50} was subsequently using a sigmoidal dose response function within the Graphpad Prism.

2.4.12. Phytochemical modulation of BCRP transport function in a primary porcine *in-vitro* permeable insert BBB model

To assess the ability of modulators to impact upon the efflux function of BCRP, modulators were incubated with primary porcine brain microvascular endothelial cells grown on permeable inserts as described in section 2.4.11.2.

2.4.13. Statistical analysis

All statistical analyses were performed in Graphpad Prism (La Jolla, California, USA). One-way ANOVA and t-tests were carried out to determine the differences between the mean values. For all multi-well based assay replicates of at least 6 were used in three independent experiments. For western blot and transport studies replicates of at least three were used and repeated in three independent experiments. IC_{50} and EC_{50} metrics were calculated using sigmoidal fit functions within Graphpad Prism. A significance p-value of < 0.05 (*P≤0.05, **P≤0.01, *** P ≤ 0.001 and **** P ≤ 0.0001) was considered as statistically significant.

2.5. Results

2.5.1. PBMEC/C1-2 cell morphology

PBMEC/C1-2 cells were grown on gelatine-coated flasks and visually observed using light microscopy. Cells demonstrated typical endothelial cellular morphology with elongated to cobblestone shaped cells (Figure 2.1).

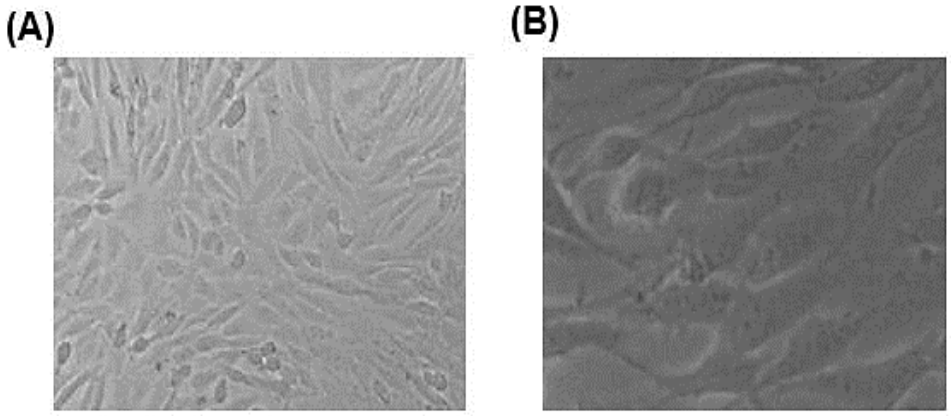

Figure 2.1: Morphology of PBMEC/C1-2 cells.

The PBMEC/C1-2 cells were seeded on a gelatine-coated flasks for 3 days at 37°C in a humidified atmosphere of 5% CO_2 in air. The cells morphology were examined under light microscope at 10x (A) and 40x (B) lenses.

2.6. Development of a PBMEC/C1-2 *in-vitro* BBB model

2.6.1. Assessment of monolayer formation and barrier integrity

The formation of a stable monolayer was determined by measuring TEER values for 4 days post seeding. TEER values significantly increased on day 2 (42 ± 10 $\Omega.cm^2$) and 3 (78 ± 6 $\Omega.cm^2$) post-seeding ($p \leq 0.0001$) compared to day 1 (22 ± 3 $\Omega.cm^2$), before declining thereafter (Figure 2.2).

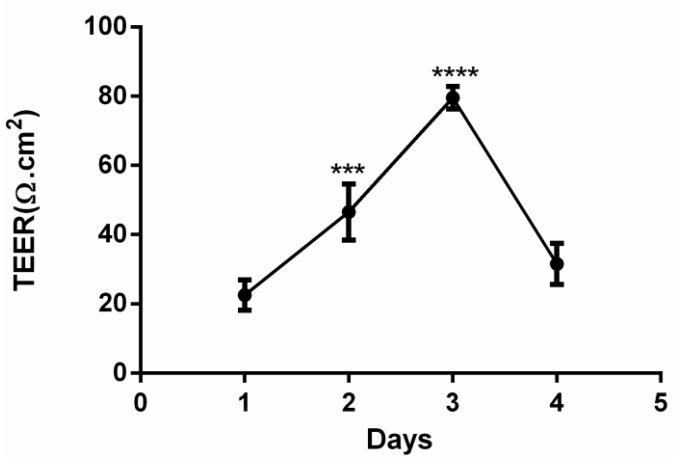

Figure 2.2: Measurement of TEER values.

PBMEC/C1-2 cells were seeded onto collagen coated permeable inserts and grown for 4 days at 37°C in a humidified atmosphere of 5% CO_2 in air. Serum free media supplemented with 250µM CPT-cAMP, 17.5µM RO20-1724 and 500nM hydrocortisone was added for 24 h post seeding and TEER values were measured. Statistical analysis compares TEER values to day 1. *** P ≤ 0.001 and **** P ≤ 0.0001.

2.6.2. Stability of ACM

ACM was initially frozen once collected but it was discovered that using fresh ACM significantly (P ≤ 0.01) increased TEER values on day 2 (45 ± 3 Ω.cm^2) and day 3 (78 ± 6 Ω.cm^2) when compared with media supplemented with frozen ACM on day 2 (41 ± 6 Ω.cm^2) and day 3 (60 ± 3 Ω.cm^2) (Figure 2.3).

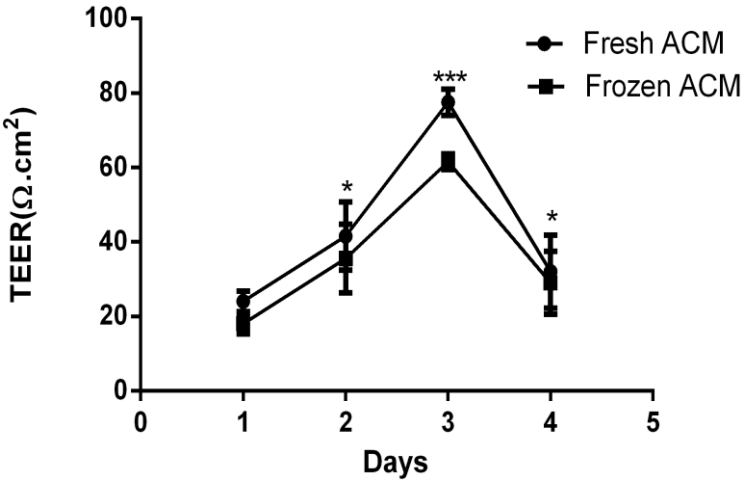

Figure 2.3: Stability of ACM

80,000 cells were seeded onto collagen coated permeable inserts and cells maintained in PBMEC media prepared with using either freshly collected or frozen ACM media to assess the impact of ACM stability on monolayer formation. The media was changed every day for 4 days and TEER values were measured using EVOM Voltmeter. Significant differences between freshly collected ACM and frozen ACM are indicated above the appropriate error bars * P ≤ 0.05 and ** P ≤ 0.01.

2.7. Cellular toxicity of modulators towards PBMEC/C1-2 cells

To investigate the cellular toxicity of modulators towards the PBMEC/C1-2 cells, a MTT cellular toxicity assay was conducted whereby cells were exposed to a 7-fold log concentration range of modulators, 0.001 µM-1000 µM, for 24 h. Modulators demonstrated a range of toxicities towards PBMEC/C1-2 cells. The lowest IC_{50} (1.5 ± 2.7 µM) was observed for α-napthoflavone (Figure 2.4L). Similarly, baiclain (Figure 2.4B), 17-β-estradiol (Figure 2.4F), hesperidin (Figure 2.4J) and hesperetin (Figure 2.4I) demonstrated low micromolar IC_{50} values of 27.9 ± 6 µM, 48.9 ± 1.1 µM, 36.9 ± 1.5 µM and 57.5 ± 3.54 µM respectively. Additionally a number of modulators demonstrated minimal toxicities up to 1000 µM and included chrysin (Figure 2.4D), fistein (Figure 2.4G) and naringin (Figure 2.4M)

All other modulators possessed IC_{50} of > 100 µM (Figure 2.4).

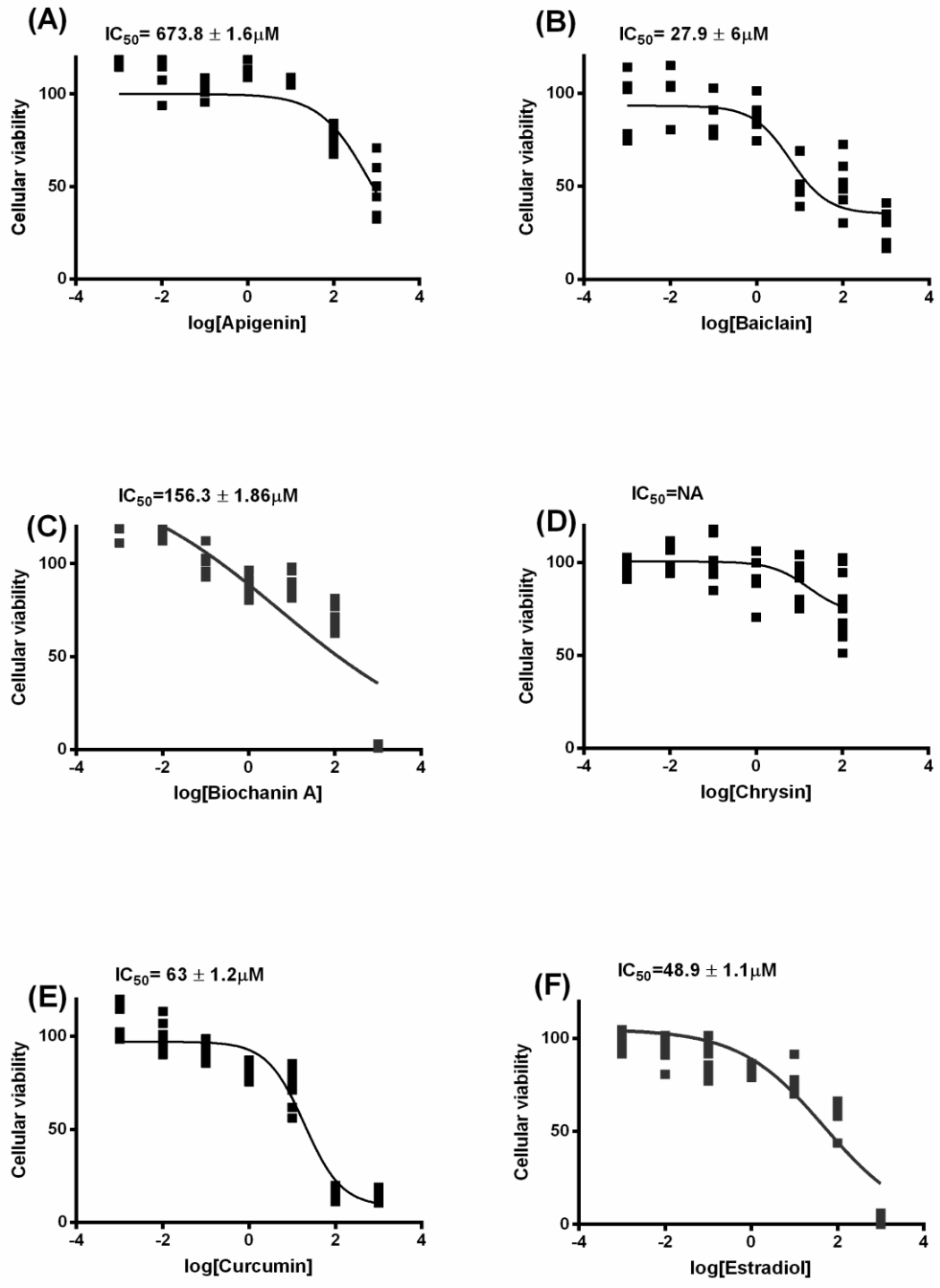

Figure 2.4: Cytotoxic assessment of modulators (A-F).

PBMEC/C1-2 cells were seeded onto gelatine coated 96-well plates at 37°C in a humidified atmosphere of 5% CO_2 in air for 24 h. Media was aspirated and cells were subsequently incubated with a 7-fold log concentration range (0.001 μM-1000 μM) of apigenin (A), baiclain (B), biochanin A (C), chrysin (D), curcumin (E) and 17-β-estradiol (F) for 24 h, prior to an MTT assay being performed. Data reported as IC_{50} ± SD.

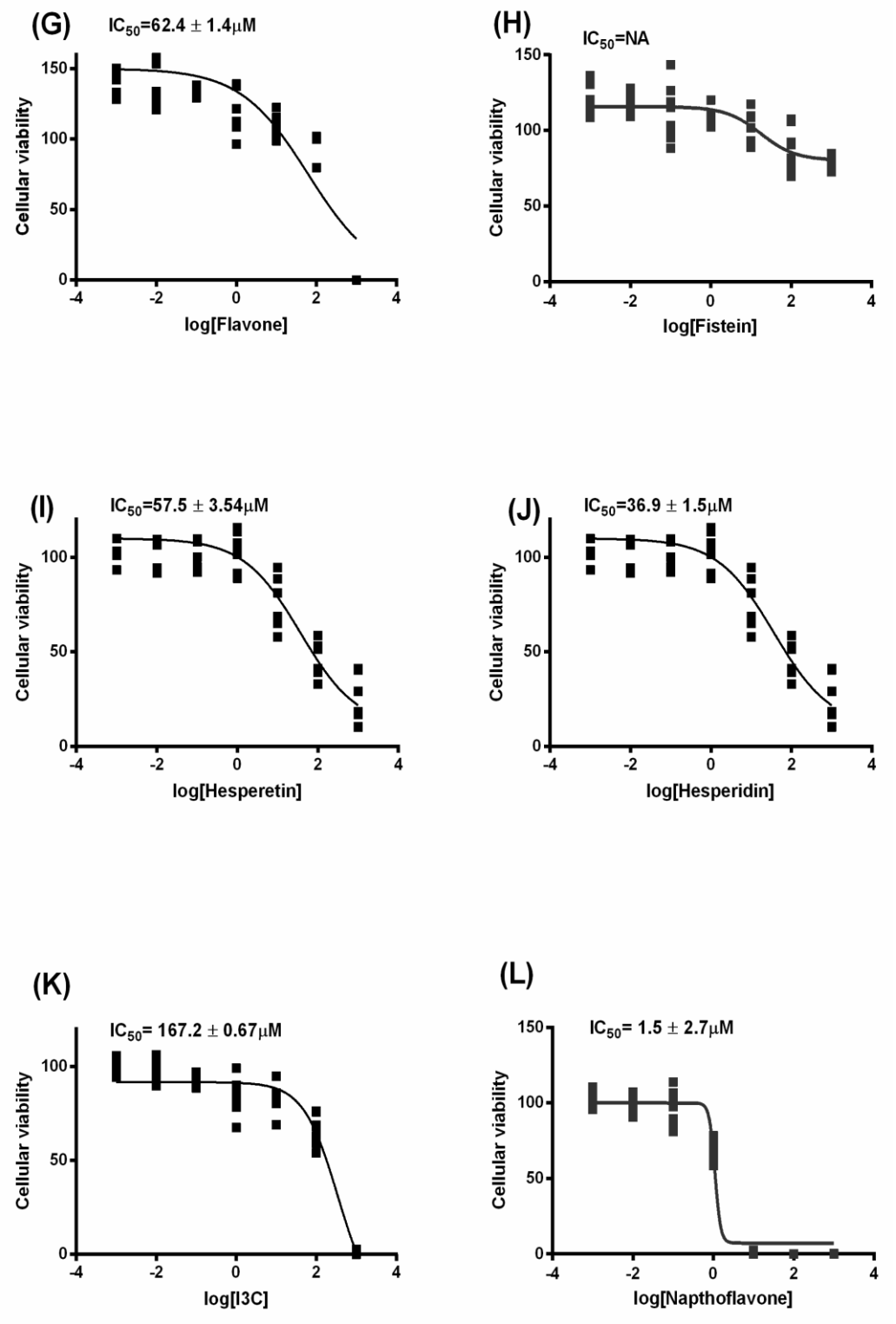

Figure 2.4: Cytotoxic assessment of modulators (G-L)

PBMEC/C1-2 cells were seeded onto gelatine coated 96-well plates at 37°C in a humidified atmosphere of 5% CO_2 in air for 24 h. Media was aspirated and cells were subsequently incubated with a 7-fold log concentration range (0.001 µM-1000 µM) of fistein (G), flavone (H), hesperetin (I), hesperidin (J), indole -3-carbinol (I3C) (K) and α-napthoflavone (L) for 24 h prior to an MTT assay being performed. Data reported as IC_{50} ± SD.

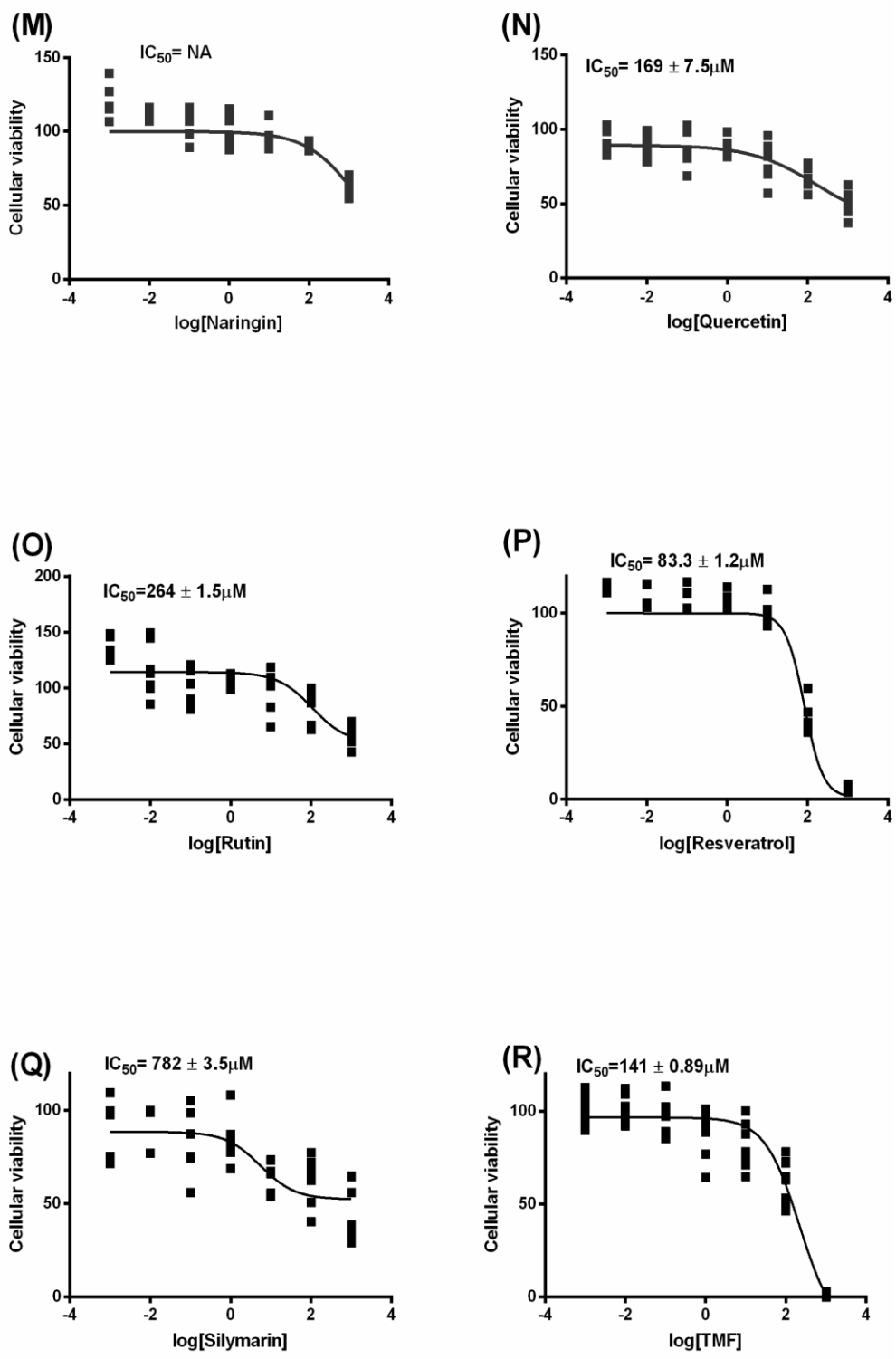

Figure 2.4: Cytotoxic assessment of modulators (M-R)

PBMEC/C1-2 cells were seeded onto gelatine coated 96-well plates at 37°C in a humidified atmosphere of 5% CO_2 in air for 24 h. Media was aspirated and cells were subsequently incubated with a 7-fold log concentration range (0.001 μM-1000 μM) of naringin (M), quercetin (N), resveratrol (O), rutin (P), silymarin (Q) and TMF(R) for 24 h, for 24 h prior to an MTT assay being performed. Data reported as IC_{50} ± SD.

2.8. Determination of BCRP expression in PBMEC/C1-2 cells

2.8.1. Determination of BCRP genomic and protein expression

PBMEC/C1-2 cells were characterised to determine the protein and genomic expression of BCRP. Reverse–transcriptase PCR confirmed the genomic expression of BCRP in PBMEC/C1-2 cells with an expected product size of 652 base pairs alongside the presence of β- actin (BA) loading control product size of 806 base pairs (Figure 2.5A). Western blot analysis further confirmed BCRP protein in PBMEC/C1-2 cells with an expected product size of 72 kDa (Figure 2.5B).

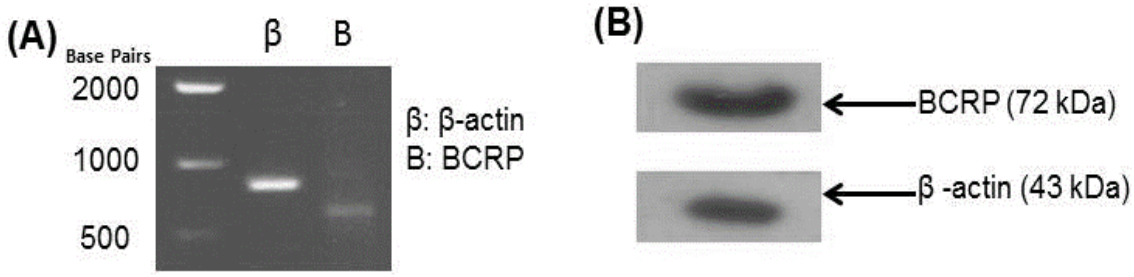

Figure 2.5: Genomic expression of BCRP in PBMEC/C1-2 cells.

(A) Genomic expression of BCRP. Cells were seeded onto a 6-well plate for 24 h. Total RNA was extracted and 400 ng of RNA was loaded reverse transcribed prior to PCR being performed. cDNA was resolved using a 2% agarose gel. A 1 kbp DNA ladder was used a size marker. (B) Protein expression of BCRP. Cells were seeded onto a 6-well plate for 24 h. Whole cell protein was extracted using RIPA buffer. Approximately 50 µg of the protein was loaded to the gel and transferred onto the PVDF membrane. The membrane was blocked and incubated with primary ABCG2 antibody for 24 h at 4°C and then incubated with goat anti-rabbit IgG-horse radish peroxidise-conjugated (Santa Cruz biotechnology, Sc-2004). Chemiluminesence detection was performed with lab made ECL.

2.8.2. Immunostaining detection of BCRP

The localisation of BCRP in PBMEC/C1-2 cells was investigated using immunostaining techniques. Following immunostaining of cells grown on cover slips, confocal laser microscopy was used to detect the membrane localisation of BCRP in PBMEC/C1-2 cells (Figure 2.6).

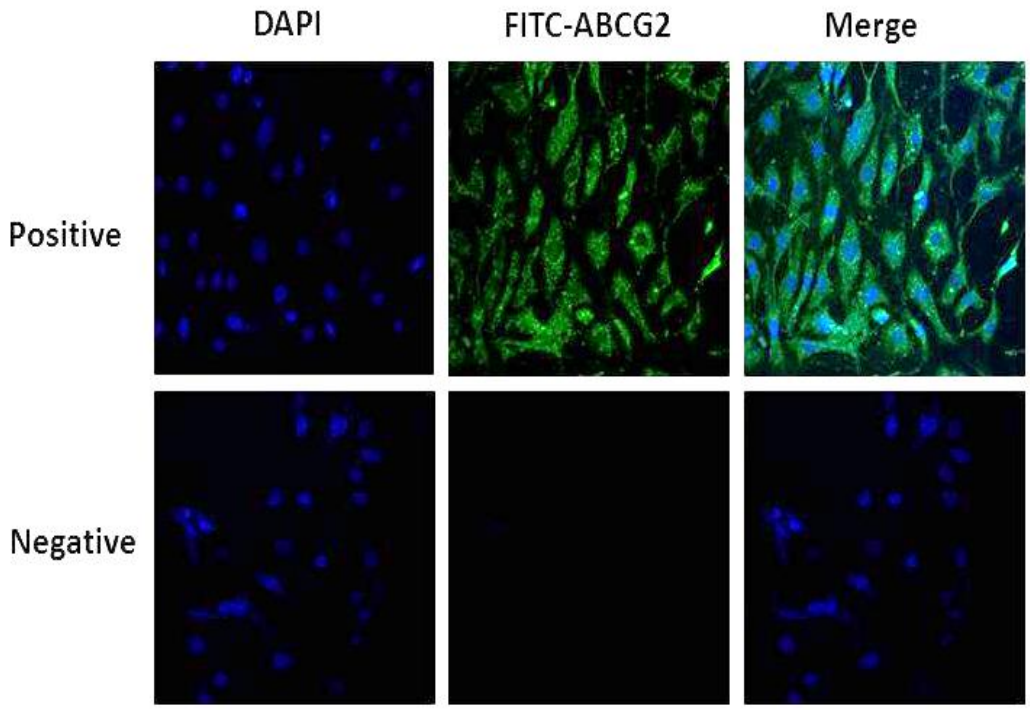

Figure 2.6: Localisation of BCRP in PBMEC/C1-2 cells.

Cells were grown on coverslips for 2-3 days and fixed with 4% paraformaldehyde and stained for BCRP using the anti-ABCG2 primary antibody and goat anti-rabbit IgG-FITC secondary antibody (green). Cell nuclei were visualised using DAPI (blue). A negative control excludes antibodies.

2.9. Measurement of BCRP cellular functional activity in PBMEC/C1-2 cells

2.9.1. Determination of optimum seeding density and incubation time

To identify an optimal seeding density and incubation time to assess the intracellular accumulation of H33342 through fluorescence measurements, H33342 accumulation was assessed under three cell densities of 1000, 10,000 and 50,000 cells per well, with incubation times of 30, 60 and 90 mins. Significantly higher ($p \leq 0.01$) intracellular H33342 accumulation was observed with 50,000 cells per well after 30 minutes of

incubation when compared with 1000 and 10,000 cells per well and 60 and 90 minutes incubation time (Figure 2.7).

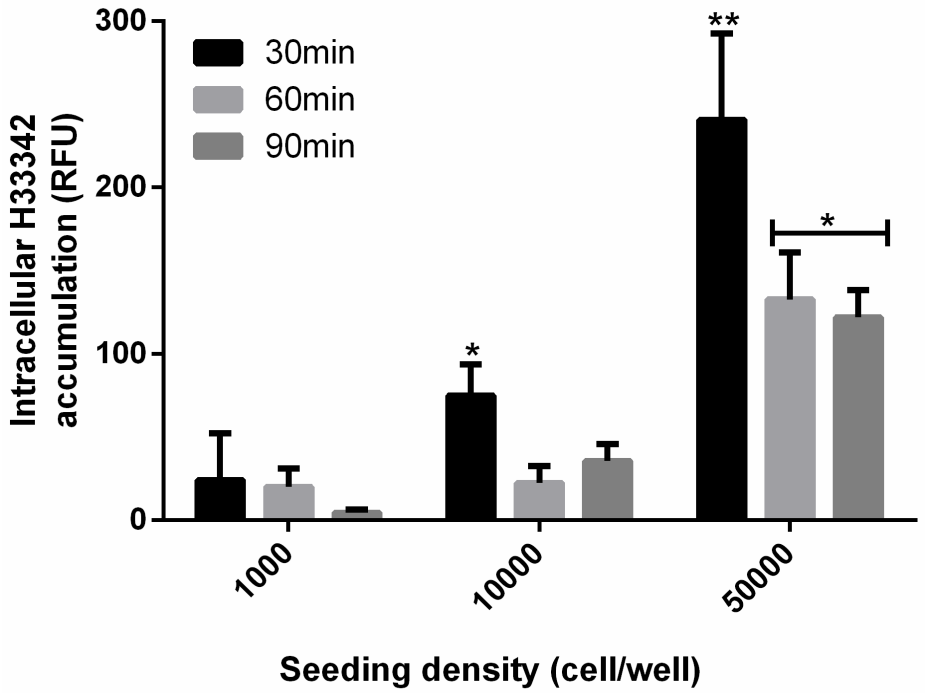

Figure 2.7: Optimisng the seeding density and incubation time of PBMEC/C1-2 cells to assess the intracellular accumulation of H33342

PBMEC/C1-2 cells were seeded with a seeding density of 1000, 10000 and 50000 cells per well of 96-well plate for 24 h. After 24 h cells were washed with HBSS and incubated with HBSS for 30 min. The cells were washed with warm HBSS prior to the addition of H33342 (10 µM) prepared in HBSS and incubated for 30 min, 60 min and 90 min. After each time point, cells were washed with ice cold HBSS twice and plates lysed at at -80°C for 2 min before the intracellular accumualtion of H33342 assessed using a fluoresecent plate reader with an excitation wavelength of 355 nm and an emission wavelength of 460 nm. Significant differences between cell number (1000,10,000 and 50,000) and incubation times (30,60 and 90 min) with control (1000,10,000 and 50,000 cells but without H33342) are indicated above the appropriate error bars (** $P \leq 0.01$).

2.9.2. Assessment of the intracellular H33342 accumulation in the absence and presence of Ko143

The intracellular accumulation of H33342 in the absence and presence of Ko143, a known potent inhibitor of BCRP, was assessed to investigate the functional expression of BCRP in PBMEC/C1-2 cells. Our results demonstrated that the intracellular accumulation of H33342 was significantly increased ($p < 0.0001$) following a 1 h incubation with Ko143 over a wide concentration range of Ko143 (0.0039 µM - 5 µM)

leading to an approximately 3.5-fold increase in H33342 accumulation (Figure 2.8) over all concentration studied.

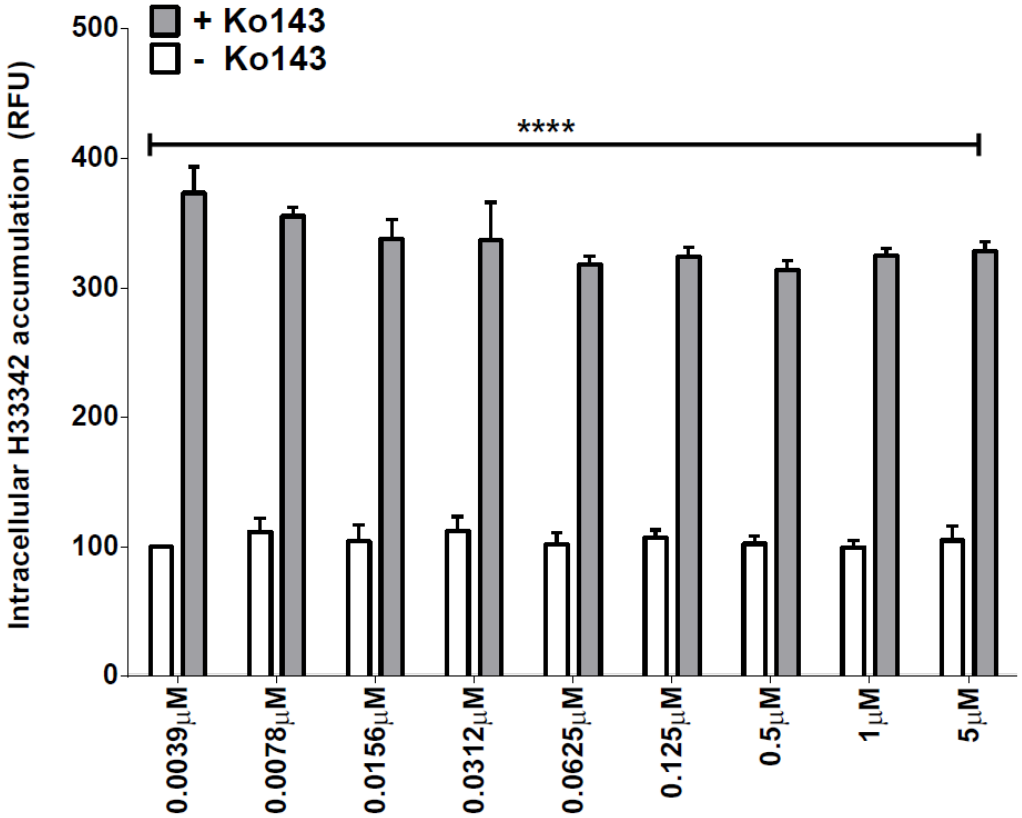

Figure 2.8: Ko143 mediated inhibition of BCRP efflux function in PBMEC/C1-2

20,000 cells/well were seeded into a clear 96-well plate and left to attach at 37°C and 5% CO_2 for 24 h. Subsequently cells were washed with PBS to remove media and 200 µL of growth media a range of Ko143 concentration (0.0039 µM-5 µM) was added and the plate pre-incubated for 1 h before the media was removed. Thereafter the cells were again incubated with media containing Ko143 (0.0039 µM-5 µM) in addition to 10 µM H33342 for 30 min before the intracellular accumualtion of H33342 assessed using a fluoresecent plate reader with an excitation wavelength of 355 nm and an emission wavelength of 460 nm. Significant differences between control and Ko143 concentrations are indicated above the appropriate error bars (**** $p \leq 0.0001$).

2.9.3. Measurement of the auto-fluorescence of phytochemicals

The inherent fluorescent properties of modulators were important to assess when using a fluorescent probe substrate for BCRP in an intracellular accumulation studies. Modulators were screening for their fluorescent properties using H33342 as a reference. The majority of modulators demonstrated no fluorescence signals when compared to H33342 (data not shown, $p < 0.05$). However, fistein, α-napthoflavone and baiclain demonstrated no statistically significant differences in fluorescence when

compared to H33342, and hence were classified as compounds that possessed auto-fluorescence which overlaps with H33342 (Figure 2.9).

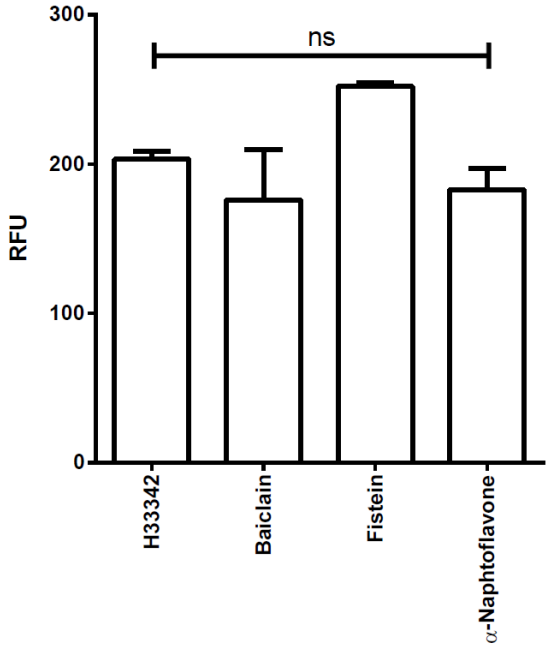

Figure 2.9: Auto-fluorescence of modulators.

25µM working stocks of baiclain, fistein and napthoflavone were prepared and transferred to a black 96-well plate. The autofluorescence of modulators was measured on a fluorescence plate reader at an excitation wavelength of 360 nm and emission wavelength of 460 nm. Statistical comparison were made between background (HBSS+) and H33342/modulators. **** $p \leq 0.0001$.

2.9.4. Modulator mediated inhibition of BCRP function in a H33342 intracellular accumulation assay

To assess the potential for modulators to directly inhibit BCRP function, the intracellular accumulation of H33342 was assessed following the incubation PBMEC/C1-2 cells with modulators. Our results demonstrated significant increase of H33342 accumulation ($p \leq 0.0001$) with most of the modulators studied across a concentration range of 1-100 µM (Figure 2.10). Furthermore the fold change in H33342 was significantly greater than that observed for Ko143 for apigenin (1 µM), hesperidin (1 µM), I3C (1-100 µM) and 2,6,4-trimethoxyflavone (TMF) (1-100 µM) and increasing H33342 accumulation by 2.5 ± 0.2 fold, 2.6 ± 0.5 fold, 3.5 - 4.5 mean fold range and 4.5 - 6.5 mean fold range respectively when compared with the known inhibitor of BCRP, Ko143 (represented by the grey shaded area in figure 2.10). Interestingly, quercetin, resveratrol and rutin did not show any significant accumulation when compared to Ko143.

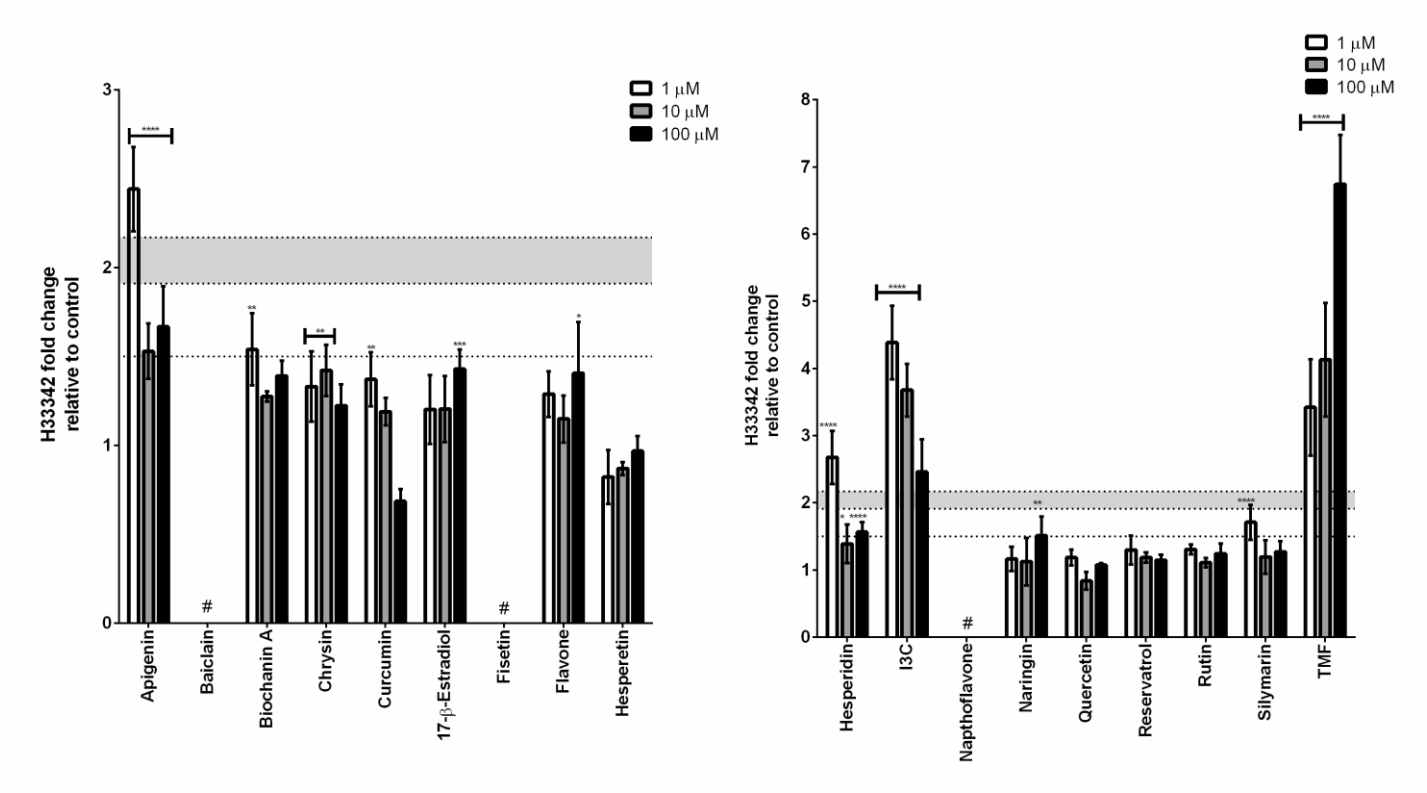

Figure 2.10: Modulation of intracellular accumulation of H33342 following a 1-hour incubation with modulators.

Cells were grown in a 96 well plate for 48 h and washed with warm HBSS supplemented and incubated for 1 h with media containing 1-100μM of test compound. Subsequently cells were incubated with media containing H33342 for 30 min and lysed. The change in H33342 intracellular accumulation in the presence of Ko143 is highlighted by the shaded region. Significant differences between Ko143 and modulators are indicated above the appropriate error bars. * P ≤ 0.05, ** P ≤ 0.01, *** P ≤ 0.001 and **** P ≤ 0.0001. The hash symbol (#) indicates modulators excluded due to auto-fluorescence.

2.9.5. Modulator mediated changes in BCRP function following 24 hours incubation

Time dependent functional activity of BCRP was also evaluated following incubation of H33342 in the presence of modulators for a 24 h period. PBMEC/C1-2 cells were exposed to modulators at 1 µM, 10 µM and 100 µM. Our results demonstrated that apigenin (1 µM and 10 µM), chrysin (1-100 µM),17-β-estradiol (1 µM and 10 µM), I3C (10 µM and 100 µM), silymarin (1-100 µM) and (TMF) (1-100µM) has shown significant increase in intracellular H33342 accumulation by 1.15-1.25, 1.26-1.35, 1.3, 1.25 -1.26, 1.25-1.6 and 1.20-1.45 mean fold change when compared to control (Figure 2.11). Furthermore, hesperetin (0.7-0.8 mean fold change), naringin (0.3-0.71 mean fold change) and quercetin (0.75-1 mean fold change) demonstrated significant downregulation of intercellular H33342 accumulation by when compared to control across all concentration (1-100 µM) studied.

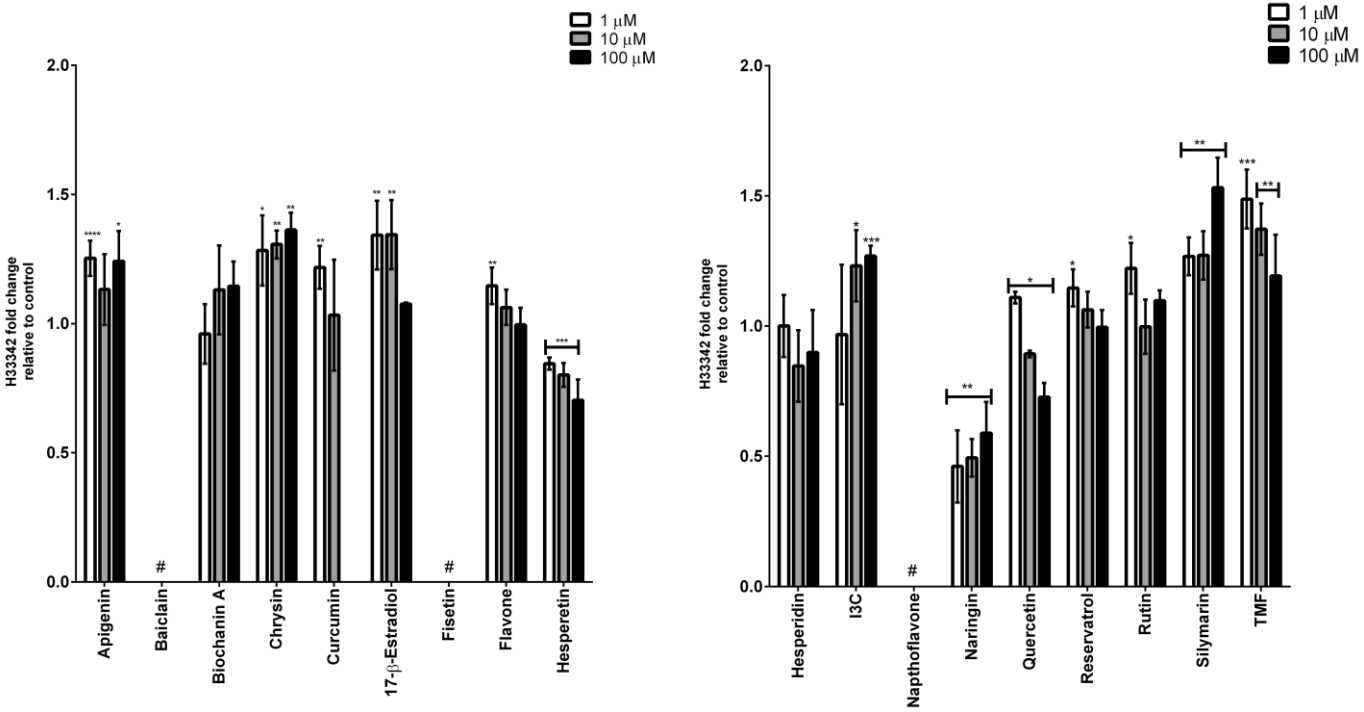

Figure 2.11: Modulation of intracellular accumulation of H33342 following a 24-hour incubation with modulators.

Cells were grown in a gelatine coated 96 well plate for 24 h and washed with pre- warm HBSS supplemented and incubated for 24h with media containing 1-100μM of test compound . After 24 h cells were incubated with media containing H33342 for 30 min and lysed. Significant differences between control and modulators are indicated above the appropriate error bars. * P ≤ 0.05, ** P ≤ 0.01, *** P ≤ 0.001 and **** P ≤ 0.0001. The hash symbol (#) indicates modulators excluded due to autofluorescence.

2.10. Modulation of BCRP protein expression by phytochemical modulators

To assess the impact of modulators on the protein expression of BCRP, PBMEC/C1-2 cells were exposed to modulators for 24 hours and changes in protein expression were assessed through western blotting. A significant induction of BCRP protein was observed for biochanin A (2.65 ± 0.12 fold), hespiridin (2.42 ± 0.19 fold), I3C (1.4 ± 0.09 fold), naringin (2.2 ± 0.17 mean fold change) and quercetin (2.3 ± 0.12 fold). Furthermore, a significant ($p \leq 0.01$) down-regulation of BCRP was observed with curcumin (0.4 ± 0.2 fold) and 17-β-estradiol (0.41 ± 0.1 fold) (Figure 2.12 and 2.13).

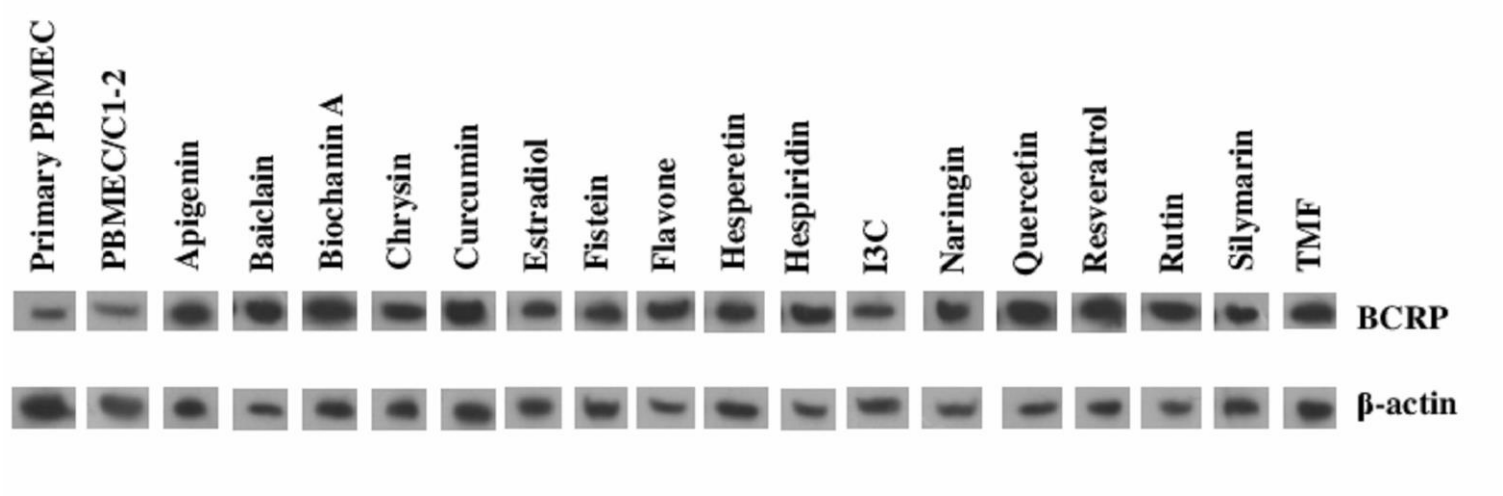

Figure 2.12: Changes in BCRP protein expression under 24-hours exposure to modulators

Cells were seeded in a 6-well plate for 24 h to attach and subsequently incubated with 25 µM modulator except for 17-β-estradiol (100nM) for 24 h. Whole cell protein was extracted using RIPA buffer and approximately 50 µg of isolated protein was loaded onto a SDS-PAGE gel to separate proteins bands. The resulting gel was then transferred onto a PVDF membrane and incubated with anti-ABCG2 antibody for 24 h at 4°C followed by incubation with goat anti-rabbit IgG-horse radish peroxidise-conjugated antibody. Chemiluminesence detection was performed with lab made ECL and a representative image is displayed. Primary PBMEC and PBMEC/C1-2 bands are non-modulator (control) samples for each cell line.

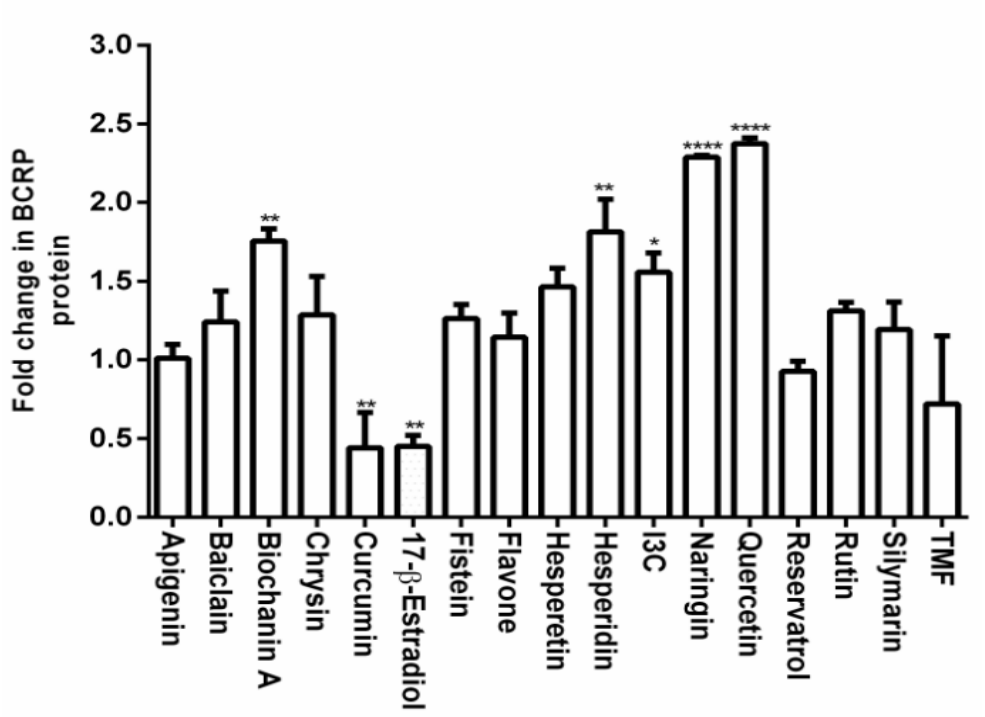

Figure 2.13: Fold change in BCRP protein expression following 24-hours exposure to modulators

Cells were seeded in a 6-well plate for 24 h to attach and subsequently incubated with 25 µM modulator except for 17-β-estradiol (100nM) for 24 h. Significant differences in protein expression when compared to control are indicated above the appropriate error bars. * $p \leq 0.05$, ** $p \leq 0.01$ and **** $p \leq 0.0001$.

2.11. Quantitative PCR assessment of the changes in BCRP genomic following exposure to modulators

The modulation of BCRP genomic expression was evaluated by qPCR with two up-regulators (quercetin and naringin) and two down-regulators (curcumin and 17-β-estradiol) selected from the western blot results. A significant increase ($p \leq 0.0001$) in the genomic expression of BCRP was observed for quercetin (1.63 ± 0.28 fold) and naringin (1.36 ± 0.71 fold), relative to control samples, whereas curcumin and 17-β-estradiol demonstrated significant down-regulation of 1.78 ± 0.05 fold ($p \leq 0.0001$) and 1.54 ± 0.05 fold ($p \leq 0.01$) respectively (Figure 2.14).

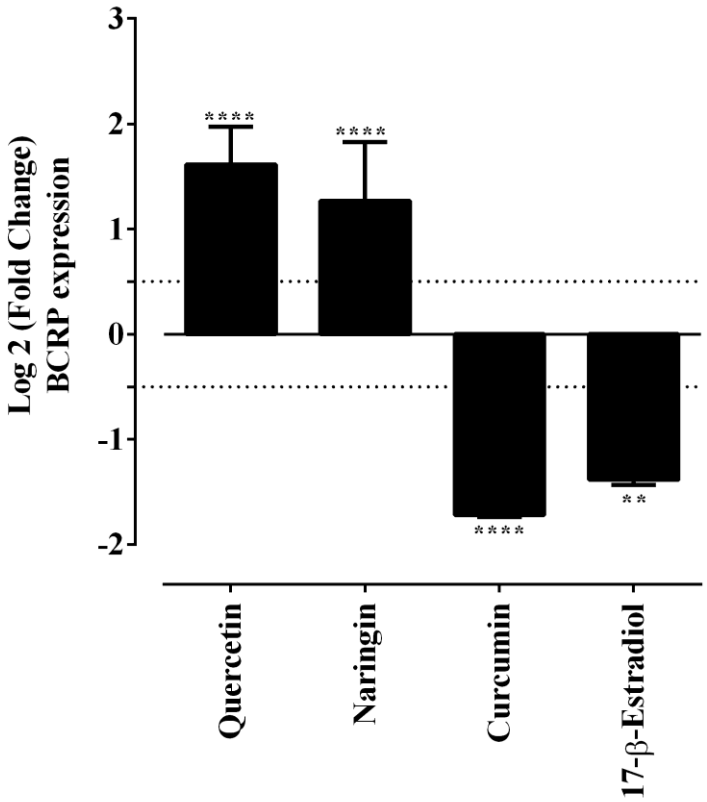

Figure 2.14: Modulation of BCRP gene expression after 24 h incubation with modulator compounds.

PBMEC/C1-2 cells were seeded onto a 6-well plate and allowed to attach for 24 h. The media was removed and modulators prepared in media were added to the wells and incubated for 24 h. After 24 h the media was removed and cells washed with pre-warmed PBS prior to RNA extraction. Total RNA was reverse transcribed and gene expression assessed by qPCR using a SYBR green master mix. Dashed line indicated 0.5-fold change. Significant differences between control and modulators are indicated above the appropriate error bars. *** $P \leq 0.001$ and **** $P \leq 0.0001$.

2.12. Modulation of BCRP transport function in an *in-vitro* permeable insert BBB model

2.12.1. Generation of a PhA standard curve

A standard curve for the fluorescent detection of PhA was developed over a concentration range of 0.01-50 µM. A linear correlation was displayed over this concentration range with an r^2 =0.9967 (Y=1.5897 x-3.4248) (Figure 2.15). The lowest limits of quantification was found to be 0.01 µM.

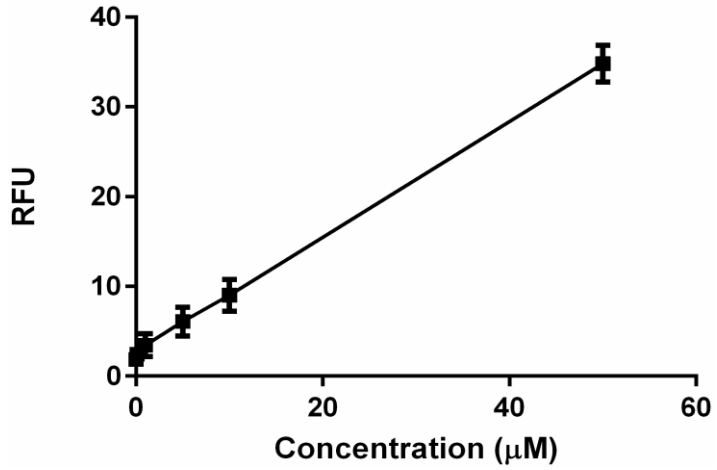

Figure 2.15: PhA standard curve

Concentrations of PhA (0.1µM-100µM) were prepared in serum free transport media and 100 µL transferred into wells of a 96-well for fluorescence measurement.

2.12.2. Impact of transport media on *in-vitro* BBB monolayer integrity

To assess the impact of transport media on the stability of the monolayer formation, preliminary transport studies were conducted assessing the impact of HBSS transport media (HBSS supplemented 10mM glucose and 10 mM HEPES) and SFM on the resistance of the monolayer. It was demonstrated that the TEER of the inserts maintained in HBSS media started to significantly decrease ($p \leq 0.05$) over the study period from 75-80Ω.cm^2 at 30 min to 32-35 Ω.cm^2 at 150 min (Figure 2.16). In contrast, TEER values of the inserts maintained in SFM were relatively consistent over 210 min with no significant decrease in TEER when compared to 30 min.

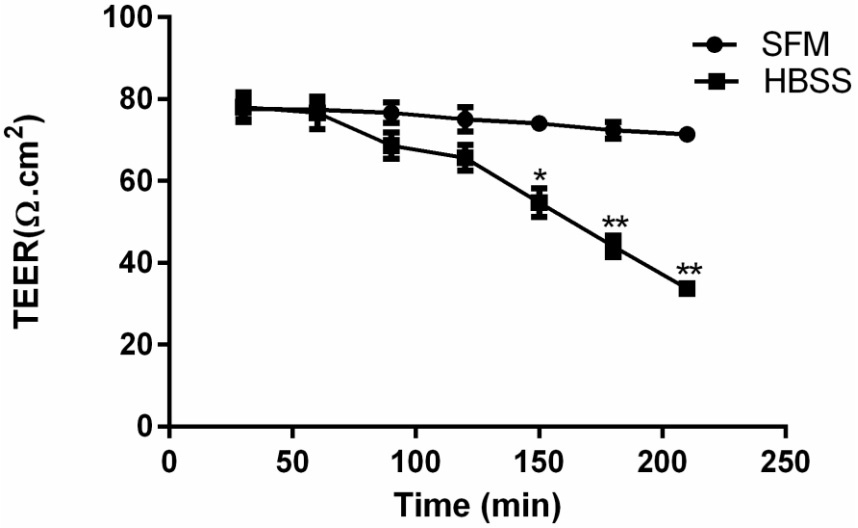

Figure 2.16: TEER values of PBMEC/C1-2 cells maintained in HBSS and SFM, grown on permeable inserts.

Cells were seeded onto collagen coated permeable inserts and allowed to grown for 4 days. The inserts were transferred to either HBSS or SFM media and maintained for up to 210 min, with TEER values measured during the study period. Significant, differences between HBSS and serum free media are indicated above the appropriate error bars * $p \leq 0.05$, ** $p \leq 0.01$.

2.12.3. Functional assessment of BCRP in an *in-vitro* permeable insert BBB model

The function of BCRP in a representative *in-vitro* BBB model was assessed by measuring the transport of PhA in the presence or absence of Ko143, a known BCRP inhibitor. Our results demonstrated that 1 h incubation with Ko143 (1 µM) significantly increased the apical-to-basolateral (AB) flux of PhA from 90 min onwards during our transport studies ($p < 0.05$) (Figure 2.17) and this was associated with an increase in $P_{app,AB}$ from 27.2 ± 0.23 $x10^{-6}$ cm/s to 43.23 ± 0.32 x 10^{-6} cm/s following Ko143 incubation.

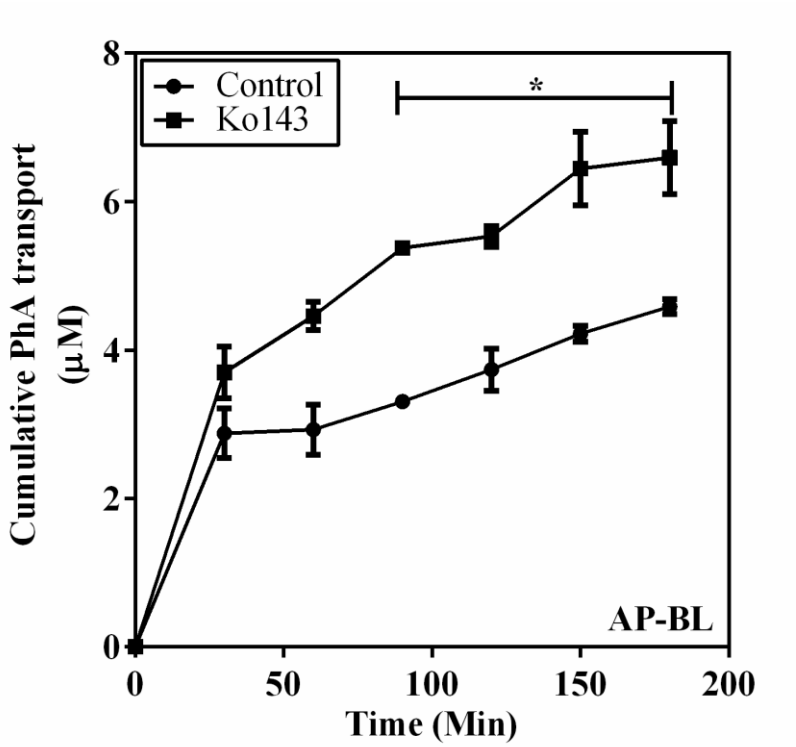

Figure 2.17: Cumulative transport of PhA across an *in-vitro* BBB model.

Cells were grown on permeable inserts and transport studies were performed on day 4 in the presence and absence of Ko143. Statistically significant differences between control and Ko143 samples at each data point are indicated. * $P \leq 0.05$.

2.12.4. Modulation of BCRP function in the absence and presence of up-regulators

To assess the impact of BCRP protein up-regulators on the functional efflux of PhA, quercetin and naringin were incubated with PBMEC/C1-2 cells, grown on permeable inserts, for 24 h prior to the initiation of a transport studying with PhA alone. When the transport study was initiated with PhA added to the apical compartment and sampling from the basolateral compartment, no significant differences in the transport kinetics of PhA were observed for quercetin and naringin when compared to control (Figure 2.18)

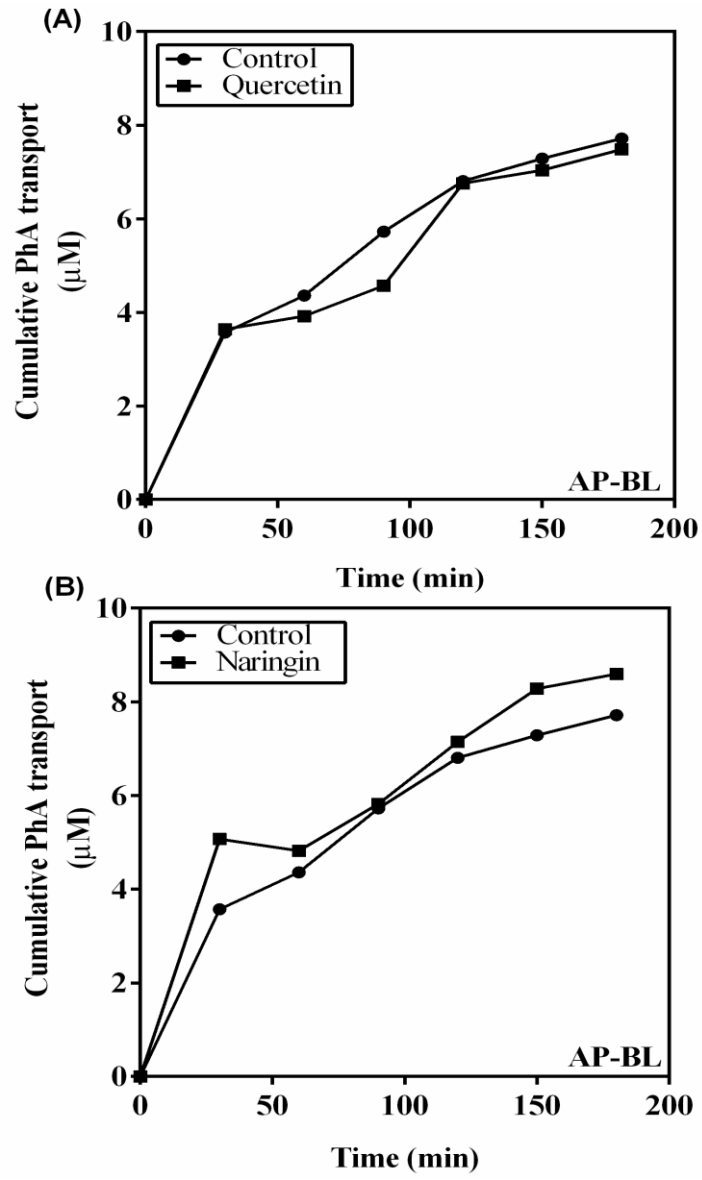

Figure 2.18: Transport of PhA across an *in-vitro* BBB cell culture model following 24 hour incubation with quercetin or naringin

Cells were grown on permeable inserts and pre-treated for 24 h with quercetin and naringin. Thereafter the transport of PhA was assessed on day 4 following the addition of PhA to the apical compartment and sampling basolaterally.

As an induction-effect was expected, incubation was repeated by the addition of compounds into the basolateral compartment with sampling from the apical compartments. Our results demonstrated that 24 h incubation of naringin (25 µM) significantly increased the basolateral-to-apical (BA) transport of PhA during our transport studies ($p < 0.01$) (Figure 2.19), with a BA permeability ($Papp_{,BA}$) of PhA of 74.23 ± 0.29 x10^{-6} cm/s when compared to the absence of naringin (23.13 ± 0.31 x 10^{-6} cm/s). Similarly for quercetin (25 µM), our results demonstrated a significant

increase ($p \leq 0.01$) in the BA transport of PhA with a BA permeability ($Papp_{,BA}$) of PhA of 63.21 ± 0.54 $x10^{-6}$ cm/s.

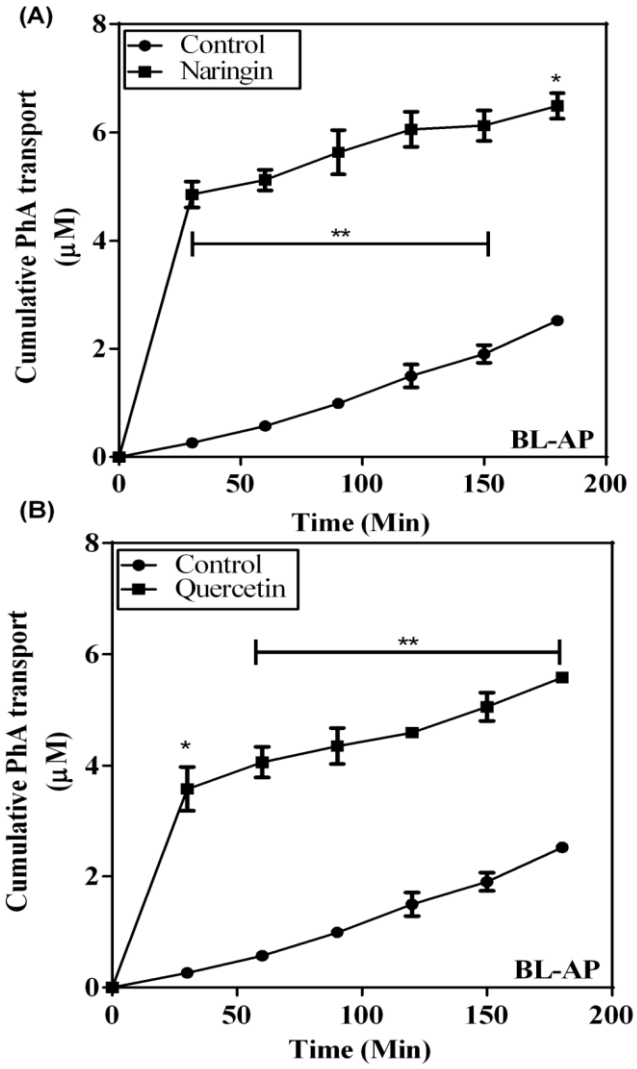

Figure 2.19: Transport of PhA across an *in-vitro* BBB cell culture model following 24 hour incubation with quercetin or naringin.

Cells were grown on permeable inserts and pre-treated for 24 h with quercetin and naringin. Thereafter the transport of PhA was assessed on day 4 following the addition of PhA to the basolateral compartment and sampling apically. Statistically significant differences between control and modulator exposed conditions are indicated as * $P \leq 0.05$, ** $P \leq 0.01$.

2.12.5. Functional assessment of BCRP in the presence of BCRP down-regulating modulators

The functional assessment of BCRP was evaluated in the presence of BCRP down-regulators namely, curcumin (1 µM) and 17-β-estradiol (100 nM) in an *in-vitro* BBB model by measuring the transport of PhA. Our results demonstrated that 24 h incubation of curcumin and 17-β-estradiol significantly increased the apical-to-basolateral (AB) passive permeability ($Papp_{,AB}$) of PhA from 27.20 ± 0.23 $x10^{-6}$ cm/s in the absence of modulators to 78.81 ± 0.65 $x10^{-6}$ cm/s and 48.11 ± 0.34 $x10^{-6}$ cm/s in the presence of curcumin and 17-β-estradiol respectively (Figure 2.20).

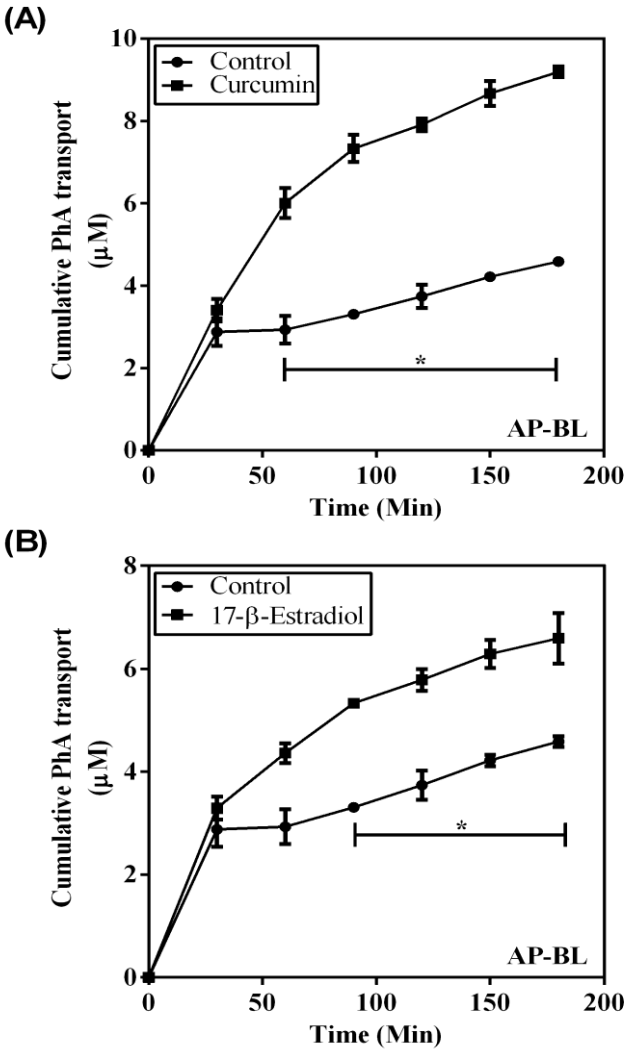

Figure 2.20: Transport of PhA across an *in-vitro* BBB cell culture model following 24 hour incubation with curcumin or 17-β-estradiol.

Cells were grown on permeable insert and transport studies were performed on day 4 using 1 µM curcumin and 100 nM 17-β-estradiol. Statistically significant differences between control and modulator exposed conditions are indicated as * P ≤ 0.05.

2.13. Characterisation of an *in-vitro* primary porcine brain BBB model

2.13.1. Morphology of porcine brain primary endothelial cells

Primary porcine brain microvascular endothelial cells were successfully isolated and grown on collagen coated T75 flasks. Explants seeded on the coated flasks were visually observed under light microscope using 10x and 40x lenses. The isolated capillaries explants were observed initially as short fragments. On the day 3, explants had fully attached and endothelial cells proliferated from the explants and formed island of cells. On day 5, the cell patches began to reveal a uniform packed monolayer and reached confluence on day 10 (Figure 2.21).

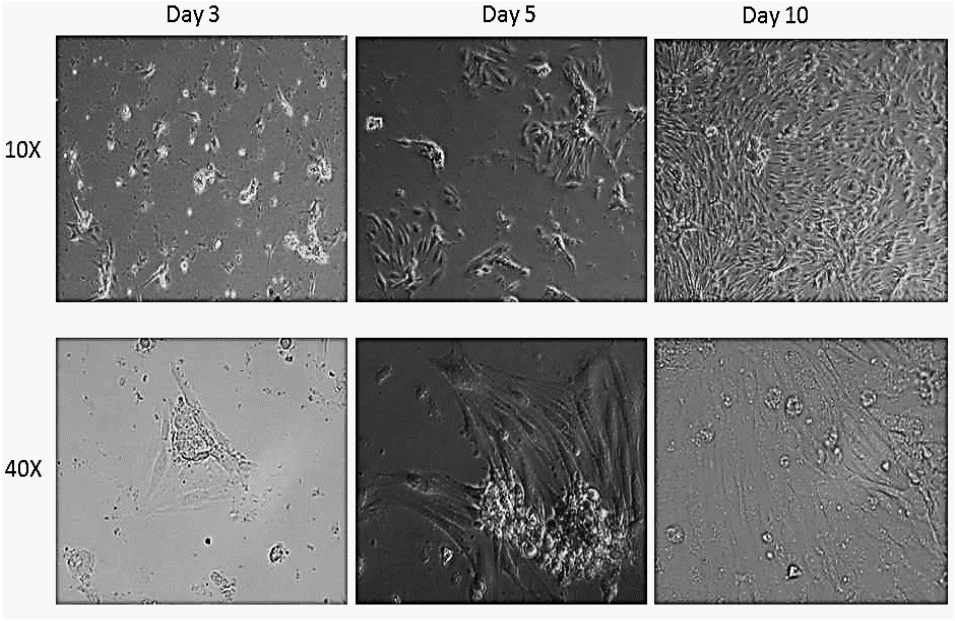

Figure 2.21: Growth of primary porcine brain endothelial cells

Explant cells were seeded on collagen coated flasks for 10 days at 37°C in a humidified atmosphere of 5% CO_2 in air. Cells morphology was examined under light microscope at 10x and 40x lenses.

2.13.2. Treatments to enhance barrier integrity

Monolayer formation and barrier integrity was assessed by measuring TEER values 24 h post-seeding and for a total of 5 days. TEER values increased significantly on day 3 reaching 80-95 $\Omega.cm^2$ ($p \leq 0.01$) and 120-125 $\Omega.cm^2$ on day 4 ($p \leq 0.001$) before declining thereafter (Figure 2.22).

Cells were treated with cAMP, RO 20-1724 and hydrocortisone for 24 h on day 3 and demonstrated TEER values that were significantly increased to 120-125$\Omega.cm^2$ on day 4 ($p \leq 0.01$) (Figure 2.22).

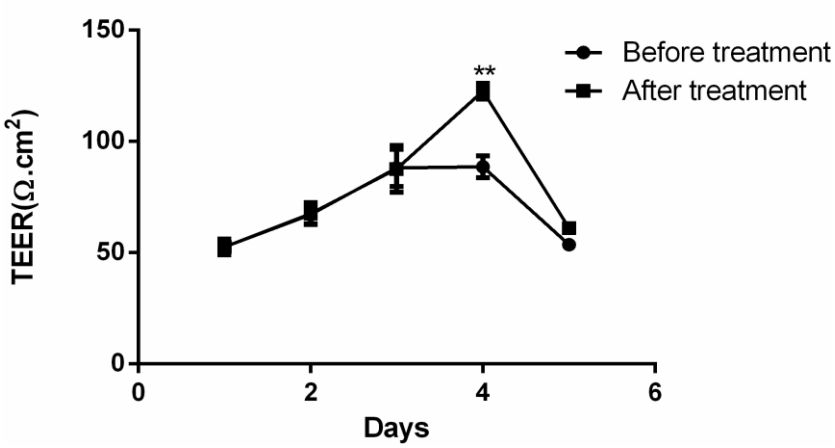

Figure 2.22: The impact of media additives to enhance monolayer formation.

Primary porcine brain endothelial cells were seeded onto collagen coated permeable inserts for 4 days at 37°C in a humidified atmosphere of 5% CO_2 in air. TEER values were measured and treatment with cAMP, RO 20-1724 and hydrocortisone initiated on day 3 for 24 h. Statistically significant differences before treatment and after treatment are indicated as ** $P \leq 0.01$.

2.13.3. Immunostaining detection of BCRP in primary porcine brain endothelial cells

The expression of BCRP in porcine primary brain endothelial cells (‘60s’) cultured on a permeable insert monolayer was investigated using immunostaining techniques. BCRP was found to be localised primarily in the plasma membrane regions. Furthermore, the formation of a monolayer structure was apparent by the overlapping nature of the brain endothelial cells (Figure 2.23)**.**

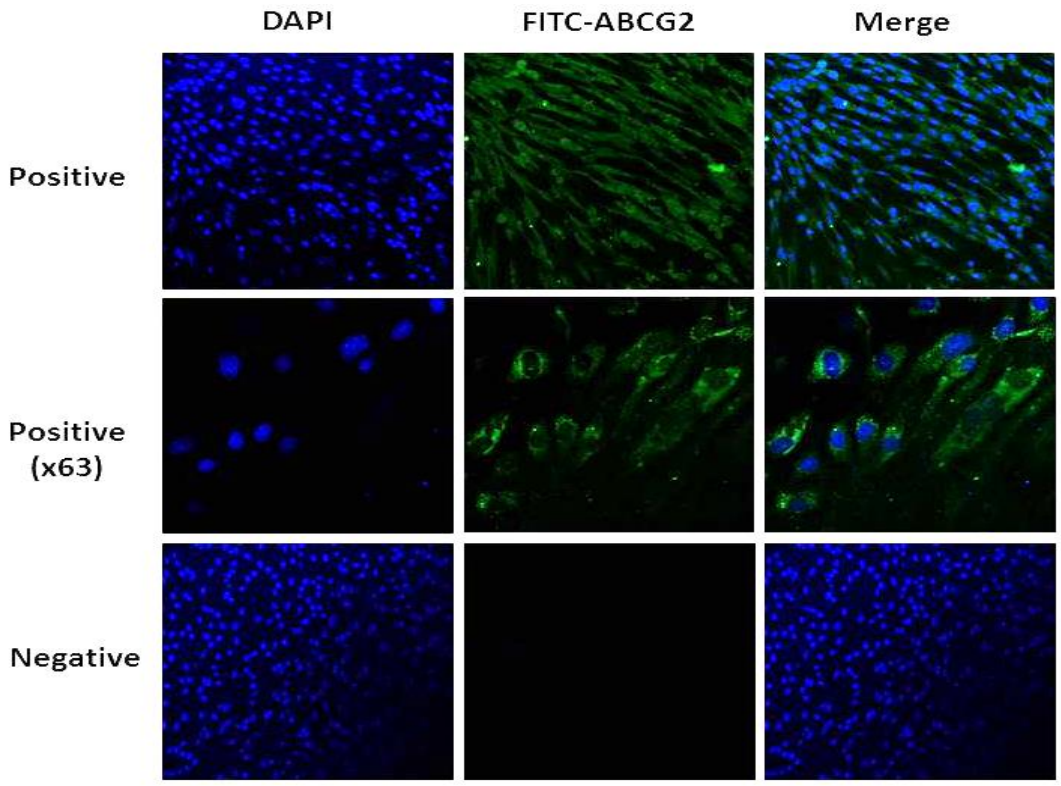

Figure 2.23: Localisation of BCRP in primary brain endothelial cells.

Cells were grown on permeable inserts for 3-4 days and fixed with 4% paraformaldehyde and stained for BCRP using the anti-ABCG2 primary antibody and goat anti-rabbit IgG-FITC secondary antibody (Green). Cell nuclei were visualised using DAPI (blue). Positive control included staining for anti-ABCG2 whereas the negative control did not include the primary antibody.

2.13.4. Determination of BCRP protein expression

The protein expression of BCRP in primary endothelial cells was determined by western blot analysis. BCRP was successfully demonstrated to be expressed in primary porcine brain cells with an expected size of 72 kDa (Figure 2.24).

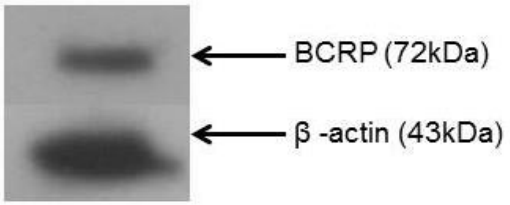

Figure 2.24: Protein expression of BCRP in primary porcine brain microvascular endothelial cells.

Cells were seeded onto a 6-well plate for 24 h. Whole cell protein was extracted using RIPA buffer. Approximately 50 µg of the protein was loaded to the gel and transferred onto the PVDF membrane. The membrane was blocked and incubated with primary ABCG2 antibody for 24 h at 4°C and then incubated with goat anti-rabbit IgG-horse radish peroxidise-conjugated. Chemiluminesence detection was performed with lab made ECL.

2.13.5. Determination of cytotoxicity of modulators in primary cells

The cellular toxicity of modulators towards the primary porcine brain endothelial cells was investigated using MTT toxicity assay. Cells were exposed to 25 µM and 100 µM of modulators for 24 h. The highest cytotoxicity was observed for curcumin and α-napthoflavone at 100 µM leading to 80-75% reduction in cell growth (Figure 2.25). Similarly, apigenin, baiclain, biochanin A (100µM), 17-β-estradiol (100µM), flavone (100µM), hesperetin (100µM) and TMF demonstrated 25-50 % reduction in cellular viability. Additionally a number of modulators demonstrated minimal toxicities up to 100 µM and included biochanin A (10µM), chrysin, fistein, hesperidin, naringin, quercetin, resveratrol, rutin and silymarin (Figure 2.25).

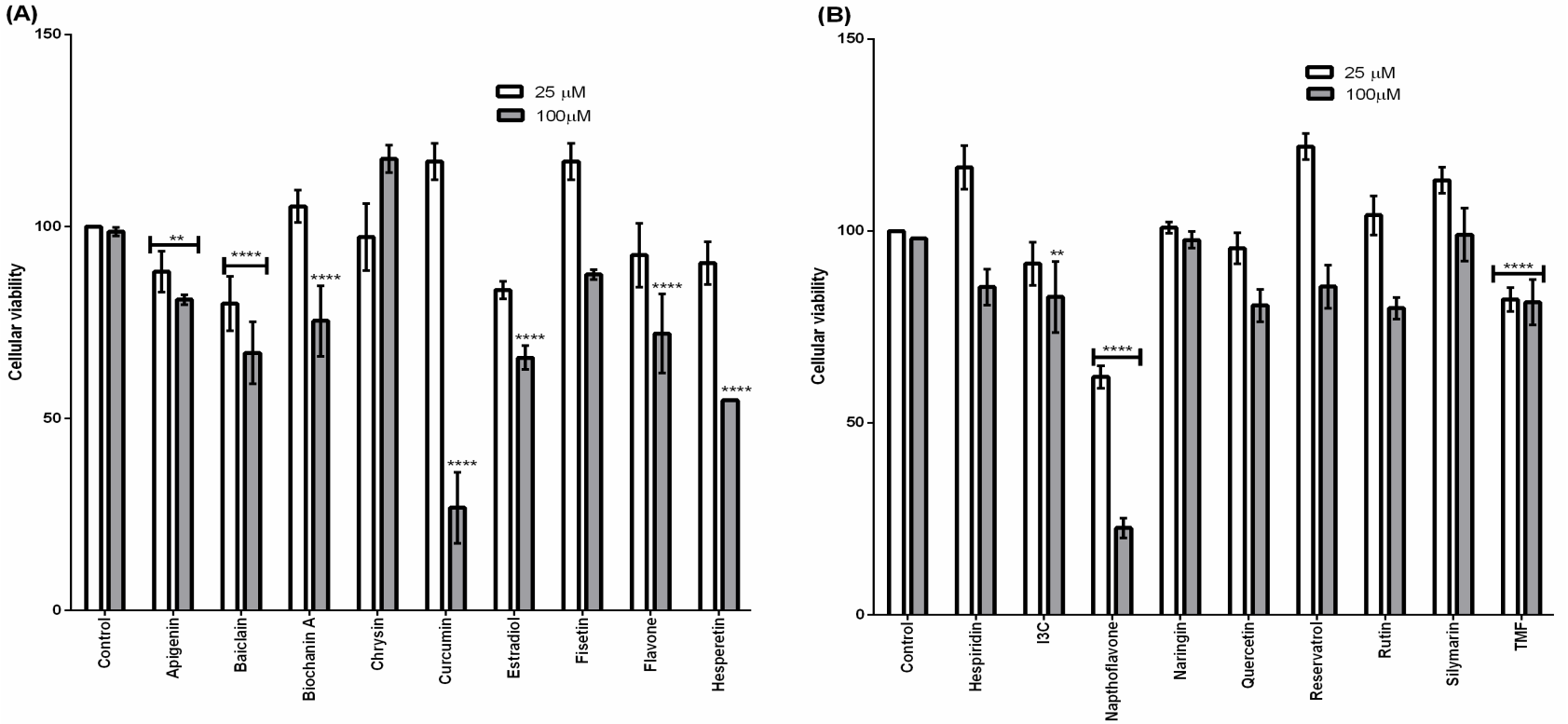

Figure 2.25: Cellular toxicity of modulators towards primary porcine brain endothelial cells.

Cells were seeded onto collagen coated 96-well plates for 10 days. The media was aspirated and cells were incubated for 24 h with 25 µM and 100 µM of modulators. Thereafter the media was replaced and 20 µl of MTT solution added to each well and plate was incubated at 37°C for 4h. The media was carefully aspirated and 100µl of the DMSO was added to each well and the UV-absorbance was measured at wavelength of 560nm.

2.13.6. Modulation of BCRP transport function in a permeable insert based *in-vitro* BBB model

2.13.6.1. Functional assessment of BCRP

BCRP functionality was investigated in a representative *in-vitro* BBB permeable insert model by measuring the transport of PhA in the presence or absence of Ko143, a known BCRP inhibitor. Our results demonstrated that a 1 h incubation with Ko143 (1 µM) significantly increased the apical-to-basolateral (AB) transport of PhA from 30 min onwards during our transport studies ($p < 0.05$) with a $P_{app,AB}$ of 109.75 ± 1.21 $x10^{-6}$ cm/s compared to the absence of Ko143, 60.57 ± 1.32 $x10^{-6}$ cm/s (Figure 2.26).

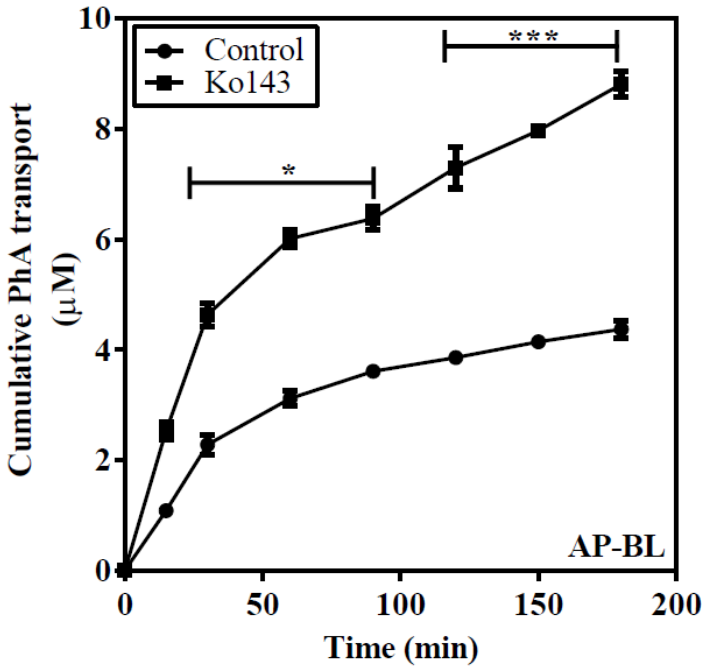

Figure 2.26: Transport of PhA across an *in-vitro* primary BBB cell culture model following 1-hour incubation Ko143.

Cells were grown on permeable inserts and transport studies were performed on day 4 in the absence and presence of Ko143.Statistically significant differences between control and Ko143 are indicated.* P ≤ 0.05.

2.13.6.2. Modulation of BCRP function in the absence and presence of up-regulators

Naringin and quercetin demonstrated up-regulation of BCRP protein expression in PBMEC/C1-2 cells and were selected as modulators to assess in the primary cell culture model. Primary cells were seeded onto permeable inserts and incubated with quercetin and naringin for 24 h with the addition of PhA and modulators into the basolateral chamber and sampling from the apical chamber.

Our results demonstrated that 24 h incubation of quercetin (25 µM) significantly increased the basolateral-to-apical (BA) transport of PhA during our transport studies ($p < 0.01$) (Figure 2.27A), with a BA permeability ($Papp_{,BA}$) of PhA of 102.93 ± 1.98 x 10^{-6} cm/s in the presence of quercetin compared to 38.57 ± 2.15 x10^{-6} cm/s in the absence of quercetin. Similarly for naringin (25 µM), our results demonstrated a significant increase ($p \leq 0.01$) in the BA transport of PhA with a BA permeability ($Papp_{,BA}$) of PhA of 98.21 ± 1.23 x10^{-6} cm/s (Figure 2.27B).

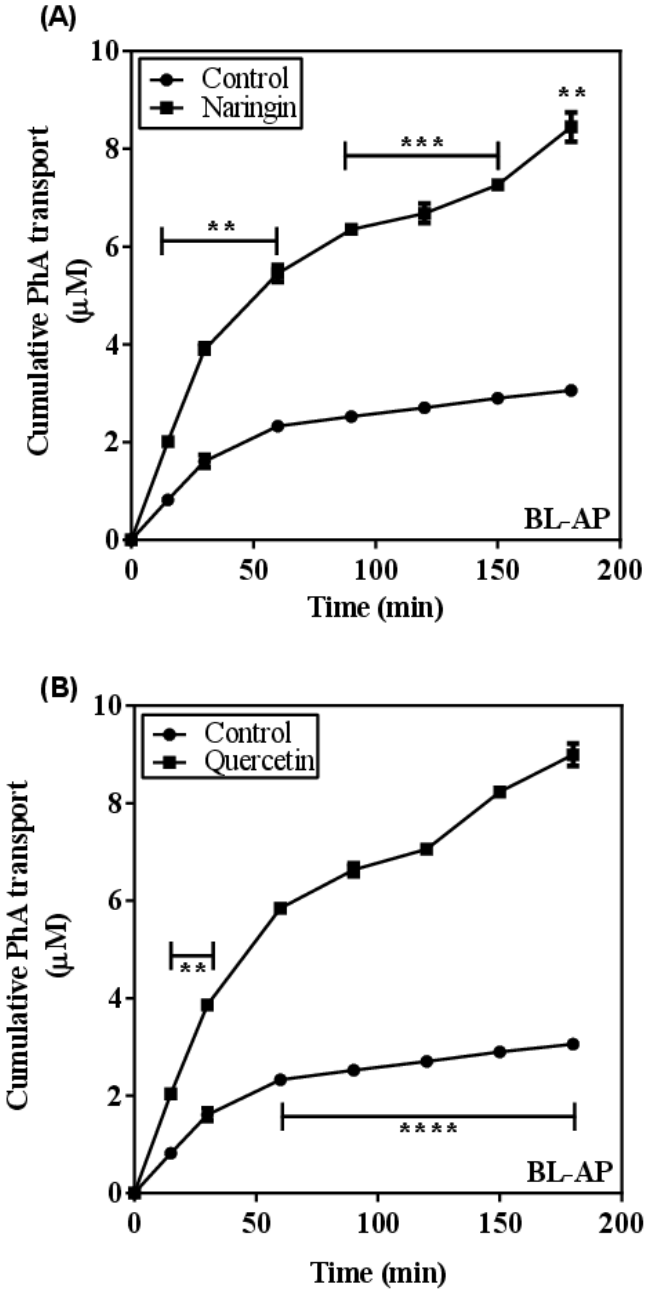

Figure 2.27: Transport of PhA across an *in-vitro* primary BBB cell culture model following 24 hour incubation with naringin or quercetin.

Cells were grown on permeable inserts and (A) naringin or (B) quercetin at 25 µM were added on day 3 followed by the initiation of the transport study 24 h later. Statistically significant differences between control and modulator exposed conditions are indicated. ** P ≤ 0.01 and **** P ≤ 0.001.

2.13.6.3. Modulation of BCRP function in the absence and presence of down-regulators

Curcumin and 17-β-estradiol demonstrated downregulation of BCRP protein expression in PBMEC/C1-2 cells and were selected as modulators to assess in the primary cell culture model. Primary cells were seeded onto permeable inserts and incubated with curcumin or 17-β-estradiol for 24 h with the addition of PhA and modulators into the apical chamber and sampling from the basolateral chamber.

Our results demonstrated that 24 h incubation of curcumin (1 µM) significantly increased the apical-to-basolateral (AB) transport of PhA during our transport studies ($p < 0.01$) (Figure 2.28A), with an AB permeability ($Papp_{,AB}$) of PhA of 83.23 ± 1.25 x 10^{-6} cm/s in the presence of curcumin compared 60.57 ± 1.32 x10^{-6} cm/s in the absence of curcumin. Similarly for 17-β-estradiol (100 nM), our results demonstrated a significant increase ($p \leq 0.01$) in the AB transport of PhA with a AB permeability ($Papp_{,AB}$) of PhA of 83.87 ± 3.25 x10^{-6} cm/s (Figure 2.28B).

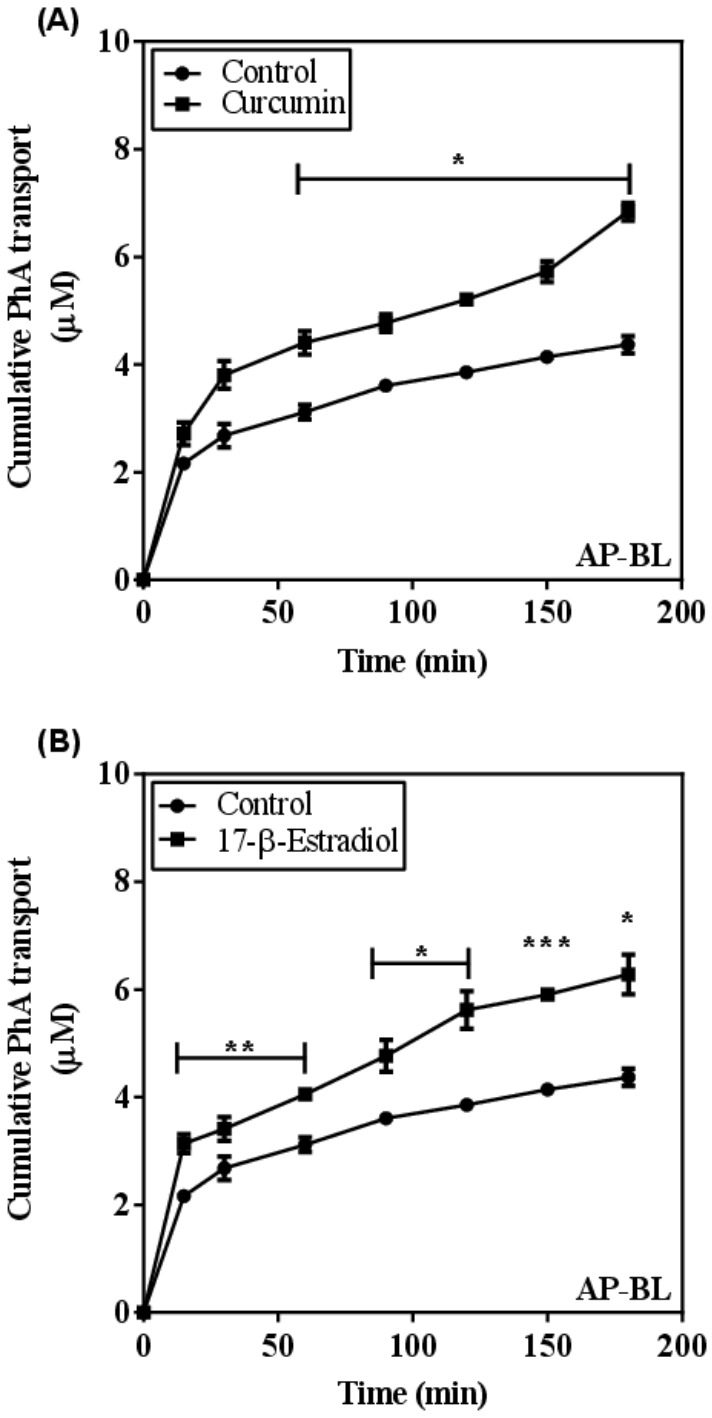

Figure 2.28: Transport of PhA across an *in-vitro* primary BBB cell culture model following 24 hour incubation with curcumin or 17-β-estradiol.

Cells were grown on permeable inserts and (A) curcumin (1 µM) or (B) 17-β-estradiol (100 nM) were added on day 3 followed by the initiation of the transport study 24 h later. Statistically significant differences between control and modulator exposed conditions are indicated. *P ≤ 0.05, ** P ≤ 0.01,***P ≤ 0.001.

2.14. Discussion

Drug delivery to the CNS has become a major challenge due to the presence of the BBB, which acts as a physical and metabolic barrier for the transport of therapeutic agents into the wider CNS. The endothelial cells forming the cerebral capillaries act as a physical barrier by limiting the transport of molecules in and out of the brain. (Pardridge, 2007, Ulrike Tontsch and Bauer, 1989). Drug metabolising enzymes present at the BBB and within the brain mass metabolise drugs and reduce circulating concentrations and the expression of a range of drug transporter at the BBB play an important role in limiting the penetration of drugs into the brain (Pardridge, 2007).

Breast cancer resistance protein (BCRP) is a member of ATP-binding cassette family of membrane transporters and is known to be expressed at the BBB of humans, cows, rats, mice and pigs (Cooray et al., 2002, Warren et al., 2009). Chemotherapeutic agents were the first identified substrates for BCRP and it is now known that BCRP possess a diverse substrate specificity (Mao, 2005) (Breedveld et al., 2004).

The use of inhibitor molecules to modulate the efflux transport function of BCRP is a viable approach to enhance CNS delivery of BCRP substrates. Ko143 (Choi et al., 2012) and fumitremorgin C (FTC) (Allen et al., 2002a) are specific known potent inhibitors of BCRP but their clinical translation is limited due to the neurotoxic and cytotoxic effects. In an attempt to identify novel candidates that may modulate BCRP expression and function, phytochemicals (primarily flavonoids) show promise. Flavonoids are important constituents of diet and are present in fruits, fruit juices, vegetables, nuts, potatoes and corn (Spencer, 2008). The daily intake of flavonoids through the human diet is approximately 200-1000 mg (Kühnau, 1976). It has also been reported that phytochemical also reach the plasma circulation, for example hesperetin, naringin and quercetin plasma concentrations have been reported as 325 nmoL/L, 112.9 nmoL/L and 52 nmoL/L in healthy females on high vegetables diet (Erlund et al., 2002). Similarly, another study demonstrated increased plasma concentrations of epicatechin to 204.4 nmoL/L in adult human after giving flavonoid-rich dark chocolate (Engler et al., 2004).

The interest in phytochemicals and flavonoids has stemmed from their proposed health benefits flavonoids includes antioxidant, anti-inflammatory, cell proliferation, angiogenesis, estrogen biosynthesis and detoxification of carcinogens (Havsteen, 2002).

The ability of flavonoids and other phytochemical compounds to modulate the expression and function of BCRP has been reported previously. The exposure of rat brain capillaries to 17-β-estradiol was shown to decrease BCRP function and protein expression, by down-regulating BCRP transcription and translation through interactions with regulatory mechanism resulting the expression of BCRP (Hartz et al., 2010). Genistein and naringenin has also been shown to inhibit BCRP at a concentration of 3 µM (Imai et al., 2004).

The primary aim of the chapter was to characterise a porcine brain microvascular endothelial cell culture model (PBMEC/C1-2 cells) and to develop an *in-vitro* BBB model which could be used to investigate the gene and protein modulation of BCRP when exposed to a range of modulators compounds. These studies were developed to identify suitable modulator compounds, which were then further assessed in a primary porcine brain microvascular endothelial cell culture model. Our rationale for this approach was that the primary cell cultures model utilised has been reported to better resemble the *in-vivo* BBB model with higher transporter expression levels and a more representative BBB phenotype (as judged by the presence of tight junctions proteins and BBB markers) (Patabendige et al., 2013).

2.14.1. The use of PBMEC/C1-2 cells to develop an *in-vitro* BBB model

PBMEC/C1-2 are immortalised cells and developed from the porcine primary brain endothelial cells after transfection with SV 40 large T-antigen by lipofection (Teifel and Friedl, 1996). The cells show typical morphology of endothelial cells and presence of blood brain barrier markers such as γ-glutamyltranspeptidase (γ-GT), the glucose transporter Glut-1, and apolipoprotein A-1(Teifel and Friedl, 1996).

Our results have shown that when grown on the correct extracellular matrix, gelatine, PBMEC/C1-2 cells demonstrated a typical elongated to cobblestone endothelial cell morphology (Figure 2.1 A and B). Although the PBMEC/C1-2 cells were immortalised to induce the barrier integrity, the cells were recommended to be grown in a 50:50 mixture of astrocytes conditioning media (ACM) obtained from rat glioma C6 cells. The use of C6 astrocyte conditioning media with the addition of cyclic AMP and the type IV phosphodiesterase inhibitor (RO20-1724) induced TEER values up to 78 ± 6 $\Omega.cm^2$ on a 12-well permeable inserts (1.1 cm^2). Lauer et al (Lauer et al., 2004) and Novotna et al (Novotna et al., 2014) achieved the TEER values of 300 $\Omega.cm^2$ on 6-well transwell insert (4.4 cm^2) after the addition of additives. It was also demonstrated that the use of freshly obtained ACM showed better effects on the integrity of the monolayer compared to frozen ACM (Figure 2.2).

Our studies demonstrated that when PBMEC/C1-2 cells were grown on 12-well permeable inserts, we achieved TEER values of 78 ± 6 Ω.cm^2 which was in a good agreement with the published TEER values of 300 Ω.cm^2 that were reported from 6-well inserts (Lauer et al., 2004). Our results are consistent with the TEER values reported as we used 12-well permeable inserts with surface area of 1.12 cm^2 where as other studies reported have used 6-well inserts with surface area of 4.67cm^2.

Several studies have also shown that astrocyte interactions with endothelial cells help to induce the BBB morphology, function and protein expression of junctional proteins (Denison et al., 1988, Lee et al., 2015, Revalde et al., 2015a). Soluble factors such as transforming growth factor β (TGFβ), interferon and Interleukin present in the ACM are known to induce the development of BBB (Katayama et al., 2007). Our results demonstrated that the use of fresh ACM has enhanced the TEER values significantly (Figure 2.3). Freeze thawing ACM might inactivate or degrade the soluble factors in the ACM and reduces the TEER values when compared to fresh ACM.

2.14.2. Cytotoxicity of modulators towards PBMEC/C1-2 cells

A total of 18 phytochemicals, primarily flavonoids (Appendix A) were selected from literature for this project, and which had previously demonstrated significant modulation of BCRP expression and function in other non-cerebral cell lines. To our knowledge there have been no studies reporting the cytotoxicity of phytochemical modulators on PBMEC/C1-2 cells. Our results demonstrated that the majority of modulators exhibited IC_{50} values in excess of 100 µM (Figure 2.4). However a number of modulators demonstrated low IC_{50} values ranging from 1.5 - 63 µM and included flavones such as baiclain (Figure 2.4B), α-napthoflavone (Figure 2.4L) and flavonones such as hesperidin (Figure 2.4J) and hesperetin (Figure 2.4I) and 17-β-estradiol (Figure 2.4F) and curcumin (Figure 2.4E).

Whilst difficult to compare with reported studies, the IC_{50} values determined for modulators were found to be within the same order of magnitude as published reports from, often, non-cerebral origin cell lines. For example, the IC_{50} for apigenin was demonstrated to be 673.8 ± 1.6µM in PBMEC/C1-2 cells, however Bai et al (Bai et al., 2014) used 80-100 µM to induce apoptosis in human breast cancer line (MCF-7). Similarly, the IC_{50} reported for apigenin in lung epithelium cancer (A549) cells was 93.7 ± 3.7 µM (Livak and Schmittgen, 2001).

Baiclain demonstrated an IC_{50} of 4.96 µg/ml (11.12 nM) in enterovirus 71 (Rice-Evans, 1995), similarly the IC_{50} for curcumin has been reported in the literature for CCRF-CM human T cell leukaemia cells as 8.68 µM (Morris and Zhang, 2006). α-napthoflavone (Figure 2.4L) demonstrated a very low IC_{50} values of 1.5 µM in PBMEC/C1-2 cells, and this concerns with other reports of concentrations ranging from 10-1000 nM (Middleton Jr, 1998, Narayana et al., 2001).

Bacanli et al (Bacanli et al., 2015) reported the IC_{50} of naringin as 1976 µM in Chinese hamster fibroblast cell line (V79). Our results were consistent with the study showing no cytotoxicity caused up to 1000 µM (Figure 2.4M). Zhang et al (Zhang et al., 2005) demonstrated limited cytotoxicity with chrysin at 50 µM in MCF-7 MX100 cells. In our study chrysin was demonstrated to show no toxicity, even at higher concentration of 1000 µM (Figure 2.4 D). The IC_{50} calculated for quercetin in PBMEC/C1-2 cells was 169 µM (Figure 2.4 N). This was within the range used *in -vivo* studies in rats, from 1-400 µM (van Zanden et al., 2007).

2.14.3. Assessment of BCRP expression in PBMEC/C1-2 cells

To date, BCRP expression in PBMEC/C1-2 cells has not been reported previously. Our results confirmed the presence of BCRP protein expression in PBMEC/C1-2 cells using reverse transcriptase PCR (Figure 2.5A), western blotting (Figure 2.5B), immunofluorescence confocal microscopy (Figure 2.6) and qPCR (Figure 2.14).

BCRP expression at the BBB and other cerebral cell lines has previously been reported. Eisenblatter et al (Eisenblätter et al., 2003), confirmed the genomic expression and localisation of BCRP by northern blot, RT-PCR and immunostaining in porcine brain capillary endothelial cells. Genomic expression of BCRP was demonstrated by RT-PCR in primary porcine brain endothelial cells (Thomsen et al., 2015). Furthermore, human brain tissues and cerebro-microvascular endothelial cells have shown protein and genomic expression of BCRP (Zhang et al., 2003b). Thomsen et al (Thomsen et al., 2015) recently demonstrated the genomic expression of BCRP in porcine brain endothelial cells. Furthermore, BCRP has been found to be expressed in human, cow rat and mouse BBB (Warren et al., 2009, Cooray et al., 2002, Lee et al., 2007, Revalde et al., 2015b). Furthermore, when assessing the expression of BCRP in porcine primary brain microvascular endothelial cells, we confirmed the presence of BCRP using immunostaining techniques (Figure 2.23) and western

blotting (Figure 2.24), giving the expect protein size of 72 kDa and demonstrating primarily membrane localisation.

2.14.4. Functional assessment of BCRP in the absence or presence of modulators

The functional activity of BCRP has been extensively studied through the use of the BCRP fluorescent substrate H33342 (Zhang et al., 2000, Lai et al., 2004, Choi et al., 2004). We adapted these studies to initially assess whether we could detect BCRP in PBMEC/C1-2 by measuring its intracellular accumulation. This was then followed by assessing the impact of modulator incubation in a short-term assay of 1 h to mimic a direct inhibition of functional activity study, followed by a 24 h incubation to detect potential genomic/proteomic changes in BCRP, which are translated to changes in functional activity.

We were able to successfully demonstrate functional activity through inhibition of BCRP efflux activity by using Ko143 (1 µM), which manifested itself in a significant increases in intracellular H33342 concentrations (Figure 2.10) of 1.8-2.3 mean fold that of H33342 in the absence of Ko143.

To then screen the modulators for their ability to directly impact upon the functional activity of BCRP, we incubated cells with modulators for 1 h and assessed changes in intracellular H33342 accumulation. Our results demonstrated highly significant ($p \leq 0.0001$) increases in intracellular H33342 accumulation after 1 h incubation with apigenin (2.5 ± 0.2 fold), hesperidin (2.6 ± 0.5 fold), indole-3-carbinol (4.5 ± 0.4 fold), and TMF (6.5 ± 0.8 fold) when compared to Ko143 (Figure 2.10).

TMF demonstrated the greatest increases in intracellular H33342 accumulation and hence appears to be a potent inhibitor of BCRP efflux activity at the BBB. Katayama et al (Katayama et al., 2007) also identified TMF as a potent BCRP inhibition in a screening study where 32 flavonoids were screened for their anti-BCRP activity, 20 demonstrated inhibition of BCRP in BCRP-transduced human leukaemia K562 cells (Katayama et al., 2007). Of these, TMF showed the strongest anti-BCRP activity and very low levels of P-gp inhibitor activity. Thus, TMF is a highly potent inhibitor of BCRP activity at the BBB. Furthermore, other flavonoids have also demonstrated similar inhibitor activity of BCRP-mediate mitoxantrone efflux and include apigenin, chrysin, hesperetin, naringin and quercetin (Zhang et al., 2004a). In addition, chrysin (50 µM)

and benzoflavone (BF) (5 μM) have been reported to also act as potent inhibitors of BCRP-mediated mitoxantrone efflux in MCF-7 MX100 cells (Zhang et al., 2005).

These finding indicate that modulators may play a role in directly inhibiting BCRP at the BBB. The exact mechanism of BCRP inhibition is not clear. But it has been reported that glycosylated flavonoids have anti-BCRP activity due to their water solubility (Imai et al., 2004). Modulators lacking significant inhibitory activity may be hindered by their low lipophilicity and reduced permeability. This may explains why we observed no inhibitory effects for hesperetin, resveratrol and rutin which are glycosides and have lower lipophilicity compared with their respective aglycons (Kühnau, 1976). Furthermore, the binding of flavonoids to the nucleotide-binding domain of BCRP has been identified as being important the inhibition process (Fleisher et al., 2015, Katayama et al., 2007), leading to inhibition of the ATPase function and hence halting of the conformational changes required to transport substrates across the cell membrane. Additionally QSAR analyses have demonstrated a strong structure-inhibition relationship between BCRP and flavonoids. Flavonoids with a hydroxyl group at position 5, double bond between position 2 and 3 and methoxyl moiety at position 3 or 6 (Pick et al., 2011) show preference for binding to BCRP and inhibiting the functional transport. This may explain why the greatest intracellular accumulation of H33342 was observed with TMF, as O-methylation at position 2, 4 and 6 increases the local hydrophobicity and hence signifies TMF mediated anti-BCRP activity.

We were also interested to identify the effects of flavonoids on BCRP gene or protein expression over longer periods of exposure, namely 24 h. Our results demonstrated that incubation with the majority of flavonoids studied resulted in limited change in H33342 intracellular accumulation. Of those studied, apigenin, chrysin, curcumin, 17-β-estradiol, I3C, rutin, silymarin and TMF demonstrated at least a 1.25 fold increase (relative to control) in H33342 intracellular accumulation at 1-10 μM (Figure 2.11) and hence suggesting a ‘down-regulation’ type effect. Also of note, is naringin and quercetin, which resulted in a reduction in H33342 intracellular accumulation of < 0.75 fold of control, suggesting an ‘up- regulation’ effect (Figure 2.11).

Of the published reports available, curcumin has been reported to inhibit BCRP function in HEK293 cells without altering protein levels over 72-hours of incubation nor inhibiting the ATPase function of the NBD (Wolfman et al., 1994). Furthermore, it has recently been recommended that curcumin be used as the ‘best’ *in-vivo* inhibitor of BCRP (Lee et al., 2015).

Our results also demonstrated that 17-β-estradiol increased H33342 accumulation to 1.35 ± 0.2 fold compared to control. 17-β-estradiol is another widely reported inhibitor of BCRP function (Hartz et al., 2010, Mahringer and Fricker, 2010). Estrogens are known to regulate BCRP in human *in-vitro*, rat, and mice *in-vivo* models (Imai et al., 2005a, Tanaka et al., 2005, Wang et al., 2006, Wang et al., 2008a). An estrogen responsive element in the promoter region of ABCG2 (gene-encoding BCRP) was identified in human ovarian cancer cells (Ee et al., 2004b) hence suggesting 17-β-estradiol may play a role in the down-regulation of BCRP transcription/translation via regulatory network.

Naringin and quercetin were also highlighted as leading to reduced H33342 intracellular accumulation, suggesting they possess BCRP down-regulatory properties. Of the reported studies available, quercetin has been demonstrated to induce BCRP expression by 5.3 fold in Caco-2 cells at concentration of < 25 µM (Ebert et al., 2007). Interestingly, naringin at 50 µM, did not show any effect on the accumulation of mitoxantrone in BCRP-overexpressing MCF-7 MX100 cells (Zhang et al., 2004a), potentially as a result of being a flavonoids glycoside.

2.14.5. Modulation BCRP protein expression in PBMEC/C1-2 cells

In order to further explore the potential modulation of BCRP protein expression in the presence of modulators, western blotting analysis was conducted on all modulators at identical concentrations studied for the H33342 accumulation assays. Our results demonstrated that biochanin A, hesperidin, I3C, naringin and quercetin significantly induced BCRP protein expression leading fold change of 1.7 ± 0.1, 1.7 ± 0.3, 1.5 ± 0.1, 2.2 ± 0.2 and 2.3 ± 0.1 respectively (Figure 2.12 and 2.13). Notably, naringin and quercetin demonstrated the greatest fold-change (> 2 fold) in BCRP protein expression and concurs with the H33342 accumulation observations. Additionally, in contrast to the study, naringin lead to an induction of BCRP protein expression (Zhang et al., 2004a). It has been reported that exposure of 25 µM of quercetin, chrysin and I3C to Caco-2 cells, for 24 h, leads to a BCRP protein induction-effect and concurs with our studies demonstrated induction of BCRP expression with I3C and quercetin (Ebert et al., 2007). The lack of correlation following exposure to chrysin, flavone and resveratrol is uncertain by may be a result of differences in study time-scales (24 h *vs*. 72 h) or differences in the cell lines utilised (endothelial *vs.* epithelial).

Our studies also identified curcumin (0.4 ± 0.2) and 17-β-estradiol (0.4 ± 0.1) as 'down-regulators' of BCRP protein expression (Figure 2.12 and 2.13). It has been recently investigated that curcumin and 23 analogous of curcumin are highly potent than curcumin in inhibiting BCRP mediated efflux and reversed BCRP mediated drug resistance. However, there are no current studies that have investigated changes in BCRP protein expression when exposed to curcumin for prolonged time-period (Revalde et al., 2015a). On the other hand, a number of studies have demonstrated the down-regulation of BCRP protein and genomic expression with 17-β-estradiol and includes modulation of BCRP activity in the mice brain capillaries (Hartz et al., 2010). Furthermore Mahringer and Fricker (Mahringer and Fricker, 2010) reported the reduced functional and protein expression of BCRP following 6 h incubation with 17-β-estradiol (1-10 nM) in rat brain capillaries.

2.14.6. Functional assessment of BCRP activity in an *in-vitro* permeable insert BBB model

The functionality of BCRP was further demonstrated using the BCRP substrate pheobhorbide A (PhA) and assessing its transport across the PBMEC/C1-2 monolayer in the absence and presence of Ko143 or modulators. Initial studies demonstrated significant increase in PhA transport when exposed to Ko143 after 90 min and lasting until the final time point (180 min) (Figure 2.17), demonstrating the presence of functional BCRP. Furthermore, the apparent permeability in the apical-to-basolateral direction ($P_{app,AB}$) significantly increased ($p < 0.01$) when cells were exposed to Ko143, rising from 27.2 ± 0.23 $x10^{-6}$ cm/s to 43.23 ± 0.32 $x10^{-6}$ cm/s.

Cells grown on permeable inserts were then exposed to modulators for 24 h followed by assessing the transport of PhA. Western blot and qPCR results (Figure 2.13 and 2.14) confirmed that quercetin and naringin are potential up-regulators of BCRP at the BBB, and these were selected for transport studies. The apical-to-basolateral transport of PhA with quercetin and naringin was negligible (Figure 2.18). Thereafter the modulators were pre-incubated for 24 h in a similar fashion, but PhA was added into the basolateral compartment and the flux of PhA from basolateral-to-apical was assessed. Under these conditions both naringin and quercetin demonstrated significant increases ($p \leq 0.01$) in PhA transport from basolateral-to-apical at all time points when compared to control (Figure 2.19) leading to increases in $P_{app,BA}$ to 74.23

± 0.29 x10^{-6} cm/s and 63.21 ± 0.54 x10^{-6} cm/s respectively when compared to control $P_{app,BA}$ 23.13 ± 0.31 x10^{-6} cm/s ($p \leq 0.01$).

As the modulators were inducing BCRP expression, the addition of PhA in the apical compartment would not alter the concentrations of PhA over the time-course of the study due to the 'retention' of PhA in the donor compartment as a result of BCRP efflux. When the donor compartment was switched to the basolateral compartment, alterations in BCRP transporter activity resulted in a more apparent change in receiver (apical) compartment concentration.

Western blot and qPCR (Figure 2.13 and Figure 2.14) confirmed that curcumin and 17-β-estradiol are potential down-regulators of BCRP at the BBB, and these were selected for transport studies. In our studies curcumin (1 µM) and 17-β-estradiol (100 nM) significantly increased PhA $P_{app,AB}$ to 78.81 ± 0.65 x10^{-6} cm/s and 48.11 ± 0.34 x10^{-6} cm/s when compared to control $P_{app,AB}$ 27.20 ± 0.23 x10^{-6} cm/s ($p \leq 0.001$) representing BCRP down-regulation (Figure 2.20). In both cases the increase in $P_{app,AB}$ is indicative of an increase in the apical-to-basolateral flux, and is a result of the associated changes in BCRP protein expression potentially reducing the abundance of BCRP in the monolayer and hence reducing the overall kinetic flux of PhA molecules across the monolayer. Furthermore, the increase apical-to-basolateral PhA flux when exposed to 17-β-estradiol concurs with reports highlighting the potent down-regulation imparted by 17-β-estradiol on BCRP expression (Mahringer and Fricker, 2010, Hartz and Bauer, 2010).

2.14.7. Characterisation of a primary porcine brain endothelial cell BBB model

Whilst immortalised cell models are widely used in BBB research, the use of primary cell culture models often leads to a more representative and viable model system. Primary porcine brain microvascular endothelial cells were successfully isolated in the lab from the fresh porcine brain hemispheres. Cells became confluent after 10-12 days post seeding and demonstrated typical elongated, spindle shape morphology under light microscopy (Figure 2.21). Patabendige et al (Patabendige et al., 2013) recently reported the detailed isolation process, morphology and characteristics of primary brain endothelial cells. Our results were consistent with Patabendige and other studies reported (Imai et al., 2003, Spencer, 2008). The primary porcine brain endothelial cells were seeded onto collagen coated permeable inserts and 3 µg/mL was used to kill the

contaminating cells and obtain pure monolayers. On a 12-well permeable inserts (1.1 cm^2) the primary endothelial cells showed the TEER values of 150-200 $\Omega.cm^2$.

The type of collagen and amount of collagen is very important for growth of primary cells. Our results found that primary porcine brain microvascular endothelial cells take longer 12-13 days to confluent when compared with other studies (10 days) (Patabendige et al., 2013, Spencer, 2008). The discrepancies between the numbers of days could be a result of the use of commercial collagen rather than collagen extracted from rat tails, as conducted by Patabendige et al (Patabendige et al., 2013). Furthermore, the barrier integrity of the *in-vitro* was enhanced by switching on day 4 to serum free media supplemented with 250 µM CPT-cAMP, 17.5 µM RO20-1724 and 500 nM of hydrocortisone, as reported elsewhere (Woodward et al., 2009, Ishiwata et al., 2005, Schwerk et al., 2012).

The cytotoxicity for the primary cells was also investigated. PBMEC/C1-2 cells provided a broad understanding of the potential cellular toxicities of modulators and this was used as a basis with which to select two concentrations (25 µM and 100 µM) (Figure 2.25), for screening against primary porcine brain endothelial cells. Our results demonstrated higher cellular viabilities for most modulators at both 25 µM and 100 µM. Where cell viability reduced, this was typically in the range of a viability of between 50-100%. Of note however is the reduction of cellular viability for modulators at 25 µM for baiclain (76 ± 11 %) and α-napthoflavone (63 ± 7 %) and at 100 µM for baiclain (62 ± 12 %), curcumin (29 ± 18 %), 17-β-estradiol (64 ± 4 %), hesperetin (53 ± 0.8 %) and α-napthoflavone (25 ± 7 %) (Figure 2.25).

When compared to cytotoxicity with PBMEC/C1-2 cells, baicalin, curcumin, 17-β-estradiol, flavone, hesperetin, hesperidin, napthoflavone and resveratrol demonstrated similar trends of cytotoxicity in both cell lines although the toxicity with primary cells was found to be lower than PBMEC/C1-2 cells. Furthermore, chrysin, fistein, naringin and silymarin demonstrated no cytotoxicity above 100 µM and similar trends were found in primary cells with no toxicity observed under 100 µM.

Structural and functional relationship of flavonoids has suggested that flavones and flavonols are more cytotoxic, whereas flavanones are less toxic (Wen et al., 2005) to cells. Our results have demonstrated that flavanones such as naringin did not demonstrate any cytotoxicity at higher concentrations unlike baiclain, α-napthoflavone, curcumin and hesperidin in PBMEC/C1-2 cells. Naringin is identical to apigenin with

the exception of the 2,3-double bond on the C-ring (Figure 2.4 M). In our results, we have shown that naringin did not cause any cytotoxicity and apigenin has shown IC_{50} of 673.8 µM (Figure 2.4 A) in PBMEC/C1-2 cells. The planar nature of the compound and presence of B-ring attached at the 2-position of the benzopyran core is required to induce cytotoxicity. The planarity of the compound can help them to cross the cell membrane and enter the cytoplasm and B-ring is important to bind to protein targets (Wen et al., 2005).

The localisation of BCRP protein expression was further confirmed by immunostaining (Figure 2.23) and western blot (Figure 2.24), demonstrating both elongated, tightly packed endothelial cell morphology when grown on permeable insert, in addition to the confirmed of the expected 72 kDa BCRP protein in western blotting studies. To identify and confirm functional BCRP in primary porcine brain microvascular endothelial cells, a permeable insert model was developed and the transport of PhA across the monolayer was assessed in the absence and presence of Ko143. Our results demonstrated a significant increase ($p \leq 0.01$) in apical-to-basolateral transport of PhA at all time points studied in the presence of Ko143 demonstrating the inhibition of BCRP (Figure 2.26). This is highlighted when considering increase in $P_{app,AB}$ from $60.57 \pm 1.32 \times 10^{-6}$ cm/s in the absence of and $109.75 \pm 1.21 \times 10^{-6}$ cm/s in the presence of Ko143 (Figure 2.26). Furthermore, quercetin and naringin were identified as BCRP inducers (Figure 2.13) and when studied in the transport model, demonstrated significant increases ($p \leq 0.01$) in PhA transport from basolateral-to-apical at all time points when compared to control (Figure 2.27). This led to an increase in $P_{app,BA}$ for quercetin and naringin to $102.93 \pm 1.98 \times 10^{-6}$ cm/s and $98.21 \pm 1.23 \times 10^{-6}$ cm/s respectively when compared to the absence of modulators, $38.57 \pm 2.15 \times 10^{-6}$ cm/s. In a similar fashion the BCRP down-regulators curcumin and 17-β-estradiol demonstrated increased apical-to-basolateral transport of PhA and significantly increased $P_{app,AB}$ to a Papp $83.23 \pm 1.25 \times 10^{-6}$ cm/s and $83.87 \pm 3.25 \times 10^{-6}$ cm/s respectively when compared to PhA alone $60.57 \pm 1.32 \times 10^{-6}$ cm/s (Figure 2.28).

Whilst gene or protein changes in BCRP expression may suggest at a possible change in the functional expression of BCRP, without conducting transport studies using a BBB monolayer model, the consequences of any gene/protein level changes in BCRP cannot be assessed in a functional sense. Across both PBMEC/C1-2 and primary cell culture model we identified similar behaviours of induction or down-regulation of BCRP expression and the functional consequences of this was confirmed using the permeable insert models.

In this chapter, we characterise the PBMEC/C1-2 cells and primary porcine brain microvascular endothelial cells for the protein, genomic and functional expression of BCRP. Our results confirmed that BCRP is expressed in PBMEC/C1-2 cells and primary porcine brain microvascular endothelial cells. Furthermore, the interaction of flavonoids with BCRP was investigated in the presence or absence of modulators. Our results indicated that modulators interact with BCRP and can modulate BCRP function, protein and genomic expression at BBB.

The findings presented in this chapter suggest that 17-β-estradiol and curcumin are viable down-regulators of BCRP expression and efflux function whereas quercetin and naringin are viable inducers of BCRP expression and efflux function. This has clear implications for modulating the efflux role of BCRP at the BBB towards either clearing agents from the brain biophase back into the systemic blood or forcing equilibrium towards enhanced brain delivery of therapeutic compounds.

2.15. Conclusion

Due to the limited impose by structural barrier (BBB) the drug delivery to the CNS remains a challenge. The Porcine brain endothelial microvascular cell culture model has been extensively used due to more close resemblance with human model. The phytochemicals have shown less or no cytotoxicity in PBMEC/C1-2 cells whereas primary cells have shown more cytotoxicity. This chapter demonstrated that the quercetin and naringin has shown to up-regulate the BCRP protein, genomic and functional expression, whereas curcumin and 17β-estradiol were down-regulators of BCRP. This work can be further exploited to investigate the modulation of BCRP in disease conditions to enhance the CNS drug delivery.

Chapter 3

Assessment of the interactions of phytochemicals on BCRP expression and function at the rat blood cerebrospinal fluid barrier

3. Introduction

The choroid plexus (CP) epithelium represents an important site controlling the development and maintenance of brain and CNS biophase and presents itself as the key barrier between the systemic blood and the CSF, often termed the blood-CSF-barrier (BCSFB). Despite the importance, the CP only accounts for approximately 0.25 % of the total brain weight. However, due to its limited tissue mass, the isolation of primary choroid plexus epithelial cells for laboratory studies is labour and time consuming.

A well-characterised *in-vitro* BCSFB cellular model would present itself as a valuable tool to understand the important role the BCSFB plays in controlling entry of compounds into the CNS. As a result of this, a number of immortalised choroid plexus cell culture models have become important tools to study pathological diseases of the CP (Nutt et al., 2003, Rennels et al., 1985), drug permeability (Szentistvanyi et al., 1984), transporter function (Baehr et al., 2006) and modulation of transporters expression (Oldendorf, 1967). The rat chorodial epithelial Z310 cell culture model was developed by Dr Wei Zheng, (Zheng and Zhao, 2002) and has been widely characterised to assess the epithelial cell morphology, tight junctions and functional, genomic and protein expression of drug transporters (Zheng and Zhao, 2002, Goodman, 1985, Juliane Kläs et al., 2010, Halwachs et al., 2011), and is therefore a viable *in-vitro* model for the study of the function of the BCSFB.

3.1. Aims and objectives

The aim of the experimental work reported in this chapter was to develop and characterise the use of an *in-vitro* BCSFB cell culture model to investigate the genomic and proteomic modulation of the drug transporter BCRP. To accomplish this, a range of phytochemical modulators was screened for the ability to modulate the functional, genomic and protein expression of BCRP in Z310 cells.

To achieve the aims the objectives were:

- To demonstrate the formation of an *in-vitro* BCSFB model using Z310 cells
- To investigate the genomic and protein expression of BCRP in the Z310 cells
- To investigate the cytotoxicity of phytochemical modulators towards Z310 cells
- To demonstrate the efflux function of BCRP in Z310 cells
- To identify phytochemical modulators capable of eliciting genomic/proteomic changes in BCRP expression

3.2. Materials

Dulbecco's modified essential media with glucose (DMEM), fetal bovine serum (FBS), amphotericin B, penicillin/streptomycin and gentamycin were obtained from Biosera (Sussex, UK); Resveratrol and Ko143 from Santa Cruz Biotechnology (Texas, USA); Curcumin from Cayman Chemical (Cambridge, UK); GenElute Total RNA extraction kits were purchased from Sigma (Dorset, UK); Rat-tail I collagen solution from First Link (Birmingham, UK) and all other chemicals were sourced from Sigma (Dorset, UK). My Taq^{TM} One-step RT-PCR kit and Easy Ladder I obtained from Bioline (London, UK). All reverse transcriptase PCR primers were synthesised by IDT Dna (Leuven, Belgium); Real time PCR housekeeping primers were obtained from Invitrogen, *AhR* and *BCRP* were custom designed by Primer Design (Sheffield, UK), Total RNA extraction kits were purchased from Qiagen (Manchester, UK) and SYBR-green master mix were obtained from Primer Design (Sheffield, UK), Optiblot SDS-page gel and western blot reagents obtained from Abcam (Cambridge, UK); ABCG2 (M-70), beta-actin (C4), broad range markers, goat anti-rabbit IgG-FITC and protease inhibitor cocktail were obtained from Santa Cruz Biotechnology (Texas, USA). Stock solutions of all test compounds were prepared in dimethylsulfoxide (DMSO) and stored at -20°C until use.

A total of 18 phytochemical derived modulators were selected for studies and their structures are detailed in Appendix A.

3.3. Methods

3.3.1. Culture of Z310 cells

Z310 cells were grown in T25 flasks containing Z310 media: DMEM, 10 % v/v FBS, 1% v/v amphotericin B, 1 % v/v penicillin/streptomycin and gentamycin (20 mg in 500 mL of media) and epidermal growth factor (EGF) at the final concentration of 10 ng/mL. Cells were allowed to attach at 37°C for 24 h. Thereafter the media was changed cells grown until 70-80 % confluent before 1 mL of trypsin-EDTA was added to the flask. The flask was placed maintained for 5 min at 37°C and the cell suspension was resuspended in a 5 mL of media. This cell suspension was transferred to a 15 mL centrifuge tube and centrifuged at 1500 rpm for 5 min. The pellet was resuspended in 2 mL of media and transferred into T75s for subsequent experiments.

3.3.2. Cryopreservation of cells

After harvesting cells, the pellet was resuspended in cryopreservation media (10% DMSO and 90% FBS). 1 mL aliquots of the cell suspension was aliquoted into cryovials and stored overnight at -80˚C in a controlled freezing environment (Mr. Frosty, Nalgene®, Thermo Fisher Scientific, UK) before being transferred to the liquid nitrogen for long term storage.

3.3.3. Development of an *in-vitro* permeable insert based model of the BCSFB

3.3.3.1. Extracellular matrix coating with collagen

12-well permeable inserts (Greiner ThinCert®) were coated with 200 µL of 0.01% rat tail collagen type 1 solution in sterile water, and incubated for 3-4 h in a laminar air flow hood. Excess collagen solution was then aspirated and inserts washed with pre-warmed PBS. The permeable inserts were then immediately used for seeding of cells. 1 mL of a cell suspension containing 2 x10^5 cells were seeded onto the permeable inserts and cells were grown in the Z310 medium supplemented with 1 µM dexamethasone (Shi and Zheng, 2005).

3.3.3.2. Visualisation of cell monolayers under light microscopy

Approximately 2-3 days after seeding, cell monolayers were examined using a DMI400B microscope (Leica microscope systems (UK) Ltd, Milton Keynes, UK) with a 10x and 40x objective lenses.

3.3.3.3. Measurement of transcellular electrical resistance

The media was changed every other day and the trans-cellular electrical resistance (TEER) values were measured every day up to 8 days post seeding. Monolayer formation was monitored by measuring the TEER using a voltohmmeter (EVOM) (World Precision Instrument) directly before and after all transport studies.

TEER values were calculated as follows:

$$\text{TEER Values } (\Omega.\text{cm}^2) = (\text{R}_{\text{Cell monolayer}} - \text{R}_{\text{Blank Filter}})\text{xA} \qquad (1)$$

where A = surface area of the permeable insert (cm^2), $R_{Cell\ monolayer}$ = resistance across permeable insert with cell monolayer and $R_{Blank\ filter}$ = resistance across permeable insert without cells. Control measurements were made using filters without cells (blank filter). A cut-off TEER range of 95 ± 8 $\Omega.cm^2$ (Zheng and Zhao, 2002, Juliane Kläs et al., 2010) was used a measure of a suitable BCSFB model.

3.3.4. Cellular toxicity of modulators towards Z310 cells: methylthiazolyldiphenyl-tetrazolium bromide assay

Stock solutions of all modulators were prepared in DMSO. Sterile working stocks of each compound were freshly prepared on the day. Culture medium was used as the diluent and the final solvent concentrations in all test drug concentrations did not exceed 1 % (v/v). Cells were seeded with an optimum density of 10,000 cells per well onto clear flat bottom 96-well plates and at 60-70 % confluency the media was carefully removed and fresh media containing phytochemical modulators over a 7-fold log concentration range (0.001 µM-1000 µM) was added and incubated for 24 h. The media was then removed and cells were carefully washed with the pre-warmed PBS to 37°C and incubated with fresh media for 30 min for the cells to equilibrate. MTT powder was dissolved in PBS (5 mg/mL) and filtered through a 0.2 µm pore size filter

to sterilise the solution and remove any insoluble residues. 20 µL of the pre- warmed MTT solution was added to each well. The plates were protected from light and incubated at 37 °C in a humidified atmosphere of 5 % CO_2 in air for 4 h. After 4 h medium was removed and 100 µL of DMSO was added to the each well of the 96-well plate to stop the reaction and solubilise the purple formazan crystals. The plates were incubated for 10-15 min at room temperature under dark conditions.

The UV-absorbance of the samples was measured on a multi-plate reader (Bio-Rad laboratories, Hercules, CA) using 570 nm as a test wavelength and 600 nm as a reference wavelength. The mean of the blank UV-absorbance was subtracted from the UV-absorbance of each controls and samples and percentage viability was calculated. The percentage of cellular viability was calculated using the equation below:

$$\%\ \text{cell viability} = \frac{\text{absorbance of sample}}{\text{absorbance of control}} * 100 \qquad (2)$$

The IC_{50} was subsequently using a sigmoidal dose response function within the Graphpad Prism version 5.0 (GraphPad Software, Inc. USA).

3.3.5. Immunostaining detection of breast cancer resistance protein in Z310 cells

A 2 mL cell suspension containing 30,000 cells were seeded onto uncoated coverslips for 24 h in an air humidified atmosphere of 5% CO_2. Subsequently cell culture media was aspirated and coverslips were washed three times with pre-warmed PBS. Cells were then fixed with methanol at -20°C for 20 min and washed three times with pre-warmed PBS. Coverslips were then exposed to blocking solution (1 % BSA in PBS) incubated for 30 min at room temperature before being incubated with primary ABCG2 antibody M-70 (1:200) for 2 h at 37°C. Coverslips were washed twice with PBS and incubated with secondary antibody fluorescein iso-thiocyanate (FITC) -labelled mouse anti-rabbit IgG (1:500) in blocking solution, for 45 min at room temperature in the dark. The secondary antibody was aspirated and cells were washed three times with pre-warmed PBS.

The coverslips were then carefully removed from the 12-well plate, rinsed with MilliQ water and mounted onto glass slides with mounting media containing 4',6-diamidino-2-phenylindole (DAPI). The coverslips were analysed using an upright confocal

microscope (Leica SP5 TCS II MP) and visualised with an oil immersion objective. All images were acquired using an argon laser to visualise FITC localisation and a helium laser to visualise DAPI localisation at 494 nm and 461 nm respectively.

3.3.6. Measurement of BCRP functional activity in Z310 cells

3.3.6.1. Functional activity of BCRP in Z310 cells using a 96-well plate assay

The functional activity of BCRP in Z310 cells was assessed using the BCRP inhibitor Ko143. 20,000 cells per well were seeded into a 96-well plate and allowed to attach for 24 h. Thereafter the cells were washed with pre-warmed HBSS at 37°C and fresh media added containing 3.9 nm - 5 µM Ko143 and left to pre-incubate for 1 h. 100 µL of media containing 10 µM of H33342 and 3.9 nm - 5 µM Ko143 were added to the appropriate wells and incubated for a further 30 min at 37°C. Wells were then washed twice with ice cold HBSS and cells lysed by storage of plates at -80°C for 20 minutes before being read on a fluorescent plate reader at an excitation wavelength of 355 nm and emission wavelength of 460 nm.

3.3.6.2. Assessment of the intracellular accumulation of H33342 in the presence of modulators in Z310 cells.

The potential of modulators to alter the functional activity of BCRP in Z310 cells was assessed by measuring changes in the intracellular accumulation of H33342 in the absence and presence of modulators. Z310 cells were seeded onto clear-bottomed 96-well plates for 24 h. The experimental assessment for modulators to directly inhibit BCRP function or modulate BCRP protein expression was conducted as described in section 2.4.5.3 and 2.4.7.

3.3.7. Determination of BCRP gene expression by reverse-transcriptase PCR in Z310 cells

3.3.7.1. Extraction of total RNA

Isolation of total RNA from Z310 cells was obtained as described in section 2.4.6.1.

3.3.7.2. One-step reverse-transcriptase PCR

A one-step RT-PCR assay was developed as described in section 2.4.6.2 using 100 ng of template (Table 3.1).

Table 3.1: Preparation of PCR samples

Reagents	Volume
My Taq One-Step Mix	25 µL
Primer Forward	1.5 µL
Primer Reverse	1.5 µL
Reverse Transcriptase Enzyme	0.5 µL
Ribosafe Inhibitor	1 µL
DEPC Water	15.5 µL
Template(100ng)	5 µL
Total Volume	50 µL

Forward and reverse primers (HKG: β-actin and TTR; GOI: BCRP) were designed using the PrimerQuest tool (http://www.idtdna.com/primerquest/home/index) and custom synthesised (IDTDna, Germany) (Table 3.2). The thermal cycling was conducted using a Hybaid OmniGene Thermal Cycler using a three-step protocol (Table 3.3).

Table 3.2: Primers used for RT-PCR

Gene	Gene Accession	Forward Primers	Reverse Primers
TTR	NM_022712	CCACAAGCCAAACAATATCCG	CCAAATGCTCAACGACCACA
BCRP	NM_181381	CTTCTCCATTCACCAGCCTC	TGTAGGGCTCACAGTGGTAA
β-actin	NM_031144	CATGAAGATCCTGACCGAGC	CAGCTCAGTAACAGTCCGC

Table 3.3: Thermal cycle reactions for PCR

Cycles	Temperature	Time	Procedure
1	45°C	20 min	Reverse Transcription
1	95°C	1 min	Polymerase Activation
40	95°C	10 s	Denaturation
	55°C	10 s	Annealing
	72°C	30 s	Extension

3.3.7.3. Gel electrophoresis

Visual confirmation of successful PCR product was conducted by agarose gel electrophoresis as described in section 2.4.6.3.

3.3.8. Determination of BCRP protein expression in Z310 cells

3.3.8.1. Preparation of cell lysate

Z310 cells were grown on 6-well plates for 48 h and whole cell obtained as described in section 2.4.7.1. To assess the impact of modulators on BCRP protein expression, Z310 cells were also incubated with modulators at 25 µM (unless otherwise stated) for a further 24 h post-seeding and the whole cell lysate subsequently extracted.

3.3.8.2. Determination of protein concentration: bicinchoninic acid assay

Protein concentration was quantified by a bicinchoninic acid (BCA) assay (Novagen, BCA assay protein kit) as described in section 2.4.7.2.

3.3.8.3. Sodium dodecyl sulphate polyacrylamide gel electrophoresis

Sodium dodecyl sulphate polyacrylamide gel electrophoresis (SDS-PAGE) was conducted using 8% SDS precast gels (Abcam, Cambridge, UK) as described in section 2.4.7.3.

3.3.8.4. Electrophoretic transfer and blotting of proteins

Electrophoretic transfer and blotting of proteins was conducted as described in section 2.4.7.4.

3.3.8.5. Immunological detection of BCRP

The electrophoretic transferred protein membrane was washed with TBST buffer for 30 min and then blocked with the blocking buffer (5% milk and TBST) for 1 h at room temperature. The membrane was subsequently incubated with polyclonal ABCG2

antibody (M-70) in blocking buffer (1:500) and incubated overnight at 4 °C. Thereafter the membrane was placed on an orbital shaker for 2 h and washed with TBST for 30 min before being blocked with blocking buffer for 30 min at room temperature. The membrane was then incubated for 2 h at room temperature with goat anti-rabbit IgG-horse radish peroxidise-conjugated (1:5000) in blocking buffer.

3.3.8.6. Chemiluminescent detection of BCRP

Laboratory prepared enhanced chemiluminescent solution was freshly prepared to detect BCRP, as described in section 2.4.7.6.

3.3.8.7. Membrane stripping

To allow reprobing of the membrane, a mild stripping agents was used to remove attached antibodies (Bendayan et al., 2006) and is described in section 2.4.7.7.

3.3.8.8. Immunological detection of β-actin

To reprobe the membrane for the loading control (β-actin) the membrane was incubated with blocking buffer, followed by mouse β-actin horseradish peroxidase conjugated monoclonal antibody (1:7500) in blocking buffer for 24 h at 4°C. The membrane was then washed with TBST for 2 h. Chemiluminescent detection was performed as described in section 2.4.7.6.

3.3.9. Determination of modulation of BCRP gene expression by phytochemical compounds using quantitative PCR in Z310 cells

3.3.9.1. Isolation of RNA

Z310 cells were grown on 6-well plates for 24 h followed by the addition of modulators at 25 µM (unless otherwise stated) before being incubated for a further 24 h. RNA was extracted as detailed in section 2.4.6.1.

3.3.9.2. Reverse transcription

A two-step reverse transcription protocol was utilised involving both annealing and extension steps and is detailed in section 2.4.8.2.

3.3.9.3. qPCR cycle parameters

The qPCR reaction mixture was prepared as outlined in Table 3.4.

Table 3.4: Preparation of PCR samples

Reagents	Volume
10x Master Mix	10 µL
Primer Forward (6 pmol)	1 µL
Primer Reverse (6 pmol)	1 µL
RNase-free Water	3 µL
Template (25 ng)	5 µL
Total Volume	20 µL

qPCR primers were custom synthesised as follows: *GADPH* (NCBI Accession: NM_017008) forward primer GGTCAAGCAGCATAATCCAAAG, reverse primer CAAGGGCATAGCCTACCACAA and a custom synthesised porcine *BCRP* (NCBI Accession: NM_181381) gene primers (PrimerDesign, UK). Samples were loaded onto a Stratagene MX3000p thermal cycler (Agilent technologies, United States) using a SYBR-green detection probe and a two-step cycling protocol (Table 3.5).

Table 3.5: qPCR thermal cycles

Cycles	Step	Time	Temperature
	Enzyme activation	2 min	95°C
40 Cycles	Denaturation	15 s	95°C
40 Cycles	Data Collection	60 s	60°C

3.3.9.4. qPCR quantification method

Relative quantification determines the mRNA changes in gene of interest (*BCRP*) relative to the levels of a housekeeping gene (*GADPH*) RNA. Threshold cycle (Ct)

values were determined and changes in the expression of target gene normalised with GADPH calculated for each reaction condition (ddCT method) (Livak and Schmittgen, 2001) (Equation 3)

$$\text{Fold change} = 2^{-\Delta(\Delta Ct)} \quad (3)$$

where $\Delta Ct = C_{T,BCRP} - C_{T,GADPH}$

The efficiency of all genes were pre-validated for specificity by the manufacturer.

3.3.10. Assessing the functional activity of BCRP in an *in-vitro* BCSFB monolayer model

3.3.10.1. HPLC detection of sulfasalazine

To assess the function of BCRP *in-vitro*, the BCRP substrate sulfasalazine was used. A isocratic HPLC method was utilised for the HPLC-UV detection of sulfasalazine, (Gurvitch and Metzler, 2009). HPLC analysis (Shimadzu, LC- 2010A HT) of sulfasalazine was performed using a reversed-phase C18 column (Phenomenex Luna 5-µm) with a mobile phase consisting of 70:29:1 methanol:millQ water:acetic acid and flow rate of 1 mL/min. The method was validated by evaluating the parameters such as linearity, limit of quantification (LOQ) and limit of detection (LOD). The linearity was determined by analysing the sulfasalazine standards (0.01-50 µM). The standards were prepared in triplicates and a calibration curve was generated to determine the coefficient (r^2). The LOD is the lowest amount of a substance that can be detected and LOQ is the concentration at which the quantitative results can be reported. The LOD and LOQ was determined by as follows:

$$\text{LOD} = 3.3(\sigma/S) \quad (4)$$

$$\text{LOQ} = 10(\sigma/S) \quad (5)$$

where σ is the standard deviation of the response; S is slope of the calibration curve. Regression analysis was performed with the standards to calculate the standard deviation and slope of the calibration curve.

3.3.10.2. Optimisation of *in-vitro* transport media

Permeable Z310 inserts were prepared according to section 3.4.3. TEER values were used a measure of monolayer formation and suitability of transport media. Preliminary experiments were performed to assess integrity of monolayers when incubated with either HBSS supplemented with glucose (10 mM) and HEPES (10 mM) or Z310 serum free media. TEER values were determined after 30 min, 60 min, 90 min, 120 min, 150 min and 180 min exposure to media.

3.3.10.3. Lucifer yellow permeability assay

To assess the formation of a suitable monolayer, lucifer yellow was used as a permeation marker, as described in section 2.4.9.3. Inserts were rejected for permeability assays if the percentage LY transported was greater than 1 %.

3.3.10.4. Modulation of BCRP transport function

To assess the potential for phytochemical modulators to modulate the *in-vitro* transporter function of BCRP in the permeable insert BCSFB model, modulators identified as resulting in induction or down-regulation of BCRP protein from western blotting studies (section 3.4.8) were selected to assess their potential to modulate the efflux of the BCRP substrate sulfasalazine. Cells were seeded onto collagen-coated permeable inserts (see section 3.4.3) and TEER values used to assess the formation of a monolayer.

Z310 seeded permeable inserts were washed with pre-warmed PBS and freshly prepared working stocks of modulators (optimal non-toxic concentrations were used and determined from cytotoxicity and western blotting studies) and Ko143 in serum free media were added to the permeable inserts and incubated for either 1 h (Ko143: to pre-load cells with inhibitor) or 24h (modulators: to modulate the protein expression of BCRP) at 37°C.

Cells were subsequently washed with pre-warmed PBS followed by the addition of serum free media (SFM) containing Ko143 (1 µM) or modulators and 10 µM sulfasalazine into the apical compartment. The basolateral compartment received media with modulators only. 50 µL aliquots were taken at 0, 30, 60, 90, 120, 150, 180 and 210 min and the transport of sulfasalazine determined by HPLC-UV methods. For

modulators demonstrating induction of BCRP, all compounds were added into the basolateral compartment and sampling of the apical compartment was conducted.

3.3.10.5. Calculation of permeability coefficients

The apparent membrane permeability (Papp: $x10^{-6}$ cm/s) of sulfasalazine was calculated according to equation 6.

$$\text{Papp} = {}^{dQ}/_{dt} \cdot \frac{1}{AC_0} \qquad (6)$$

where dQ/dt is the rate of appearance of sulfasalazine on the receiver side (calculated from the slope of the cumulative transport graph), C_0 is the initial concentration of sulfasalazine in the donor compartment and A (cm^2) is the surface area of the insert.

3.3.11. Statistical analysis

All statistical analyses were performed in Graph pad Prism (La Jolla, California, USA). One-way ANOVA and t-tests were carried out to determine the differences between the mean values. For all multi-well based assay replicates of at least 6 were used in three independent experiments. For western blot and transport studies replicates of at least three were used and repeated in three independent experiments. IC_{50} and EC_{50} metrics were calculated using sigmoidal fit functions within Graph pad Prism. A significance p-value of < 0.05 was considered as statistically significant.

3.4. Results

3.4.1. Z310 cell morphology

Z310 cells were grown on uncoated plastic surfaces and typically became confluent in 2-3 days. Cells show formation of closely packed islands under light microscopy with typical polygonal epithelial morphology at 10X and 40X (Figure 3.1).

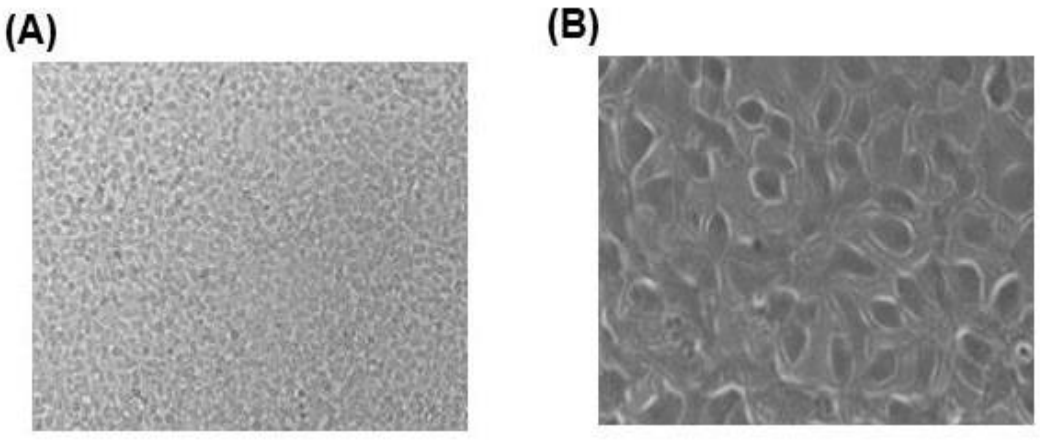

Figure 3.1: Morphology of Z310 cells grown on tissue culture surfaces.

Z310 cells were seeded at a density of $4x10^4$ cells/cm^2 and incubated at 37˚C with 5% CO2 in a humidified atmosphere for two days. The cells were examined under 10x (A) and 40x (B) objective lens.

3.4.2. Development of a Z310 *in-vitro* BCSFB model

3.4.2.1. Assessment of monolayer formation and barrier integrity

The formation of a monolayer was determined by assessing the TEER values for 12 days post seeding in order to identify the optimal growth time on inserts. TEER values demonstrated a steady increase as the monolayer started to form and reached 92 ± 5 Ω.cm^2 on day 8 before starting to decline thereafter (Figure 3.2).

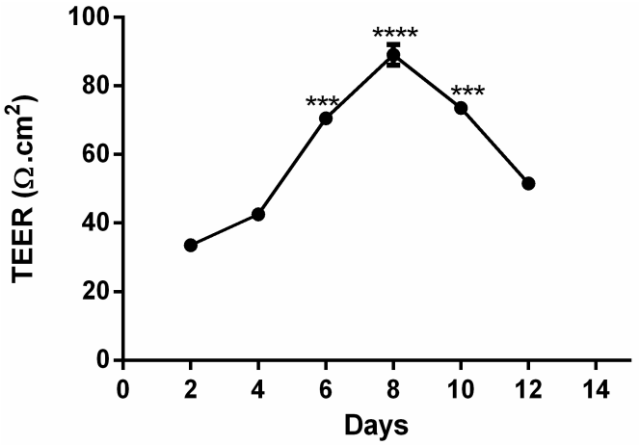

Figure 3.2: Monolayer resistance of Z310 grown on permeable inserts.

Z310 cells were seeded at a density of 2.0 x10^5 cells/cm^2 onto collagen coated inserts at 37˚C with 5% CO_2 in a humidified atmosphere. The media was replaced every other day and TEER values were measured with EVOM voltammeter up to 12 days. Statistical analysis compares TEER at day 2 to all other data points. *** P ≤ 0.001 and ****P≤0.001.

3.4.2.2. Measurement of CSF formation

A key function of the choroid plexus epithelial cells is the production of cerebrospinal fluid (CSF). Z310 cells grown on permeable inserts demonstrated the production of fluid in the inner chamber and an increase in the volume height, which was maintained at > 2 mm for 48 h (Figure 3.3).

Figure 3.3: Measurement of fluid formation in permeable inserts

Z310 cells were seeded at a density of 2.0 x10^5 cells/cm^2 onto the collagen coated inserts for 7 days at 37˚C with 5% CO_2 in a humidified atmosphere. The media was replaced every other day. After 3-4 days when the monolayer was formed the volume of inner chamber was increased and remained consistent for at least 48 h.

3.4.3. Cellular toxicity of modulators towards Z310 cells

To investigate the cellular toxicity of modulators towards the Z310 cells, a MTT cellular toxicity assay was conducted whereby cells were exposed to a 7-fold log concentration range of modulators, 0.001 µM-1000 µM, for 24 h.

The majority of modulators demonstrated IC_{50} values above 140 ± 1.5 µM. The lowest IC_{50} values (1.4 ± 0.8 µM) was identified for α-napthoflavone (Figure 3.4L) followed by quercetin (107 ± 2.3 µM) (Figure 3.4N). Additionally a number of modulators demonstrated minimal toxicities up to 1000 µM and included chrysin (Figure 3.4D), 17-β-estradiol (Figure 3.4F), hesperidin (Figure 3.4J), naringin (Figure 3.4M), silymarin (Figure 3.4Q) and TMF (Figure 3.4R).

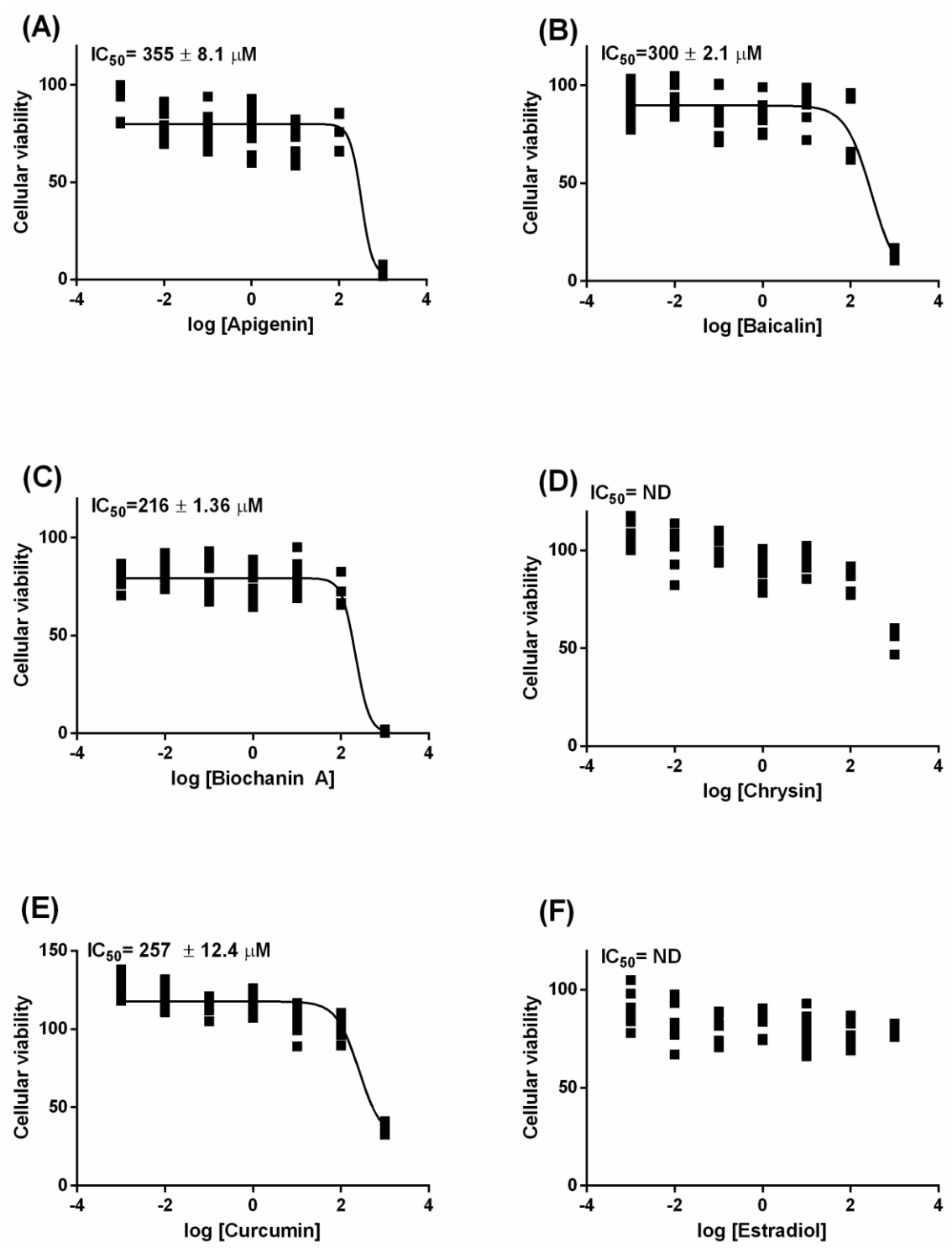

Figure 3.4: Phytochemical cytotoxicity towards Z310 cells (A-F)

The Z310 cells were seeded on to the 96-well plates at 37°C in a humidified atmosphere of 5% CO_2 in air for 24h. The media was aspirated and cells were incubated with 7-fold log concentration range (0.001 μM-1000 μM) of apigenin (A), baiclain (B), biochanin A (C), chrysin (D), curcumin (E) and 17-β-estradiol (F) for 24 h, prior to the assessment of cytotoxicity.

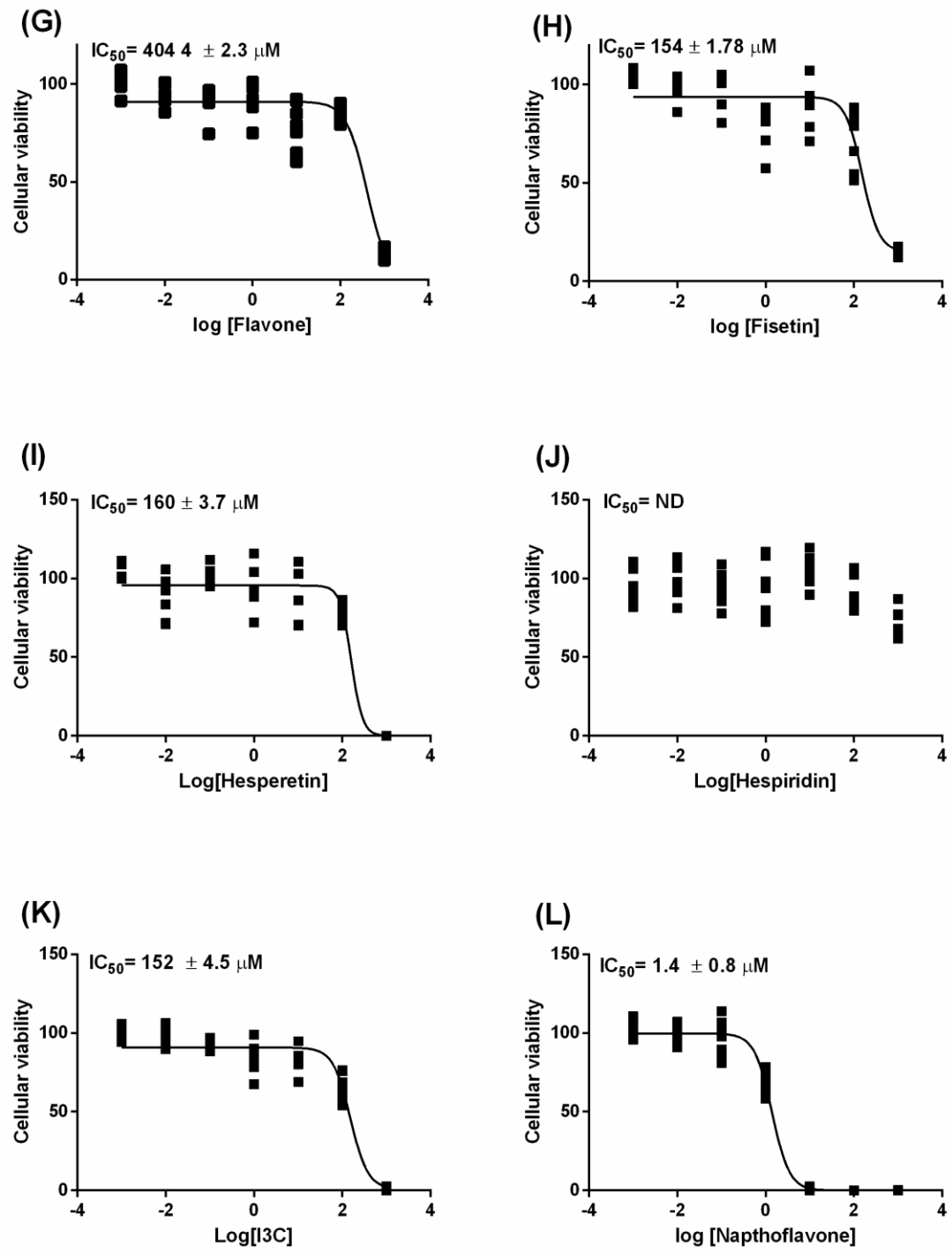

Figure 3.4: Phytochemical cytotoxicity towards Z310 cells (G-L)

The Z310 cells were seeded on to the gelatine coated 96-well plates at 37°C in a humidified atmosphere of 5% CO_2 in air for 24h. The media was aspirated and cells were incubated with a 7-fold log concentration range (0.001 µM-1000 µM) of fistein (G), flavone (H), hesperetin (I), hesperidin (J), indole 3 carbinol (K) and α-napthoflavone (L) for 24h prior to the assessment of cytotoxicity.

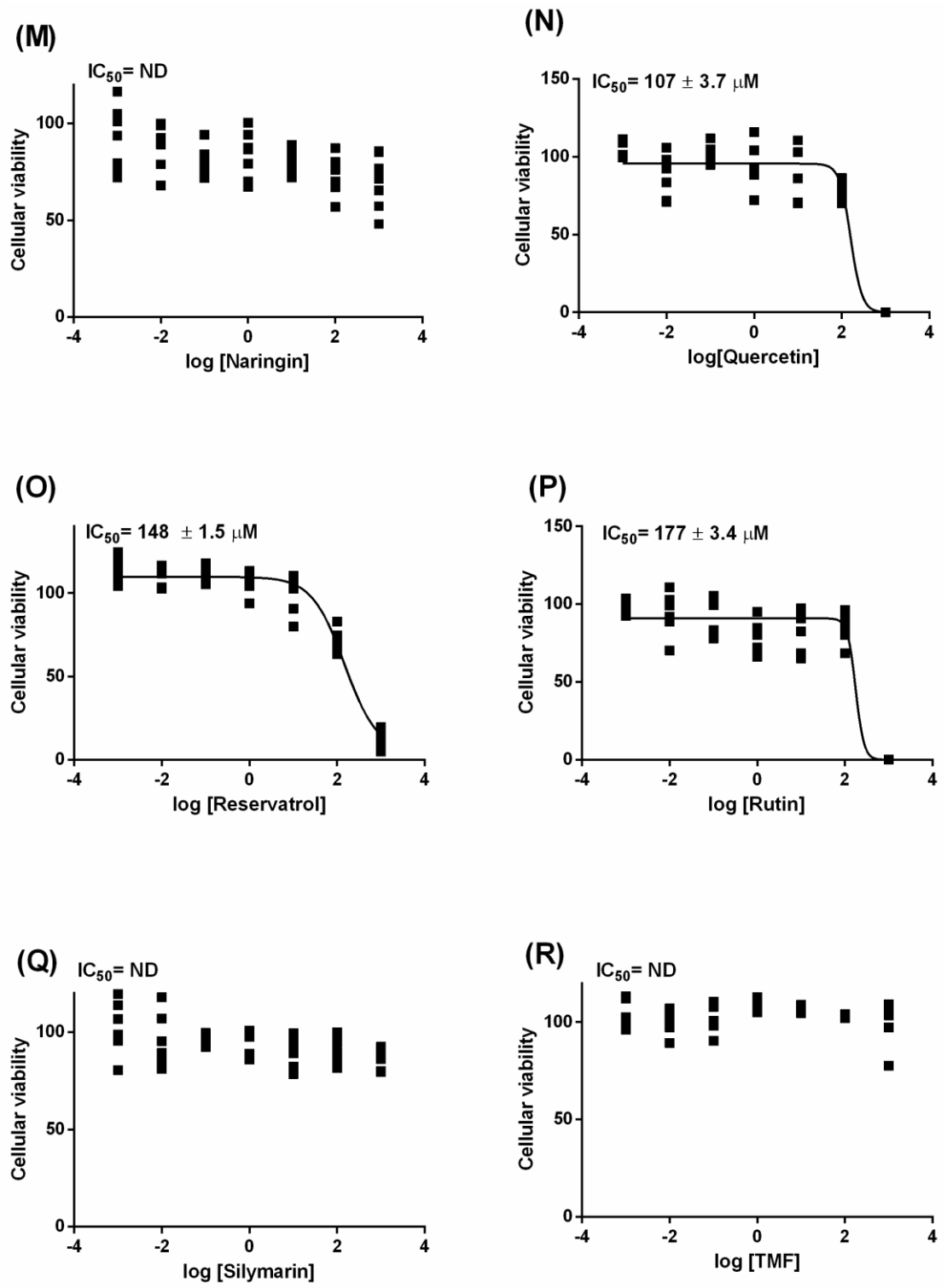

Figure 3.4: Phytochemical cytotoxicity towards Z310 cells (M-R)

The Z310 cells were seeded on to the 96-well plates at 37°C in a humidified atmosphere of 5% CO_2 in air for 24h. The media was aspirated and cells were incubated with a 7-fold log concentration range (0.001 µM-1000 µM) of naringin (M), quercetin (N), resveratrol (O), rutin (P), silymarin (Q) and TMF (R) for 24h prior to the assessment of cytotoxicity.

3.5. Determination of BCRP expression in Z310 cells

3.5.1. Determination of BCRP genomic and protein expression

Z310 cells were characterised to determine the expression of BCRP along with the choroid plexus marker transthyretin (TTR). Reverse–transcriptase PCR confirmed the genomic expression of BCRP in Z310 cells with an expected product size of 146 base pairs alongside the presence of choroid plexus phenotypic markers transthyretin (TTR) and β-actin (BA) loading control (Figure 3.5A). Western blot analysis confirmed the BCRP protein expression in Z310 cells with an expected size of 72 kDa (Figure 3.5B).

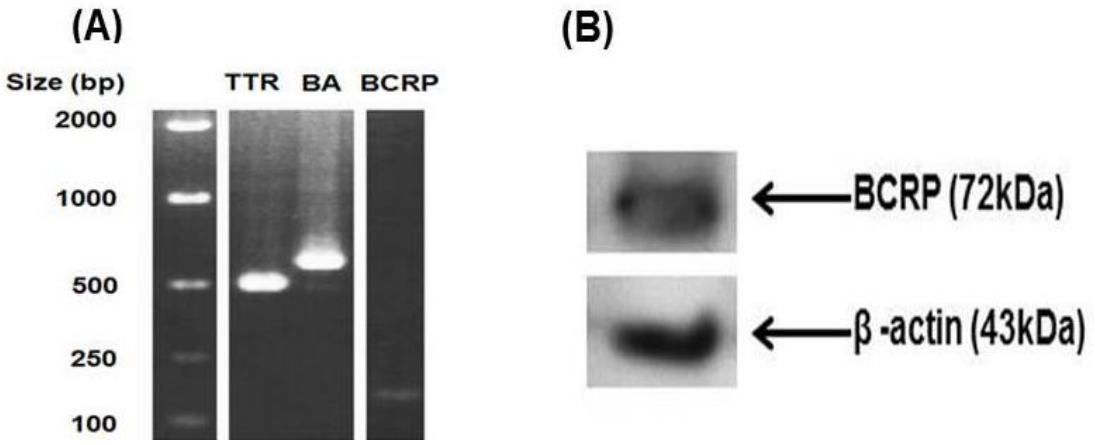

Figure 3.5: Genomic expression of BCRP in Z310 cells.

(A) Cells were seeded to a 6-well plate for 48h. Total RNA was extracted and 500ng of the RNA was loaded to the reverse transcriptase prior to PCR. Gel electrophoresis was performed with the PCR product. The amplicon products for transthyretin (TTR), loading control β-actin and BCRP were detected (B) Protein expression of BCRP in Z310 cells. Cells were seeded into a 6-well plate for 48 h. Whole cell protein was extracted using RIPA buffer. Approximately 80 µg of the protein was loaded to the gel and transferred onto the PVDF membrane. The membrane was blocked and incubated with ABCG2 M-70 antibody for 24h at 4°C and then incubated with goat anti-rabbit IgG-horse radish peroxidise-conjugated (Santa Cruz biotechnology, Sc-2004).

3.5.2. Immunostaining detection of BCRP in Z310 cells

The expression of BCRP in Z310 cells was investigated using immunostaining techniques. Confocal laser microscopy was able to demonstrate BCRP localisation in Z310 cells with staining against BCRP throughout the cells and greater localisation in the cell membrane (Figure 3.6).

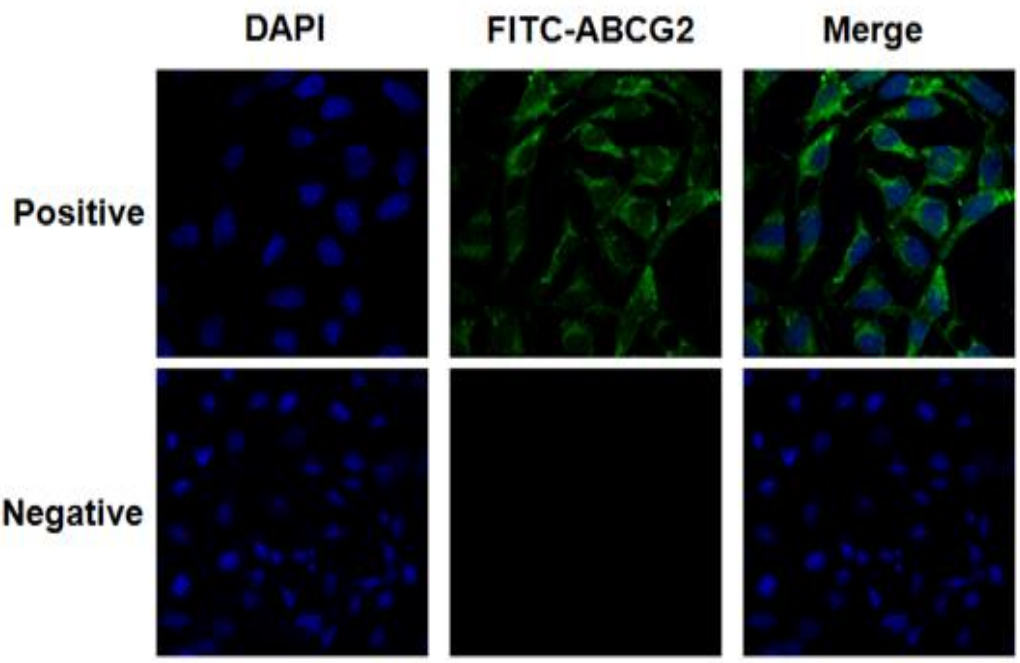

Figure 3.6: Localisation of BCRP in Z310 cells.

Cells were grown on coverslips for 2-3 days and fixed with 4% paraformaldehyde and stained for BCRP using the ABCG2-M70 primary antibody and goat anti-rabbit IgG-FITC secondary antibody (green). Cell nuclei were visualised using DAPI (blue). The positive control includes ABCG2-M70 and FITC secondary whereas a negative control excludes the primary antibody.

3.6. Measurement of BCRP cellular functional activity in Z310 cells

3.6.1. Assessment of intracellular H33342 accumulation in the absence and presence of Ko143

To assess the functional activity of BCRP in Z310 cells a 96-well plate assay was utilised to measure the intracellular accumulation of H33342, a substrate of BCRP in the absence and presence of Ko143, a known potent inhibitor of BCRP. When exposed to Ko143 over a concentration range of 0.039 nM-5 µM, the intracellular accumulation

was significantly increased by approximately 3-fold ($p \leq 0.0001$), regardless of the Ko143 concentration used (Figure 3.7).

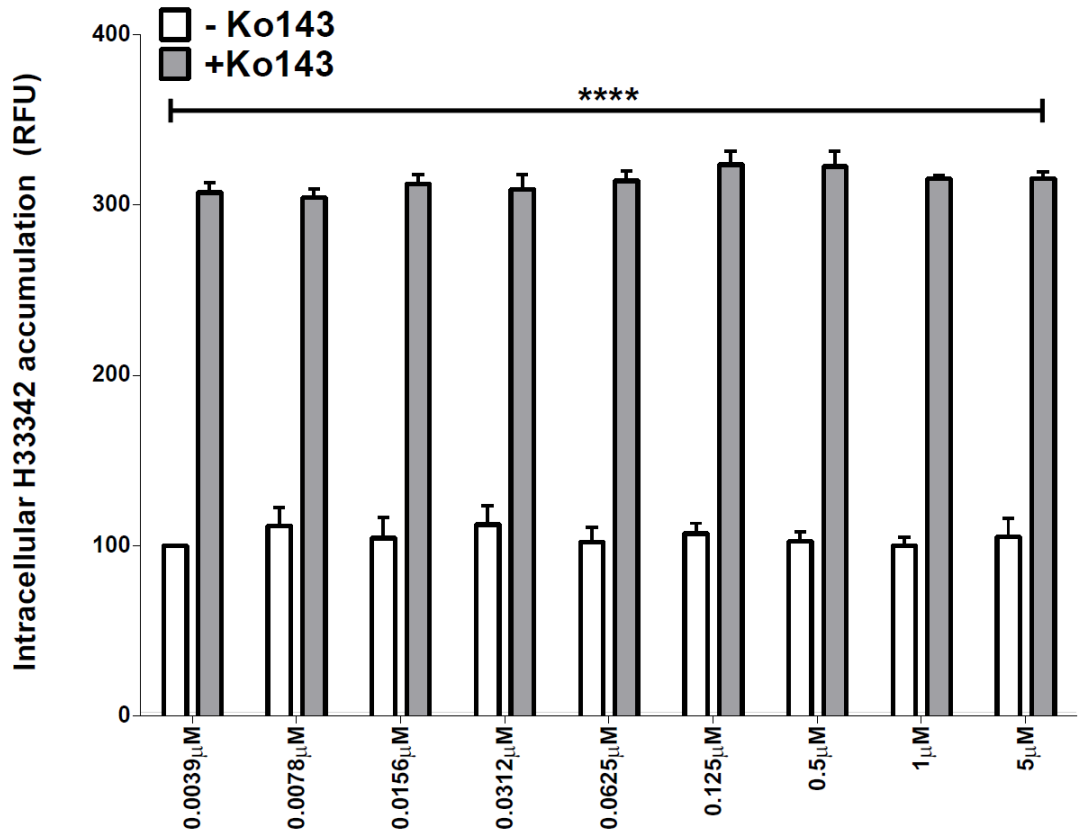

Figure 3.7: Functionality of BCRP in Z310 cells.

15,000 cells/well were seeded into wells of a clear 96-well plate at 37°C and 5% CO_2 for 24 h. Subsequently cells were washed with PBS to remove media and 200 µL of growth media a range of Ko143 concentration (0.0039 µM-5 µM) was added and the plate pre-incubated for 1 h before the media was removed. Thereafter the cells were again incubated with media containing Ko143 (0.0039 µM-5 µM) in addition to 10 µM H33342 for 30 min before the intracellular accumualtion of H33342 assessed using a fluoresecent plate reader with an excitation wavelength of 355 nm and an emission wavelength of 460 nm. Significant differences between control and Ko143 concentrations are indicated above the appropriate error bars (**** $p \leq 0.0001$).

3.6.2. Modulator inhibition of BCRP function in an H33342 intracellualr accumulation assay

To assess the potential of modulators to directly inhibit BCRP, BCRP functional activity was assessed by measuring the accumulation of H33342 in the presence of modulators and Ko143 for 1 h. Our results demonstrated significant increase of intracellular H33342 accumulation for apigenin, chrysin (100 µM), curcumin (1µM), 17-β-estradiol (1 µM), hesperetin (10 and 100 µM) ($P \leq 0.01$), naringin and TMF (100µM) ($p \leq 0.001$) by a fold change of 1.05-1.35 (mean fold change), 1.35 ± 0.5, 1.37 ± 0.2, 1.40 ± 0.70, 1.35-1.42 (mean fold change), 1.6 ± 0.1 and 1.6 ± 0.2 respectively when compared to control (Figure 3.8).

Similarly, flavone (100 µM), indole 3 carbinol (1 and 100 µM), rutin (100µM), silymarin (100µM) and TMF (10 µM) also shown significant increases ($P \leq 0.05$) of intracellular H33342 accumulation by 1.15 ± 0.4, 1.28-1.32 (mean fold change), 1.29 ± 0.5, 1.32 ± 0.1 and 1.33 ± 0.3 respectively when compared to control.

Furthermore, 17-β-estradiol (100 µM), flavone (1 µM), quercetin (100 µM) demonstrated significant reduction in H33342 intracellular accumulation leading to a fold change of 0.25 ± 0.1, 0.26 ± 0.2, 0.45 ± 0.05. Whereas, biochanin A, hesperidin and resveratrol did not demonstrate any change in intracellular H33342 accumulation.

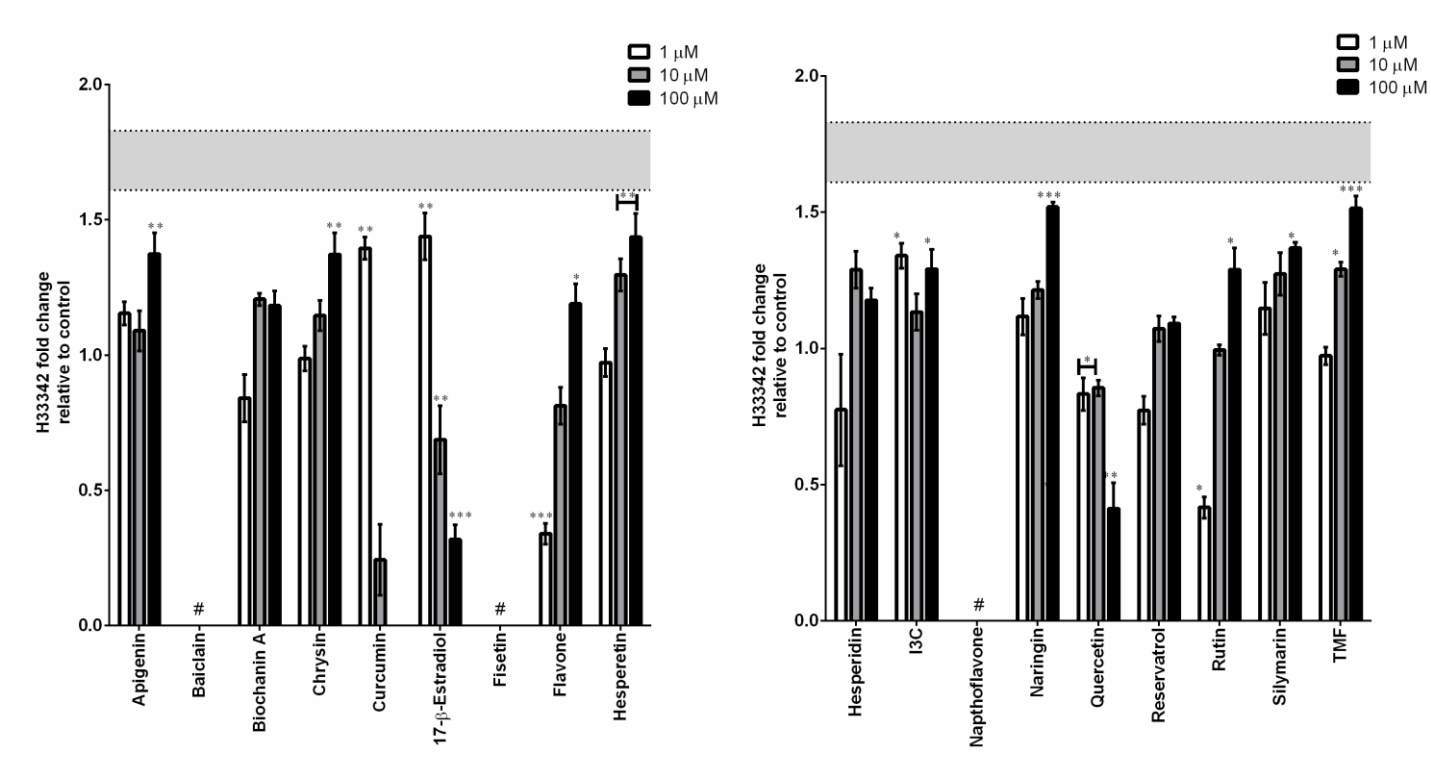

Figure 3.8: Modulation of intracellular accumulation of H33342 following a 1-hour incubation with modulators.

Cells were grown in a 96 well plate for 48 h and washed with warm HBSS supplemented and incubated for 1 h with media containing 25 µM of test compound, except α-napthoflavone (1µM) and 17-β-estradiol (100nM). Subsequently cells were incubated with media containing H33342 for 30 min and lysed. The change in H33342 intracellular accumulation in the presence of Ko143 is highlighted by the shaded regions (2-fold change). Significant differences between Ko143 and modulators are indicated above the appropriate error bars. * P ≤ 0.05, ** P ≤ 0.01, *** P ≤ 0.001 and **** P ≤ 0.0001. The hash symbol (#) indicates modulators excluded due to auto fluorescence.

3.6.3. Modulator mediated changes in BCRP function following 24 hours incubation

The time dependent functional activity of BCRP was also evaluated following incubation of H33342 in the presence of modulators for a 24 h period. Z310 cells were exposed to modulators at 1 µM, 10 µM and 100 µM.

Our results demonstrated that I3C (1 µM) and naringin (1 µM) significantly increased ($p \leq 0.001$) the intracellular H33342 accumulation by 1.65 ± 0.1 and 1.75 ± 0.2 fold respectively, when compared to Ko143 a known potent inhibitor of BCRP. Similarly, apigenin (1-100 µM), biochanin A (10 and 100 µM), chrysin (1-100 µM), curcumin (1 µM), 17-β-estradiol (1 and 10 µM), hesperetin (1 µM), resveratrol (100µM), rutin (100µM), silymarin (1-100 µM) and TMF (1 µM) also increased the H33342 accumulation leading to a fold change of 1.15 -1.35 (mean fold change), 1.20-1.22 (mean fold change), 1.25-1.27 (mean fold change), 1.25 ± 0.2, 1.25-1.30 (mean fold change), 1.45 ± 0.5, 1.35 ± 0.3, 1.35 ± 0.1, 1.25-1.27 (mean fold change) and 1.35 ± 0.1 respectively when compared to control. Interestingly, 17-β-estradiol (100 µM), quercetin, resveratrol and rutin (1 µM) significantly reduced ($p \leq 0.01$) intracellular H33342 accumulation (Figure 3.9).

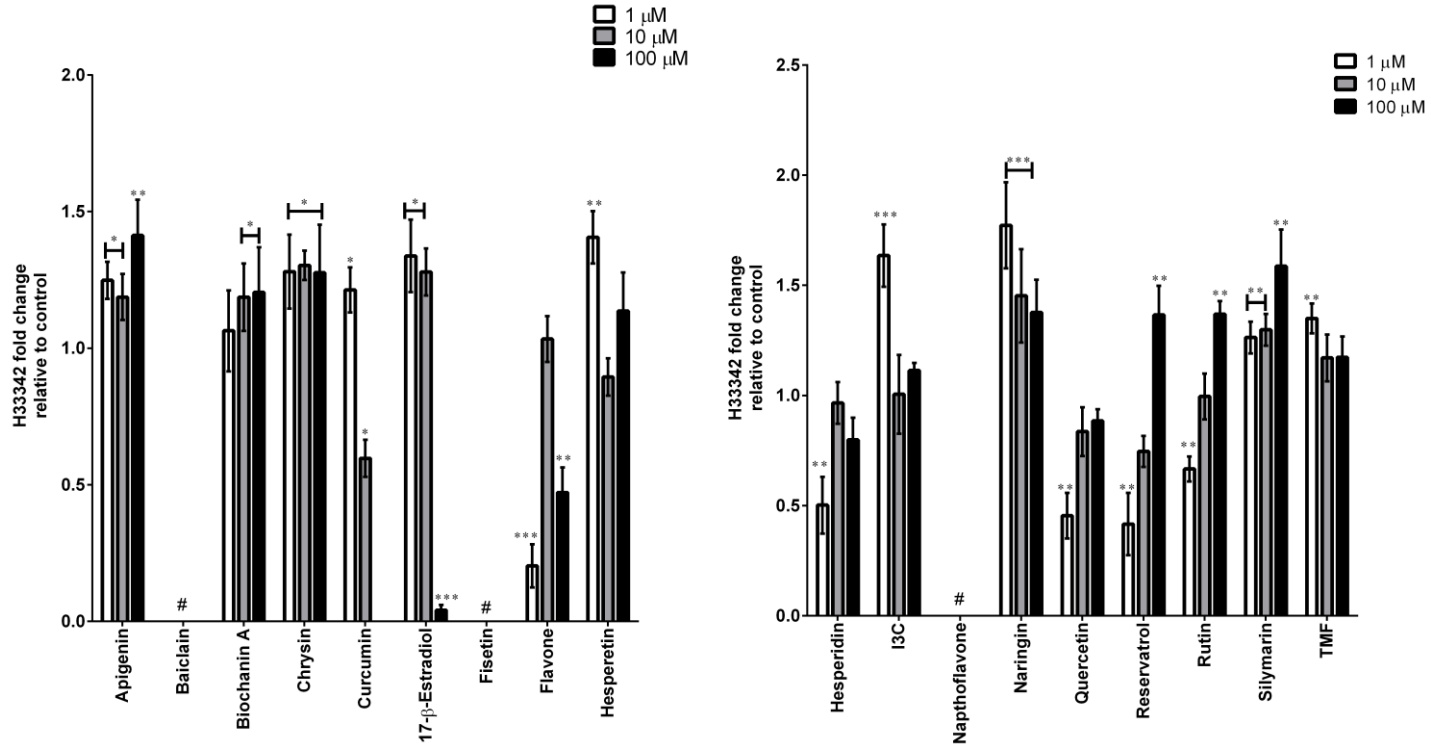

Figure 3.9: Modulation of intracellular accumulation of H33342 following a 24-hour incubation with modulators

Cells were grown in a 96 well plate for 24 h and washed with pre- warm HBSS supplemented and incubated for 24h with media containing 1-100 μM of test compound, except α-napthoflavone (1 μM) and 17-β-estradiol (100 nM). After 24h cells were incubated with media containing H33342 for 30 min and lysed. H33342 fold change in the control is represented by shade. Significant differences between control and modulators are indicated above the appropriate error bars. * P ≤ 0.05, ** P ≤ 0.01, *** P ≤ 0.001 and **** P ≤ 0.0001. The hash symbol (#) indicates modulators excluded due to auto fluorescence.

3.7. Modulation of BCRP protein expression by phytochemical modulators

To assess the effect of modulators on BCRP protein expression, Z310 cells were incubated with modulators for 24 h and western blot analysis was performed. Our results demonstrated a significant increase ($p \leq 0.0001$) in BCRP protein for flavone (2.65 ± 0.12 fold), baicalin (2.42 ± 0.19 fold) and hesperidin (2.43 ± 0.09 fold) (Figure 3.10 and 3.11). Furthermore, a significant down-regulation in BCRP was observed for naringin ($p \leq 0.001$) (0.16 ± 0.07 fold) and silymarin ($p \leq 0.001$) (0.22 ± 0.09 fold), quercetin ($p \leq 0.01$) (0.29 ± 0.08 fold) and 17-β estradiol ($p \leq 0.05$) (0.49 ± 0.11 fold). α-napthoflavone was excluded from the study due to its cytotoxicity.

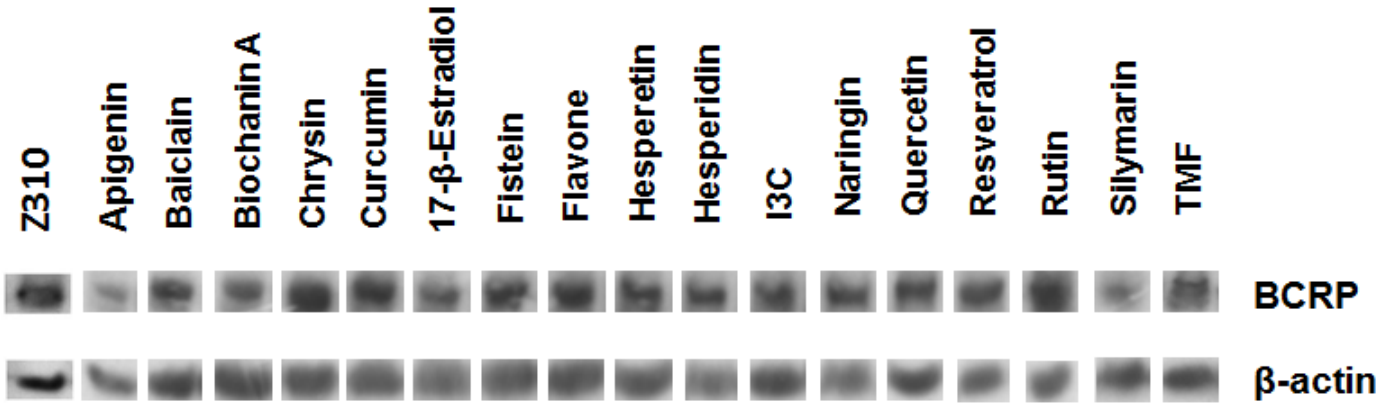

Figure 3.10: Changes in BCRP Protein expression under 24-hours exposure to modulators

Cells were seeded in a 6-well plate for 24 h to attach and subsequently incubated with 25µM modulators except 17-β-estradiol (100 nM) for 24 h. Whole cell protein was extracted using RIPA buffer. Approximately 100 µg of the protein was loaded onto a SDS-PAGE gel to separate proteins bands. The resulting gel was then transferred onto a PVDF membrane and incubated with ABCG2 M-70 antibody for 24 h at 4°C and then incubated with goat anti-rabbit IgG-horse radish peroxidise-conjugated (Santa Cruz biotechnology, Sc-2004). Chemiluminescence detection was performed with lab made ECL and a representative image is displayed. Z310 represent BCRP expression in the absence of modulators.

.

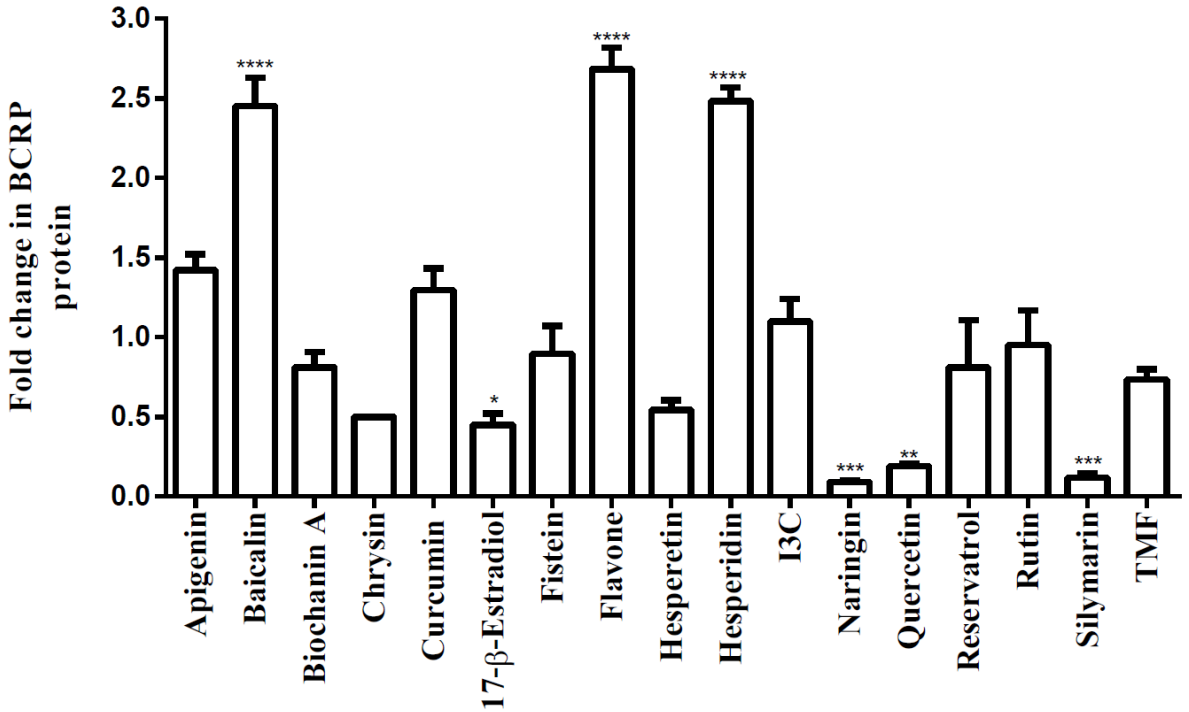

Figure 3.11: Fold change in BCRP protein expression.

The cells were seeded to a 6-well plate for 24h. The cells were incubated with 25µM modulators except 17-β-estradiol (100 nM) for 24h. Whole cell protein was extracted using RIPA buffer. 100 µg of the protein was loaded to the gel and transferred onto the PVDF membrane. The membrane was blocked and incubated with ABCG2 M-70 antibody for 24h at 4°C and then incubated with goat anti-rabbit IgG-horse radish peroxidise-conjugated (Santa Cruz biotechnology, Sc-2004). Chemiluminescence detection was performed with lab made ECL. Significant differences in protein expression are indicated above the appropriate error bars. * $P \leq 0.05$, ** $P \leq 0.01$, *** $P \leq 0.001$ and **** $P \leq 0.0001$.

3.8. Quantitative PCR assessment of the changes in BCRP genomic expression following exposure to modulators

The modulation of BCRP genomic expression was evaluated by qPCR using 4 identified modulators of BCRP protein expression, namely baiclain, flavone as up-regulators and naringin and quercetin as down-regulators. A significant increase ($p \leq 0.0001$) in genomic expression of BCRP for baiclain (1.48 ± 0.23 fold) and flavone (1.22 ± 0.25 fold), whereas naringin was slightly downregulated but this was not significant. On the other hand quercetin was significantly ($p \leq 0.01$) down regulated by 0.75 ± 0.11 fold of control (Figure 3.12).

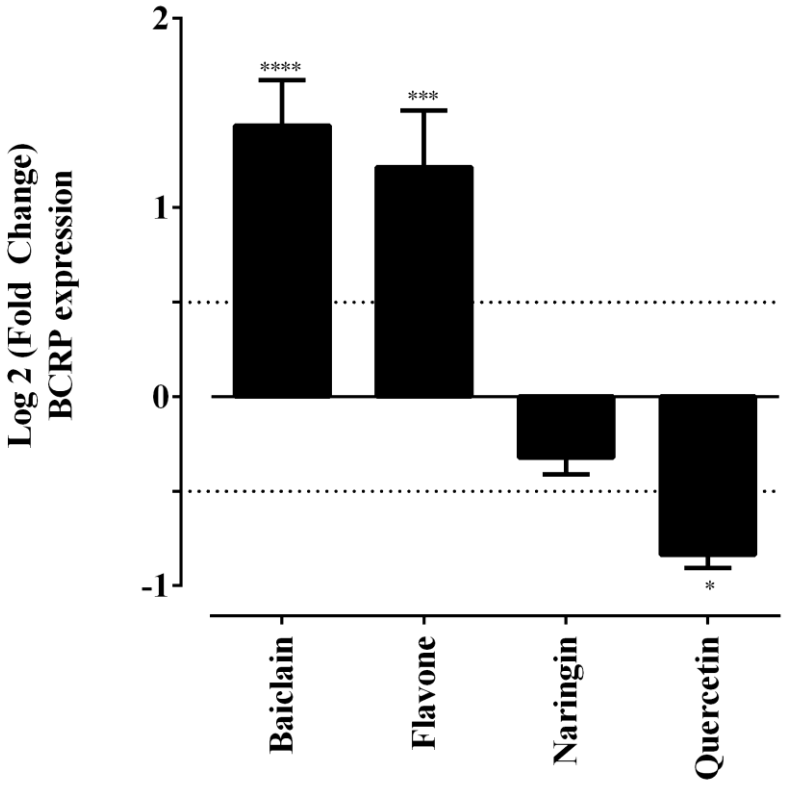

Figure 3.12: Modulation of BCRP gene expression after 24 h incubation with modulator compounds.

Z310 cells were seeded onto a 6-well plate in the growth medium and incubated at 37°C and 5% CO_2 for 24h. The media was removed and modulators prepared in media were added to the wells and incubated for 24h. After 24 h the media was removed cells were washed with the pre-warmed PBS and RNA was extracted according to manufacture s instructions. Total RNA was reverse transcribed and gene expression assessed by qPCR using a SYBR green master mix. Dashed line indicated 0.5-fold change. Significant differences between control and modulators are indicated above the appropriate error bars *** $P \leq 0.001$ and **** $P \leq 0.0001$.

.

3.9. Modulation of BCRP transport function using an i*n -vitro* BCSFB model

3.9.1. HPLC-UV Detection of sulfasalazine

A HPLC method for the detection of sulfasalazine successfully detected sulfasalazine with a consistent retention time of 3.36 min (Figure 3.13) with a second smaller solvent front peak at 1.81 min. The serum free media was used as a solvent in the transport study and the solvent front is more likely glucose as for the Z310 cells DMEM high glucose was used as stated in methods.

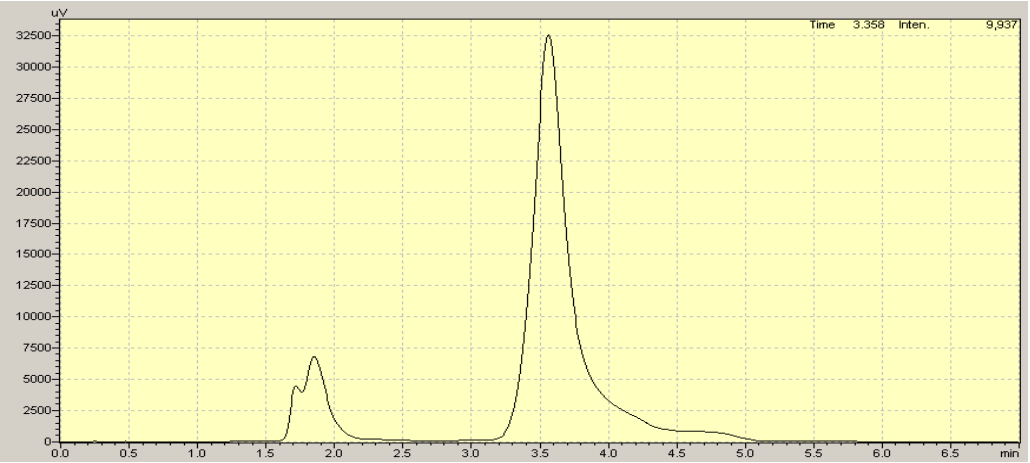

Figure 3.13: Chromatogram of sulfasalazine.

Sulfasalazine was detected with a rentetion time of 3.36 min using a reversed-phase C18 column (Phenomenex Luna 5-µm) with a mobile phase consisting of 70:29:1 methanol:millQ water:acetic acid and flow rate of 1 mL/min.

3.9.2. Linearity

The linearity of the HPLC method determined by constructing a calibration curve with over a concentration range of 0.1 µM-50 µM. The area under the curve was linearly regressed under the concentration range used and the coefficient of correlation (r^2) was 0.9998. The slope and intercept were 31872.15 ± 3181 and 4991.831 ± 586 respectively. The LOD and LOQ were found to be 0.081 ± 0.004 and 0.089 ± 0.006 µM respectively.

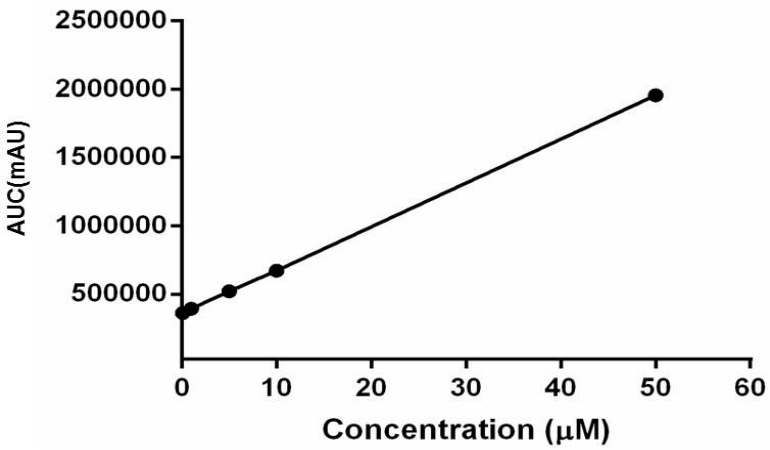

Figure 3.14: Linearity of sulfasalazine.

Concentrations of sulfasalazine (0.1 µM-100 µM) were prepared in serum free transport media and 20 µL of the each concentration was injected to the HPLC machine and area under curve was obtained. Calibration curve was constructed by plotting average peak area against concertation. LOD and LOQ was calculated by using regression analysis.

3.9.3. The impact of transport media on *in-vitro* BCSFB monolayer integrity

To assess the impact of transport media on the stability of the monolayer formation, preliminary transport studies were conducted assessing the impact of HBSS transport media (HBSS supplemented with 10 mM glucose and HEPES (10 mM) and serum free media (SFM) on the TEER of the monolayer.

It was demonstrated that SFM provided a more stable media for the preservation of TEER values over the duration of the incubation study with no significant difference in TEER values when compared to the start of the study (Figure 3.15). Furthermore, the

use of HBSS resulted in a significant ($p \leq 0.001$) decline in TEER values 92 ± 5 $\Omega.cm^2$ to 25 ± 8 $\Omega.cm^2$ after 180 min (Figure 3.15).

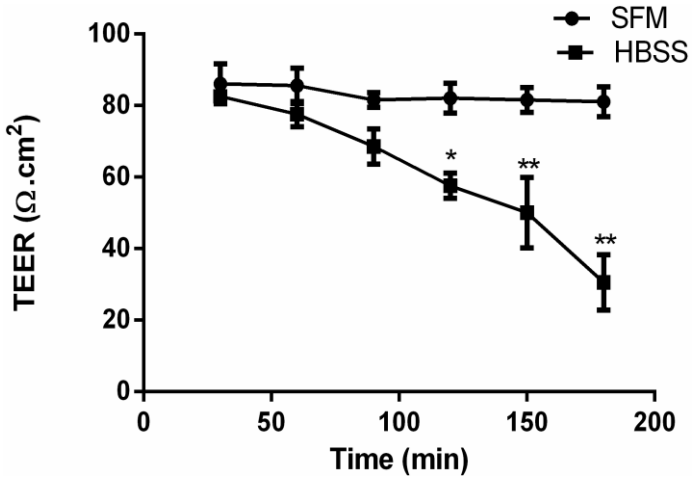

Figure 3.15: TEER values of Z310 cells maintained in HBSS and SFM, grown in permeable inserts

Cells were seeded onto the collagen coated permeable inserts for 8 days, TEER values were measured on the day before, and after running the assay for 210 min. Significant, differences between HBSS and serum free media are indicated above the appropriate error bars * $P \leq 0.05$, ** $P \leq 0.01$.

3.9.4. Functional assessment of BCRP in an *in-vitro* permeable insert BCSFB model

The *in-vitro* BCSFB model was developed by growing Z310 cells on permeable inserts for 8-10 days. The functionality of BCRP was assessed by measuring the transport of sulfasalazine, a substrate of BCRP, in the presence or absence of Ko143, a known BCRP inhibitor. Our results demonstrated a significant increase in sulfasalazine transport from apical-to-basolateral from all time points when compared with control, signifying the functional presence of BCRP with a 10% increase in sulfasalazine transport in the presence of Ko143 (Figure 3.16) and causing an apical-to-basolateral apparent permeability ($P_{app,AB}$) increase from 1.32 ± 0.12 $x10^{-6}$ cm/s to 2.11 ± 0.09 $x10^{-6}$ cm/s when exposed to Ko143.

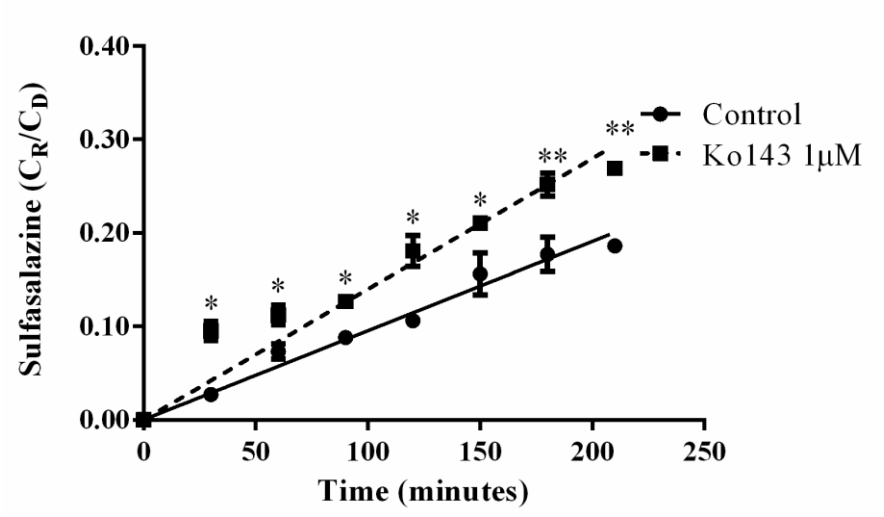

Figure 3.16: Assessment of BCRP functionality in an *in-vitro* BCSFB model.

Cells were grown on permeable insert and transport studies were performed on day 8 (TEER ≥ 60 Ω.cm^2) following 1 h incubation with Ko143. Results are reported as the fraction of sulfasalazine transporter (receiver concentration/ donor concentration). Statistically significant differences between control and Ko143 conditions are indicated. * P ≤ 0.05 and ** P ≤ 0.01.

3.9.5. Functional assessment of BCRP in the presence of BCRP up-regulating modulators

Modulators identified as demonstrating significant up-regulation of BCRP at in Z310 cells, namely baiclain and flavone were assessed for their ability to modulate BCRP function in an *in-vitro* transport model. Baicalin (Figure 3.17A) demonstrated a significant decrease ($p \leq 0.05$) the transport of sulfasalazine across the insert by approximately 10 % (C_R/C_D) for portions of the assay and this was coupled with a significant ($p < 0.05$) decrease in $P_{app,AB}$ from 1.32 ± 0.12 x10^{-6} cm/s to 1.10 ± 0.08 x10^{-6} (Figure 3.17A). However exposure to flavone did not result in any significant change in the transport of sulfasalazine across the in-vitro BCSFB barrier model (Figure 3.17B)**.**

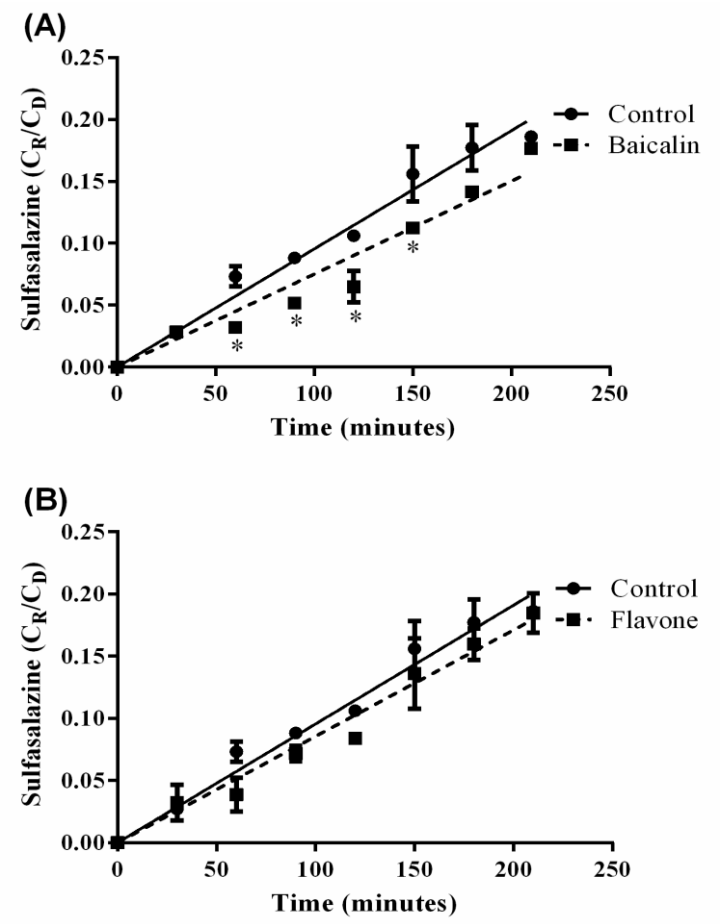

Figure 3.17: Transport of sulfasalazine across an *in vitro* BCSFB model following 24 hour incubation with baicalin or flavone.

Cells were grown on permeable insert and transport studies were performed on day 8 (TEER ≥ 60 Ω.cm^2) following 24 h incubation with modulators, baicalin (A) or flavone (B). Results are reported as the fraction of sulfasazine transporter (receiver concentration/ donor concentration). Statistically significant differences between control and modulator are indicated. * P ≤ 0.05 and ** P ≤ 0.01.

3.9.6. Functional assessment of BCRP in the presence of BCRP down-regulating modulators

The functional assessment of BCRP was evaluated in the presence of BCRP down-regulators namely, naringin, silymarin and 17-β-estradiol in the *in-vitro* BCSFB model by measuring the transport of sulfasalazine. Naringin, silymarin and 17-β-estradiol resulted in significant increases in sulfasalazine $P_{app,AB}$ to 3.83 ± 0.34 x10^{-6} cm/s, 3.33 ± 0.61 x10^{-6} cm/s and 2.01 ± 0.23 x10^{-6} cm/s respectively, when compared to the absence of modulators 1.32 ± 0.12 x10^{-6} cm/s (Figure 3.18). This translated into an increase of 43% in sulfasalazine transport for naringin and 36% increase for silymarin with a smaller 11% increase for 17-β-estradiol.

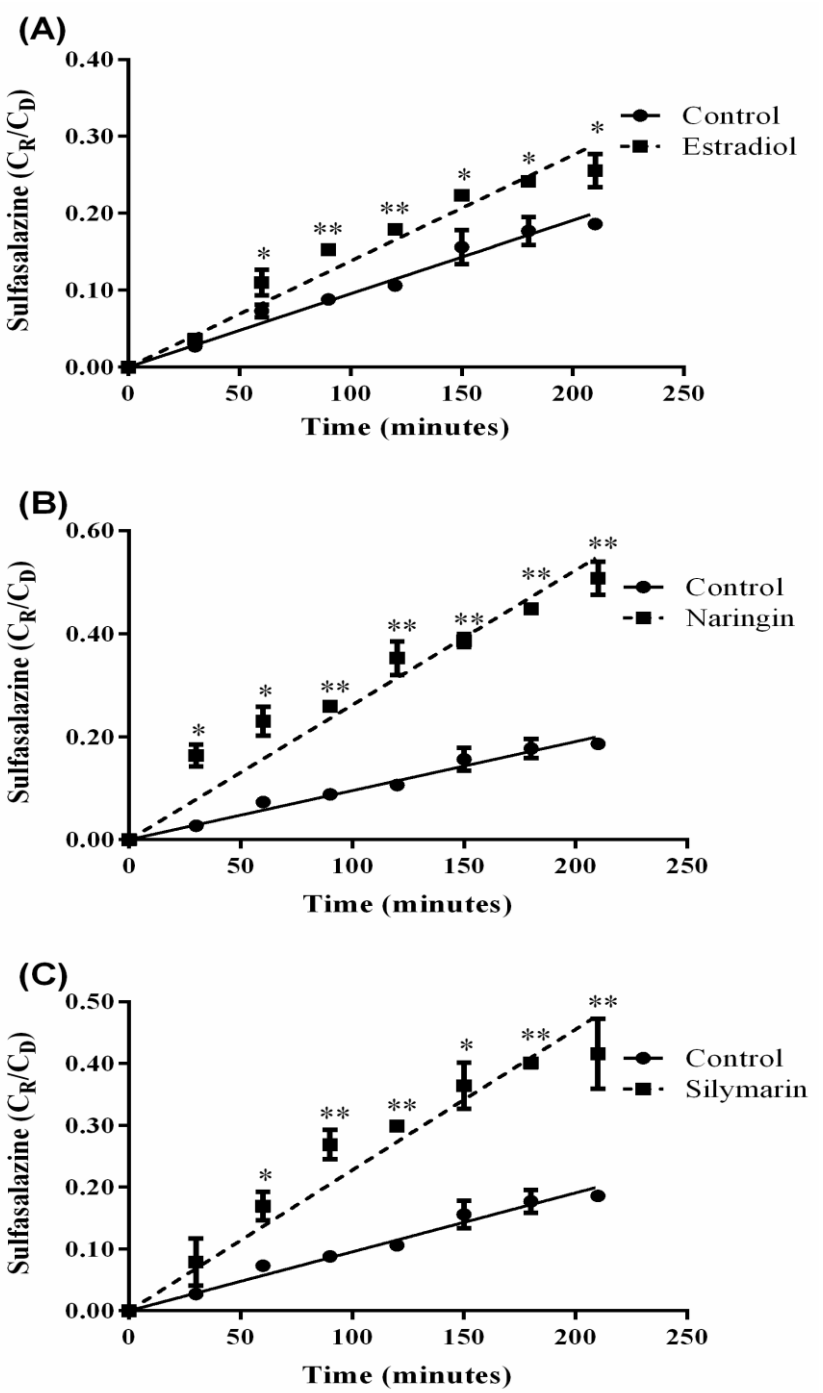

Figure 3.18: Transport of sulfasalazine across an *in vitro* BCSFB model following 24 hour incubation with 17-β-estradiol, naringin or silymarin.

Cells were grown on permeable insert and transport studies were performed on day 8 (TEER ≥ 60 $\Omega.cm^2$) following 24 h incubation with modulators, namely 17-β-estradiol (A), naringin (B) or silymarin (C). Results are reported as the fraction of sulfasalazine transporter (receiver concentration/ donor concentration). Statistically significant differences between control and modulator are indicated. * $P \leq 0.05$ and ** $P \leq 0.01$.

3.10. Discussion

The BBB and the BCSFB regulate the influx and efflux of endogenous substrates and drugs into the brain. Drug transporters at the BBB limit the ability of drugs to permeate into the brain biophase but not in the CSF (Abbott and Romero, 1996), similarly, the transporters at the BCSFB affects the transport of drugs into the CSF not into the brain parenchymal tissues.

ABC transporters are key membrane localised proteins, which often serve a xenobiotic protective mechanism for the CNS but are often the primary cause of poor therapeutic distribution into the CNS. BCRP is an ABC efflux transporter that has been shown to confer resistance to large number of therapeutic agents such as mitoxantrone, methotrexate, topotecan, SN38, doxorubicin and flavopiridol (Doyle and Ross, 2003b, Maliepaard et al., 2001). Although the body of work assessing the important role the BBB plays in governing CNS drug distribution is significant, very little has been reported on the functional role of BCRP at the BCSFB and the role it plays in controlling drug transport across the BCSFB. Knock-out animals data have demonstrated that cells at the BCSFB differ from the BBB in the distribution of ABC transporters and, therefore, the effects of changes in transporter expression on drug distribution. For example, topotecan distribution into the brain was reported to be increased but its penetration into the ventricular CSF was reduced with Bcrp KO mice (Shen et al., 2009) as a result of the asymmetrical expression of the transporter at the BBB and BCSFB (Urquhart and Kim, 2009, Rao et al., 1999). However results can be contrasting depending on the site/location of CSF sampling (i.e. ventricular CSFs vs bulk CSF sampling from the cisterna magna) (Doran et al., 2005, Shen et al., 2009). Furthermore, the complexities in site-specific knock-down of Bcrp (in the CP alone, the CP+BBB or the CP +parenchymal cells) would further compound the interpretation of the changes in gross drug transport.

Several strategies have been considered to enhance drug accumulation into the CNS, the most common of which is to directly inhibit BCRP using chemical modulators such GF120918 (elacridar) or Ko143 (Breedveld et al., 2006, Pick et al., 2008). Unfortunately these inhibitors cause severe neurotoxicity which limits their clinical applications (Thomas and Coley, 2003, Varma et al., 2003).

In an attempt to identify novel candidates that may modulate BCRP expression and function, phytochemicals (primarily flavonoids) show promise as potential BCRP expression and transport function modulators (see section 2.14.5 and 2.14.6).

The key focus of this chapter was to characterise the Z310 rodent choroid plexus epithelial cell line to assess whether BCRP is expressed and to subsequently examine the role phytochemical modulators may play in the cytotoxicity towards Z310 cells but also their ability to modulate BCRP expression and transport functions.

3.10.1. The use of Z310 cells to develop an *in-vitro* BCSFB model

Z310 were first established by Zheng and Zhao (Zheng and Zhao, 2002) by transfection with a viral plasmid (pSV3neo). The cells show typical epithelial cell morphology and presence of BCSFB markers such as transthyretin (TTR), a thyroxine transport protein (Zheng and Zhao, 2002). Z310 cells were selected for their high reported TEER values (130-200 $\Omega.cm^2$) and expression of important transporter proteins such as P-gp, Mrp1, Mrp4 and BCRP (Juliane Kläs et al., 2010) and presence of the key choroid plexus marker (TTR) (Zheng and Zhao, 2002, Juliane Kläs et al., 2010, Szmydynger-Chodobska et al., 2007, Shi et al., 2008b). In contrast other CP cell lines, such as TR-CSFB, demonstrate low TEER value (30-35 $\Omega.cm^2$) and require growth at reduced lower temperatures (Juliane Kläs et al., 2010) (Kitazawa et al., 2001).

Our results demonstrated that Z310 cells, when grown on uncoated tissue culture surfaces, demonstrate typical uniform polygonal epithelial cell morphology, with tendency to form closely packed islands (Figure 3.1 A and B). The formation of a cell monolayer was assessed by measuring the height of the media in the inner chamber when compared to permeable inserts without cells. The height of the medium was about 2 mm higher for up to 24 h representing the formation of CSF (Shi et al., 2008a) (Figure 3.2) and achieved TEER values of 92 ± 5 $\Omega.cm^2$ at day 8 post seeding (Figure 3.3), which would place it within the range of reported TEER values when accounting the growth surface area (1.12 cm^2 versus 4.4. cm^2).

3.10.2. Cytotoxicity assessment of modulators

To date no studies have been reported to our knowledge, assessing the interaction of phytochemical modulators with Z310 cells. As a result, a clear indication of the cytotoxicity for each modulator needed to be identified for subsequent experiments.

Our results reported that most modulators demonstrated IC_{50} values of > 100 µM (Figure 3.4), with the exception of α-napthoflavone (1.4 ± 0.8 µM) (Figure 3.4 L). Furthermore, a number of flavonoids demonstrated no appreciable toxicity at 1000 µM and included chrysin, 17-β-estradiol, hesperidin, naringin, silymarin and TMF (Figure 3.4 D, F, J, M, Q and R, respectively). To date, there is a lack of published cytotoxicity data reported for phytochemical modulators against Z310 cells. However, with some level of caution, comparisons can be made with other cell lines. α-napthoflavone is a synthetic flavonoid and known as a strong inhibitor of CYP1B1 (Vincent et al., 1998). The IC_{50} calculated to inhibit CYP1B1 in MCF-7 cells was 0.2 nM (Zeichner, 2010), which is significantly below our reported values but highlight the potentially cytotoxic nature of this modulator. Zhang, et al (Zhang et al., 2005) demonstrated limited cytotoxicity with chrysin at 50 µM in MCF-7 MX100 cells. Furthermore in another study HepG2 were incubated with 5 µM chyrin to assess changes in the expression of UGT1A1 (Sugatani et al., 2004). In Caco-2 cells 150 µM biochanin A was reported to show no significant decrease in cellular viability, which compares with our calculated IC_{50} 216 ± 1.36 µM (Figure 3.4C).

In another study (Dornan et al., 2007) it was reported the lack of cytotoxicity of apigenin up to 250 µM in rat hepatoma H4IIE cells and C6 glioma cells. Similarly, our results report an IC_{50} of apigenin of 355 ± 8.1µM in Z310 cells (Figure 3.4A). Furthermore, 120 µM fistein reduced the viability of human colonic cancer (COLO205) cells by 27.6% (Wu et al., 2013). Our results demonstrated a 50% reduction in Z310 cell viability by fistein at 154 ± 1.78 µM (Figure 3.4H).

Quercetin has been used *in-vivo* studies in rats, from 1- 400 µM (van Zanden et al., 2007) with no resultant toxicity and concurns with our calculated IC_{50} of 107 ± 2.3 µM (Figure 3.4N). In contrast, naringin was found to use to inhibit BCRP at 3 µM concentration in K562 cells (Imai et al., 2004), however our results demonstrated that narignin was not toxic to Z310 cells up to 1000 µM (Figure 3.4 M). Interestingly, the IC_{50}` for for α-napthoflavone was similar to that reported at the BBB (section 2.7and Figure 2.4 L), however limited correlation was observed with other modulators such as

17-β- estradiol, chrysin and naringin, which demonstrated reduced or no toxicity in Z310 and PBMEC/C1-2 cells.

In contrast to their widely cited beneficial effects, flavonoids also have been found to be pro-oxidant or mutagenic and to produce toxicity (Sahu and Gray, 1997, Galati et al., 2002). The beneficial effects of flavonoids (outside of interacting with BCRP) is often perceived to be because of their antioxidant properties (Kris-Etherton and Keen, 2002, Kelly, 1998, Bonnefoy et al., 2002). In a study comparing 20 flavonoids for their sensitivities towards L-02 and HepG2 cells, it was noted that L-02 cells were more sensitive towards the flavonoids studied. It was proposed that this was related to the fact that L-02 cells possessed a greater level of intracellular antioxidant enzymes and GSH, which are essential and beneficial to help maintain the redox balance in cells due to the fact that the cytotoxic effects of flavonoids are associated with their pro-oxidant activity (Rietjens et al., 2002, Dickancaite et al., 1998, Galati et al., 2002). Furthermore, flavonoid cytotoxicity may have also occurred through apoptosis-inducing properties in cells by interactions with protein kinase, lipid kinase, or other apoptosis related signalling pathways (Kampa et al., 2007, Hadi et al., 2000, Cunningham et al., 1992), which may produce different extents of toxicity in different cell lines, particularly where the expression/abundance of signalling pathway elements are diminished/different.

It is also possible that flavonoids produce both an effect on BCRP whilst at the same time being highly cytotoxic and act in this manner as conventional hydrogen donators, particularly for flavonoids with multihydroxyls, which may form phenoxyl radicals to induce cytotoxicity (Galati et al., 2001, Galati et al., 2002). Furthermore flavonoids may result in cytotoxicity by destroying the intracellular antioxidant systems or negatively impacting on antioxidant-sensitive signalling pathways (Son et al., 2004, Ramos, 2007, Haddad, 2004). Finally, other reports have also suggested the disruption of the mitochondrial respiratory chain or depletion of GSH by forming GSSG or GSH conjugates (Sabzevari et al., 2004).

GST is the most abundant phase-II enzyme in the brain and hence may predispose the BBB to greater levels of sensitives towards phytochemicals compared to the CP. However, given the complex nature of the proposed mechanism of cytotoxicity, the difference in cell origin species (porcine versus rats) the potential for inter-species variability of the abundance of signally pathway elements or metabolism enzymes may confound the mechanism understanding the nature of this toxicity.

3.10.3. Assessment of BCRP expression in Z310 cells

Our results have confirmed the expression of BCRP in Z310 cells using reverse-transcriptase polymerase chain reaction (Figure 3.5A), western blot analysis (Figure 3.5B) and immunosfluoresecene confocal microscopy (Figure 3.6). Our results were consistent with previous study reported the portein expression of BCRP in Z310 cells (Halwachs et al., 2011). Reichel et al (Reichel et al., 2011) reported BCRP genomic and protein expression in rat choroid plexus. Furthermore, BCRP protein expression was demonstrated in rat choroid plexus TR-CSFB cell lines (Hosoya et al., 2004).

3.10.4. Functional assessment of BCRP in the absence and presence of modulators

BCRP functional activity was assessed using a H33342 accumulation assay in the presence of BCRP inhibitor Ko143 (1 µM), and our results demonstrated a significant 1.8 ± 0.2 fold increase in intracellular H33342 accamulation (Figure 3.8), signifing the presence of functional BCRP in Z310 cells. This was then followed by assessing the impact of modulator incubation in a short-term assay of 1 h to mimic a direct inhibition of functional activity study and a 24 h incubation to detect potential genomic/proteomic changes in BCRP, which are translated to changes in functional activity. Our results demonstrated highly significant ($p \leq 0.001$) increases of 1.35 ± 0.5 to 1.6 ± 0.2 fold in intracellular H33342 accumulation for a number of modulators following a 1 h incubation, however none were able to elicit a similar fold-change as observed with Ko143 expect for hesperetin (100 µM), naringin (100 µM) and TMF (100 µM) (Figure 3.8). This indicated that these modulators may act as competitive inhibitors of BCRP, given the short incubation time. In contrast flavone (1 µM), quercetin (100 µM) and rutin (1 µM) demonstrated reduced H33342 accumulation (< 0.5 fold) suggesting an induced/increased efflux effect has occurred (Figure 3.8). Of the published studies available, TMF, apigenin, chrysin, hesperetin, naringin and quercetin have previously demonstrated an ability to inhibit BCRP functional efflux of substrates (see section 2.14.4 for further discussion of these modulators). The role of glycosylation status, resultant hydrophobicity and potential targeting of the ATPase site within the NBD of BCRP may also be an important factor governing the eventual effect observed over short incubation periods (see section 2.14.4 for further discussion of these modulators).

We were also interested to identify the effects of flavonoids on BCRP gene or protein expression over longer periods of exposure, namely 24 h. Our results demonstrated that incubation with the majority of modulators studied resulted significant changes to H33342 intracellular accumulation. The majority of modulators studied resulted in an increase in H33342 accumulation by > 25 % (1.25 fold of greater) with naringin (1 µM), IC3 (1 µM) and silymarin (100 µM) eliciting a > 1.5 fold increase in H33342 accumulation, and hence demonstrating potential down-regulation of BCRP to enhance H33342 intracellular accumulation. In contrast curcumin (10 µM), flavone (1 µM), quercetin (1 µM) and resveratrol (1 µM) significantly reduced intracellular H33342 accumulation by to 0.5 fold or lower, suggesting at a possible induction of BCRP to reduce H33342 intracellular accumulation (Figure 3.9).

Of the published reports available, curcumin, 17-β-estradiol, naringin and quercetin have demonstrated the ability to modulate BCRP expression over similar concentration ranges studied (see section 2.9.5. for further discussion of these modulators).

When comparing modulators eliciting inhibitor effects between PBMEC/C1-2 and Z310 cells, there is some clear discord between the extents of inhibition. For example in PBMEC/C1-2 apigenin and hesperidin elicits a strong inhibition at 1 µM but these effects are absent in Z310. Furthermore in Z310 concentration dependant effects on BCRP modulation are more apparent and which are absent from PBMEC/C1-2 studies and examples include chrysin, flavone, naringin, rutin, silymarin and TMF. The rationale for this is relatively unclear. However a primary cause may be the differences in the species that each cell line is derived from. A BLAST (www.blast.ncbi.nlm.nih.gov) comparison of both porcine and rat BCRP nucleotide sequeces highlights a sequence identity of 80 %, with the key mutation causing non-functioning BCRP at position 482 missing. This difference in sequence identity may alter the three-dimensinoal structrure of the protein and hence potentially alter the extent of modulator-BCRP interactions. Similar mismatches between *in-vitro* and *in-vivo* inhibition across species have been observed (Zhang et al., 2005), however this requires further investigation in each cell line to identify the primary cause of this mismatch.

3.10.5. Modulating BCRP protein expression in Z310 cells

In order to further explore the potential modulation of BCRP protein expression in the presence of modulators, western blotting analysis was conducted on all modulators at identical concentrations studied for the H33342 accumulation assays.

Our results demonstrated that out of the 18 modulators studied, only 8 showed a statistically significant change in BCRP expression with baiclain, hesperidin and flavone demonstrating a BCRP up-regulation effect (2.5 fold or more) and 17-β-estradiol, naringin, quercetin and sliymarin demonstrating a down-regulation effect (0.16-4.9 fold) (Figure 3.11). Of the non-phytoestrogenic compounds 17-β-estradiol demonstrated the expected trend of downregulation of BCRP. This down regulation could be the result of interference with 17-β-estradiol signalling pathways by ERα and ERβ.

Despite the fact that H33342 accumulation assay demonstrated a significant increase in intracellular accumulation under prolonged exposure (24 h), it is apparent that this effect is only tangible in influencing the expression of BCRP in the highlighted modulators. It has been reported that H33342 may also be substrate for P-gp, and hence the discord between the increased intracellular accumulation of H33342 for all modulators and selective changes in BCRP protein expression observed may be indicative of a potential change in P-gp expression (Werner and Schneider 1974). Imai et al (Imai et al., 2005a) demonstrated that 17-β-estradiol significantly reduced the expression of BCRP in MCF-7 cells at low nanomolar concentrations (3 nmol/L) for 1,2 and 4 days (2-,5- and 10-fold down regulation respectively). Furthermore, Hartz et al (Hartz et al., 2010) found that the protein expression of BCRP was down regulated in the presence of 17-β-estradiol in rat brain capillaries. It has been (Ebert et al., 2007) reported that 25 µM and 50 µM quercetin increased BCRP protein expression in Caco-2 by 2.6 and 5.3 fold after 72h incubation. Furthermore at the genomic level a 19-37 fold increase in BCRP mRNA was reported when exposed to 50µM of chrysin, quercetin, resveratrol and flavone.

When comparing the modulation of BCRP protein expression in PBMEC/C1-2 and Z310, the lack of similarity in the modulation of protein expression is evident. For example quercetin and naringin are clear up-regulators of BCRP gene and protein expression in PBMEC/C1-2 cells (Figure 2.13 and 2.14) whereas in Z310 the opposing trend is evident with quercetin being a down-regulator in gene (Figure 3.12) and protein expression (Figure 3.11) but naringin shows no significant down-regulation of BCRP gene expression (Figure 3.12) but a highly significant decrease in BCRP protein

(Figure 3.11). This would suggest that naringin does not interfere with a transcriptional element of BCRP but rather is capable of initiate a translational change in BCRP expression. The discord between PBMEC/C1-2 and Z310 changes in BCRP protein expression may be indicative of differences in cellular mechanisms such as differences in the abundance of transcriptional/translational signalling pathways. Some species differences have been identified with AhR, for example differences in the regulation of AhR has been reported between humans and rodents (Flaveny et al., 2010), and the AhR-mediated BCRP regulator pathway was not able to be demonstrated in mouse cell lines but were evident in human intestinal cells (Tan et al., 2010).

3.10.6. Functional assessment of BCRP activity in an *in-vitro* permeable insert BCSFB model

The functionality of BCRP was further demonstrated using the BCRP substrate sulfasalazine and assessing its transport across the Z310 monolayer in the absence and presence of Ko143 or modulators, using the SFM as the optimal transport study media (Figure 3.15). In the *in-vitro* construct developed, the apical chamber represents the CSF and the basolateral the blood, hence the direction of efflux for BCRP is towards the CSF. Initial studies demonstrated that Ko143 significantly increased the apical-to-basolateral sulfasalazine flux at all time points leading to an increase in $P_{app,AB}$ from 1.32 ± 0.12 $x10^{-6}$ cm/s to 2.11 ± 0.17 $x10^{-6}$ cm/s, and hence demonstrating functional activity of BCRP (Figure 3.16) and it's inhibition leading to enhanced penetration across the *in-vitro* BCSFB and delivery into the basolaterial (blood) compartment.

Cells grown on permeable inserts were further exposed to modulators for 24 h followed by assessing the transport of sulfasalazine across the *in-vitro* BCSFB. Western blot and qPCR result (Figure 3.11 and 3.12) confirmed that baiclain and flavone are up-regulators of BCRP protein at the BCSFB and these were selected to study further to assess the functional consequences of this up-regulation. Baiclain demonstrated a significant decrease ($p \leq 0.05$) in the transport of sulfasalazine across the insert by approximately 10 % (C_R/C_D) for portions of the assay and this was coupled with a decrease in $P_{app,AB}$ from 1.32 ± 0.12 x 10^{-6} cm/s to 1.10 ± 0.08 x 10^{-6} and hence diminishing of the overall apical-to-basolateral flux (Figure 3.17A). However, when examining the impact of flavone on BCRP, no significant differences were observed in apical-to-basolateral flux for the duration of the study (Figure 3.17B). This was surprising as flavone demonstrated the greatest up-regulation of BCRP protein in

western blots (Figure 3.11) and may indicate time-dependant protein decay following the up-regulation phenomena.

When investigating the impact of the down-regulators 17-β-estradiol, naringin and silymarin, we observed statistically significant differences across all time-points with 11 %, 43% and 36% increase in sulfasalazine transport, for 17-β- estradiol, naringin and silymarin leading to an increase in $P_{app,AB}$ from 1.32 ± 0.12 $x10^{-6}$ cm/s to 2.01 ± 0.23 $x10^{-6}$ cm/s, 3.83 ± 0.34 $x10^{-6}$ cm/s and 3.33 ± 0.61 $x10^{-6}$ cm/s respectively (Figure 3.18). Of interest is the translational effect of downregulation in BCRP protein when exposed to naringin and silymarin (0.16 ± 0.07 fold and 0.22 ± 0.09 fold change in protein expression, respectively, Figure 3.11) and the resultant effect on 'CSF-to-blood' sulfasalazine transport where $P_{app,AB}$ for naringin and silymarin was increased by 2.9- and 2.5-fold, respectively. This effect clearly highlights the potential impact of prolonged exposure of flavonoids to BCRP may have on substrate transport and how this may influence the disposition of transporter substrate at the BCSFB and wider CNS.

It is important to note that the design of the transport study, namely pre-incubation with modulators for 24 h followed by a short washout-period and subsequent initiation of a transport study in the presence of the substrate along, would negate the impact of modulators themselves inhibiting the transporters directly. It is more likely that this approach would lead to a change in BCRP protein as evident from western blotting studies and the transport studies have therefore demonstrated that the down-regulators are able to significantly alter the equilibrium of sulfasalazine across the BCSFB leading to an increase in flux towards the blood. As the formation of CSF is, in part, related to the draining of ISF from the brain, the bulk flow from ISF-to-CSF would drive the equilibrium within the cranium towards the CSF and this would then be followed by CSF draining, driving largely by gravity back into the systemic blood via dural venous sinuses drainage (Pollay, 2010, Johanson et al., 2008b, Wraith and Nicholson, 2012). Hence, both naringin and silymarin and phytochemical modulators along with 17-β-estradiol, are potential viable candidates, which may limit the entry of systemically administered BCRP substrates into the CSF or enhance the removal of compounds from the CSF. This may be an important application in age-associated diseases states such as Alzheimer's disease where the amyloid beta plaques circulating the CSF and originating from the brain are drained into the systemic circulation through CSF drainage and passage across the BCSFB (Pascale et al., 2011) . As amyloid-beta peptides (Aβ) has previously been reported to be a substrate of BCRP (Xiong et al., 2009, Candela et al., 2010, Carrano et al., 2014). it is possible

that down-regulation of BCRP at the BCSFB may enhance the opportunities for clearance of Aβ out of the CNS through the traditional sinuses drainage routes and enhance flux across the BCSFB, as a result of diminished BCRP protein.

3.11. Conclusion

In this chapter, the modulation of BCRP by phytochemicals at the BCSFB was investigated. Our results confirmed the presence of genomic, protein and functional expression of BCRP in choroid plexus Z310 cells. Baiclain and flavone has shown to be the up-regulators of BCRP protein, genomic and functional expression whereas, 17β-estradiol, quercetin and naringin were the down-regulators. From this study, it is concluded that phytochemicals can modulate the expression of BCRP at the BCSFB model, which can help to enhance the drugs to the CSF or remove neurotoxins from the CSF.

Chapter 4

Transcriptional regulation of BCRP by the aryl hydrocarbon receptor at the BBB and BCSFB

4.1. Introduction

The aryl hydrocarbon receptor (AhR) is involved in a wide range of cellular processes such as cell proliferation, xenobiotic metabolism and the development of the immune system (Lindsey and Papoutsakis, 2012, Ma and Whitlock, 1996, Boitano et al., 2010, Mulero-Navarro et al., 2006). AhR is a member of the basic helix-loop-helix (bHLH) PER-AhR nuclear translocator (ARNT)-SIM superfamily of transcription factors. AhR is localised in the form of a complex with two molecules of heat shock protein 90 (hsp90) and Ah receptor-interacting protein (AIP) in the cytoplasm. Upon ligand binding the AhR with its associated heat shock proteins, forms a dimer complex and is translocated to the nucleus where it binds with ARNT and transcribes the required target genes (Nebert et al., 2004).

The activity of AhR has been shown to be modulated by several compounds including phytochemicals (Ashida et al., 2000, Ciolino et al., 1998a, Nishiumi et al., 2007b). Furthermore, AhR has previously been shown to play a role in the induction of BCRP through interactions with a range of compounds, including phytochemicals (Ebert et al., 2007, Tan et al., 2010). Examples include quercetin, chrysin, flavone and indole-3-carbinol which have all shown to significantly induce BCRP genomic and proteomic levels following exposure concentration of 25µM and 50µM concentration (Ebert et al., 2007).

The direct inhibition of BCRP, through the use of existing inhibitors has not yielded fruition of viable clinical inhibitors as a result of their severe neurotoxicity (Nutton, 1973, Allen et al., 2002a) (Allen et al., 2002b).The modulation of regulatory pathways is a new promising approach to target BCRP to enhance delivery to BCRP substrates into the brain. The expression of drug transporters and drug metabolising enzymes at the BBB is thought to be regulated by a network of regulatory pathways including the pregnane-X-receptor (PXR), the peroxisome proliferator-activated receptor α (PPARα), the constitutive androstane receptor (CAR), and the aryl hydrocarbon receptor (AhR) (Jacob et al., 2011, Xu et al., 2005, Dauchy et al., 2008a, Granberg et al., 2003, Hoque et al., 2012).

Whilst most studies have focussed on the role of AhR in regulating the expression of xenobiotic metabolism pathways (e.g. CYP isozymes), a few studies have demonstrated the role AhR plays in regulating BCRP expression. A known AhR agonists, 3-methylcholanthrene (3MC), has been demonstrated to cause an AhR mediated 80-fold induction of BCRP in LS174T cells when exposed to 3MC, with reversal of this induction (by 65 %) when AhR was knock-down (Tompkins et al., 2010). Wang et al (Wang et al., 2011) also demonstrated that the well-known AhR agonist, TCDD, up-regulated the expression and transporter activity of BCRP in rat brain capillaries. In a further study (Campos et al., 2012), exposure of the AhR agonist TCDD to rat spinal cord capillaries increased BCRP protein expression.

Although BCRP is known to play an important role in governing the entry of a range of therapeutic compounds into the brain, approaches to target its transcriptional regulation have been poorly studied. This chapter will explore the role AhR plays in regulating the expression of BCRP and will attempt to identity suitable candidate compounds, which modulate the genomic regulation of BCRP by AhR at the BBB and BCSFB.

4.2. Aims and objectives

The aim of the work reported in this chapter was to investigate whether modulators identified from earlier studies with their interactions at the BBB and BCSFB, regulated the expression of BCRP by AhR pathways. The objectives were:

- To demonstrate activation of AhR by a chemically-activated luciferase assay system (H1L6.1c2 cells)
- To assess modulation of BCRP and AhR following modulator exposure in PBMEC/C1-2 and Z310 cells
- To silence the AhR gene by dicer substrate siRNA approaches and assess subsequent changes in BCRP expression in PBMEC/C1-2 and Z310 cells.

4.3. Materials

Alpha-MEM (Corning, USA); fetal bovine serum (FBS) (Biosera, UK); Opti-MEM® (Life Technologies, USA); Transfection reagents and fluorescent control plasmid (TYE-563) (Mirus, USA); Curcumin (Cayman Chemical, UK); all other chemicals were sourced from Sigma (Dorset, UK).

Stock solutions of all test compounds were prepared in dimethylsulfoxide (DMSO) and stored at -20°C until use.

The materials used to grow PBMEC/C1-2 cells and Z310 were detailed in chapter 2 (section 2.3) and chapter 3 (section 3.3).

4.4. Culture of H1L6.1c2 cells

H1L6.1c2 cells are mouse hepatoma cell lines, which were a kind gift from Dr.Michael Denison and was stably transfected with a luciferase firefly plasmid (Garrison et al., 1996, Nagy et al., 2002). Cells were seeded into a T25 flask containing alpha-MEM supplemented with 10% FBS at 37°C and allowed to attach for 24 h before the media was changed. At 70-80% confluency, cells were washed with warm PBS and 1 mL of trypsin-EDTA was added to the flask. The flask was placed in the incubator for 5 min and cell suspension was resuspened in a 5 mL of media before the being transferred to a 15 mL centrifuge tube and centrifuged at 1000 rpm for 5 min. The pellet was resuspened in 2 mL of the media and transferred to a T75 for subsequent experiments.

4.4.1. Cryopreservation of the cells

After harvesting cells as described in section 4.4, the pellet was resuspended in freezing media (10% DMSO and 90% FBS). A 1 mL volume of the cell suspension was aliquot to the cryovials and stored overnight at -80˚C in cell cooling box (Mr. Frosty, Nalgene®, Thermo Fisher Scientific, UK). After 24 h, vials were transferred to the liquid nitrogen for long-term storage.

4.4.2. Activation of AhR by omeprazole in H1L6.1c2 cells

Omeprazole is a known non-toxic AhR antagonist. To assess the functional activity of AhR in H1L6.1c2 cells, the activation of AhR was assessed across a concentration range of omeprazole, to identify an EC_{50}. Sterile working stocks of omeprazole were freshly prepared on the day. Culture medium was used as the diluent and the final solvent concentrations in all test drug concentrations did not exceed 1 % (v/v).
Cells were seeded with a density of 75,000 cells per well onto a clear flat bottom 96-well plates and grown to 60-70% confluence. Media was then carefully removed and

fresh media containing 0.5 µM -100 µM omeprazole or lacking omeprazole (control) incubated for 24 h.

To assess the activation of AhR, a commercial luciferase-based luminescence assay (Promega, USA) was utilised. Cells were washed with pre-warmed PBS followed by the addition of 20 µL of Lysis Buffer (Promega, USA) to each well. The plates were transferred to an orbital plate shaker and shaken at 1000 rpm for 20 minutes. 20 µL of the cell lysate was then transferred into opaque 96-well plate and 100 µL of Luciferase Reagent was added to each well. The luminescence was measured immediately and at 10 seconds intervals for duration of 60 seconds using a Spectra Max MX5 plate reader (Molecular Devices LLC, Sunnyvale, CA). The peak average time-resolved stable luminescence signal was calculated as a measure of luminosity.

4.4.3. Activation of AhR by modulators in H1L6.1c2 cells

To assess the potential activation of AhR by phytochemical modulators, a luciferase-based assay was developed as described in section 4.4.2. All modulators were prepared at 25 µM concentration (unless otherwise indicated) and 100 µL added to the appropriate wells. The plates were incubated at 37°C for 24 h prior to the luciferase assay.

4.5. Silencing AhR gene expression

4.5.1. Preparation of siRNA reaction

A commercial transfection kit, TransIT-TKO (Mirus Bio, USA), was used for transfection studies. 100 µL of Opti-MEM® was added into a sterile tube, followed by 3 µL of the TransIT-TKO and 1.4 µL of the siRNA (final concentration 25 nM) and mixed gently by pipetting up and down. The tube was incubated for 30 min at room temperature. Dicer substrate siRNA duplexes were custom synthesised by IDTDna against porcine AhR (Table 4.1) and rodent AhR (Table 4.2) and obtained in a commercial gene transfection kit, TriFECTa® (IDTDna, Belgium).

Table 4. 1: Porcine AhR siRNA duplexes

Duplex	Size	Sense	Anti-sense
1	16566	GAACAUUAUCACUUCCCAUUGGUGCAA	CTUGUAAUAGUGAAGGGUAACCACG
2	16520	UUUCUGACACAGUUGUUGCUGCUGCUC	AAAGACUGUGUCAACAACGACGACG
3	16490	ACACAUUGAAAUAGGUGCCUUAUUCUU	TGUGUAACUUUAUCCACGGAAUAAG

Table 4.2: Rodent AhR siRNA duplexes

Duplex	Size	Sense	Anti-sense
1	16506	ACCAAAGACACGGGAUAAACUCACA	UUUGGUUUCUGUGCCCUAUUUGAGUGU
2	16544	CGACAUAACAGACGAAAUCCUGACG	UAGCUGUAUUGUCUGCUUUAGGACUGC
3	16544	AGCAUCAUGAGAAACCUAGGGAUCG	UAUCGUAGUACUCUUUGGAUCCCUAGC

4.5.2. Culture of PBMEC/C1-2 and Z310 cells

PBMEC/C1-2 and Z310 cells were grown in 12-well plates for studies as described in chapter 2 (section 2.4.2) and chapter 3 (section 3.4.1). Media was aspirated and cells were washed with the pre-warmed Opti-MEM®. The three sets of dicer substrate siRNA were added to the individual wells to identify the most efficient silencing 'set', and incubated at 37°C for 6 h. Thereafter the media was removed and replaced with the pre-warmed Opti-MEM and incubated for a further 18 h.

4.5.3. Measurement of transfection efficiency using a fluorescent plasmid

To assess transfection efficiency, PBMEC/C1-2 and Z310 cells were seeded at a density of 25,000 and 15,000 into wells of a 6-well plate and allowed to attach for 24 h. Thereafter, cells were incubated with a fluorescent transfection control duplex (TYE-563®) (IDTDna, Belgium) at 5, 10 and 25 nM for 24 h and visually inspected every 6 hours to assess transfection efficiency. Cells were observed under inverted DMI400B microscope (Leica microscope systems (UK) Ltd, Milton Keynes, UK).

4.5.4. Chemically mediated antagonism of AhR

In addition to gene silencing through siRNA, the AhR antagonist CH223191 (Choi et al., 2012) was assessed for its ability to silence AhR. 1 µM and 10 µM CH223191 solutions were prepared in cell culture media and incubated with cells seeded in 24-well plates (as described in section 4.4). RNA was subsequently extracted and AhR expression was quantified.

4.5.5. Quantification of AhR and BCRP gene expression

4.5.5.1. Extraction of RNA

RNA was extracted in triplicate from wells for each set of siRNA or CH223191 as described in Chapter 2 section 2.4.8.1.

4.5.5.2. Reverse transcription and qPCR analysis of AhR and BCRP gene expression

To confirm the presence of BCRP and AhR genes in cells, reverse transcription and qPCR was conducted as described in chapter 2 4.8.2 and for AhR and for BCRP in the absence of siRNA. Furthermore to identify AhR mediated regulation of *BCRP*, knockdown of AhR by siRNA was then used to both confirm successful AhR knockdown and also assess any associated changes in *BCRP*.

Gene expression levels was measured using a relative quantification method as discussed in Chapter 2 (Section 2.4.8.4 and equation 3) and Chapter 3 (Section 3.4.9.4).

4.5.6. Phytoestrogen mediated modulation of AhR gene expression

To assess whether phytoestrogen identified as modulators of BCRP protein and functional expression:

(i) Could directly alter *AhR* expression

(ii) Could directly alter *BCRP* expression

(iii) Will show diminished effects on BCRP when silencing AhR (i.e. modulator mediated effects on BCRP and directly related to AhR)

phystoestrogenic modulators were prepared in an incubation mixture combined with either siRNA (25 nM) or CH223191 (1 µM or 10 µM) and incubated with cells for 24 h (see section 4.4.2). In PBMEC/C1-2 cells, modulators which induced BCRP protein included quercetin (25 µM) and naringin (25 µM), with curcumin (1 µM) and estradiol (100 nM) selected as down-regulators of BCRP. In Z310 cells, modulators studied which induced BCRP protein included baiclain (25 µM) and flavone (25 µM), with quercetin (25 µM) and naringin (25 µM) selected as down-regulators of BCRP. RNA was extracted and qPCR was performed as described in section 4.5.5.

4.6. Statistical Analysis

All statistical analyses were performed in Graph pad Prism (La Jolla, California, USA). One-way ANOVA and t-tests were carried out to determine the differences between the mean values. For all multi-well based assay replicates of at least 3 were used in three independent experiments. EC_{50} metrics were calculated using sigmoidal fit functions within Graph pad Prism.

A significance p-value of < 0.05 was considered as statistically significant.

4.7. Results

4.7.1. Activation of AhR by omeprazole in H1L6.1c2 cells

The concentration dependent activation of AhR in H1L6.1c2 cells by the AhR activator omeprazole was assessed by measuring the luminescence produced from transfected firefly luciferase gene. The concentration dependent activation of AhR was confirmed over the concentration range, with a sigmoidal response curve (Figure 4.1) with a calculated EC_{50} of 9.73 ± 0.05 µM.

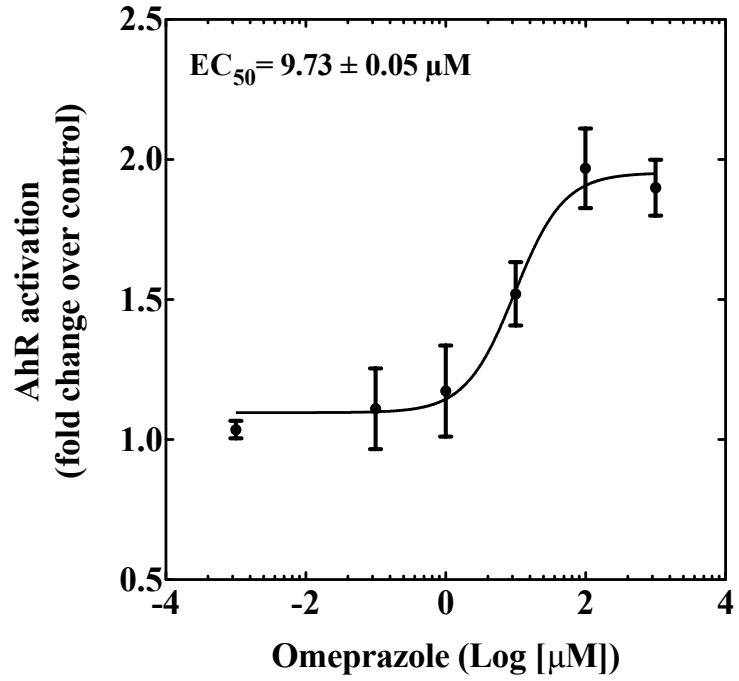

Figure 4.1: Concentration dependent activation of AHR activity.

The luciferase firefly stably transfected mouse hepatoma cell line, H1L6.1c2, was seeded to a 96-well plate and incubated for 24 h with omeprazole (0.5 µM-100 µM). A luciferase assay was subsequently performed and luminescence was measured and reported as the fold change compared to non-activated control.

4.7.2. Activation of AhR by modulators in H1L6.1c2 cells

To assess the activation of AhR by modulators, a chemically-activated luciferase (CALUX) assay was employed to screen modulators at optimal concentration of 25 µM known to modulate BCRP protein expression in both Z310 and PBMEC/C1-2 cells Chapter 2 (section 2.10) and Chapter 3 (section 3.8). Using the luminescence quantified from the maximum activation of AhR by omeprazole, the activation of AhR by modulators was reported as percentage maximum omeprazlole induction, with values greater than 1 % indicating induction, 50 % reflecting the 50 % of the maximum induction and 100% reflecting identical induction as achieved with omeprazole. To simplify the analysis, a cut off which equated to 50 % maximum induction was used as a metric for identified modulators, with values of greater than 75 % being classified as 'potent' activators of AhR.

Modulators identified as 'potent' included biochanin a (73.9 % $\pm$ 4.8 %), chrysin (80.6 % $\pm$ 2.7 %), curcumin (81.21 % $\pm$ 3.8 %), hesperidin (88.16 % $\pm$ 9.3 %) and rutin (81.17 % $\pm$ 6.3 %). All other flavonoids demonstrated > 50 % maximum induction (when considering the SD) (Figure 4.2).

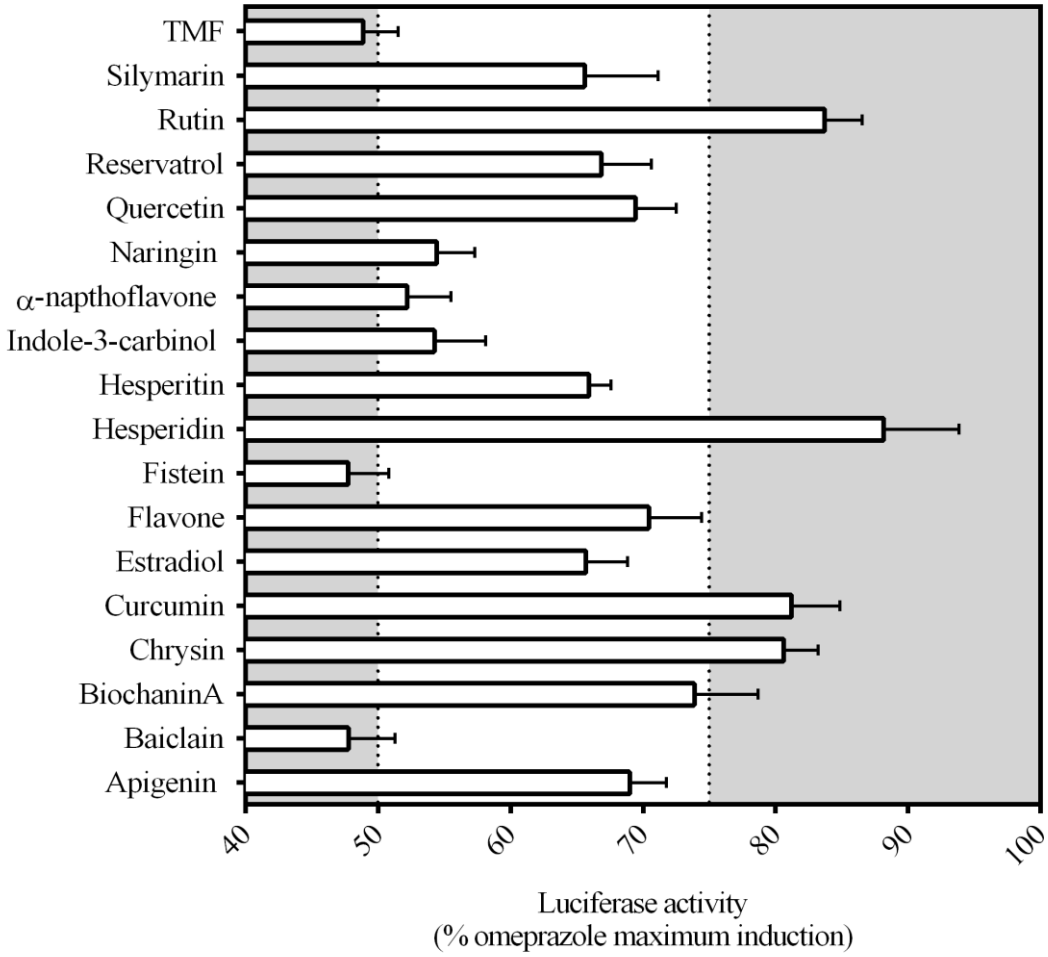

Figure 4.2: The activation of AhR by phytochemical modulators.

H1L6.1c2 cells were seeded to a 96-well plate and incubated with modulators for 24 h and CALUX assay was performed. Shaded areas reflect modulators activation of AhR by up to 50% and greater than 75%.

4.7.3. Assessing transfection efficiency using a fluorescent plasmid

Transfection efficacy was assessed using a concentration range of 5, 10 and 25 nM for 24 h and visually inspected every 6 h to assess transfection efficiency. Optimal transfection efficiency was demonstrated at 24 h post-seeding for 25 nM concentrations of plasmid which demonstrated successful transfection of the TYE™-563 labelled plasmid in PBMEC/C1-2 (Figure 4.3) and Z310 cells (Figure 4.4).

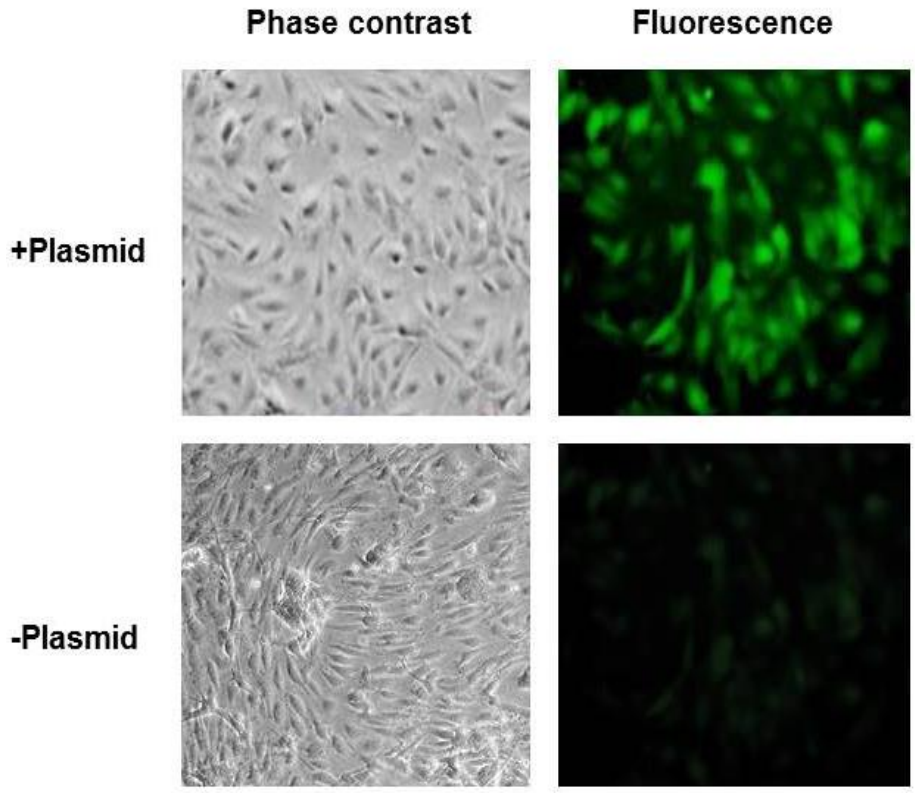

Figure 4.3: Assessment of fluorescence efficiency in PBMEC/C1-2 cells.

PBMEC1-2 cells were seeded onto a 6-well plate and incubated with fluorescently-labelled transfection control duplex (TYE 563™) for 24 h and 25 nM. Cells were visualised 24 h post-transfection under fluorescent microscope (excitation 556 nm, emission max 570 nm).

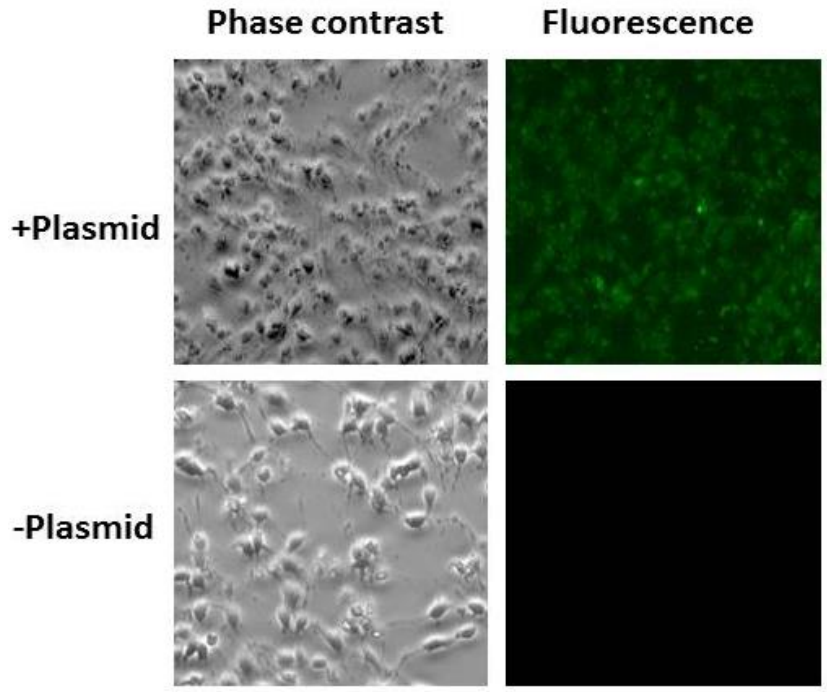

Figure 4.4: Assessment of fluorescence efficiency in Z310 cells.

Z310 cells were seeded onto a 6-well plate and incubated with fluorescently-labelled transfection control duplex (TYE 563™) for 24 h and 25 nM. Cells were visualised 24 h post-transfection under fluorescent microscope (excitation 556 nm, emission max 570 nm).

4.7.4. Modulation of BCRP and AhR gene expression in PBMEC/C1-2 cells

4.7.4.1. Assessment of AhR down-regulation by siRNA and CH223191

To identify whether AhR and BCRP were present in PBMEC/C1-2 cells, qPCR was conducted using porcine specific AhR primers. The primers were designed and pre-validated by PrimerDesign (Sheffield, UK). qPCR was successfully performed with single-peak dissociation-curves for both AhR (Figure 4.5A) and BCRP (Figure 4.5B).

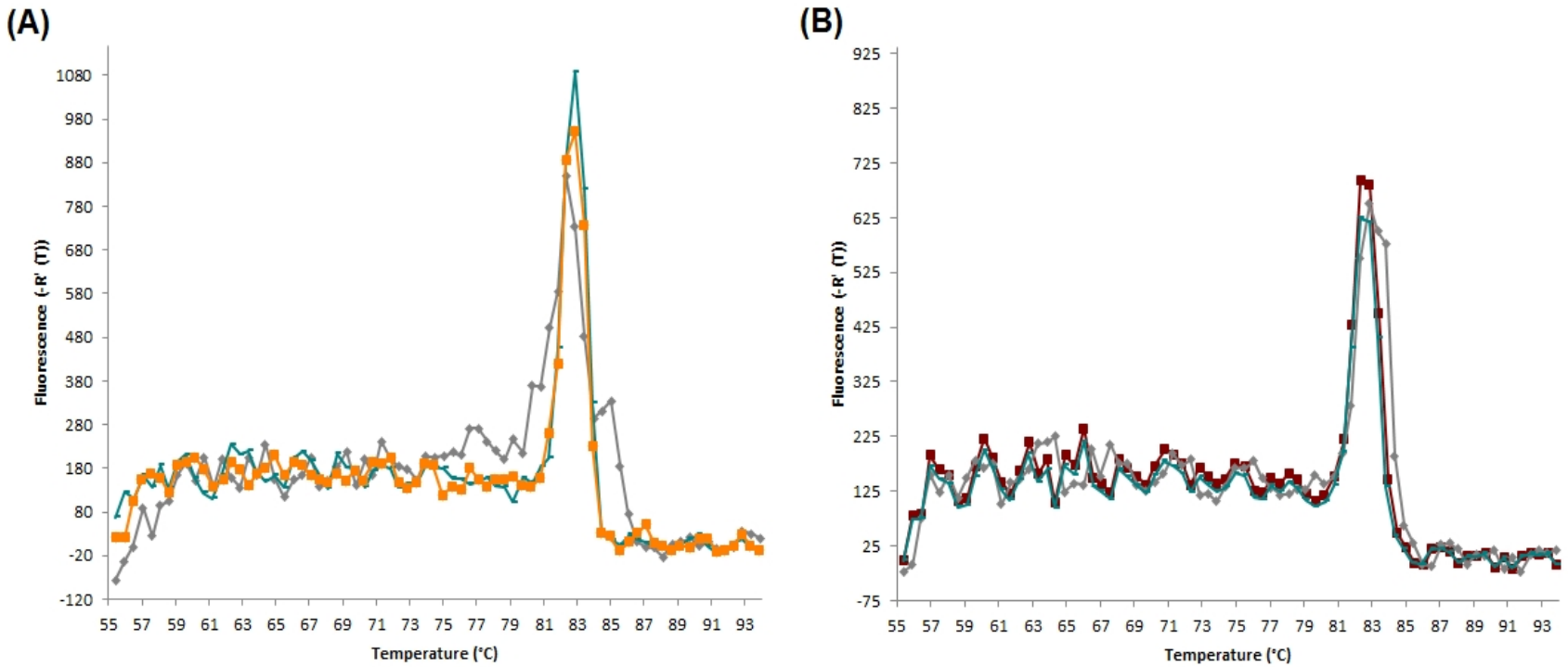

Figure 4.5: qPCR dissociation curves for AHR and BCRP in PBMEC/C1-2.

(A) Representative dissociation curves showing the primer specificity for AhR gene and (B) Representative dissociation curves showing primer specificity for the BCRP gene in PBMEC/C1-2 cells.

AhR knockdown in PBMEC/C1-2 cells was performed using siRNA and CH223191. AhR gene expression was successfully detected in PBMEC/C1-2 cells using qPCR approaches (Figure 4.6). Following incubation with the AhR antagonist CH223191, a significant down-regulation of AhR was observed at 1 µM ($p \leq 0.001$) and 10 µM ($p \leq 0.05$) resulting in down-regulation of AhR by 1.71 ± 0.12 and 1.17 ± 0.16 fold change in AhR gene levels (Figure 4.6). Furthermore, dicer siRNA set 2 demonstrated successful down-regulation of AhR ($P \leq 0.01$) leading to a 2.31 ± 0.08 fold change in gene expression.

BCRP gene expression was also quantified in the same samples that were treated with CH223191 and demonstrated down-regulation when exposed to 1 µM ($P \leq 0.001$) and 10 µM ($P \leq 0.05$) leading to a 1.12 ± 0.09 and 0.79 ± 0.12 fold change respectively. In samples exposed to dicer AhR siRNA set 2, BCRP gene expression was also significantly down-regulated ($P < 0.01$) leading to a 1.75 ± 0.08 fold change (Figure 4.6)

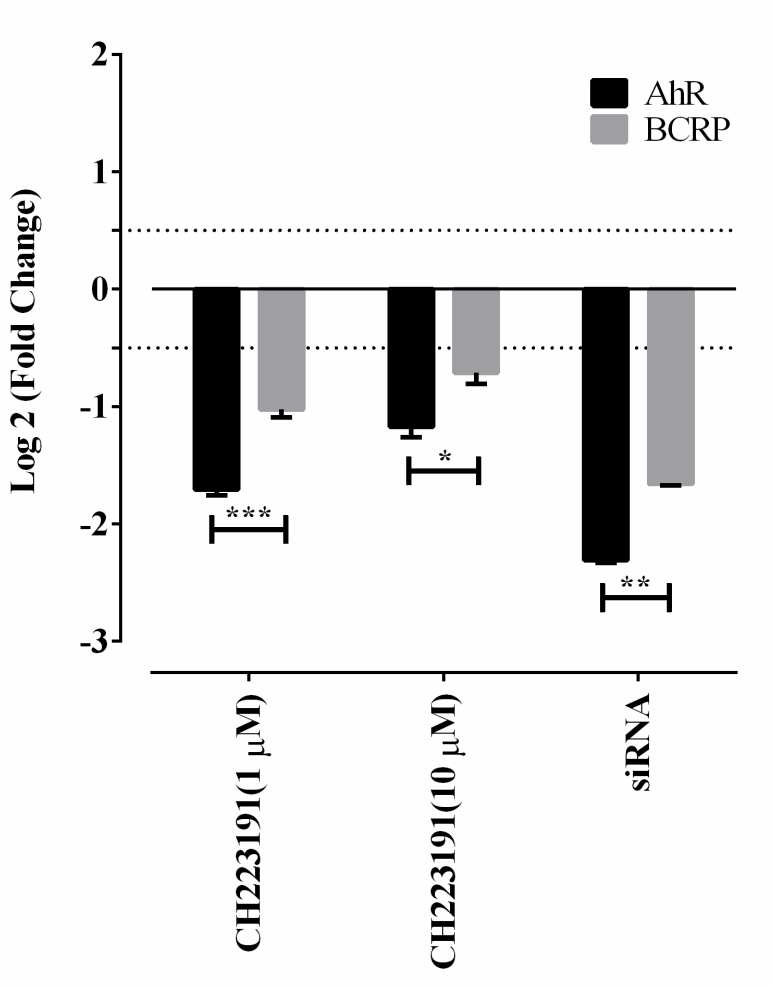

Figure 4.6: Modulation of *AhR* and *BCRP* gene expression in the presence of siRNA or CH223191 in PBMEC/C1-2 cells.

PBMEC/C1-2 cells were seeded onto a 24-well plate and incubated with siRNA or CH223191 (1 and 10 μM), followed by RNA isolation and qPCR quantification of *AhR* and *BCRP* gene expression. Change in gene expression was calculated relative to normalised control samples (absence of siRNA or CH223191). Significant differences between control and siRNA or CH223191 exposed samples are indicated above the appropriate error bars (*P ≤ 0.05; **P ≤ 0.01; ***P ≤ 0.001).

4.7.4.2. Phytochemical mediated modulation of AhR gene expression

Modulation of AhR and BCRP gene expression mediated by phytochemicals was investigated in PBMEC/C1-2 cells. siRNA transfected cells were incubated with modulators which instigated an induction of BCRP protein, quercetin (25 µM) and naringin (25 µM) and those causing a down-regulation of BCRP protein, curcumin (1 µM) and 17-β-estradiol (100 nM).

In the absence of siRNA, AhR gene expression was significantly increased ($p \leq 0.0001$) when exposed to BCRP protein inducers, namely quercetin (0.62 ± 0.31 fold) and naringin (0.84 ± 0.08 fold), relative to control samples (Figure 4.7). However for BCRP protein down-regulates namely curcumin and 17-β-estradiol, no significant differences in AhR gene expression was detected (Figure 4.7).

When AhR was silenced using siRNA, AhR gene expression was significantly reduced (when compared to control samples), when exposed to BCRP protein inducers, namely quercetin (1.26 ± 0.06 fold) ($p \leq 0.0001$) and naringin (0.64 ± 0.08 fold) ($p \leq 0.05$). Additionally, significant differences existed when compared the absence and presence of siRNA ($p < 0.0001$). Furthermore AhR gene expression was significantly reduced when exposed to BCRP protein down-regulators, namely curcumin (1.06 ± 0.09 fold) ($p \leq 0.01$) and 17-β-estradiol (0.97 ± 0.09 fold) ($p \leq 0.01$ (Figure 4.7). However, no significant difference was detected when comparing samples in the absence or presence of siRNA (Figure 4.7).

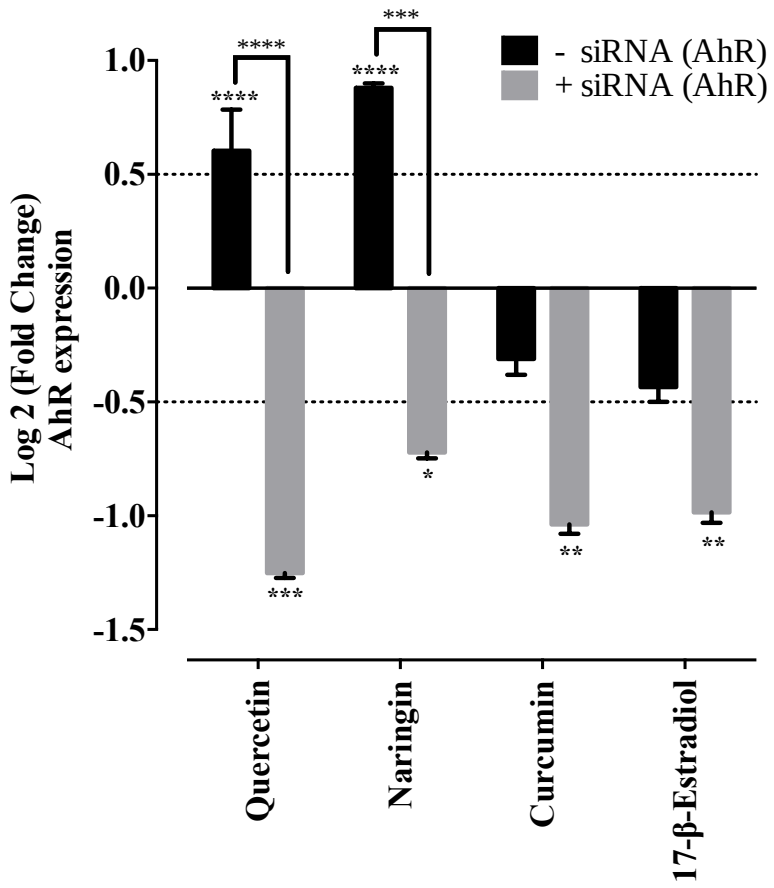

Figure 4.7: Phytoestrogen modulation of *AhR* gene expression in the absence and presence of AhR specific siRNA in PBMEC/C1-2 cells.

PBMEC/C1-2 cells were seeded onto 24-well plates and incubated with quercetin, naringin, curcumin and 17-β-estradiol for 24 h along with siRNA targeted to AhR. RNA was extracted and qPCR analysis conducted. Significant differences between groups are indicated above the appropriate error bars (*P ≤ 0.05; **P ≤ 0.01; ***P ≤ 0.001 and **** P ≤ 0.0001).

4.7.4.3. Phytoestrogen mediated modulation of BCRP gene expression in PBMEC/C1-2 cells

In the absence of siRNA, BCRP gene expression was significantly increased (P ≤ 0.0001) for BCRP protein inducers, namely quercetin (1.63 ± 0.28 fold) and naringin (1.36 ± 0.71 fold), relative to control samples (Figure 4.8). Similarly BCRP protein down-regulators demonstrated significant decrease in BCRP gene expression, curcumin (1.78 ± 0.05 fold) (P ≤ 0.0001) and 17-β-estradiol (1.54 ± 0.05 fold) (P ≤ 0.01) (Figure 4.8).

When AhR gene expression was silenced using siRNA, BCRP gene expression was reduced compared to control samples for BCRP protein inducers, quercetin (0.18 ± 0.12 fold) and naringin (0.41 ± 0.09 fold) and were not significantly

different from control (absence of modulators) (Figure 4.8) but were significantly different from results obtained for BCRP expression in the absence of siRNA. For BCRP protein down-regulators, BCRP gene expression increased when compared to samples in the absence of siRNA for curcumin (0.62 ± 0.10 fold) and 17-β-estradiol (0.22 ± 0.21 fold) but were not significantly different from control (absence of modulators) (Figure 4.8). Furthermore, when compared to samples in the absence of siRNA significant differences between –siRNA and +siRNA samples existed for curcumin ($P \leq 0.01$) and naringin ($P \leq 0.05$) (Figure 4.8).

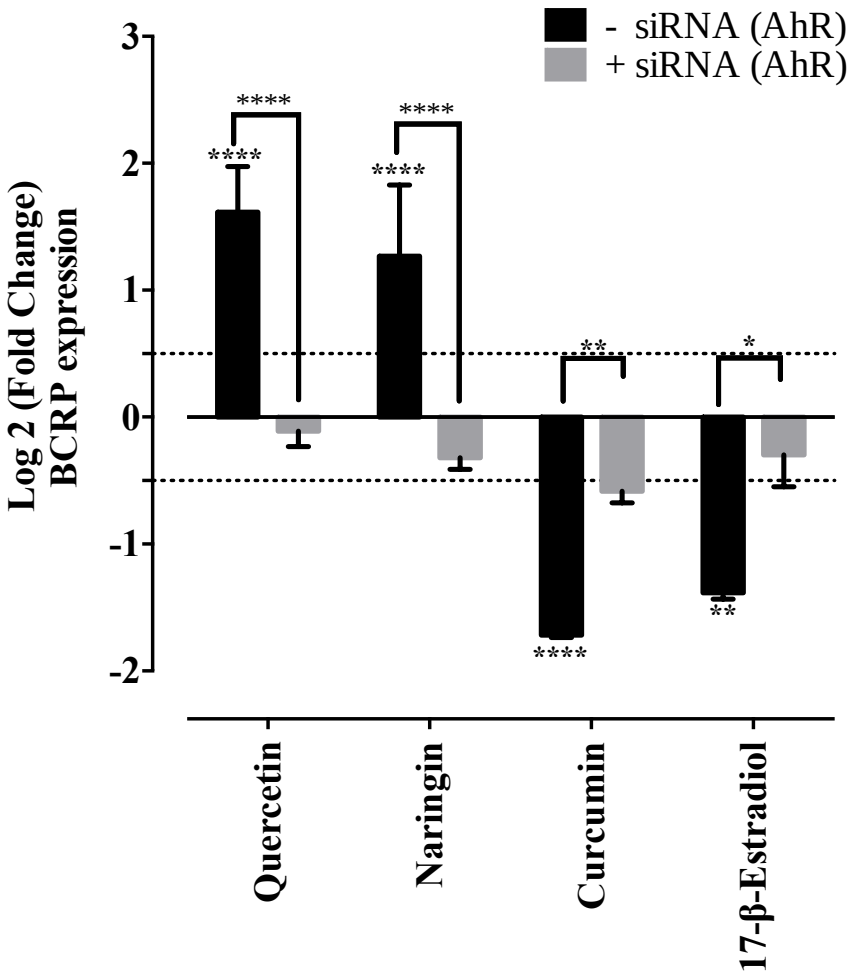

Figure 4.8: Phytoestrogen modulation of *BCRP* gene expression in the absence and presence of AhR specific siRNA in PBMEC/C1-2 cells.

PBMEC/C1-2 cells were seeded onto 24-well plates and incubated with quercetin, naringin, curcumin and 17-β-estradiol for 24 h along with siRNA for AhR. RNA was extracted and qPCR analysis conducted. Significant differences between groups are indicated above the appropriate error bars (*P ≤ 0.05; **P ≤ 0.01; ***P ≤ 0.001).

4.7.5. Modulation of BCRP and AhR gene expression in Z310 cells

4.7.5.1. Assessment of AHR downregulation with siRNA and CH223191

To identify whether AhR and BCRP were present in Z310, qPCR was conducted using rodent specific AhR primers. The primers were designed and pre-validated by PrimerDesign (Sheffield, UK). qPCR was successfully performed with single-peak dissociation-curves for both AhR (Figure 4.9A) and BCRP (Figure 4.9B).

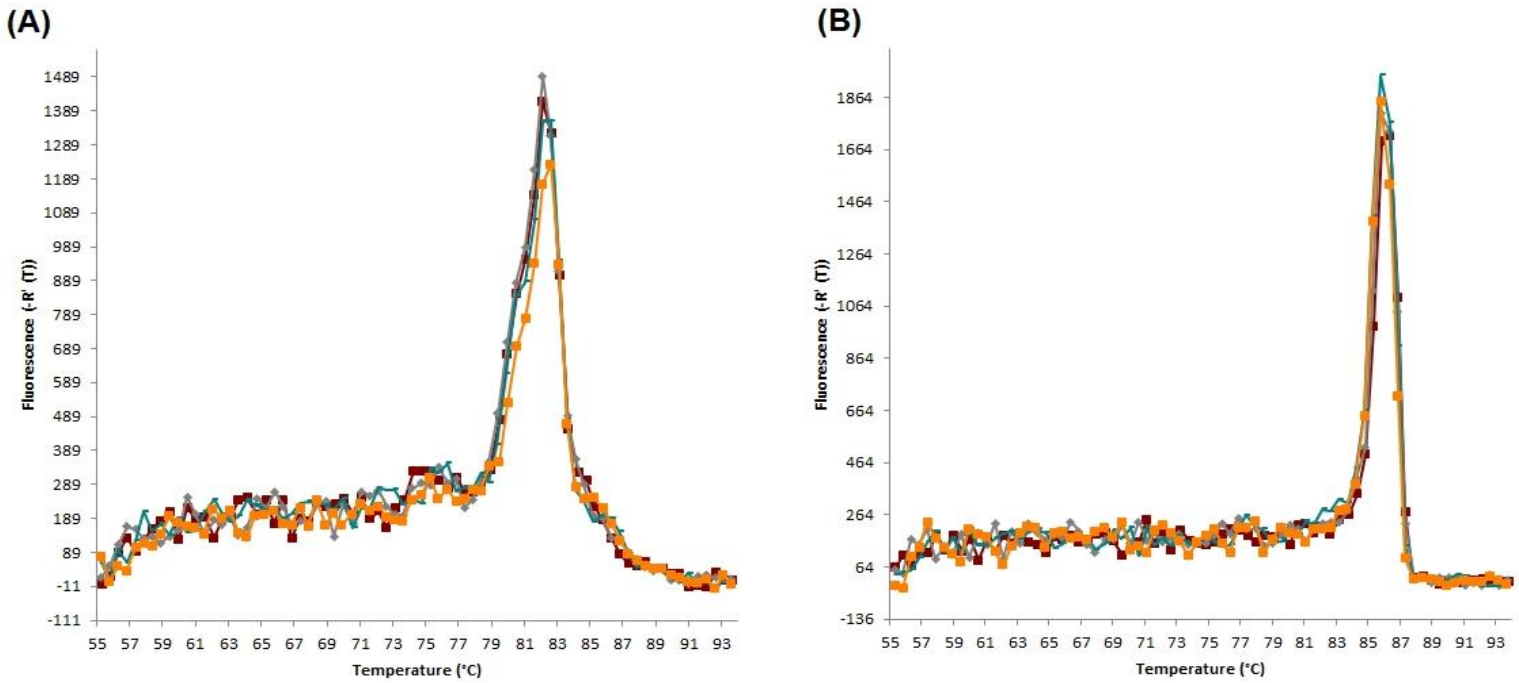

Figure 4.9: qPCR dissociation curves for AHR and BCRP in Z310 cells.

A) Representative dissociation curves showing the primer specificity for AhR gene and (B) Representative dissociation curves showing primer specificity for the BCRP gene in PBMEC/C1-2 cells.

AhR knockdown in Z310 cells was performed using siRNA and CH223191. AhR gene expression was successfully detected in Z310 cells using qPCR approaches (Figure 4.10). Following incubation with the AhR antagonist CH223191, a significant down-regulation of AhR was observed at 1 µM ($p \leq 0.001$) and 10 µM ($p \leq 0.05$) resulting in down-regulation of AhR by 1.81 ± 0.05 and 1.09 ± 0.07 fold change in AhR gene levels (Figure 4.10). Furthermore, dicer siRNA set 3 demonstrated successful down-regulation of AhR ($P \leq 0.01$) leading to a 1.01 ± 0.04 fold change in gene expression.

BCRP gene expression was also quantified in the same samples that were treated with CH223191 and demonstrated down-regulation when exposed to 1 µM ($P \leq 0.001$) and 10 µM ($P \leq 0.001$) leading to a 1.86 ± 0.10 and 1.47 ± 0.09 fold change respectively. In samples exposed to dicer AhR siRNA set 3, BCRP gene expression was also significantly down-regulated ($P < 0.01$) leading to a 0.75 ± 0.08 fold change (Figure 4.10).

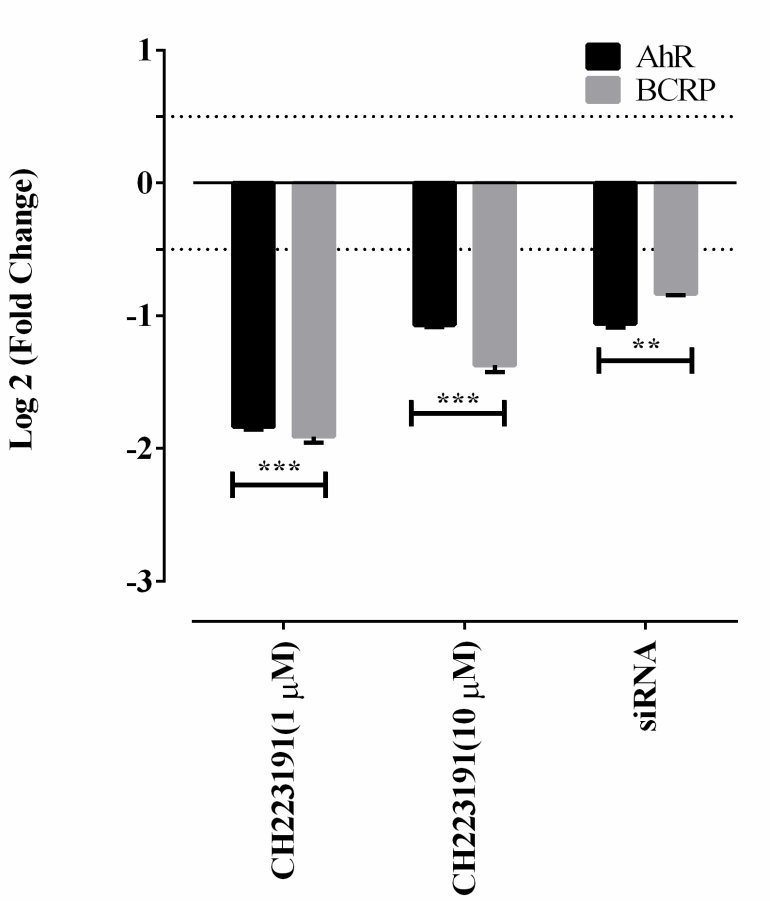

Figure 4.10: Modulation of *AhR* and *BCRP* gene expression in the presence of siRNA or CH223191 in Z310 cells.

Z310 cells were seeded onto a 24-well plate and incubated with siRNA or CH223191 (1 and 10 μM), followed by RNA isolation and qPCR quantification of AhR and BCRP gene expression. Change in gene expression was calculated relative to normalised control samples (absence of siRNA or CH223191). Significant differences between control and siRNA or CH223191 exposed samples are indicated above the appropriate error bars (*P ≤ 0.05; **P ≤ 0.01; ***P ≤ 0.001).

4.7.5.2. Phytoestrogen mediated modulation of *AhR* gene expression

Modulation of AhR and BCRP gene expression mediated by phytochemicals was investigated in Z310 cells. siRNA transfected cells were incubated with modulators which instigated an induction of BCRP protein, baiclain (25 μM) and flavone (25 μM) and those causing a down-regulation of BCRP protein, narinign (25 μM) and quercetin (25 μM).

In the absence of siRNA, AhR gene expression was significantly increased ($p \leq 0.0001$) when exposed to BCRP protein inducers, namely baiclain (1.23 ± 0.31 fold) and flavone (1.28 ± 0.35 fold), relative to control samples (Figure 4.11). However, for BCRP protein down-regulators, namely naringin and quercetin, a decrease in AhR gene levels were detected but this was not significant when compared to control (absence of modulators), < 0.4 fold (Figure 4.11).

When AhR was silenced using siRNA, AhR gene expression was significantly reduced (when compared to the samples in the absence of siRNA) when exposed to BCRP protein inducers, namely baiclain (0.25 ± 0.06 fold) ($p \leq 0.0001$) and flavone (0.09 ± 0.16 fold) ($p \leq 0.0001$). Additionally, when compared to control (absence of modulators), no significant differences were observed. However for BCRP protein down-regulators namely naringin and quercetin, decrease in AhR gene levels were detected but this was not significant when compared to control (absence of modulators), < 0.4 fold (Figure 4.11).

Furthermore, when compared to 1 µM CH223191, AhR gene expression was significantly reduced compared to the samples in the absence of siRNA for BCRP inducers, namely baiclain (0.41 ± 0.09 fold) ($P \leq 0.0001$) and flavone (0.68 ± 0.09 fold) ($P \leq 0.0001$). When compared to samples in the absence of siRNA significant differences between –siRNA and +siRNA or CH223191 existed for baiclain ($P \leq 0.0001$) and quercetin ($P \leq 0.0001$) (Figure 4.11).

However BCRP protein down-regulators (naringin and quercetin) demonstrated a non-significant decrease in AhR gene levels, when compared to control (absence of modulators), < 0.4 fold (Figure 4.11).

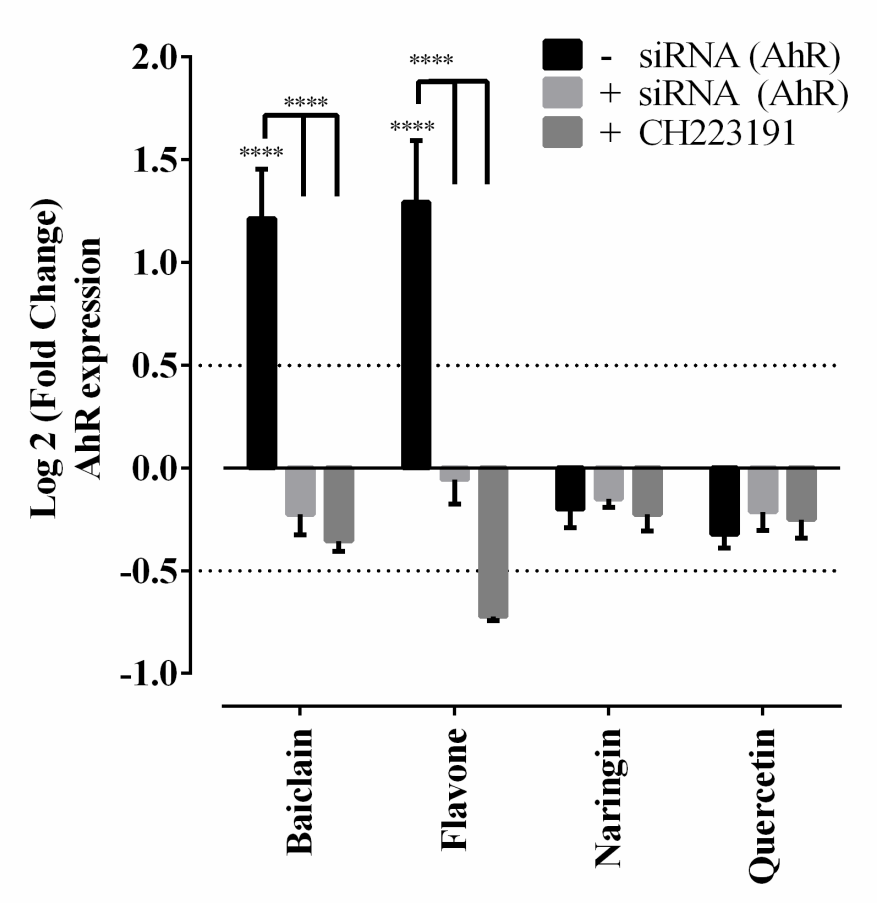

Figure 4.11: Phytoestrogen modulation of *AhR* gene expression in the absence and presence of AhR specific siRNA or CH223191 in Z310 cells.

Z310 cells were seeded onto 24-well plates and incubated with baiclain, flavone, naringin and quercetin for 24 h along with siRNA for AhR. RNA was extracted and qPCR analysis conducted. Significant differences between groups are indicated above the appropriate error bars (*P ≤ 0.05; **P ≤ 0.01; ***P ≤ 0.001).

4.7.5.3. Phytoestrogen mediated modulation of BCRP gene expression in Z310 cells

Modulation of BCRP gene expression mediated by phytochemicals was investigated in Z310 cells. In the absence of siRNA, BCRP gene expression was significantly increased ($p \leq 0.0001$) when exposed to BCRP protein inducers, namely baiclain (1.28 ± 0.31 fold) and flavone (1.21 ± 0.35 fold), relative to control samples (Figure 4.12). However for BCRP protein down-regulators namely naringin and quercetin, a decrease in BCRP gene levels were detected but this was not significant for naringin when compared to control (absence of

modulators), < 0.4 fold but was significant for quercetin (0.74 ± 0.13 fold) ($p \leq 0.05$) (Figure 4.12).

When AhR was silenced using siRNA, BCRP gene expression was significantly reduced (when compared to the samples in the absence of siRNA) when exposed to BCRP protein inducers, namely baiclain (0.15 ± 0.12 fold) ($p \leq 0.001$) and flavone (0.02 ± 0.16 fold) ($p \leq 0.01$). Additionally, when compared to control (absence of modulators), no significant differences were observed.

However for the BCRP protein down-regulator naringin, a significant downregulation of BCRP was observed (1.78 ± 0.12 fold) ($p \leq 0.0001$) when compared to control and this was also significantly difference when compared to the absence of siRNA ($p \leq 0.01$). For quercetin, a non-significant change in BCRP was observed when compared to control (absence of modulators) but this was highly significant when compared to modulators in the absence of siRNA (Figure 4.12).

Furthermore, when compared to 1 µM CH223191, BCRP gene expression was significantly reduced compared to the samples in the absence of siRNA for the BCRP inducers baiclain (0.51 ± 0.09 fold) ($P \leq 0.001$) but was not significantly different for flavone, which has recovered to control levels. When compared to samples in the absence of siRNA significant differences between –siRNA and +siRNA for CH223191 existed for baiclain ($P \leq 0.0001$) and quercetin ($P \leq 0.0001$) (Figure 4.12). However BCRP protein down-regulators (naringin and quercetin) demonstrated a non-significant decrease in AhR gene levels, when compared to control (absence of modulators), < 0.4 fold (Figure 4.11).

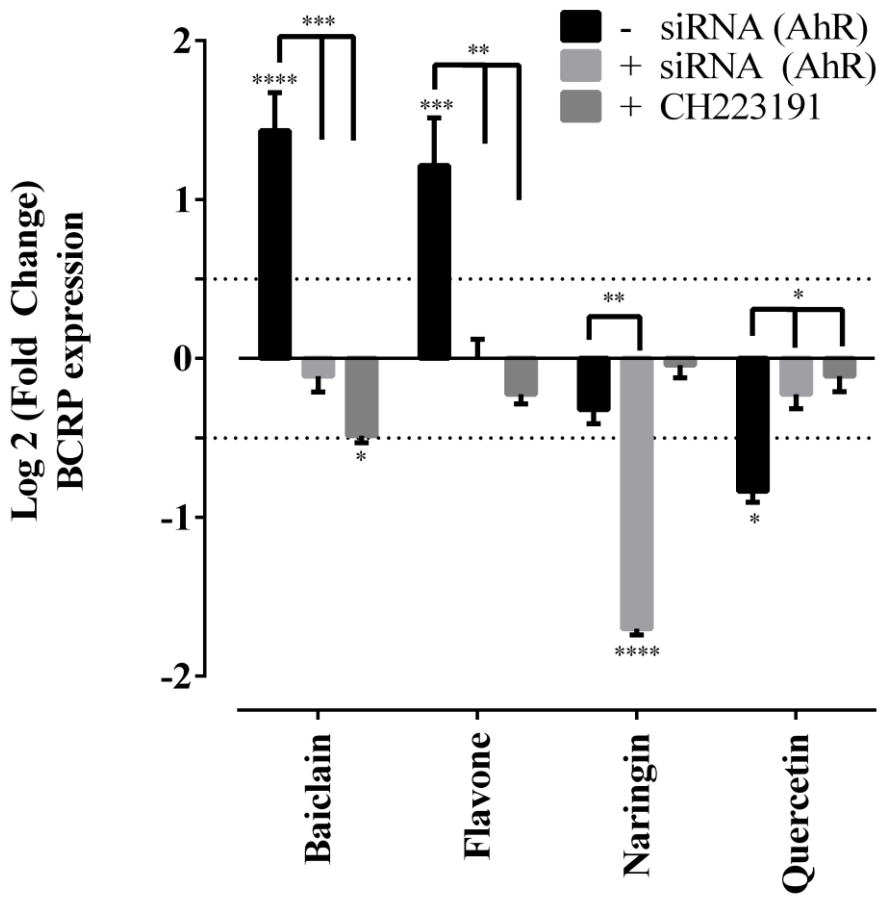

Figure 4.12: Phytoestrogen modulation of *BCRP* gene expression in the absence and presence of AhR specific siRNA or CH223191 in Z310 cells.

Z310 cells were seeded onto 24-well plates and incubated with baiclain, flavone, naringin and quercetin for 24 h along with siRNA for AhR. RNA was extracted and qPCR analysis conducted. Significant differences between groups are indicated above the appropriate error bars (*P ≤ 0.05; **P ≤ 0.01; ***P ≤ 0.001).

4.8. Discussion

AhR plays a vital role in controlling and mediating transcription signals from environment toxins such as polycyclic aromatic hydrocarbons (PAHs) (Denison and Nagy, 2003), with the classical common environmental pollutants such as 2, 3, 7, 8-tetrachlorodibenzo-*p*-dioxin (TCDD) and benzo[*a*]pyrene (BaP) known to induce or activate the activity of AhR.

AhR, to date, has primarily been studied for the role it plays in xenobiotic signalling. In its non-active state, it can be found in the cytoplasm of cells in an intricate protein complex. Activation of AhR leads to nuclear transformation (Perdew, 1988) and binding to promoter regions of target genes that contains an AhR binding consensus (5'-T/GNGCGTGA/CG/CA-3') (Denison et al., 1988).

The role of AhR at the BBB is not well understood. However it has been reported that the higher expression of AhR at the human BBB compared to other regulatory genes such CAR and PXR, potentially highlights the important role AhR may play in transcriptional regulation of xenobiotic clearance mechanisms such as BCRP (Dauchy et al., 2008b). At the BBB, AhR regulates the expression of drug metabolising enzymes such as CYP1A1 and CYP1B1 and ABC transporters (Granberg et al., 2003, Dauchy et al., 2008a). Furthermore, activation or modulation of AhR has previously been shown to alter the expression of BCRP. For example 3-methylcholanthrene (3MC) is a known AhR agonists and has been demonstrated to lead to an AhR mediated, 80-fold induction of BCRP in LS174T cells, which was reduced by 65% in AhR knockdown cells (Tompkins et al., 2010). Furthermore TCDD has been demonstrated to up-regulated BCRP expression and in rat brain capillaries (Wang et al., 2011) and rat spinal cord capillaries (Campos et al., 2012).

In light of the current clinical failures in specific BCRP inhibitor molecules (Nutton, 1973, Allen et al., 2002a) (Allen et al., 2002b), the identification of new candidates that show limited cellular toxicity and an ability to mediate alterations in BCRP expression (transcriptional and translational) is of interest. In this respect, phytochemicals such as flavonoids are promising leads.

Phytochemicals (primarily flavonoids) are natural compounds found in the foods consumed as part of the human diet, with an estimated intake of 1g/per day

(Formica and Regelson, 1995). Several studies have demonstrated that flavonoids act as agonists and antagonist of AhR in a concentration dependant manner (Ashida et al., 2000) (Ciolino et al., 1998a, Zhang et al., 2003a). The exact mechanism of action is unclear, but is thought to supress the nuclear translocation of AhR (Mukai et al., 2010) with flavonoids such as quercetin, flavone, apigenin, kaempferol and galangin (Ebert et al., 2007) (Mukai et al., 2010) (Tan et al., 2010).

The primary focus of this chapter was to evaluate whether flavonoids were capable of modulating AhR, and to further assess the impact of any potential modulation of BCRP expression at the BBB and BCSFB. AhR activation by all modulators was evaluated using a chemically activated luciferase assay (CALUX). Thereafter the regulatory control of BCRP by AhR was demonstrated by AhR silencing (dicer substrate siRNA) in both PBMEC/C1-2 and Z310 cells. Finally, the impact of up- and down-regulators of BCRP at the BBB and BCSFB on BCRP and AhR were identified in +AhR and –AhR cells.

We selected the stably transfected H1L6.1c2 cell lines along with an associated luciferase assay based on the CALUX assay developed by He et al (He et al., 2004). We confirmed the functional activity of the luciferase plasmid within the cells with a non-toxic agonist of AhR, omeprazole, which has previously been used as an AhR activator for the CALUX assay (Zhao et al., 2013).

Our results have shown that omeprazole demonstrated AhR activation in a concentration dependent manner by forming typical sigmoidal curve (Figure 4.1). The EC_{50} for omeprazole induction of AHR gene was estimated to be 9.73 ± 0.05 µM in H1L6.1c2 cells. AhR is known to induce the expression of CYP1A1 and omeprazole induction of CYP1A1 in human cancer cells and primary human hepatocytes was determined over a concentration range of 10-100 µM (Novotna et al., 2014). Furthermore, the EC_{50} for omeprazole induction of the human CYP1A1 gene was found to be 100 µM (Quattrochi and Tukey, 1993). Our calculated EC_{50} is within the same order of magnitude to other reports and highlights the functionally active luciferase firefly response.

It should be noted that the most appropriate agonist to use would have been TCDD (He et al., 2004). However TCDD is considered a highly carcinogenic compound, even at very low concentrations (Kociba and Schwetz, 1982), and

was deemed unsafe for use in this project. However, the similarity of EC_{50} calculations for omeprazole, coupled with the concentration dependent sigmoidal profile justifies its use.

We next assessed whether modulators were capable of modulating AhR by activating a luciferase response following a period of 24 h incubation in H1L6.1c2 cells. Modulators were assessed for the ability to activate a maximum luminesce response based on the maximum fold-change to control obtained with omeprazole (Figure 4.1). To aid in categorising the response, a marker of 50% maximum induction and 75% maximum induction of luciferase activity (relative to omeprazole maximum induction) was chosen as a moderate and good respectively. Chrysin, curcumin, hesperidin and rutin resulted in luciferase activity of 75% or above ('good') and hence can be classified as potentially potent AhR activators, whereas BaP, biochanin A, 17-β-estradiol, flavone, hesperetin, I3C, napthoflavone, naringin, quercetin, resveratrol, silymarin and TBHQ demonstrated 50% or above ('moderate') AhR activation (Figure 4.2).

It has been reported that quercetin significantly increased AhR activity by inducing CYP1A1 in human hepatoma HepG2 cells, whereas rutin a glycoside of quercetin failed to induce AHR and activation of CYP1A1 (Vrba et al., 2012). Our results demonstrated that both quercetin and rutin elicited a luciferase response, although the response from rutin (84 ± 1.8 %) was greater than that elicited by quercetin (70 ± 2.3 %). However, the concentration used by Vrba et al was similar to those used in this study (10-50 µM) (Vrba et al., 2012). Additionally, other studies have also confirmed AhR activation by similar modulators identified in our studies. For example quercetin has been shown to activate AhR mediated CYP1A1 mRNA expression in Caco-2 cells (Pohl et al., 2006, Niestroy et al., 2011) and MCF-7 cells (Ciolino et al., 1999) at concentrations of 0.5-10 µM. Another study also reported that chrysin, baiclain, galangin and genistein induced the luciferase activity in stably transfected Hepa-1 cells whereas quercetin, emodin and apigenin demonstrated inhibitory effect on AHR induction relative to TCDD and act in a concentration dependant manner(Amakura et al., 2008).

Having identified the modulation of AhR activity by modulators studied, the relationship between BCRP expression and AhR regulation was important to elucidate. To this end we first assessed each cell line (PBMEC/C1-2 and Z310) for the ability to be transfected using a TYE™-563 fluorescently labelled plasmid

with a view to subsequently silencing AhR using dicer substrate siRNA. Both cells lines were amenable to transfection and demonstrate successful transfection at 24 hours with an optimal plasmid concentration of 25 nM (PBMEC/C1-2: Figure 4.3; Z310: Figure 4.4).

Thereafter, gene silencing of AhR was conducted using siRNA specific to AhR and changes in both AhR and BCRP expression was assessed using qPCR approaches. Furthermore, we utilised the selective antagonist of AhR, CH223191 (Zhao et al., 2010), as a positive control to compare against siRNA-based *AhR* silencing. Using both a chemical antagonist of AhR and siRNA, we were demonstrated successful down-regulation of AhR in both PBMEC/C1-2 and Z310 cells. In PBMEC/C1-2 cells, CH223191 at 1 µM and 10 µM resulted in a 1.71 ± 0.12 and 1.17 ± 0.16 fold down-regulation of AhR expression, with 2.31 ± 0.08 fold down-regulation with siRNA (Figure 4.6). In Z310 cells CH223191 at 1 µM and 10 µM successfully down-regulated *AhR* expression by 1.81 ± 0.05 and 1.09 ± 0.07 fold respectively with siRNA knockdown resulting in 1.01 ± 0.04 fold down-regulation (Figure 4.10).

Of interest however, is the associated downregulation of BCRP under all treatment conditions in both cells lines (PBMEC/C1-2- CH223191 1 µM: 1.12 ± 0.09, 10 µM: 0.79 ± 0.12; siRNA: 1.75 ± 0.08 (Figure 4.6); Z310- CH223191 1 µM: 1.86 ± 0.10, 10 µM: 1.47 ± 0.09; siRNA: 0.75 ± 0.08) (Figure 4.10). This associated down-regulation of BCRP confirms the role that AhR regulates BCRP at transcriptional level, which is clearly evident when considering the statistical analysis of results, which show statistically significant differences in AhR and BCRP expression under both CH223191 and siRNA treatment when compared to control (untreated: fold-change = 0).

Previously, only one study has reported the modulation of BCRP through AhR dependent manner in Caco-2 cells (Tan et al., 2010). It is demonstrated that a 1.5-2.0 fold induction in BCRP expression when cells were treated with AhR agonist TCDD, and after knockdown of AhR, gene expression of BCRP was significantly reduced (Tan et al., 2010). The relationship between AhR and its transcriptional regulation of BCRP was also identified by Tompkins et al (Tompkins et al., 2010), who reported that activation of BCRP expression in human colon adenocarcinoma-derived LS174T cells is regulated by AhR. Taken

together, our results suggest that AhR plays a significant role in the transcriptional regulation of BCRP.

Having identified this relationship, we then wished to assess the potential impact of modulators on both AhR and BCRP expression. From the H33342 accumulation assays, western blots and transport assays we were able to identify modulations possessed BCRP induction or down-regulation properties. In PBMEC/C1-2 cells, two up-regulators of BCRP protein (quercetin and naringin) and two down-regulators (curcumin and 17-β-estradiol) were selected based on the western blot (Figure 2.13) and qPCR (Figure 2.14) results in PBMEC/C1-2 cells. Similarly, for Z310 cells two up-regulators (baiclain and flavone) and two down-regulators (quercetin and naringin) were selected (Figure 3.11 and 3.12).

In PBMEC/C1-2 cells, in the absence of siRNA treatment, quercetin and naringin significantly ($p < 0.0001$) up-regulated AhR expression by 0.62 ± 0.31 and 0.84 ± 0.08 fold (Figure 4.7) which was abolished when treated with siRNA (1.26 ± 0.06 and 0.64 ± 0.08 fold down-regulated, respectively). Similarly, BCRP expression was also up-regulated in the absence of AhR siRNA by 1.63 ± 0.28 and 1.36 ± 0.71 fold which was abolished when treated with siRNA (0.18 ± 0.12 and 0.41 ± 0.09 fold down-regulated, respectively). In both cases highly statistically significant differences ($p < 0.0001$) are evident when comparing – with + siRNA, highlighting the important role AhR plays as one potential target site for quercetin and naringin interactions. Interestingly the lack of statistically significant differences between control and + siRNA for changes in BCRP expression highlight a 'normalisation' of BCRP gene expression as it returns to baseline and hence no significant difference in gene expression compared to control.

Curcumin and 17-β-estradiol were identified as down-regulators of BCRP. When assessing their impact on AhR, no significant differences were observed between modulator treated and control in the absence of siRNA, suggesting that curcumin and 17-β-estradiol do not alter AhR gene expression (Figure 4.7 and 4.8). However when considering their effects on *BCRP*, curcumin down-regulates BCRP to 1.78 ± 0.05 of control and 17-β-estradiol to 1.54 ± 0.05 of control (Figure 4.8). Furthermore, in the presence of siRNA, AhR is confirmed as being down regulated for both modulators and BCRP expression recovers to 0.51 ± 0.09 and

0.29 ± 0.19 of control and is not significantly different from control, again suggesting a return to baseline expression for BCRP.

At the BBB (using PBMEC/C1-2 cells), this confirms that AhR has a significant role to play in the regulation of BCRP. Furthermore, the modulators identified as up- or down-regulators of BCRP expression may, in part, act to impact directly upon the activity of AhR, such as nuclear translocation (Mukai et al., 2010) (Li et al., 2009), as a possible mechanism which can alter the gene expression of BCRP.

In Z310 cells, in the absence of siRNA treatment, baiclain and flavone significantly ($p < 0.0001$) up-regulated AhR expression by 1.23 ± 0.31 and 1.28 ± 0.35 fold (Figure 4.11) which was down-regulated when treated with siRNA (< 0.5 fold and not significantly different from control). Similarly, BCRP expression was also up-regulated in the absence of AhR siRNA by 1.28 ± 0.31 and 1.21 ± 0.35 fold (Figure 4.12) which was also down-regulated when treated with siRNA (< 0.5 fold). In both cases statistically significant differences are evident when comparing – with + siRNA, highlighting the important role AhR plays in causing the up-regulating phenomena with baiclain and flavone. A similar 'normalisation' of BCRP gene expression effect was also observed between control and + siRNA as it returns to baseline.

Naringin and quercetin were identified as down-regulators of BCRP in Z310 cells. When assessing their impact on AhR, no significant differences were observed between modulator treated and control in the absence or presence of siRNA, suggesting that naringin and quercetin do not alter AhR gene expression. We also confirmed no significant difference in AhR expression when using the chemical antagonist CH223191. However when considering their effects on BCRP, naringin does not significantly down-regulate BCRP whereas quercetin significantly ($p < 0.05$) down-regulates BCRP 0.86 ± 0.09 of control. Furthermore, in the presence of siRNA, BCRP expression is further down-regulated to 1.78 ± 0.12 for naringin but recovers to 0.22 ± 0.21 for quercetin and is not significantly different from control, suggesting a return to baseline expression for BCRP.

At the BCSFB (using Z310 cells), this again confirms that AhR has a significant role to play in the regulation of BCRP. Interestingly, the trends in modulation of

BCRP and AhR were different for Z310 cells compared to PBMEC/C1-2, particularly for the down-regulators, where both naringin and quercetin seemed to have no significant direct effect on AhR levels. Furthermore, naringin demonstrated no significant effects on BCRP expression in the absence of siRNA whereas quercetin significantly downregulated BCRP expression. The differences observed between the up-/down-regulators of BCRP, with PBMEC/C1-2 and Z310 cells, may be a result of the inherently lower expression of AhR in Z310 cells compared to PBMEC/C1-2 cells. Indeed, studies have reported a similar phenomenon in rodent primary choroid plexus cells and TR-CSFB cell lines (Halwachs et al., 2011, Reichel et al., 2011).

4.9. Conclusion

This chapter has highlighted the transcriptional regulation of BCRP by AhR in both PBMEC/C1-2 and Z310 cells. We further investigated the up-regulators and down-regulators of BCRP in both cell culture models. All phytochemicals were shown to the AhR activators when compared to omeprazole. Furthermore, we have identified that up-regulators and down-regulators studied are able to directly alter BCRP gene expression, which is mediated by AhR.

Chapter 5

Conclusion

5.1. Conclusion

The overall aim of this work was to investigate whether phytochemical modulators were capable of modulating the expression and efflux function of BCRP at both the BBB and BCSFB, with a secondary aim of assessing whether BCRP transcriptional regulation is mediated by AhR, and whether phytochemicals act upon this regulatory pathway.

In the first part of the work in this thesis, *in-vitro* models of the BBB and BCSFB were used to assess the cytotoxicity of selected modulators. We determined that, in general, most modulators demonstrated relatively little toxicity below 100 μM, but that species differences between the *in-vitro* model cell systems resulted in distinct differences in the level of toxicity mediated by some modulators.

In order to screen modulators for the ability to impact upon BCRP, a high-throughput 96-well plate assay was developed to assess the intracellular accumulation of a fluorescent BCRP substrate. In this model system, we demonstrated that many phytochemicals are capable of eliciting inhibition of BCRP efflux function in both cell lines during a 1 h pre-incubation. Furthermore, during a longer incubation time-period (24 h) we also demonstrated that modulators mediated potential up-regulation or down-regulation of BCRP functional activity resulting in alterations of H33342 intracellular accumulation. To confirm that these alterations were at the level of the proteome, western blotting identified a number of modulators in both cell lines which significantly altered protein expression by induction (2-3 fold) or down-regulation (0.2-0.4 fold).

Next, we identified phytochemical modulators from both up- and down-regulation categories and assessed their ability to mediate functional changes in BCRP substrate transport in an *in-vitro* BBB or BCSFB permeable insert cell culture model. We identified significant changes in BCRP substrate transport under both groups at the BBB and BCSFB, however when assessing the transcriptional changes using qPCR the down-regulators of protein expression did not seen to initiate similar changes in BCRP genome.

The final part of this work focussed on examining the role AhR plays in regulating BCRP expression in knock-down studies employing dicer substrate siRNA directed towards AhR. We demonstrated that with knockdown of AhR came a significant decrease in BCRP gene expression that was also confirmed when

using the AhR antagonist CH223191. This demonstrated that BCRP transcription is indeed regulated by the AhR. We then demonstrated that the phytochemical modulators were also capable of acting directly upon AhR, resulting in changes in AhR gene expression but also initiating subsequent alteration of BCRP gene expression, the effects of which were diminished when silencing AhR.

In summary we have demonstrated that phytochemicals demonstrate little cytotoxicity *in-vitro* at both the BBB and the BCSFB and are indeed capable of modulating BCRP expression and functional transport of BCRP substrates. However further work is required to assess the importance of the translation of this work to humans as distinct differences in the impact of phytochemicals on BCRP expression and function were also observed between each cell system. A potential cause of this could be the differences in species from which the cell systems were developed (BBB: porcine and BCSFB: rat), but also differences in regulatory networks and other cascade systems are required to be characterised in order to make better comparisons between results obtained from each cell system/barrier site. Furthermore, the permeation of flavonoids into the CNS and their distribution around the CNS would allow an understanding of the temporal changes in phytochemical concentrations within the CNS and therefore whether the exposure concentrations are significant enough to translate our *in-vitro* observations into an *in-vivo* effect, and the role of pharmacokinetic modelling may aid in this translation.

REFERENCES

ABBOTT, N. J. 2002. Astrocyte-endothelial interactions and blood-brain barrier permeability. *J Anat,* 200**,** 629-38.

ABBOTT, N. J. 2005. Dynamics of CNS barriers: evolution, differentiation, and modulation. *Cell Mol Neurobiol,* 25**,** 5-23.

ABBOTT, N. J., PATABENDIGE, A. A. K., DOLMAN, D. E. M., YUSOF, S. R. & BEGLEY, D. J. 2010. Structure and function of the blood–brain barrier. *Neurobiology of Disease,* 37**,** 13-25.

ABBOTT, N. J. & ROMERO, I. A. 1996. Transporting therapeutics across the blood-brain barrier. *Molecular Medicine Today,* 2**,** 106-113.

ABDELRAHIM, M., ARIAZI, E., KIM, K., KHAN, S., BARHOUMI, R., BURGHARDT, R., LIU, S., HILL, D., FINNELL, R., WLODARCZYK, B., JORDAN, V. C. & SAFE, S. 2006. 3-Methylcholanthrene and other aryl hydrocarbon receptor agonists directly activate estrogen receptor alpha. *Cancer Res,* 66**,** 2459-67.

ALATA, W., PARIS-ROBIDAS, S., EMOND, V., BOURASSET, F. & CALON, F. 2014. Brain uptake of a fluorescent vector targeting the transferrin receptor: a novel application of in situ brain perfusion. *Mol Pharm,* 11**,** 243-53.

ALAVIJEH, M. S., CHISHTY, M., QAISER, M. Z. & PALMER, A. M. 2005. Drug metabolism and pharmacokinetics, the blood-brain barrier, and central nervous system drug discovery. *NeuroRx,* 2**,** 554-571.

ALLEN, J. D., VAN LOEVEZIJN, A., LAKHAI, J. M., VAN DER VALK, M., VAN TELLINGEN, O., REID, G., SCHELLENS, J. H., KOOMEN, G. J. & SCHINKEL, A. H. 2002a. Potent and specific inhibition of the breast cancer resistance protein multidrug transporter in vitro and in mouse intestine by a novel analogue of fumitremorgin C. *Mol Cancer Ther,* 1**,** 417-25.

ALLEN, J. D., VAN LOEVEZIJN, A., LAKHAI, J. M., VAN DER VALK, M., VAN TELLINGEN, O., REID, G., SCHELLENS, J. H. M., KOOMEN, G. J. & SCHINKEL, A. H. 2002b. Potent and Specific Inhibition of the Breast Cancer Resistance Protein Multidrug Transporter in Vitro and in Mouse Intestine by a Novel Analogue of Fumitremorgin C 1 This work was supported in part by grant NKI 97-1433 from the Dutch Cancer Society (to AHS). Synthesis investigations by A. v. L. and GJ. K. were supported by the Netherlands Research Council for Chemical Sciences (NWO/CW) and the Netherlands Technology Foundation (STW). 1. *Molecular Cancer Therapeutics,* 1**,** 417-425.

ALLIKMETS, R., SCHRIML, L. M., HUTCHINSON, A., ROMANO-SPICA, V. & DEAN, M. 1998. A human placenta-specific ATP-binding cassette gene (ABCP) on chromosome 4q22 that is involved in multidrug resistance. *Cancer Res,* 58**,** 5337-9.

AMAKURA, Y., TSUTSUMI, T., SASAKI, K., NAKAMURA, M., YOSHIDA, T. & MAITANI, T. 2008. Influence of food polyphenols on aryl hydrocarbon receptor-signaling pathway estimated by in vitro bioassay. *Phytochemistry,* 69**,** 3117-30.

ASAKAWA, C., OGAWA, M., KUMATA, K., FUJINAGA, M., KATO, K., YAMASAKI, T., YUI, J., KAWAMURA, K., HATORI, A., FUKUMURA, T. & ZHANG, M. R. 2011. [11C]sorafenib: radiosynthesis and preliminary PET study of brain uptake in P-gp/Bcrp knockout mice. *Bioorg Med Chem Lett,* 21**,** 2220-3.

ASHIDA, H., FUKUDA, I., YAMASHITA, T. & KANAZAWA, K. 2000. Flavones and flavonols at dietary levels inhibit a transformation of aryl hydrocarbon receptor induced by dioxin. *FEBS Lett,* 476**,** 213-7.

BACANLI, M., BASARAN, A. A. & BASARAN, N. 2015. CYTOTOXICITY EVALUATION of SOME PHENOLIC COMPOUNDS in V79 CELLS. *Turkish Journal of Pharmaceutical Sciences,* 12**,** 53-61.

BADHAN, R. K. S., CHENEL, M. & PENNY, J. I. 2014. Development of a Physiologically-Based Pharmacokinetic Model of the Rat Central Nervous System. *Pharmaceutics,* 6**,** 97-136.
BAEHR, C., REICHEL, V. & FRICKER, G. 2006. Choroid plexus epithelial monolayers–a cell culture model from porcine brain. *Cerebrospinal Fluid Res,* 3**,** 13.
BAI, H., JIN, H., YANG, F., ZHU, H. & CAI, J. 2014. Apigenin induced MCF-7 cell apoptosis-associated reactive oxygen species. *Scanning,* 36**,** 622-31.
BALL, K., BOUZOM, F., SCHERRMANN, J.-M., WALTHER, B. & DECLÈVES, X. 2012. Development of a physiologically based pharmacokinetic model for the rat central nervous system and determination of an in vitro–in vivo scaling methodology for the blood–brain barrier permeability of two transporter substrates, morphine and oxycodone. *Journal of Pharmaceutical Sciences,* 101**,** 4277-4292.
BANKSTAHL, J. P., BANKSTAHL, M., ROMERMANN, K., WANEK, T., STANEK, J., WINDHORST, A. D., FEDROWITZ, M., ERKER, T., MULLER, M., LOSCHER, W., LANGER, O. & KUNTNER, C. 2013. Tariquidar and elacridar are dose-dependently transported by P-glycoprotein and Bcrp at the blood-brain barrier: a small-animal positron emission tomography and in vitro study. *Drug Metab Dispos,* 41**,** 754-62.
BART, J., HOLLEMA, H., GROEN, H., DE VRIES, E., HENDRIKSE, N., SLEIJFER, D., WEGMAN, T., VAALBURG, W. & VAN DER GRAAF, W. 2004. The distribution of drug-efflux pumps,< i> P</i>-gp, BCRP, MRP1 and MRP2, in the normal blood–testis barrier and in primary testicular tumours. *European Journal of Cancer,* 40**,** 2064-2070.
BAUER, B., HARTZ, A. M., FRICKER, G. & MILLER, D. S. 2004. Pregnane X receptor up-regulation of P-glycoprotein expression and transport function at the blood-brain barrier. *Mol Pharmacol,* 66**,** 413-9.
BAUER, B., HARTZ, A. M. S., LUCKING, J. R., YANG, X., POLLACK, G. M. & MILLER, D. S. 2008a. Coordinated nuclear receptor regulation of the efflux transporter, Mrp2, and the phase-II metabolizing enzyme, GST[pi], at the blood-brain barrier. *J Cereb Blood Flow Metab,* 28**,** 1222-1234.
BAUER, B., HARTZ, A. M. S., PEKCEC, A., TOELLNER, K., MILLER, D. S. & POTSCHKA, H. 2008b. Seizure-Induced Up-Regulation of P-Glycoprotein at the Blood-Brain Barrier through Glutamate and Cyclooxygenase-2 Signaling. *Molecular Pharmacology,* 73**,** 1444-1453.
BAUER, B., YANG, X., HARTZ, A. M., OLSON, E. R., ZHAO, R., KALVASS, J. C., POLLACK, G. M. & MILLER, D. S. 2006. In vivo activation of human pregnane X receptor tightens the blood-brain barrier to methadone through P-glycoprotein up-regulation. *Mol Pharmacol,* 70**,** 1212-9.
BEGLEY, D. 2003. Understanding and circumventing the blood-brain barrier. *Acta Paediatrica,* 92**,** 83-91.
BENDAYAN, R., RONALDSON, P. T., GINGRAS, D. & BENDAYAN, M. 2006. In situ localization of P-glycoprotein (ABCB1) in human and rat brain. *J Histochem Cytochem,* 54**,** 1159-67.
BERNOUD, N., FENART, L., BENISTANT, C., PAGEAUX, J. F., DEHOUCK, M. P., MOLIERE, P., LAGARDE, M., CECCHELLI, R. & LECERF, J. 1998. Astrocytes are mainly responsible for the polyunsaturated fatty acid enrichment in blood-brain barrier endothelial cells in vitro. *J Lipid Res,* 39**,** 1816-24.
BILLIAU, H., HEREMANS, D., VERVERKEN, J., VAN DAMME, H., CARTON, P. & DE SOMER 1981. Tissue distribution of human interferons after exogenous administration in rabbits, monkeys, and mice. *Arch Virol,* 68**,** 19 - 25.
BLASBERG, R., PATLAK, C. & FENSTERMACHER, J. 1975. Intrathecal chemotherapy: brain tissue profiles after ventriculocisternal perfusion. *J Pharmacol Exp Ther,* 195**,** 73 - 83.
BOITANO, A. E., WANG, J., ROMEO, R., BOUCHEZ, L. C., PARKER, A. E., SUTTON, S. E., WALKER, J. R., FLAVENY, C. A., PERDEW, G. H., DENISON, M. S., SCHULTZ, P. G. & COOKE, M. P.

2010. Aryl hydrocarbon receptor antagonists promote the expansion of human hematopoietic stem cells. *Science,* 329**,** 1345-8.
BONNEFOY, M., DRAI, J. & KOSTKA, T. 2002. [Antioxidants to slow aging, facts and perspectives]. *Presse Med,* 31**,** 1174-84.
BREEDVELD, P., BEIJNEN, J. H. & SCHELLENS, J. H. M. 2006. Use of P-glycoprotein and BCRP inhibitors to improve oral bioavailability and CNS penetration of anticancer drugs. *Trends in Pharmacological Sciences,* 27**,** 17-24.
BREEDVELD, P., ZELCER, N., PLUIM, D., SÖNMEZER, Ö., TIBBEN, M. M., BEIJNEN, J. H., SCHINKEL, A. H., VAN TELLINGEN, O., BORST, P. & SCHELLENS, J. H. M. 2004. Mechanism of the pharmacokinetic interaction between methotrexate and benzimidazoles potential role for breast cancer resistance protein in clinical drug-drug interactions. *Cancer Res,* 64**,** 5804-5811.
BROWN, P., DAVIES, S., SPEAKE, T. & MILLAR, I. 2004. Molecular mechanisms of cerebrospinal fluid production. *Neuroscience,* 129**,** 955-968.
CALDWELL, G. W. & YAN, Z. 2013. *Optimization in Drug Discovery: In Vitro Methods*, Humana Press.
CAMPOS, C. R., SCHROTER, C., WANG, X. & MILLER, D. S. 2012. ABC transporter function and regulation at the blood-spinal cord barrier. *J Cereb Blood Flow Metab,* 32**,** 1559-1566.
CANDELA, P., GOSSELET, F., SAINT-POL, J., SEVIN, E., BOUCAU, M. C., BOULANGER, E., CECCHELLI, R. & FENART, L. 2010. Apical-to-basolateral transport of amyloid-beta peptides through blood-brain barrier cells is mediated by the receptor for advanced glycation end-products and is restricted by P-glycoprotein. *J Alzheimers Dis,* 22**,** 849-59.
CARDOSO, F. L., BRITES, D. & BRITO, M. A. 2010. Looking at the blood–brain barrier: Molecular anatomy and possible investigation approaches. *Brain Research Reviews,* 64**,** 328-363.
CARRANO, A., SNKHCHYAN, H., KOOIJ, G., VAN DER POL, S., VAN HORSSEN, J., VEERHUIS, R., HOOZEMANS, J., ROZEMULLER, A. & DE VRIES, H. E. 2014. ATP-binding cassette transporters P-glycoprotein and breast cancer related protein are reduced in capillary cerebral amyloid angiopathy. *Neurobiol Aging,* 35**,** 565-75.
CARVEY, P. M., HENDEY, B. & MONAHAN, A. J. 2009. The blood-brain barrier in neurodegenerative disease: a rhetorical perspective. *J Neurochem,* 111**,** 291-314.
CHAN, G. N., HOQUE, M., CUMMINS, C. L. & BENDAYAN, R. 2011. Regulation of P-glycoprotein by orphan nuclear receptors in human brain microvessel endothelial cells. *Journal of neurochemistry,* 118**,** 163-175.
CHANG, T. K. 2009. Activation of pregnane X receptor (PXR) and constitutive androstane receptor (CAR) by herbal medicines. *Aaps j,* 11**,** 590-601.
CHEN, Y. & LIU, L. 2012. Modern methods for delivery of drugs across the blood–brain barrier. *Advanced Drug Delivery Reviews,* 64**,** 640-665.
CHIANG, M. H., CHANG, L. W., WANG, J. W., LIN, L. C. & TSAI, T. H. 2015. Herb-drug pharmacokinetic interaction of a traditional chinese medicine jia-wei-xiao-yao-san with 5-Fluorouracil in the blood and brain of rat using microdialysis. *Evid Based Complement Alternat Med,* 2015**,** 729679.
CHODOBSKI, A., LOH, Y. P., CORSETTI, S., SZMYDYNGER-CHODOBSKA, J., JOHANSON, C. E., LIM, Y. P. & MONFILS, P. R. 1997. The presence of arginine vasopressin and its mRNA in rat choroid plexus epithelium. *Brain Res Mol Brain Res,* 48**,** 67-72.
CHOI, E. Y., LEE, H., DINGLE, R. W., KIM, K. B. & SWANSON, H. I. 2012. Development of novel CH223191-based antagonists of the aryl hydrocarbon receptor. *Mol Pharmacol,* 81**,** 3-11.

CHOI, J. S., JO, B. W. & KIM, Y. C. 2004. Enhanced paclitaxel bioavailability after oral administration of paclitaxel or prodrug to rats pretreated with quercetin. *European Journal of Pharmaceutics and Biopharmaceutics,* 57**,** 313-318.

CHRISTY, N. & FISHMAN, R. 1961. Studies of the blood-cerebrospinal fluid barrier to cortisol in the dog. *J Clin Invest,* 40**,** 1997 - 2006.

CIOLINO, H. P., DASCHNER, P. J. & YEH, G. C. 1998a. Resveratrol inhibits transcription of CYP1A1 in vitro by preventing activation of the aryl hydrocarbon receptor. *Cancer Research,* 58**,** 5707-5712.

CIOLINO, H. P., DASCHNER, P. J. & YEH, G. C. 1998b. Resveratrol inhibits transcription of CYP1A1 in vitro by preventing activation of the aryl hydrocarbon receptor. *Cancer Res,* 58**,** 5707-12.

CIOLINO, H. P., DASCHNER, P. J. & YEH, G. C. 1999. Dietary flavonols quercetin and kaempferol are ligands of the aryl hydrocarbon receptor that affect CYP1A1 transcription differentially. *Biochemical Journal,* 340**,** 715-722.

CISTERNINO, S., ROUSSELLE, C., DAGENAIS, C. & SCHERRMANN, J. M. 2001. Screening of multidrug-resistance sensitive drugs by in situ brain perfusion in P-glycoprotein-deficient mice. *Pharm Res,* 18**,** 183-90.

COHEN-KASHI-MALINA, K., COOPER, I. & TEICHBERG, V. I. 2012. Mechanisms of glutamate efflux at the blood-brain barrier: involvement of glial cells. *J Cereb Blood Flow Metab,* 32**,** 177-89.

COLE, S. P., BHARDWAJ, G., GERLACH, J. H., MACKIE, J. E., GRANT, C. E., ALMQUIST, K. C., STEWART, A. J., KURZ, E. U., DUNCAN, A. M. & DEELEY, R. G. 1992. Overexpression of a transporter gene in a multidrug-resistant human lung cancer cell line. *Science,* 258**,** 1650-4.

COOK, B. D., FERRARI, G., PINTUCCI, G. & MIGNATTI, P. 2008. TGF-β1 INDUCES REARRANGEMENT OF FLK-1 – VE-CADHERIN– β- CATENIN COMPLEX AT THE ADHERENS JUNCTION THROUGH VEGF-MEDIATED SIGNALING. *Journal of cell biochemistry,* 105**,** 1367-1373.

COORAY, H. C., BLACKMORE, C. G., MASKELL, L. & BARRAND, M. A. 2002. Localisation of breast cancer resistance protein in microvessel endothelium of human brain. *Neuroreport,* 13**,** 2059-63.

CORDON-CARDO, C., O'BRIEN, J. P., CASALS, D., RITTMAN-GRAUER, L., BIEDLER, J. L., MELAMED, M. R. & BERTINO, J. R. 1989. Multidrug-resistance gene (P-glycoprotein) is expressed by endothelial cells at blood-brain barrier sites. *Proc Natl Acad Sci U S A,* 86**,** 695-8.

CORNFORD, E. M., VARESI, J. B., HYMAN, S., DAMIAN, R. T. & RALEIGH, M. J. 1997. Mitochondrial content of choroid plexus epithelium. *Experimental Brain Research,* 116**,** 399-405.

CUNNINGHAM, B. D., THREADGILL, M. D., GROUNDWATER, P. W., DALE, I. L. & HICKMAN, J. A. 1992. Synthesis and biological evaluation of a series of flavones designed as inhibitors of protein tyrosine kinases. *Anticancer Drug Des,* 7**,** 365-84.

DAUCHY, S., DUTHEIL, F., WEAVER, R. J., CHASSOUX, F., DAUMAS-DUPORT, C., COURAUD, P. O., SCHERRMANN, J. M., DE WAZIERS, I. & DECLEVES, X. 2008a. ABC transporters, cytochromes P450 and their main transcription factors: expression at the human blood-brain barrier. *J Neurochem,* 107**,** 1518-28.

DAUCHY, S., DUTHEIL, F., WEAVER, R. J., CHASSOUX, F., DAUMAS-DUPORT, C., COURAUD, P. O., SCHERRMANN, J. M., DE WAZIERS, I. & DECLÈVES, X. 2008b. ABC transporters, cytochromes P450 and their main transcription factors: Expression at the human blood-brain barrier. *Journal of Neurochemistry,* 107**,** 1518-1528.

DAUCHY, S., MILLER, F., COURAUD, P. O., WEAVER, R. J., WEKSLER, B., ROMERO, I. A., SCHERRMANN, J. M., DE WAZIERS, I. & DECLEVES, X. 2009. Expression and transcriptional regulation of ABC transporters and cytochromes P450 in hCMEC/D3 human cerebral microvascular endothelial cells. *Biochem Pharmacol,* 77**,** 897-909.

DAVARINOS, N. A. & POLLENZ, R. S. 1999. Aryl hydrocarbon receptor imported into the nucleus following ligand binding is rapidly degraded via the cytosplasmic proteasome following nuclear export. *J Biol Chem,* 274**,** 28708-15.

DAY, A. J., CANADA, F. J., DIAZ, J. C., KROON, P. A., MCLAUCHLAN, R., FAULDS, C. B., PLUMB, G. W., MORGAN, M. R. & WILLIAMSON, G. 2000. Dietary flavonoid and isoflavone glycosides are hydrolysed by the lactase site of lactase phlorizin hydrolase. *FEBS Lett,* 468**,** 166-70.

DEELEY, R. G. & COLE, S. P. C. 2006. Substrate recognition and transport by multidrug resistance protein 1 (ABCC1). *FEBS Letters,* 580**,** 1103-1111.

DENISON, M. S., FISHER, J. M. & WHITLOCK, J. P., JR. 1988. The DNA recognition site for the dioxin-Ah receptor complex. Nucleotide sequence and functional analysis. *J Biol Chem,* 263**,** 17221-4.

DENISON, M. S. & NAGY, S. R. 2003. Activation of the Aryl Hydrocarbon Receptor by Structurally Diverse Exogenous and Endogenous Chemicals. *Annual Review of Pharmacology and Toxicology.*

DI MASI, A., DE MARINIS, E., ASCENZI, P. & MARINO, M. 2009. Nuclear receptors CAR and PXR: Molecular, functional, and biomedical aspects. *Mol Aspects Med,* 30**,** 297-343.

DICKANCAITE, E., NEMEIKAITE, A., KALVELYTE, A. & CENAS, N. 1998. Prooxidant character of flavonoid cytotoxicity: structure-activity relationships. *Biochem Mol Biol Int,* 45**,** 923-30.

DOHRMANN, G. 1970a. The choroid plexus: a historical review. *Brain Res,* 18**,** 197 - 218.

DOHRMANN, G. J. 1970b. Dark and light epithelial cells in the choroid plexus of mammals. *Journal of Ultrasructure Research,* 32**,** 268-273.

DONOVAN, J. L., MANACH, C., FAULKS, R. M. & KROON, P. A. 2006. Absorption and metabolism of dietary secondary metabolites. *In:* CROZIER, A., CLIFFORD, M. N. & ASHIHARA, H. (eds.) *Plant Secondary Metabolites. Occurrence, Structure and Role in the Human Diet.* Oxford, UK: Blackwell Publishing.

DORAN, A., OBACH, R. S., SMITH, B. J., HOSEA, N. A., BECKER, S., CALLEGARI, E., CHEN, C., CHEN, X., CHOO, E., CIANFROGNA, J., COX, L. M., GIBBS, J. P., GIBBS, M. A., HATCH, H., HOP, C. E., KASMAN, I. N., LAPERLE, J., LIU, J., LIU, X., LOGMAN, M., MACLIN, D., NEDZA, F. M., NELSON, F., OLSON, E., RAHEMATPURA, S., RAUNIG, D., ROGERS, S., SCHMIDT, K., SPRACKLIN, D. K., SZEWC, M., TROUTMAN, M., TSENG, E., TU, M., VAN DEUSEN, J. W., VENKATAKRISHNAN, K., WALENS, G., WANG, E. Q., WONG, D., YASGAR, A. S. & ZHANG, C. 2005. The impact of P-glycoprotein on the disposition of drugs targeted for indications of the central nervous system: evaluation using the MDR1A/1B knockout mouse model. *Drug Metab Dispos,* 33**,** 165-74.

DORNAN, T., BOSHUIZEN, H., KING, N. & SCHERPBIER, A. 2007. Experience-based learning: a model linking the processes and outcomes of medical students' workplace learning. *Medical Education,* 41**,** 84-91.

DOYLE, L. & ROSS, D. D. 2003a. Multidrug resistance mediated by the breast cancer resistance protein BCRP (ABCG2). *Oncogene,* 22**,** 7340-58.

DOYLE, L. A. & ROSS, D. D. 2003b. Multidrug resistance mediated by the breast cancer resistance protein BCRP (ABCG2). *Oncogene,* 22**,** 7340-7358.

DOYLE, L. A., YANG, W., ABRUZZO, L. V., KROGMANN, T., GAO, Y., RISHI, A. K. & ROSS, D. D. 1998. A multidrug resistance transporter from human MCF-7 breast cancer cells. *Proceedings of the National Academy of Sciences,* 95**,** 15665-15670.

EBADA, S., HELAL, A. & ALKAFAFY, M. 2011. Morphological Studies on the Choroid Plexus in Balady Goat (Capra hircus). *J. Vet. Anat. Vol,* 4**,** 79-92.

EBERT, B., SEIDEL, A. & LAMPEN, A. 2005. Identification of BCRP as transporter of benzo[a]pyrene conjugates metabolically formed in Caco-2 cells and its induction by Ah-receptor agonists. *Carcinogenesis,* 26**,** 1754-63.

EBERT, B., SEIDEL, A. & LAMPEN, A. 2007. Phytochemicals induce breast cancer resistance protein in Caco-2 cells and enhance the transport of benzo[a]pyrene-3-sulfate. *Toxicol Sci,* 96**,** 227-36.

EDWARDS, J. E., ALCORN, J., SAVOLAINEN, J., ANDERSON, B. D. & MCNAMARA, P. J. 2005. Role of P-glycoprotein in distribution of nelfinavir across the blood-mammary tissue barrier and blood-brain barrier. *Antimicrob Agents Chemother,* 49**,** 1626-8.

EE, P. L., KAMALAKARAN, S., TONETTI, D., HE, X., ROSS, D. D. & BECK, W. T. 2004a. Identification of a novel estrogen response element in the breast cancer resistance protein (ABCG2) gene. *Cancer Res,* 64**,** 1247-51.

EE, P. L. R., KAMALAKARAN, S., TONETTI, D., HE, X., ROSS, D. D. & BECK, W. T. 2004b. Identification of a novel estrogen response element in the breast cancer resistance protein (ABCG2) gene. *Cancer research,* 64**,** 1247-1251.

EIGENMANN, D. E., XUE, G., KIM, K. S., MOSES, A. V., HAMBURGER, M. & OUFIR, M. 2013. Comparative study of four immortalized human brain capillary endothelial cell lines, hCMEC/D3, hBMEC, TY10, and BB19, and optimization of culture conditions, for an in vitro blood–brain barrier model for drug permeability studies. *Fluids and Barriers of the CNS,* 10**,** 1-17.

EISENBLÄTTER, T., HÜWEL, S. & GALLA, H.-J. 2003. Characterisation of the brain multidrug resistance protein (BMDP/ABCG2/BCRP) expressed at the blood–brain barrier. *Brain Research,* 971**,** 221-231.

ENGLER, M. B., ENGLER, M. M., CHEN, C. Y., MALLOY, M. J., BROWNE, A., CHIU, E. Y., KWAK, H. K., MILBURY, P., PAUL, S. M., BLUMBERG, J. & MIETUS-SNYDER, M. L. 2004. Flavonoid-rich dark chocolate improves endothelial function and increases plasma epicatechin concentrations in healthy adults. *J Am Coll Nutr,* 23**,** 197-204.

ERLUND, I., SILASTE, M. L., ALFTHAN, G., RANTALA, M., KESANIEMI, Y. A. & ARO, A. 2002. Plasma concentrations of the flavonoids hesperetin, naringenin and quercetin in human subjects following their habitual diets, and diets high or low in fruit and vegetables. *Eur J Clin Nutr,* 56**,** 891-8.

ESSER, C. 2009. The immune phenotype of AhR null mouse mutants: Not a simple mirror of xenobiotic receptor over-activation. *Biochemical Pharmacology,* 77**,** 597-607.

EVANS, E. A. & SKALAK, R. 1980. *Mechanics and thermodynamics of biomembranes*, Crc Press Boca Raton, FL.

FENSTERMACHER, J. & KAYE, T. 1988. Drug "diffusion" within the brain. *Ann N Y Acad Sci,* 531**,** 29-39.

FERNANDEZ-SALGUERO, P. M., HILBERT, D. M., RUDIKOFF, S., WARD, J. M. & GONZALEZ, F. J. 1996. Aryl-hydrocarbon receptor-deficient mice are resistant to 2,3,7,8-tetrachlorodibenzo-p-dioxin-induced toxicity. *Toxicol Appl Pharmacol,* 140**,** 173-9.

FINDLEY, L., AUJLA, M., BAIN, P. G., BAKER, M., BEECH, C., BOWMAN, C., HOLMES, J., KINGDOM, W. K., MACMAHON, D. G., PETO, V. & PLAYFER, J. R. 2003. Direct economic impact of Parkinson's disease: a research survey in the United Kingdom. *Mov Disord,* 18**,** 1139-45.

FLAVENY, C. A., MURRAY, I. A. & PERDEW, G. H. 2010. Differential gene regulation by the human and mouse aryl hydrocarbon receptor. *Toxicol Sci,* 114**,** 217-25.

FLEISHER, B., UNUM, J., SHAO, J. & AN, G. 2015. Ingredients in Fruit Juices Interact with Dasatinib Through Inhibition of BCRP: A New Mechanism of Beverage–Drug Interaction. *Journal of Pharmaceutical Sciences,* 104**,** 266-275.

FORMICA, J. V. & REGELSON, W. 1995. Review of the biology of Quercetin and related bioflavonoids. *Food Chem Toxicol,* 33**,** 1061-80.

FRANKE, H., GALLA, H.-J. & BEUCKMANN, C. T. 2000. Primary cultures of brain microvessel endothelial cells: a valid and flexible model to study drug transport through the blood–brain barrier in vitro. *Brain Research Protocols,* 5**,** 248-256.

FRIEDEMANN, U. 1942. Blood-Brain Barrier. *Physiological Reviews,* 22**,** 125-145.

FRIXIONE, E. 2006. Albrecht von Haller (1708-1777). *J Neurol,* 253**,** 265-6.

FUKUNAGA, B. N., PROBST, M. R., REISZ-PORSZASZ, S. & HANKINSON, O. 1995. Identification of functional domains of the aryl hydrocarbon receptor. *J Biol Chem,* 270**,** 29270-8.

FURUSE, M., SASAKI, H. & TSUKITA, S. 1999. Manner of interaction of heterogeneous claudin species within and between tight junction strands. *J Cell Biol,* 147**,** 891-903.

GALATI, G., MORIDANI, M. Y., CHAN, T. S. & O'BRIEN, P. J. 2001. Peroxidative metabolism of apigenin and naringenin versus luteolin and quercetin: glutathione oxidation and conjugation. *Free Radic Biol Med,* 30**,** 370-82.

GALATI, G., SABZEVARI, O., WILSON, J. X. & O'BRIEN, P. J. 2002. Prooxidant activity and cellular effects of the phenoxyl radicals of dietary flavonoids and other polyphenolics. *Toxicology,* 177**,** 91-104.

GARRISON, P. M., TULLIS, K., AARTS, J. M., BROUWER, A., GIESY, J. P. & DENISON, M. S. 1996. Species-specific recombinant cell lines as bioassay systems for the detection of 2,3,7,8-tetrachlorodibenzo-p-dioxin-like chemicals. *Fundam Appl Toxicol,* 30**,** 194-203.

GEICK, A., EICHELBAUM, M. & BURK, O. 2001a. Nuclear Receptor Response Elements Mediate Induction of Intestinal MDR1 by Rifampin. *Journal of Biological Chemistry,* 276**,** 14581-14587.

GEICK, A., EICHELBAUM, M. & BURK, O. 2001b. Nuclear receptor response elements mediate induction of intestinal MDR1 by rifampin. *J Biol Chem,* 276**,** 14581-7.

GIL, S., SAURA, R., FORESTIER, F. & FARINOTTI, R. 2005. P-glycoprotein expression of the human placenta during pregnancy. *Placenta,* 26**,** 268-70.

GOLDMANN, E. E. 1909. Die aussere und innere Sekretion des gesunden und kranken Organismus im Lichte der 'vitalen Farbung'. *Beitr. klin. Chir.,* 64**,** 192-265.

GOLDMANN, E. E. 1913. Vitalfarbung am Zentralneirvensystem. *Abh. preuss. Akad.Wims., Phys.-Math. Kl.,* I**,** 1-60.

GOODMAN, J. 1985. Field-based experience: a study of social control and student teachers' response to institutional constraints. *Journal of Education for Teaching,* 11**,** 26-49.

GOTTESMAN, M. M. & PASTAN, I. 1993. Biochemistry of multidrug resistance mediated by the multidrug transporter. *Annu Rev Biochem,* 62**,** 385-427.

GRANBERG, L., OSTERGREN, A., BRANDT, I. & BRITTEBO, E. B. 2003. CYP1A1 and CYP1B1 in blood-brain interfaces: CYP1A1-dependent bioactivation of 7,12-dimethylbenz(a)anthracene in endothelial cells. *Drug Metab Dispos,* 31**,** 259-65.

GUO, M., JOIAKIM, A. & REINERS, J. J., JR. 2000. Suppression of 2,3,7,8-tetrachlorodibenzo-p-dioxin (TCDD)-mediated aryl hydrocarbon receptor transformation and CYP1A1 induction by the phosphatidylinositol 3-kinase inhibitor 2-(4-morpholinyl)-8-phenyl-4H-1- benzopyran-4-one (LY294002). *Biochem Pharmacol,* 60**,** 635-42.

GUPTA, A., ZHANG, Y., UNADKAT, J. D. & MAO, Q. 2004. HIV protease inhibitors are inhibitors but not substrates of the human breast cancer resistance protein (BCRP/ABCG2). *Journal of Pharmacology and Experimental Therapeutics,* 310**,** 334-341.

GURVITCH, R. & METZLER, M. W. 2009. The effects of laboratory-based and field-based practicum experience on pre-service teachers' self-efficacy. *Teaching and Teacher Education,* 25**,** 437-443.

HADDAD, J. J. 2004. On the antioxidant mechanisms of Bcl-2: a retrospective of NF-kappaB signaling and oxidative stress. *Biochem Biophys Res Commun,* 322**,** 355-63.

HADI, S. M., ASAD, S. F., SINGH, S. & AHMAD, A. 2000. Putative mechanism for anticancer and apoptosis-inducing properties of plant-derived polyphenolic compounds. *IUBMB Life,* 50**,** 167-71.

HAJDU, S. I. 2003. Discovery of the cerebrospinal fluid. *Annals of Clinical & Laboratory Science,* 33**,** 334-336.

HAKVOORT, A., HASELBACH, M., WEGENER, J., HOHEISEL, D. & GALLA, H. J. 1998. The Polarity of Choroid Plexus Epithelial Cells In Vitro Is Improved in Serum-Free Medium. *Journal of neurochemistry,* 71**,** 1141-1150.

HALWACHS, S., LAKOMA, C., SCHÄFER, I., SEIBEL, P. & HONSCHA, W. 2011. The antiepileptic drugs phenobarbital and carbamazepine reduce transport of methotrexate in rat choroid plexus by down-regulation of the reduced folate carrier. *Molecular Pharmacology,* 80**,** 621-629.

HAMMARLUND-UDENAES, M. 2000. The use of microdialysis in CNS drug delivery studies. Pharmacokinetic perspectives and results with analgesics and antiepileptics. *Adv Drug Deliv Rev,* 45**,** 283-94.

HAN, M.-E., KIM, H.-J., LEE, Y.-S., KIM, D.-H., CHOI, J.-T., PAN, C.-S., YOON, S., BAEK, S.-Y., KIM, B.-S. & KIM, J.-B. 2009. Regulation of cerebrospinal fluid production by caffeine consumption. *BMC neuroscience,* 10**,** 110.

HAPPICH, M., KIRSON, N. Y. B., DESAI, U., KING, S., BIRNBAUM, H. G. B., REED, C., BELGER, M., LENOX-SMITH, A. & PRICE, D. 2016. Excess Costs Associated with Possible Misdiagnosis of Alzheimer's Disease Among Patients with Vascular Dementia in a UK CPRD Population. *Journal of Alzheimer s Disease,* 52**,** 1-13.

HARTZ, A. & BAUER, B. 2011. ABC transporters in the CNS–an inventory. *Curr. Pharm. Biotechnol,* 12**,** 656-673.

HARTZ, A. M. & BAUER, B. 2010. Regulation of ABC transporters at the blood-brain barrier: new targets for CNS therapy. *Mol Interv,* 10**,** 293-304.

HARTZ, A. M. S., MAHRINGER, A., MILLER, D. S. & BAUER, B. 2010. 17-β-Estradiol: a powerful modulator of blood–brain barrier BCRP activity. *Journal of Cerebral Blood Flow & Metabolism,* 30**,** 1742-1755.

HAVSTEEN, B. H. 2002. The biochemistry and medical significance of the flavonoids. *Pharmacology and Therapeutics,* 96**,** 67-202.

HAWKINS, B. T. & DAVIS, T. P. 2005. The blood-brain barrier/neurovascular unit in health and disease. *Pharmacol Rev,* 57**,** 173-85.

HE, G., ZHAO, J., BRENNAN, J. C., AFFATATO, A. A., ZHAO, B., RICE, R. H. & DENISON, M. S. 2004. Cell based assay for the identification of aryl hydrocarbon receptor activators *In:* CALDWELL, G. W. & YAN, Z. (eds.) *Optimisation in drug discovery.* Humana Press.

HIGGINS, C. F. 1992. ABC Transporters: From Microorganisms to Man. *Annual Review of Cell Biology,* 8**,** 67-113.

HOFFMAN, E. C., REYES, H., CHU, F. F., SANDER, F., CONLEY, L. H., BROOKS, B. A. & HANKINSON, O. 1991. Cloning of a factor required for activity of the Ah (dioxin) receptor. *Science,* 252**,** 954-8.

HOQUE, M. T., ROBILLARD, K. R. & BENDAYAN, R. 2012. Regulation of breast cancer resistant protein by peroxisome proliferator-activated receptor alpha in human brain microvessel endothelial cells. *Mol Pharmacol,* 81**,** 598-609.

HOSOYA, K.-I., HORI, S., OHTSUKI, S. & TERASAKI, T. 2004. A new in vitro model for blood–cerebrospinal fluid barrier transport studies: an immortalized choroid plexus epithelial cell line derived from the tsA58 SV40 large T-antigen gene transgenic rat. *Advanced Drug Delivery Reviews,* 56**,** 1875-1885.

HTTP://ALZHEIMERS.ORG.UK/SITE/SCRIPTS/DOWNLOAD_INFO.PHP?DOWNLOADID=1491, A. J., 2015. 2014. *Alzheimer's, Society (2014) Dementia UK* [Online].

HURD , M. D., MARTORELL , P., DELAVANDE , A., MULLEN , K. J. & LANGA , K. M. 2013. Monetary Costs of Dementia in the United States. *New England Journal of Medicine,* 368**,** 1326-1334.

IKUTA, T., EGUCHI, H., TACHIBANA, T., YONEDA, Y. & KAWAJIRI, K. 1998. Nuclear localization and export signals of the human aryl hydrocarbon receptor. *J Biol Chem,* 273**,** 2895-904.

IKUTA, T., TACHIBANA, T., WATANABE, J., YOSHIDA, M., YONEDA, Y. & KAWAJIRI, K. 2000. Nucleocytoplasmic shuttling of the aryl hydrocarbon receptor. *J Biochem,* 127**,** 503-9.

IMAI, Y., ASADA, S., TSUKAHARA, S., ISHIKAWA, E., TSURUO, T. & SUGIMOTO, Y. 2003. Breast cancer resistance protein exports sulfated estrogens but not free estrogens. *Mol Pharmacol,* 64**,** 610-8.

IMAI, Y., ISHIKAWA, E., ASADA, S. & SUGIMOTO, Y. 2005a. Estrogen-mediated post transcriptional down-regulation of breast cancer resistance protein/ABCG2. *Cancer research,* 65**,** 596-604.

IMAI, Y., ISHIKAWA, E., ASADA, S. & SUGIMOTO, Y. 2005b. Estrogen-mediated post transcriptional down-regulation of breast cancer resistance protein/ABCG2. *Cancer Res,* 65**,** 596-604.

IMAI, Y., TSUKAHARA, S., ASADA, S. & SUGIMOTO, Y. 2004. Phytoestrogens/flavonoids reverse breast cancer resistance protein/ABCG2-mediated multidrug resistance. *Cancer Res,* 64**,** 4346-52.

ISHIWATA, I., ISHIWATA, C., ISHIWATA, E., SATO, Y., KIGUCHI, K., TACHIBANA, T., HASHIMOTO, H. & ISHIKAWA, H. 2005. Establishment and characterization of a human malignant choroids plexus papilloma cell line (HIBCPP). *Hum Cell,* 18**,** 67-72.

JACOB, A., HARTZ, A. M., POTIN, S., COUMOUL, X., YOUSIF, S., SCHERRMANN, J. M., BAUER, B. & DECLEVES, X. 2011. Aryl hydrocarbon receptor-dependent upregulation of Cyp1b1 by TCDD and diesel exhaust particles in rat brain microvessels. *Fluids Barriers CNS,* 8**,** 23.

JOHANSON, C. E., DUNCAN 3RD, J., KLINGE, P. M., BRINKER, T., STOPA, E. G. & SILVERBERG, G. D. 2008a. Multiplicity of cerebrospinal fluid functions: New challenges in health and disease. *Cerebrospinal Fluid Res,* 5**,** 353-364.

JOHANSON, C. E., DUNCAN, J. A., 3RD, KLINGE, P. M., BRINKER, T., STOPA, E. G. & SILVERBERG, G. D. 2008b. Multiplicity of cerebrospinal fluid functions: New challenges in health and disease. *Cerebrospinal Fluid Res,* 5**,** 10.

JOHNSON, D. R., GUO, G. L. & KLAASSEN, C. D. 2002. Expression of rat Multidrug Resistance Protein 2 (Mrp2) in male and female rats during normal and pregnenolone-16alpha-carbonitrile (PCN)-induced postnatal ontogeny. *Toxicology,* 178**,** 209-19.

JONKER, J. W., MERINO, G., MUSTERS, S., VAN HERWAARDEN, A. E., BOLSCHER, E., WAGENAAR, E., MESMAN, E., DALE, T. C. & SCHINKEL, A. H. 2005. The breast cancer resistance protein BCRP (ABCG2) concentrates drugs and carcinogenic xenotoxins into milk. *Nature medicine,* 11**,** 127-129.

JULIANE KLÄS, HARTWIG WOLBURG, TETSUYA TERASAKI, GERT FRICKER & REICHEL1, V. 2010. Characterization of immortalized choroid plexus epithelial cell lines for studies of transport processes across the blood-cerebrospinal fluid barrier. *Cerebrospinal Fluid Research,* 7**,** 2-12.

JULIANO, R. L. & LING, V. 1976. A surface glycoprotein modulating drug permeability in Chinese hamster ovary cell mutants. *Biochim Biophys Acta,* 455**,** 152-62.
KAGE, K., TSUKAHARA, S., SUGIYAMA, T., ASADA, S., ISHIKAWA, E., TSURUO, T. & SUGIMOTO, Y. 2002. Dominant-negative inhibition of breast cancer resistance protein as drug efflux pump through the inhibition of S-S dependent homodimerization. *Int J Cancer,* 97**,** 626-30.
KAINU, T., GUSTAFSSON, J. A. & PELTO-HUIKKO, M. 1995. The dioxin receptor and its nuclear translocator (Arnt) in the rat brain. *Neuroreport,* 6**,** 2557-60.
KAMEREMAIL, A. R., PIRRAGLIA, E., YI LI, W. T., MCHUGH, P., SVETCOV, S., LINKER, R., ANNAM, K., OSORIO, R., GLODZIK, L., CORBY, P. M., JANAL, M., ZETTERBERG, H., BLENNOW, K. & DELEON, M. 2015. CSF Alzheimer's disease-related biomarkers are higher in subjects with periodontal disease. *Alzheimer's & Dementia: The Journal of the Alzheimer's Association,* 11**,** 779.
KAMPA, M., NIFLI, A. P., NOTAS, G. & CASTANAS, E. 2007. Polyphenols and cancer cell growth. *Rev Physiol Biochem Pharmacol,* 159**,** 79-113.
KAST, H. R., GOODWIN, B., TARR, P. T., JONES, S. A., ANISFELD, A. M., STOLTZ, C. M., TONTONOZ, P., KLIEWER, S., WILLSON, T. M. & EDWARDS, P. A. 2002. Regulation of multidrug resistance-associated protein 2 (ABCC2) by the nuclear receptors pregnane X receptor, farnesoid X-activated receptor, and constitutive androstane receptor. *J Biol Chem,* 277**,** 2908-15.
KATAYAMA, K., MASUYAMA, K., YOSHIOKA, S., HASEGAWA, H., MITSUHASHI, J. & SUGIMOTO, Y. 2007. Flavonoids inhibit breast cancer resistance protein-mediated drug resistance: transporter specificity and structure-activity relationship. *Cancer Chemother Pharmacol,* 60**,** 789-97.
KAUR, M. & BADHAN, R. K. 2015. Phytoestrogens Modulate Breast Cancer Resistance Protein Expression and Function at the Blood-Cerebrospinal Fluid Barrier. *J Pharm Pharm Sci,* 18**,** 132-54.
KAWAMURA, K., KONNO, F., YUI, J., YAMASAKI, T., HATORI, A., YANAMOTO, K., WAKIZAKA, H., TAKEI, M., NENGAKI, N., FUKUMURA, T. & ZHANG, M. R. 2010. Synthesis and evaluation of [11C]XR9576 to assess the function of drug efflux transporters using PET. *Ann Nucl Med,* 24**,** 403-12.
KELLY, F. J. 1998. Use of antioxidants in the prevention and treatment of disease. *J Int Fed Clin Chem,* 10**,** 21-3.
KITAMURA, A., OKURA, T., HIGUCHI, K. & DEGUCHI, Y. 2015. Cocktail-Dosing Microdialysis Study to Simultaneously Assess Delivery of Multiple Organic-Cationic Drugs to the Brain. *J Pharm Sci*.
KITAZAWA, T., HOSOYA, K., WATANABE, M., TAKASHIMA, T., OHTSUKI, S., TAKANAGA, H., UEDA, M., YANAI, N., OBINATA, M. & TERASAKI, T. 2001. Characterization of the amino acid transport of new immortalized choroid plexus epithelial cell lines: a novel in vitro system for investigating transport functions at the blood-cerebrospinal fluid barrier. *Pharm Res,* 18**,** 16-22.
KOCIBA, R. J. & SCHWETZ, B. A. 1982. Toxicity of 2, 3, 7, 8-tetrachlorodibenzo-p-dioxin (TCDD). *Drug Metab Rev,* 13**,** 387-406.
KOWAL, S. L., DALL, T. M., CHAKRABARTI, R., STORM, M. V. & JAIN, A. 2013. The current and projected economic burden of Parkinson's disease in the United States. *Mov Disord,* 28**,** 311-8.
KRIS-ETHERTON, P. M. & KEEN, C. L. 2002. Evidence that the antioxidant flavonoids in tea and cocoa are beneficial for cardiovascular health. *Curr Opin Lipidol,* 13**,** 41-9.
KRISHNAMURTHY, P., ROSS, D. D., NAKANISHI, T., BAILEY-DELL, K., ZHOU, S., MERCER, K. E., SARKADI, B., SORRENTINO, B. P. & SCHUETZ, J. D. 2004. The stem cell marker

Bcrp/ABCG2 enhances hypoxic cell survival through interactions with heme. *J Biol Chem,* 279**,** 24218-25.
KÜHNAU, J. 1976. The flavonoids. A class of semi-essential food components: their role in human nutrition. *World review of nutrition and dietetics,* 24**,** 117-191.
KUSUHARA, H. & SUGIYAMA, Y. 2005. Active efflux across the blood-brain barrier: role of the solute carrier family. *NeuroRx,* 2**,** 73-85.
LAI, M. Y., HSIU, S. L., HOU, Y. C., TSAI, S. Y. & CHAO, P. D. L. 2004. Significant decrease of cyclosporine bioavailability in rats caused by a decoction of the roots of Scutellaria baicalensis. *Planta Medica,* 70**,** 132-137.
LANGFORD, D., HURFORD, R., HASHIMOTO, M., DIGICAYLIOGLU, M. & MASLIAH, E. 2005. Signalling crosstalk in FGF2-mediated protection of endothelial cells from HIV-gp120. *BMC Neurosci,* 6**,** 8.
LAUER, R., BAUER, R., LINZ, B., PITTNER, F., PESCHEK, G. A., ECKER, G., FRIEDL, P. & NOE, C. R. 2004. Development of an in vitro blood–brain barrier model based on immortalized porcine brain microvascular endothelial cells. *Il Farmaco,* 59**,** 133-137.
LEE, A. J., CAI, M. X., THOMAS, P. E., CONNEY, A. H. & ZHU, B. T. 2003. Characterization of the oxidative metabolites of 17β-estradiol and estrone formed by 15 selectively expressed human cytochrome P450 isoforms. *Endocrinology,* 144**,** 3382-3398.
LEE, C. A., O'CONNOR, M. A., RITCHIE, T. K., GALETIN, A., COOK, J. A., RAGUENEAU-MAJLESSI, I., ELLENS, H., FENG, B., TAUB, M. E., PAINE, M. F., POLLI, J. W., WARE, J. A. & ZAMEK-GLISZCZYNSKI, M. J. 2015. Breast cancer resistance protein (ABCG2) in clinical pharmacokinetics and drug interactions: practical recommendations for clinical victim and perpetrator drug-drug interaction study design. *Drug Metab Dispos,* 43**,** 490-509.
LEE, G., BABAKHANIAN, K., RAMASWAMY, M., PRAT, A., WOSIK, K. & BENDAYAN, R. 2007. Expression of the ATP-binding cassette membrane transporter, ABCG2, in human and rodent brain microvessel endothelial and glial cell culture systems. *Pharm Res,* 24**,** 1262-74.
LEMMEN, J., TOZAKIDIS, I. E., BELE, P. & GALLA, H. J. 2013. Constitutive androstane receptor upregulates Abcb1 and Abcg2 at the blood-brain barrier after CITCO activation. *Brain Res,* 1501**,** 68-80.
LI, L., STANTON, J. D., TOLSON, A. H., LUO, Y. & WANG, H. 2009. Bioactive terpenoids and flavonoids from Ginkgo biloba extract induce the expression of hepatic drug-metabolizing enzymes through pregnane X receptor, constitutive androstane receptor, and aryl hydrocarbon receptor-mediated pathways. *Pharm Res,* 26**,** 872-82.
LI, Y., FANNING, A. S., ANDERSON, J. M. & LAVIE, A. 2005. Structure of the Conserved Cytoplasmic C-terminal Domain of Occludin: Identification of the ZO-1 Binding Surface. *Journal of Molecular Biology,* 352**,** 151-164.
LINDSEY, S. & PAPOUTSAKIS, E. T. 2012. The Evolving Role of the Aryl Hydrocarbon Receptor (AHR) in the Normophysiology of Hematopoiesis. *Stem cell reviews,* 8**,** 1223-1235.
LIPINSKI, C. A. 2000. Drug-like properties and the causes of poor solubility and poor permeability. *Journal of pharmacological and toxicological methods,* 44**,** 235-249.
LIVAK, K. J. & SCHMITTGEN, T. D. 2001. Analysis of relative gene expression data using real-time quantitative PCR and the 2(-Delta Delta C(T)) Method. *Methods,* 25**,** 402-8.
LÖSCHER, W. & POTSCHKA, H. 2005. Blood-brain barrier active efflux transporters: ATP-binding cassette gene family. *NeuroRx,* 2**,** 86-98.
MA, Q. & WHITLOCK, J. P., JR. 1996. The aromatic hydrocarbon receptor modulates the Hepa 1c1c7 cell cycle and differentiated state independently of dioxin. *Mol Cell Biol,* 16**,** 2144-50.
MAHRINGER, A. & FRICKER, G. 2010. BCRP at the blood-brain barrier: Genomic regulation by 17β-estradiol. *Molecular Pharmaceutics,* 7**,** 1835-1847.

MAHRINGER, A., OTT, M., REIMOLD, I., REICHEL, V. & FRICKER, G. 2011. The ABC of the blood-brain barrier - regulation of drug efflux pumps. *Curr Pharm Des,* 17**,** 2762-70.

MALIEPAARD, M., SCHEFFER, G. L., FANEYTE, I. F., VAN GASTELEN, M. A., PIJNENBORG, A. C. L. M., SCHINKEL, A. H., VAN DE VIJVER, M. J., SCHEPER, R. J. & SCHELLENS, J. H. M. 2001. Subcellular localization and distribution of the breast cancer resistance protein transporter in normal human tissues. *Cancer Res,* 61**,** 3458-3464.

MANJI, H. K. & DESOUZA, E. B. 2008. CNS Drug Discovery and Development: When Will We Rescue Tantalus?' Neuropsychopharmacology Reviews Volume 2 on CNS Drug Discovery and Development: Challenges and Opportunities. *Neuropsychopharmacology Reviews,* 0**,** 1-4.

MAO, Q. 2005. Role of the breast cancer resistance protein (ABCG2) in drug transport. *AAPS J,* 7**,** 118-133.

MELAINE, N., LIENARD, M. O., DORVAL, I., LE GOASCOGNE, C., LEJEUNE, H. & JEGOU, B. 2002. Multidrug resistance genes and p-glycoprotein in the testis of the rat, mouse, Guinea pig, and human. *Biol Reprod,* 67**,** 1699-707.

MIDDLETON JR, E. 1998. Effect of plant flavonoids on immune and inflammatory cell function. *Advances in Experimental Medicine and Biology.*

MILLER, D. S. 2010. Regulation of P-glycoprotein and other ABC drug transporters at the blood–brain barrier. *Trends in Pharmacological Sciences,* 31**,** 246-254.

MIYAKE, K., MICKLEY, L., LITMAN, T., ZHAN, Z., ROBEY, R., CRISTENSEN, B., BRANGI, M., GREENBERGER, L., DEAN, M., FOJO, T. & BATES, S. E. 1999. Molecular cloning of cDNAs which are highly overexpressed in mitoxantrone-resistant cells: demonstration of homology to ABC transport genes. *Cancer Res,* 59**,** 8-13.

MO, W. & ZHANG, J. T. 2009. Oligomerization of human ATP-binding cassette transporters and its potential significance in human disease.

MOORE, J. T., MOORE, L. B., MAGLICH, J. M. & KLIEWER, S. A. 2003. Functional and structural comparison of PXR and CAR. *Biochim Biophys Acta,* 1619**,** 235-8.

MORRIS, M. E. & ZHANG, S. 2006. Flavonoid–drug interactions: Effects of flavonoids on ABC transporters. *Life Sciences,* 78**,** 2116-2130.

MUKAI, R., SHIRAI, Y., SAITO, N., FUKUDA, I., NISHIUMI, S., YOSHIDA, K. & ASHIDA, H. 2010. Suppression mechanisms of flavonoids on aryl hydrocarbon receptor-mediated signal transduction. *Arch Biochem Biophys,* 501**,** 134-41.

MULERO-NAVARRO, S., CARVAJAL-GONZALEZ, J. M., HERRANZ, M., BALLESTAR, E., FRAGA, M. F., ROPERO, S., ESTELLER, M. & FERNANDEZ-SALGUERO, P. M. 2006. The dioxin receptor is silenced by promoter hypermethylation in human acute lymphoblastic leukemia through inhibition of Sp1 binding. *Carcinogenesis,* 27**,** 1099-104.

NAGY, S. R., SANBORN, J. R., HAMMOCK, B. D. & DENISON, M. S. 2002. Development of a green fluorescent protein-based cell bioassay for the rapid and inexpensive detection and characterization of ah receptor agonists. *Toxicol Sci,* 65**,** 200-10.

NAIK, P. & CUCULLO, L. 2012. In vitro blood–brain barrier models: Current and perspective technologies. *Journal of Pharmaceutical Sciences,* 101**,** 1337-1354.

NARANG, V. S., FRAGA, C., KUMAR, N., SHEN, J., THROM, S., STEWART, C. F. & WATERS, C. M. 2008a. Dexamethasone increases expression and activity of multidrug resistance transporters at the rat blood-brain barrier. *American Journal of Physiology-Cell Physiology,* 295**,** C440-C450.

NARANG, V. S., FRAGA, C., KUMAR, N., SHEN, J., THROM, S., STEWART, C. F. & WATERS, C. M. 2008b. Dexamethasone increases expression and activity of multidrug resistance transporters at the rat blood-brain barrier. *Am J Physiol Cell Physiol,* 295**,** C440-50.

NARAYANA, K. R., REDDY, M. S., CHALUVADI, M. R. & KRISHNA, D. R. 2001. Bioflavonoids classification, pharmacological, biochemical effects and therapeutic potential. *Indian Journal of Pharmacology,* 33**,** 2-16.

NAZER, B., HONG, S. & SELKOE, D. J. 2008. LRP promotes endocytosis and degradation, but not transcytosis, of the amyloid-beta peptide in a blood-brain barrier in vitro model. *Neurobiol Dis,* 30**,** 94-102.

NEBERT, D. W., DALTON, T. P., OKEY, A. B. & GONZALEZ, F. J. 2004. Role of aryl hydrocarbon receptor-mediated induction of the CYP1 enzymes in environmental toxicity and cancer. *J Biol Chem,* 279**,** 23847-50.

NEBERT, D. W., PUGA, A. & VASILIOU, V. 1993. Role of the Ah receptor and the dioxin-inducible [Ah] gene battery in toxicity, cancer, and signal transduction. *Ann N Y Acad Sci,* 685**,** 624-40.

NEBERT, D. W., ROE, A. L., DIETER, M. Z., SOLIS, W. A., YANG, Y. & DALTON, T. P. 2000. Role of the aromatic hydrocarbon receptor and [Ah] gene battery in the oxidative stress response, cell cycle control, and apoptosis. *Biochemical Pharmacology,* 59**,** 65-85.

NEUHAUS, W., MANDIKOVA, J., PAWLOWITSCH, R., LINZ, B., BENNANI-BAITI, B., LAUER, R., LACHMANN, B. & NOE, C. R. 2012. Blood-brain barrier in vitro models as tools in drug discovery: assessment of the transport ranking of antihistaminic drugs. *Pharmazie,* 67**,** 432-9.

NEUHAUS, W., STESSL, M., STRIZSIK, E., BENNANI-BAITI, B., WIRTH, M., TOEGEL, S., MODHA, M., WINKLER, J., GABOR, F., VIERNSTEIN, H. & NOE, C. R. 2010. Blood-brain barrier cell line PBMEC/C1-2 possesses functionally active P-glycoprotein. *Neurosci Lett,* 469**,** 224-8.

NICOLAZZO, J. A. & KATNENI, K. 2009. Drug transport across the blood-brain barrier and the impact of breast cancer resistance protein (ABCG2). *Curr Top Med Chem,* 9**,** 130-47.

NIES, A., JEDLITSCHKY, G., KÖNIG, J., HEROLD-MENDE, C., STEINER, H., SCHMITT, H. P. & KEPPLER, D. 2004. Expression and immunolocalization of the multidrug resistance proteins, MRP1–MRP6 (ABCC1–ABCC6), in human brain. *Neuroscience,* 129**,** 349-360.

NIESTROY, J., BARBARA, A., HERBST, K., RODE, S., VAN LIEMPT, M. & ROOS, P. H. 2011. Single and concerted effects of benzo[a]pyrene and flavonoids on the AhR and Nrf2-pathway in the human colon carcinoma cell line Caco-2. *Toxicology in Vitro,* 25**,** 671-683.

NISHIUMI, S., YOSHIDA, K. & ASHIDA, H. 2007a. Curcumin suppresses the transformation of an aryl hydrocarbon receptor through its phosphorylation. *Arch Biochem Biophys,* 466**,** 267-73.

NISHIUMI, S., YOSHIDA, K. I. & ASHIDA, H. 2007b. Curcumin suppresses the transformation of an aryl hydrocarbon receptor through its phosphorylation. *Archives of Biochemistry and Biophysics,* 466**,** 267-273.

NOLTE, J. 1988. The human brain. USA: Mosby-Year Book

NOLTE, J. 1993. *The Human Brain,* United States of America, Mosby-Year Book.

NORINDER, U. & HAEBERLEIN, M. 2002. Computational approaches to the prediction of the blood–brain distribution. *Advanced Drug Delivery Reviews,* 54**,** 291-313.

NOVOTNA, A., SROVNALOVA, A., SVECAROVA, M., KORHONOVA, M., BARTONKOVA, I. & DVORAK, Z. 2014. Differential effects of omeprazole and lansoprazole enantiomers on aryl hydrocarbon receptor in human hepatocytes and cell lines. *PLoS One,* 9**,** e98711.

NUTT, J., BURCHIEL, K., COMELLA, C., JANKOVIC, J., LANG, A., LAWS, E., LOZANO, A., PENN, R., SIMPSON, R., STACY, M. & WOOTEN, G. 2003. Randomized, double-blind trial of glial cell line-derived neurotrophic factor (GDNF) in PD. *Neurology,* 60**,** 69 - 73.

NUTTON, V. 1973. The chronology of Galen's early career. *Class Q,* 23**,** 158-71.

OLDENDORF, W. 1967. Why is cerebrospinal fluid? *Bulletin of the Los Angeles Neurological Society,* 32**,** 169 - 180.
OLDENDORF, W. H., CORNFORD, M. E. & BROWN, W. J. 1977. The large apparent work capability of the blood-brain barrier: a study of the mitochondrial content of capillary endothelial cells in brain and other tissues of the rat. *Ann Neurol,* 1**,** 409-17.
OTT, M., FRICKER, G. & BAUER, B. 2009. Pregnane X receptor (PXR) regulates P-glycoprotein at the blood-brain barrier: functional similarities between pig and human PXR. *J Pharmacol Exp Ther,* 329**,** 141-9.
PARDRIDGE, W. 1991. New York: Raven Press.
PARDRIDGE, W. 2011. Drug transport in brain via the cerebrospinal fluid. *Fluids and Barriers of the CNS,* 8**,** 7.
PARDRIDGE, W. M. 2007. Blood–brain barrier delivery. *Drug Discovery Today,* 12**,** 54-61.
PASCALE, C. L., MILLER, M. C., CHIU, C., BOYLAN, M., CARALOPOULOS, I. N., GONZALEZ, L., JOHANSON, C. E. & SILVERBERG, G. D. 2011. Amyloid-beta transporter expression at the blood-CSF barrier is age-dependent. *Fluids Barriers CNS,* 8**,** 21.
PATABENDIGE, A., SKINNER, R. A., MORGAN, L. & JOAN ABBOTT, N. 2013. A detailed method for preparation of a functional and flexible blood–brain barrier model using porcine brain endothelial cells. *Brain Research,* 1521**,** 16-30.
PENG, B. H., LEE, J. C. & CAMPBELL, G. A. 2003. In vitro protein complex formation with cytoskeleton-anchoring domain of occludin identified by limited proteolysis. *J Biol Chem,* 278**,** 49644-51.
PENG, H. W., CHENG, F. C., HUANG, Y. T., CHEN, C. F. & TSAI, T. H. 1998. Determination of naringenin and its glucuronide conjugate in rat plasma and brain tissue by high-performance liquid chromatography. *J Chromatogr B Biomed Sci Appl,* 714**,** 369-74.
PERDEW, G. H. 1988. Association of the Ah receptor with the 90-kDa heat shock protein. *J Biol Chem,* 263**,** 13802-5.
PERSIDSKY, Y., RAMIREZ, S. H., HAORAH, J. & KANMOGNE, G. D. 2006. Blood-brain barrier: structural components and function under physiologic and pathologic conditions. *J Neuroimmune Pharmacol,* 1**,** 223-36.
PICK, A., MÜLLER, H., MAYER, R., HAENISCH, B., PAJEVA, I. K., WEIGT, M., BÖNISCH, H., MÜLLER, C. E. & WIESE, M. 2011. Structure–activity relationships of flavonoids as inhibitors of breast cancer resistance protein (BCRP). *Bioorganic & Medicinal Chemistry,* 19**,** 2090-2102.
PICK, A., MÜLLER, H. & WIESE, M. 2008. Structure–activity relationships of new inhibitors of breast cancer resistance protein (ABCG2). *Bioorganic & Medicinal Chemistry,* 16**,** 8224-8236.
POHL, C., WILL, F., DIETRICH, H. & SCHRENK, D. 2006. Cytochrome P450 1A1 expression and activity in caco-2 cells: Modulation by apple juice extract and certain apple polyphenols. *Journal of Agricultural and Food Chemistry,* 54**,** 10262-10268.
POLAND, A., GLOVER, E. & KENDE, A. S. 1976. Stereospecific, high affinity binding of 2,3,7,8-tetrachlorodibenzo-p-dioxin by hepatic cytosol. Evidence that the binding species is receptor for induction of aryl hydrocarbon hydroxylase. *J Biol Chem,* 251**,** 4936-46.
POLLAY, M. 2010. The function and structure of the cerebrospinal fluid outflow system. *Cerebrospinal Fluid Res,* 7**,** 9.
POLLAY, M. & CURL, F. 1967. Secretion of cerebrospinal fluid by the ventricular ependyma of the rabbit. *Am J Physiol,* 213**,** 1031-8.
POLLER, B., DREWE, J., KRAHENBUHL, S., HUWYLER, J. & GUTMANN, H. 2010. Regulation of BCRP (ABCG2) and P-glycoprotein (ABCB1) by cytokines in a model of the human blood-brain barrier. *Cell Mol Neurobiol,* 30**,** 63-70.

PRUDHOMME, J. G., SHERMAN, I. W., LAND, K. M., MOSES, A. V., STENGLEIN, S. & NELSON, J. A. 1996. Studies of Plasmodium falciparum cytoadherence using immortalized human brain capillary endothelial cells. *International Journal for Parasitology,* 26**,** 647-655.

QUATTROCHI, L. C. & TUKEY, R. H. 1993. Nuclear uptake of the Ah (dioxin) receptor in response to omeprazole: transcriptional activation of the human CYP1A1 gene. *Mol Pharmacol,* 43**,** 504-8.

RAMOS, S. 2007. Effects of dietary flavonoids on apoptotic pathways related to cancer chemoprevention. *J Nutr Biochem,* 18**,** 427-42.

RANGEL-ORDONEZ, L., NOLDNER, M., SCHUBERT-ZSILAVECZ, M. & WURGLICS, M. 2010. Plasma levels and distribution of flavonoids in rat brain after single and repeated doses of standardized Ginkgo biloba extract EGb 761(R). *Planta Med,* 76**,** 1683-90.

RAO, V. V., DAHLHEIMER, J. L., BARDGETT, M. E., SNYDER, A. Z., FINCH, R. A., SARTORELLI, A. C. & PIWNICA-WORMS, D. 1999. Choroid plexus epithelial expression of MDR1 P glycoprotein and multidrug resistance-associated protein contribute to the blood-cerebrospinal-fluid drug-permeability barrier. *Proc Natl Acad Sci U S A,* 96**,** 3900-5.

REDZIC, Z. B., PRESTON, J. E., DUNCAN, J. A., CHODOBSKI, A. & SZMYDYNGER-CHODOBSKA, J. 2005. The Choroid Plexus-Cerebrospinal Fluid System: From Development to Aging. *Current topics in developmental biology,* 71**,** 1-52.

REDZIC, Z. B. & SEGAL, M. B. 2004. The structure of the choroid plexus and the physiology of the choroid plexus epithelium. *Advanced Drug Delivery Reviews,* 56**,** 1695-1716.

REGINALD A KAVISHE, JEROEN MW VAN DEN HEUVEL, MARGA VAN DE VEGTEBOLMER, ADRIAN JF LUTY, RUSSEL, F. G. & KOENDERINK, J. B. 2009. Localization of the ATP-binding cassette (ABC) transport proteins PfMRP1, PfMRP2, and PfMDR5 at the Plasmodium falciparum plasma membrane. *Malaria Journal,* 8**,** 9.

REICHEL, V., BURGHARD, S., JOHN, I. & HUBER, O. 2011. P-glycoprotein and breast cancer resistance protein expression and function at the blood-brain barrier and blood-cerebrospinal fluid barrier (choroid plexus) in streptozotocin-induced diabetes in rats. *Brain Res,* 1370**,** 238-45.

RENNELS, M., GREGORY, T., BLAUMANIS, O., FUJIMOTO, K. & GRADY, P. 1985. Evidence for a 'paravascular' fluid circulation in the mammalian central nervous system, provided by the rapid distribution of tracer protein throughout the brain from the subarachnoid space. *Brain Res,* 326**,** 47 - 63.

REVALDE, J. L., LI, Y., HAWKINS, B. C., ROSENGREN, R. J. & PAXTON, J. W. 2015a. Heterocyclic cyclohexanone monocarbonyl analogs of curcumin can inhibit the activity of ATP-binding cassette transporters in cancer multidrug resistance. *Biochem Pharmacol,* 93**,** 305-17.

REVALDE, J. L., LI, Y., HAWKINS, B. C., ROSENGREN, R. J. & PAXTON, J. W. 2015b. Heterocyclic cyclohexanone monocarbonyl analogs of curcumin can inhibit the activity of ATP-binding cassette transporters in cancer multidrug resistance. *Biochemical Pharmacology,* 93**,** 305-317.

REYES, H., REISZ-PORSZASZ, S. & HANKINSON, O. 1992. Identification of the Ah receptor nuclear translocator protein (Arnt) as a component of the DNA binding form of the Ah receptor. *Science,* 256**,** 1193-5.

RICE-EVANS, C. 1995. Plant polyphenols: free radical scavengers or chain-breaking antioxidants? *Biochem Soc Symp,* 61**,** 103-16.

RIETJENS, I. M., BOERSMA, M. G., HAAN, L., SPENKELINK, B., AWAD, H. M., CNUBBEN, N. H., VAN ZANDEN, J. J., WOUDE, H., ALINK, G. M. & KOEMAN, J. H. 2002. The pro-oxidant chemistry of the natural antioxidants vitamin C, vitamin E, carotenoids and flavonoids. *Environ Toxicol Pharmacol,* 11**,** 321-33.

RIORDAN, H. J. & CUTLER, N. R. 2012. The Death of CNS Drug Development: Overstatement or Omen? *Journal for clinical studies,* 3**,** 12-15.

ROBERTS, L. M., BLACK, D. S., RAMAN, C., WOODFORD, K., ZHOU, M., HAGGERTY, J. E., YAN, A. T., CWIRLA, S. E. & GRINDSTAFF, K. K. 2008. Subcellular localization of transporters along the rat blood-brain barrier and blood-cerebral-spinal fluid barrier by in vivo biotinylation. *Neuroscience,* 155**,** 423-38.

ROUX, F., DURIEU-TRAUTMANN, O., CHAVEROT, N., CLAIRE, M., MAILLY, P., BOURRE, J. M., STROSBERG, A. D. & COURAUD, P. O. 1994. Regulation of gamma-glutamyl transpeptidase and alkaline phosphatase activities in immortalized rat brain microvessel endothelial cells. *Journal of Cellular Physiology,* 159**,** 101-113.

RYOTA, N., SULEKHA, V., A, D. M., SUSUMU, S., MASAMI, N. & A, B. W. 2007. Glucose regulated blood-brain barrier transport of insulin: Pericyte-astrocyte-endothelial cell cross talk. *Journal of pharmacological science,* 3**,** 195-200.

SABZEVARI, O., GALATI, G., MORIDANI, M. Y., SIRAKI, A. & O'BRIEN, P. J. 2004. Molecular cytotoxic mechanisms of anticancer hydroxychalcones. *Chem Biol Interact,* 148**,** 57-67.

SAHU, S. C. & GRAY, G. C. 1997. Lipid peroxidation and DNA damage induced by morin and naringenin in isolated rat liver nuclei. *Food Chem Toxicol,* 35**,** 443-7.

SAITO, H., HIRANO, H., NAKAGAWA, H., FUKAMI, T., OOSUMI, K., MURAKAMI, K., KIMURA, H., KOUCHI, T., KONOMI, M. & TAO, E. 2006. A new strategy of high-speed screening and quantitative structure-activity relationship analysis to evaluate human ATP-binding cassette transporter ABCG2-drug interactions. *Journal of Pharmacology and Experimental Therapeutics,* 317**,** 1114-1124.

SCHINKEL, A. H. 1999. P-Glycoprotein, a gatekeeper in the blood–brain barrier. *Advanced Drug Delivery Reviews,* 36**,** 179-194.

SCHINKEL, A. H. & JONKER, J. W. 2012. Mammalian drug efflux transporters of the ATP binding cassette (ABC) family: an overview. *Advanced Drug Delivery Reviews*.

SCHLICHTIGER, J., PEKCEC, A., BARTMANN, H., WINTER, P., FUEST, C., SOERENSEN, J. & POTSCHKA, H. 2010. Celecoxib treatment restores pharmacosensitivity in a rat model of pharmacoresistant epilepsy. *Br J Pharmacol,* 160**,** 1062-71.

SCHWERK, C., PAPANDREOU, T., SCHUHMANN, D., NICKOL, L., BORKOWSKI, J., STEINMANN, U., QUEDNAU, N., STUMP, C., WEISS, C., BERGER, J., WOLBURG, H., CLAUS, H., VOGEL, U., ISHIKAWA, H., TENENBAUM, T. & SCHROTEN, H. 2012. Polar invasion and translocation of Neisseria meningitidis and Streptococcus suis in a novel human model of the blood-cerebrospinal fluid barrier. *PLoS One,* 7**,** e30069.

SEDLAKOVA, R., SHIVERS, R. R. & DEL MAESTRO, R. F. 1999. Ultrastructure of the blood-brain barrier in the rabbit. *J Submicrosc Cytol Pathol,* 31**,** 149-61.

SHEN, J., CARCABOSO, A. M., HUBBARD, K. E., TAGEN, M., WYNN, H. G., PANETTA, J. C., WATERS, C. M., ELMELIEGY, M. A. & STEWART, C. F. 2009. Compartment-specific roles of ATP-binding cassette transporters define differential topotecan distribution in brain parenchyma and cerebrospinal fluid. *Cancer Res,* 69**,** 5885-92.

SHI, L. Z., LI, G. J., WANG, S. & ZHENG, W. 2008a. Use of Z310 cells as an in vitro blood-cerebrospinal fluid barrier model: tight junction proteins and transport properties. *Toxicology in vitro: an international journal published in association with BIBRA,* 22**,** 190.

SHI, L. Z., LI, G. J., WANG, S. & ZHENG*, W. 2008b. Use of Z310 Cells as an In Vitro Blood-Cerebrospinal Fluid Barrier Model: Tight Junction Proteins and Transport Properties. *Toxicology in Vitro,* 22**,** 190-199.

SHI, L. Z. & ZHENG, W. 2005. Establishment of an in vitro brain barrier epithelial transport system for pharmacological and toxicological study. *Brain Res,* 1057**,** 37-48.

SHI, Z., PENG, X. X., KIM, I. W., SHUKLA, S., SI, Q. S., ROBEY, R. W., BATES, S. E., SHEN, T., ASHBY, C. R., JR., FU, L. W., AMBUDKAR, S. V. & CHEN, Z. S. 2007. Erlotinib (Tarceva, OSI-774) antagonizes ATP-binding cassette subfamily B member 1 and ATP-binding cassette subfamily G member 2-mediated drug resistance. *Cancer Res,* 67**,** 11012-20.

SIEGEL GJ, AGRANOFF BW & ALBERS RW 1999. *Basic Neurochemistry: Molecular, Cellular and Medical Aspects.,* Philadelphia, Philadelphia: Lippincott-Raven.

SKINNER, R. A., GIBSON, R. M., ROTHWELL, N. J., PINTEAUX, E. & PENNY, J. I. 2009. Transport of interleukin-1 across cerebromicrovascular endothelial cells. *Br J Pharmacol,* 156**,** 1115-23.

SON, Y. O., LEE, K. Y., KOOK, S. H., LEE, J. C., KIM, J. G., JEON, Y. M. & JANG, Y. S. 2004. Selective effects of quercetin on the cell growth and antioxidant defense system in normal versus transformed mouse hepatic cell lines. *Eur J Pharmacol,* 502**,** 195-204.

SPECTOR, R., KEEP, R. F., ROBERT SNODGRASS, S., SMITH, Q. R. & JOHANSON, C. E. 2015. A balanced view of choroid plexus structure and function: Focus on adult humans. *Experimental Neurology,* 267**,** 78-86.

SPENCER, J. P. E. 2008. Food for thought: The role of dietary flavonoids in enhancing human memory, learning and neuro-cognitive performance. *Proceedings of the Nutrition Society,* 67**,** 238-252.

STAMATOVIC, S. M., KEEP, R. F. & ANDJELKOVIC, A. V. 2008. Brain endothelial cell-cell junctions: how to "open" the blood brain barrier. *Curr Neuropharmacol,* 6**,** 179-92.

STANLEY, L. A., HORSBURGH, B. C., ROSS, J., SCHEER, N. & WOLF, C. R. 2006. PXR and CAR: nuclear receptors which play a pivotal role in drug disposition and chemical toxicity. *Drug Metab Rev,* 38**,** 515-97.

STAUD, F. & PAVEK, P. 2005. Breast cancer resistance protein (BCRP/ABCG2). *The international journal of biochemistry & cell biology,* 37**,** 720-725.

STEPHEN PORTER, CROSSLEY, A., NEWMAN, J., FINCHAM, K., FEINGOLD, M., LEVACK, B., P.M.GOUK & TYACKE, N. 1977. *THe histroy of the University of Oxford,* Oxford New York, Oxford University Press.

STINS, M. F., BADGER, J. & SIK KIM, K. 2001. Bacterial invasion and transcytosis in transfected human brain microvascular endothelial cells. *Microbial Pathogenesis,* 30**,** 19-28.

SUGATANI, J., YAMAKAWA, K., TONDA, E., NISHITANI, S., YOSHINARI, K., DEGAWA, M., ABE, I., NOGUCHI, H. & MIWA, M. 2004. The induction of human UDP-glucuronosyltransferase 1A1 mediated through a distal enhancer module by flavonoids and xenobiotics. *Biochemical pharmacology,* 67**,** 989-1000.

SUMMERFIELD, S. G., READ, K., BEGLEY, D. J., OBRADOVIC, T., HIDALGO, I. J., COGGON, S., LEWIS, A. V., PORTER, R. A. & JEFFREY, P. 2007. Central nervous system drug disposition: the relationship between in situ brain permeability and brain free fraction. *J Pharmacol Exp Ther,* 322**,** 205-13.

SUZUKI, H. & SUGIYAMA, Y. 2000. Role of metabolic enzymes and efflux transporters in the absorption of drugs from the small intestine. *European journal of pharmaceutical sciences,* 12**,** 3-12.

SUZUKI, T., FUKAMI, T. & TOMONO, K. 2015. Possible involvement of cationic-drug sensitive transport systems in the blood-to-brain influx and brain-to-blood efflux of amantadine across the blood-brain barrier. *Biopharm Drug Dispos,* 36**,** 126-37.

SZENTISTVANYI, I., PATLAK, C., ELLIS, R. & CSERR, H. 1984. Drainage of interstitial fluid from different regions of rat brain. *Am J Physiol,* 246**,** F835 - F844.

SZMYDYNGER-CHODOBSKA, J., PASCALE, C. L., PFEFFER, A. N., COULTER, C. & CHODOBSKI, A. 2007. Expression of junctional proteins in choroid plexus epithelial cell lines: a comparative study. *Cerebrospinal Fluid Res,* 4.

T, I., H, E., T, T., Y, Y. & K., K. 1998. Nuclear localization and export signals of the human aryl hydrocarbon receptor. *The journal of biological chemistry,* 273**,** 2895-2904.

TAKASHIMA, T., WU, C., TAKASHIMA-HIRANO, M., KATAYAMA, Y., WADA, Y., SUZUKI, M., KUSUHARA, H., SUGIYAMA, Y. & WATANABE, Y. 2013. Evaluation of Breast Cancer Resistance Protein Function in Hepatobiliary and Renal Excretion Using PET with 11C-SC-62807. *Journal of Nuclear Medicine,* 54**,** 267-276.

TAN, K. P., WANG, B., YANG, M., BOUTROS, P. C., MACAULAY, J., XU, H., CHUANG, A. I., KOSUGE, K., YAMAMOTO, M., TAKAHASHI, S., WU, A. M., ROSS, D. D., HARPER, P. A. & ITO, S. 2010. Aryl hydrocarbon receptor is a transcriptional activator of the human breast cancer resistance protein (BCRP/ABCG2). *Mol Pharmacol,* 78**,** 175-85.

TANAKA, Y., SLITT, A. L., LEAZER, T. M., MAHER, J. M. & KLAASSEN, C. D. 2005. Tissue distribution and hormonal regulation of the breast cancer resistance protein (Bcrp/Abcg2) in rats and mice. *Biochem Biophys Res Commun,* 326**,** 181-7.

TANG, C., CHEN, T., KAPADNIS, S., HODGDON, H., TAO, Y., CHEN, X., WEN, M., COSTA, D., MURPHY, D., NOLAN, S., FLOOD, D. G., WELTY, D. F. & KOENIG, G. 2014. Neuropharmacokinetics of two investigational compounds in rats: Divergent temporal profiles in the brain and cerebrospinal fluid. *Biochemical Pharmacology,* 91**,** 543-551.

TEIFEL, M. & FRIEDL, P. 1996. Establishment of the permanent microvascular endothelial cell line PBMEC/C1-2 from porcine brains. *Experimental cell research,* 228**,** 50-57.

TENG, S., JEKERLE, V. & PIQUETTE-MILLER, M. 2003. Induction of ABCC3 (MRP3) by pregnane X receptor activators. *Drug Metab Dispos,* 31**,** 1296-9.

THOMAS, H. & COLEY, H. M. 2003. Overcoming multidrug resistance in cancer: an update on the clinical strategy of inhibiting p-glycoprotein. *Cancer control,* 10**,** 159-159.

THOMSEN, L. B., BURKHART, A. & MOOS, T. 2015. A Triple Culture Model of the Blood-Brain Barrier Using Porcine Brain Endothelial cells, Astrocytes and Pericytes. *PLoS ONE,* 10**,** e0134765.

TOMPKINS, L. M., LI, H., LI, L., LYNCH, C., XIE, Y., NAKANISHI, T., ROSS, D. D. & WANG, H. 2010. A novel xenobiotic responsive element regulated by aryl hydrocarbon receptor is involved in the induction of BCRP/ABCG2 in LS174T cells. *Biochemical pharmacology,* 80**,** 1754-1761.

TOURNIER, N., SABA, W., GOUTAL, S., GERVAIS, P., VALETTE, H., SCHERRMANN, J. M., BOTTLAENDER, M. & CISTERNINO, S. 2015. Influence of P-Glycoprotein Inhibition or Deficiency at the Blood-Brain Barrier on (18)F-2-Fluoro-2-Deoxy-D-glucose ((18)F-FDG) Brain Kinetics. *AAPS J,* 17**,** 652-9.

UCHIDA, Y., ZHANG, Z., TACHIKAWA, M. & TERASAKI, T. 2015. Quantitative targeted absolute proteomics of rat blood-cerebrospinal fluid barrier transporters: comparison with a human specimen. *J Neurochem,* 134**,** 1104-15.

ULRIKE TONTSCH & BAUER, H.-C. 1989. Isolation, characterization, and long-term cultivation of porcine and murine cerebral capillary endothelial cells. *Microvascular research,* 37**,** 148-161.

URQUHART, B. L. & KIM, R. B. 2009. Blood-brain barrier transporters and response to CNS-active drugs. *Eur J Clin Pharmacol,* 65**,** 1063-70.

VAN ZANDEN, J. J., VAN DER WOUDE, H., VAESSEN, J., USTA, M., WORTELBOER, H. M., CNUBBEN, N. H. P. & RIETJENS, I. M. C. M. 2007. The effect of quercetin phase II metabolism on its MRP1 and MRP2 inhibiting potential. *Biochemical pharmacology,* 74**,** 345-351.

VARMA, M. V. S., ASHOKRAJ, Y., DEY, C. S. & PANCHAGNULA, R. 2003. P-glycoprotein inhibitors and their screening: a perspective from bioavailability enhancement. *Pharmacological Research,* 48**,** 347-359.

VERSANTVOORT, C. H., BAGRIJ, T., WRIGHT, K. A. & TWENTYMAN, P. R. 1995. On the relationship between the probenecid-sensitive transport of daunorubicin or calcein and the glutathione status of cells overexpressing the multidrug resistance-associated protein (MRP). *Int J Cancer,* 63**,** 855-62.

VINCENT, C., TAYLOR-ADAMS, S. & STANHOPE, N. 1998. Framework for analysing risk and safety in clinical medicine. *BMJ,* 316**,** 1154-1157.

VOLK, E. L. & SCHNEIDER, E. 2003. Wild-type breast cancer resistance protein (BCRP/ABCG2) is a methotrexate polyglutamate transporter. *Cancer Res,* 63**,** 5538-43.

VON WEDEL-PARLOW, M., WOLTE, P. & GALLA, H. J. 2009. Regulation of major efflux transporters under inflammatory conditions at the blood-brain barrier in vitro. *J Neurochem,* 111**,** 111-8.

VRBA, J., KREN, V., VACEK, J., PAPOUSKOVA, B. & ULRICHOVA, J. 2012. Quercetin, Quercetin Glycosides and Taxifolin Differ in their Ability to Induce AhR Activation and CYP1A1 Expression in HepG2 Cells. *Phytotherapy Research,* 26**,** 1746-1752.

WANG, H. & LECLUYSE, E. L. 2003. Role of orphan nuclear receptors in the regulation of drug-metabolising enzymes. *Clin Pharmacokinet,* 42**,** 1331-57.

WANG, H., LEE, E. W., ZHOU, L., LEUNG, P. C., ROSS, D. D., UNADKAT, J. D. & MAO, Q. 2008a. Progesterone receptor (PR) isoforms PRA and PRB differentially regulate expression of the breast cancer resistance protein in human placental choriocarcinoma BeWo cells. *Mol Pharmacol,* 73**,** 845-54.

WANG, H. & NEGISHI, M. 2003. Transcriptional regulation of cytochrome p450 2B genes by nuclear receptors. *Curr Drug Metab,* 4**,** 515-25.

WANG, H., UNADKAT, J. D. & MAO, Q. 2008b. Hormonal regulation of BCRP expression in human placental BeWo cells. *Pharm Res,* 25**,** 444-52.

WANG, H., ZHOU, L., GUPTA, A., VETHANAYAGAM, R. R., ZHANG, Y., UNADKAT, J. D. & MAO, Q. 2006. Regulation of BCRP/ABCG2 expression by progesterone and 17beta-estradiol in human placental BeWo cells. *Am J Physiol Endocrinol Metab,* 290**,** E798-807.

WANG, Q., RAGER, J. D., WEINSTEIN, K., KARDOS, P. S., DOBSON, G. L., LI, J. & HIDALGO, I. J. 2005. Evaluation of the MDR-MDCK cell line as a permeability screen for the blood-brain barrier. *Int J Pharm,* 288**,** 349-59.

WANG, X., HAWKINS, B. T. & MILLER, D. S. 2011. Aryl hydrocarbon receptor-mediated up-regulation of ATP-driven xenobiotic efflux transporters at the blood-brain barrier. *FASEB J,* 25**,** 644-52.

WANG, X., SYKES, D. B. & MILLER, D. S. 2010. Constitutive androstane receptor-mediated up-regulation of ATP-driven xenobiotic efflux transporters at the blood-brain barrier. *Mol Pharmacol,* 78**,** 376-83.

WARREN, M. S., ZERANGUE, N., WOODFORD, K., ROBERTS, L. M., TATE, E. H., FENG, B., LI, C., FEUERSTEIN, T. J., GIBBS, J. & SMITH, B. 2009. Comparative gene expression profiles of ABC transporters in brain microvessel endothelial cells and brain in five species including human. *Pharmacological Research,* 59**,** 404-413.

WEI, J. B., LAI, Q., SHUMYAK, S. P., XU, L. F., ZHANG, C. X., LING, J. J. & YU, Y. 2015. An LC/MS quantitative and microdialysis method for cyclovirobuxine D pharmacokinetics in rat plasma and brain: The pharmacokinetic comparison of three different drug delivery routes. *J Chromatogr B Analyt Technol Biomed Life Sci,* 1002**,** 185-93.

WEKSLER, B. B., SUBILEAU, E. A., PERRIERE, N., CHARNEAU, P., HOLLOWAY, K., LEVEQUE, M., TRICOIRE-LEIGNEL, H., NICOTRA, A., BOURDOULOUS, S., TUROWSKI, P., MALE, D. K., ROUX, F., GREENWOOD, J., ROMERO, I. A. & COURAUD, P. O. 2005. Blood-brain barrier-specific properties of a human adult brain endothelial cell line. *Faseb j,* 19**,** 1872-4.

WEN, X., WALLE, U. K. & WALLE, T. 2005. 5,7-Dimethoxyflavone downregulates CYP1A1 expression and benzo[a]pyrene-induced DNA binding in Hep G2 cells. *Carcinogenesis,* 26**,** 803-9.

WERNER , A. & SCHNEIDER , J. M. 1974. Teaching Medical Students Interactional Skills. *New England Journal of Medicine,* 290**,** 1232-1237.

WILHELMSSON, A., CUTHILL, S., DENIS, M., WIKSTROM, A. C., GUSTAFSSON, J. A. & POELLINGER, L. 1990. The specific DNA binding activity of the dioxin receptor is modulated by the 90 kd heat shock protein. *Embo j,* 9**,** 69-76.

WIMO, A. & PRINCE, M. 2010. World Alzheimer Report 2010

The Global Economic Impact of Dementia. *Alzheimer's disease international.* USA: Alzheimer's Disease International (ADI)

WOLBURG, H., NOELL, S., MACK, A., WOLBURG-BUCHHOLZ, K. & FALLIER-BECKER, P. 2009. Brain endothelial cells and the glio-vascular complex. *Cell Tissue Res,* 335**,** 75-96.

WOLFMAN, C., VIOLA, H., PALADINI, A., DAJAS, F. & MEDINA, J. H. 1994. Possible anxiolytic effects of chrysin, a central benzodiazepine receptor ligand isolated from Passiflora coerulea. *Pharmacol Biochem Behav,* 47**,** 1-4.

WOODWARD, O. M., KOTTGEN, A., CORESH, J., BOERWINKLE, E., GUGGINO, W. B. & KOTTGEN, M. 2009. Identification of a urate transporter, ABCG2, with a common functional polymorphism causing gout. *Proc Natl Acad Sci U S A,* 106**,** 10338-42.

WRAITH, D. C. & NICHOLSON, L. B. 2012. The adaptive immune system in diseases of the central nervous system. *J Clin Invest,* 122**,** 1172-9.

WU, M.-S., LIEN, G.-S., SHEN, S.-C., YANG, L.-Y. & CHEN, Y.-C. 2013. HSP90 Inhibitors, Geldanamycin and Radicicol, Enhance Fisetin-Induced Cytotoxicity via Induction of Apoptosis in Human Colonic Cancer Cells. *Evidence-based Complementary and Alternative Medicine : eCAM,* 2013**,** 987612.

XIE, R. & HAMMARLUND-UDENAES, M. 1998. Blood-brain barrier equilibration of codeine in rats studied with microdialysis. *Pharm Res,* 15**,** 570-5.

XIONG, H., CALLAGHAN, D., JONES, A., BAI, J., RASQUINHA, I., SMITH, C., PEI, K., WALKER, D., LUE, L. F., STANIMIROVIC, D. & ZHANG, W. 2009. ABCG2 is upregulated in Alzheimer's brain with cerebral amyloid angiopathy and may act as a gatekeeper at the blood-brain barrier for Abeta(1-40) peptides. *J Neurosci,* 29**,** 5463-75.

XU, C., LI, C. Y. & KONG, A. N. 2005. Induction of phase I, II and III drug metabolism/transport by xenobiotics. *Arch Pharm Res,* 28**,** 249-68.

XU, J., LIU, Y., YANG, Y., BATES, S. & ZHANG, J. T. 2004. Characterization of oligomeric human half-ABC transporter ATP-binding cassette G2. *J Biol Chem,* 279**,** 19781-9.

YOU, G. & MORRIS, M. E. 2007. Overview of drug transporter families. *Drug Transporters: Molecular Characterization and Role in Drug Disposition,* 4**,** 1.

YOUDIM, K. A., DOBBIE, M. S., KUHNLE, G., PROTEGGENTE, A. R., ABBOTT, N. J. & RICE-EVANS, C. 2003. Interaction between flavonoids and the blood-brain barrier: in vitro studies. *J Neurochem,* 85**,** 180-92.

YOUDIM, K. A., QAISER, M. Z., BEGLEY, D. J., RICE-EVANS, C. A. & ABBOTT, N. J. 2004. Flavonoid permeability across an in situ model of the blood-brain barrier. *Free Radic Biol Med,* 36**,** 592-604.

YOUSIF, S., CHAVES, C., POTIN, S., MARGAILL, I., SCHERRMANN, J. M. & DECLEVES, X. 2012. Induction of P-glycoprotein and Bcrp at the rat blood-brain barrier following a subchronic morphine treatment is mediated through NMDA/COX-2 activation. *J Neurochem,* 123**,** 491-503.

ZEICHNER, K. 2010. Rethinking the Connections Between Campus Courses and Field Experiences in College- and University-Based Teacher Education. *Journal of Teacher Education,* 61**,** 89-99.

ZHANG, H., WONG, C. W., COVILLE, P. F. & WANWIMOLRUK, S. 2000. Effect of the grapefruit flavonoid naringin on pharmacokinetics of quinine in rats. *Drug Metabolism and Drug Interactions,* 17**,** 351-363.

ZHANG, Q., WU, D., WU, J., OU, Y., MU, C., HAN, B. & ZHANG, Q. 2015. Improved blood-brain barrier distribution: effect of borneol on the brain pharmacokinetics of kaempferol in rats by in vivo microdialysis sampling. *J Ethnopharmacol,* 162**,** 270-7.

ZHANG, S. & MORRIS, M. E. 2003. Effect of the flavonoids biochanin A and silymarin on the P-glycoprotein-mediated transport of digoxin and vinblastine in human intestinal Caco-2 cells. *Pharm Res,* 20**,** 1184-91.

ZHANG, S., QIN, C. & SAFE, S. H. 2003a. Flavonoids as aryl hydrocarbon receptor agonists/antagonists: effects of structure and cell context. *Environ Health Perspect,* 111**,** 1877-82.

ZHANG, S., WANG, X., SAGAWA, K. & MORRIS, M. E. 2005. Flavonoids chrysin and benzoflavone, potent breast cancer resistance protein inhibitors, have no significant effect on topotecan pharmacokinetics in rats or mdr1a/1b (-/-) mice. *Drug Metab Dispos,* 33**,** 341-8.

ZHANG, S., YANG, X. & MORRIS, M. E. 2004a. Flavonoids are inhibitors of breast cancer resistance protein (ABCG2)-mediated transport. *Mol Pharmacol,* 65**,** 1208-1216.

ZHANG, S., YANG, X. & MORRIS, M. E. 2004b. Flavonoids are inhibitors of breast cancer resistance protein (ABCG2)-mediated transport. *Mol Pharmacol,* 65**,** 1208-16.

ZHANG, W., MOJSILOVIC-PETROVIC, J., ANDRADE, M. F., ZHANG, H., BALL, M. & STANIMIROVIC, D. B. 2003b. The expression and functional characterization of ABCG2 in brain endothelial cells and vessels. *Faseb j,* 17**,** 2085-7.

ZHANG, W., XIONG, H., CALLAGHAN, D., LIU, H., JONES, A., PEI, K., FATEHI, D., BRUNETTE, E. & STANIMIROVIC, D. 2013. Blood-brain barrier transport of amyloid beta peptides in efflux pump knock-out animals evaluated by in vivo optical imaging. *Fluids and Barriers of the CNS,* 10**,** 13-13.

ZHAO, B., BOHONOWYCH, J. E., TIMME-LARAGY, A., JUNG, D., AFFATATO, A. A., RICE, R. H., DI GIULIO, R. T. & DENISON, M. S. 2013. Common commercial and consumer products contain activators of the aryl hydrocarbon (dioxin) receptor. *PLoS One,* 8**,** e56860.

ZHAO, B., DEGROOT, D. E., HAYASHI, A., HE, G. & DENISON, M. S. 2010. CH223191 is a ligand-selective antagonist of the Ah (Dioxin) receptor. *Toxicol Sci,* 117**,** 393-403.

ZHAO, R., KALVASS, J. C. & POLLACK, G. M. 2009a. Assessment of blood-brain barrier permeability using the in situ mouse brain perfusion technique. *Pharm Res,* 26**,** 1657-64.

ZHAO, R., RAUB, T. J., SAWADA, G. A., KASPER, S. C., BACON, J. A., BRIDGES, A. S. & POLLACK, G. M. 2009b. Breast cancer resistance protein interacts with various compounds in vitro, but plays a minor role in substrate efflux at the blood-brain barrier. *Drug Metabolism and Disposition,* 37**,** 1251-1258.

ZHENG, W. & ZHAO, Q. 2002. Establishment and characterization of an immortalized Z310 choroidal epithelial cell line from murine choroid plexus. *Brain Res,* 958**,** 371-380.

Appendix A

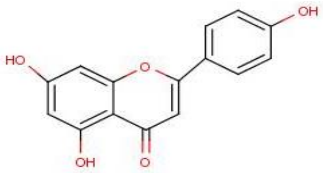

Apigenin

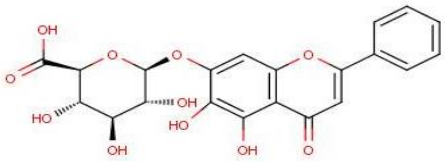

Baiclain

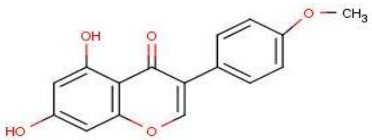

Biochanin A

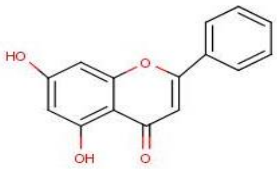

Chrysin

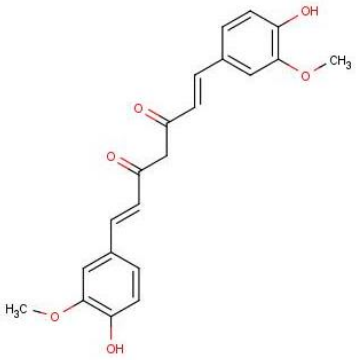

Curcumin

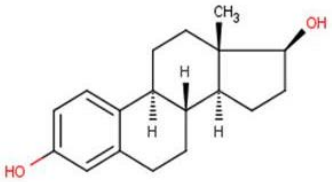

17- β-estradiol

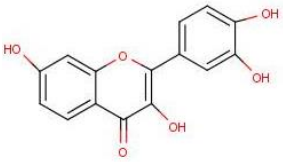

Fistein

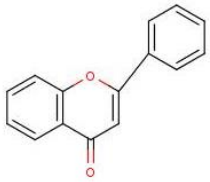

Flavone

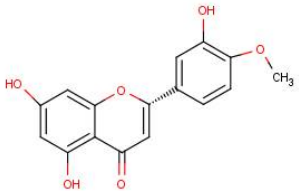

Hesperetin

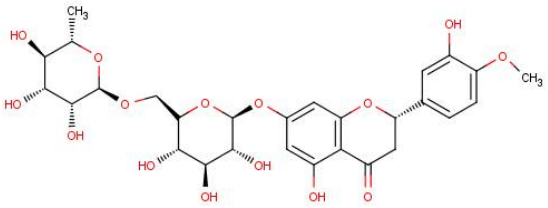

Hesperidin

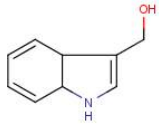

Indole-3-carbinol

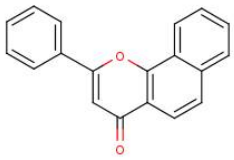

α-Napthoflavone

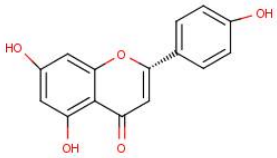

Naringin

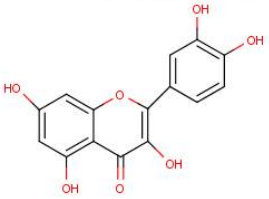

Quercetin

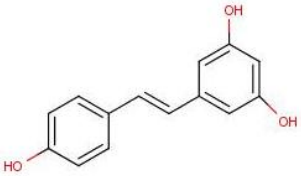

Resveratrol

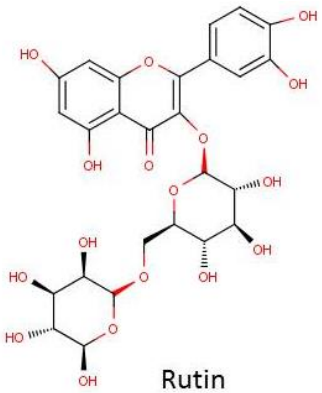

Rutin

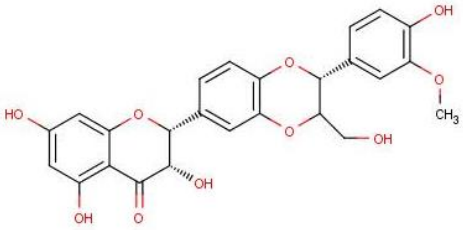

Silymarin

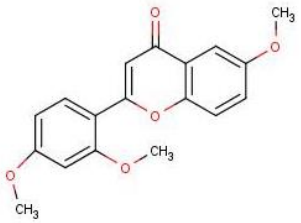

6,2,4-trimethoxyflavone